Formation of DNA complexes in aqueous and organic solvents

Dissertation

zur Erlangung des Grades

„Doktor der Naturwissenschaften“

Im Promotionsfach Chemie

Am Fachbereich Chemie, Pharmazie und Geowissenschaften

der Johannes Gutenberg Universität-Mainz

vorgelegt von

Angel Francisco Medina Oliva

geboren in Maracaibo, Venezuela

Mainz, 2012

Die vorliegende Arbeit wurde in der Zeit von Juli 2009 bis Juli 2012 am Institut fur Physikalische Chemie der Johannes Gutenberg-Universitat Mainz angefertigt.

Dekan: Prof. D. Sc. h. c. -

1. Berichterstatter: Prof. Dr. -

2. Berichterstatter: Prof. Dr. -

Datum der mundlichen Prufung: 16.07.2012

Acknowledgments

Although there is a “model” to write the acknowledgments of a PhD thesis, I would like to break the rule and write something in this work that it is not coming from my brain but from my soul.

It is a real pleasure for me to thank my supervisor, Prof. -, for his great guidance, for being there every day available for his students. That is something that not many PhD students can say. Thank you for the great knowledge, because I arrive here with almost no idea about light scattering and now I am able to spread this knowledge to others. I am grateful to the MAINZ Graduate School for financing my PhD.

I own big thanks to a person who has not only provided me with scientific guidance but also with great smiles and who encouraged me to learn more and more every day. This person is known among the PhD students as the “walking Wikipedia”. Yes, I am talking about you Dr.-, thanks a lot!

It would like to express my gratitude to Prof. -. He was hearing all the details of my PhD and providing me with very good advices. Thank you also for the non-scientific chats.

I would like to thank a person, who has impressed by letting me see with my own eyes the exciting “nanoworld”. Danke - für die AFM Bilder und für deine gute Laune. Also - had contributed to these great images, which increase my passion for science. Thank you - for the Cryo-TEM pictures of DOTAP. Ich möchte mich auch bei - für die GPC Messungen bedanken.

I would also like to thank Dr. - and my friend Prof. - for the nice discussions about my work.

I am very grateful to Dr. - for introducing to the wonderful (but complicated) world of capillary electrophoresis, for his amazingly good guidance in Sydney and for his friendship. I am also grateful to Dr. - for the same reasons. It is also a pleasure for me to thank Dr. - for the knowledge about migration of polyelectrolytes under an electric field.

I am happy to thank - for the teaching light scattering, CD spectroscopy, UV spectroscopy, and in general to work in the lab. In general, I would like to thank the whole group of - for helping me in the lab and by writing this work.

I own a big hug to - for correcting my English and for being an amazing friend.

I would like to thank - for nice scientific (and not that scientific) discussions. It is a pleasure being a friend of such a brilliant person. In this respect, I am also thankful with -. His brain is as big as his heart.

The people just mentioned before helped me directly with my PhD. But the research is at the end the result of intense work. Behind all this work, there are many people, who day by day made my life easier, more beautiful, who with a word or a hug made my day and encouraged me to keep going even if after the day, I was completely tired or not motivated. The first people that I would like to thank are all of the members of my family. Desde la paz espiritual adquirida gracias a mi abuela, pasando por las risas y las lindas palabras de mis tías - y mis primitos -, hasta la perseverancia aprendida por mi padre, la compañía infinita de mi hermana -, la asertividad y los buenos momentos compartidos con mi hermanita menor - y las infinitas enseñanzas de mi madre desde los tiempos en los cuales me cantaba "duerme negrito" en la cuna contribuyeron a hacer de este sueño una realidad. Je voudrais aussi remercier à - et sa famille pour les bons instants qu'on a partagé ensemble. Merci Madame - pour tous votre attentions.

I would like to thank a person, who helped me enormously during the first difficult months in Mainz. Without this person, I would have hesitated between staying in Germany or going back to Venezuela before finishing my PhD. Thank you very much Dr. -.

Two other people helped me from the beginning to make the start of my PhD a pleasant "journey". Thank you very much to -. You are the only friend that I met from my first day here in Germany and have helped enormously from many points of view. A person who has delighted me from the first day with interesting conversations and who also from the first time initiated a wonderful friendship that I hope it lasts for many more years is -. A life is not enough to thank you for the great moments.

I would like to thank as well the person who made me integrate into the German culture, a person who everyday with a lot of patience was talking to me in German while eating in the "Mensa". Thank you -. I mentioned you before, but this time I am thanking you as one of my best friends.

The whole group of - (including her as well), thank you for the nice talks. Thank you - for lighting my life everyday when I was going into your office.

If there are two people who have demonstrated me that good scientist can also be smiling and happy people with a great sense of humor are - y mi tocayo -. You are by far two of the most amazing people I have ever met in my life.

Also I am extremely grateful to - for changing my life (literally). Ich möchte mir auch bei - bedanken für seine Geduld und immer dabei zu sein. Also I'd like to thank my friend - and one of the most beautiful person I have ever met, -, for the nice philosophical chats at the gym.

- and -, if it weren't because of our lunches on Tuesdays, I would have not learned that much about the world. Thank you for making my life better. You are examples to follow as scientists and as a person.

- and for the even crazier - (bella!!!) and mi amigo -. You make me look at life in a completely different way than before. Thanks a lot!

Thanks a lot to -, and - for the great talks in the office. - and -, ihr seid unglaublich gute deusche Lehrerin. - thanks for taking me out when I was not feeling very well.

Mi muy querida amiga y hermana -. Desde los siete anos nos conocimos y hemos establecido una amistad que durará por siempre. Mil gracias! - bella de mi corazón, mil gracias por tu amistad. -, eres la alegría hecha persona. Gracias por las mejores carcajadas de mi vida y por tu amistad.

Finally, I would like to thank my beautiful family for its great support and for being all the time there for me. Yes, I know, I already thanked you a few paragraphs above but I was told that I should emphasize the most important part of my PhD.

Summary

From a physical-chemical point of view, it is challenging to form complexes with polyelectrolytes, consisting of only molecule of the largest component, i.e. the component with the highest number of charges. In this study, complexes are formed with DNA because of its potential applications as an artificial vector for gene delivery. The aim of this work is to prepare complexes in aqueous solutions as well as in organic solvents containing only one DNA molecule. For this purpose, the topology, equilibrium and conformation of complexes between a supercoiled DNA pUC19 (2686 base pairs) and spermine containing hydrophilic and/or hydrophobic moieties or a polylysine with a hydrophilic block are determined by means of dynamic (DLS) and static light scattering (SLS), atomic force microscopy (AFM), and circular dichroism (CD) spectroscopy. It is demonstrated that all of these complexes consisted of only one molecule of the polyanion. Only the polylysine-b-polyethylene glycol copolymer satisfied the conditions: 1) 100% neutralization of DNA charges and with a small excess of the cation (lower than 30%) and 2) form stable complexes at every charge ratio.

DNA complex formation is also investigated in organic solvents. Precipitation is induced by neutralizing the charge of the supercoiled DNA pUC19 with the surfactants dodecyltrimethylammonium bromide (DTAB) and tetradecyltrimethylammonium bromide (TTAB). After isolation and drying of the solids, the complexes are dissolved in organic solvents. DNA-TTA complexes are only soluble in methanol and DNA-DTA in DMF. The complexes again consisted of only one DNA molecule. The final topology of the complexes is different in methanol than in DMF. In the former case, DNA seems to be compacted whereas in the latter case, the DNA-DTA complexes seem to have an expanded conformation. Upon complex formation with polycations in organic solvents (with polyvilylpyridine brush (b-PVP) in methanol and with a protected polylysine in DMF), DNA aggregates and precipitates.

DNA is linearized with an enzyme (SmaI) to investigate the influence of the initial topology of the polyanion on the final conformation of the complexes in organic solvents. Two main differences are evidenced: 1. Complexes in organic solvents formed with linear DNA have in general a more expanded conformation and a higher tendency to aggregate. 2. If a polycation, i.e. the b-PVP, is added to the linear DNA-TTA complexes in methanol, complexes with the polycation are formed at a higher charge ratio. In DMF, the addition of the same b-PVP and of b-PLL did not lead to the formation of complexes.

Zusammenfassung

Vom physiko-chemischen Gesichtspunkt aus ist es eine große Herausforderung Polyelektrolytkomplexe aus nur einem Molekül des größten Komponenten, z.B. aus dem mit der größten Ladungsdichte, zu formen. In dieser Arbeit wurden die Komplexe aus DNA wegen ihrer möglichen Verwendung als künstliche Vektoren in der Gentherapie verwendet. Hierbei war es das Ziel Komplexe sowohl in wässrigen als auch organischen Lösungsmittel mit nur einem DNA-Molekül zu bilden. Zu diesem Zwecke wurden Topologie, Gleichgewicht und Konformation der Komplexe zwischen supercoiled DNA pUC19 (2686 Basenpaare) und Spermin mit dessen hydrophilen und hydrophoben Resten oder Polylysin mit dessen hydrophilen Block durch dynamische (DLS) und statischer Lichtstreuung (SLS), Rasterkraftmikroskopie oder CD-Spektroskopie untersucht. Ferner wurde nachgewiesen, dass alle Komplexe aus nur einem Molekül des Polyanions bestehen. Lediglich das Polylysin-b-Polyethylenglycol-Copolymer war in der Lage folgende Kriterien zu erfüllen: 1. 100% Neutralisation der DNA-Ladungen mit einem kleinen Überschuss an Kation (weniger 30%) und 2. Stabile Komplexe bei verschiedenen Ladungsverhältnissen

Desweitern wurde die DNA-Komplexbildung auch in organischen Lösungsmitteln untersucht. Bei der Neutralisation der supercoiled pUC19 mit den Tensiden Dodecyltrimethylammoniumbromid (DTAB) und Tetradecyltrimethylammoniumbromid (TTAB) wurde diese ausgefällt. Nach Isolierung und Trocknung der Feststoffe wurden die Komplexe in organischen Lösemittel gelöst. DNA-TTA Komplexe sind nur in Methanol löslich, DNA-DTA hingegen nur in DMF. Es wurden unterschiedliche Topologien für die die verschiedenen Lösemittel gefunden. Im ersten Fall scheint es als würde die DNA kompaktiert werden während im letzteren Fall scheint es hingegen so als würden sich die Komplexe mit Dodecylammonium in DMF ausbreiten. DNA-Komplexe mit Polykationen wie Polyvinylpyridin (b-PVP) zu in Methanol oder geschützten Polylysinbürsten (b-PLL) in DMF hingegen aggregieren und fallen aus.

Ferner wurde die DNA mit Hilfe eines Restriktionsenzyms (SmaI) linerisiert und dessen Einfluss von der ursprüngliche Topologie des Polyanions auf die finale Konformation der Komplexe in organischen Lösemittel zu untersuchen. Dabei wurden zwei große Unterschied deutlich: 1. Komplexe mit linearer DNA besitzen in organischen Lösemittel generell eine größere Ausdehnung und eine höhere Tendenz zu aggregieren. 2. Wenn ein Polykation wie zum Beispiel b-PVP zu den lineare DNA-TTA-Komplexen in Methanol hinzugegeben wird werden Komplexe mit einer höheren Ladungsdichte geformt. In DMF ist dies weder für das b-PVP noch für das b-PLL der Fall.

Table of content

1. Introduction

Polyelectrolytes are polymers containing charged or ionizable monomers [1]. These charged groups provide the polymers with certain properties, particular to this group of macromolecules, for example, higher stiffness, and an "anomalous" increment of the viscosity with dilution at salt free conditions and the capacity to form complexes with oppositely-charged molecules [2]. This last characteristic has been of particular interest to the scientific community in recent years, especially with respect to self-assembly of polyelectrolytes (PECs) and of polyelectrolytes with surfactants (PE-surf).

In order to maintain the principle of electroneutrality, the polyelectrolytes must be always surrounded by ions with opposite charges. These ions are called "counterions". The counterions can be only in the vicinity of the polymer forming a cloud of opposite charges or they could be "sitting" on the surface of the charges. In the latter case, it is said that counterions are in a "condensed" state [3].The term "condensation" is also used for DNA collapse (shrinkage) as a result of the reduction in intramolecular electrostatic repulsions. Polyelectrolytes with "hydrophobic" chains are water soluble due to the charges. Thus, the regions where the charges are condensed may become hydrophobic [4].

The main driving force for the formation of PECs is the gain in entropy due to the release of counterions together with the electrostatic interactions between opposite charges [2] (see figure 1.1). Other forces are responsible for the binding of an oppositely charged surfactant to a polyelectrolyte, i.e. hydrophobic interactions among neighboring bounded surfactants.

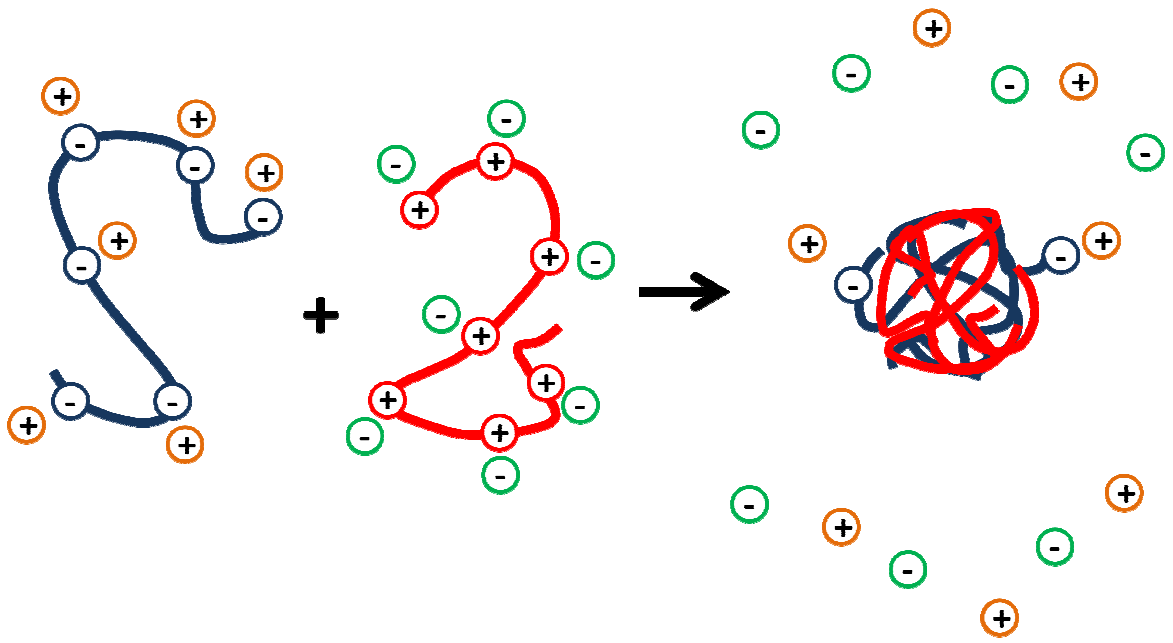

Figure 1.1. Formation of PECs driven by electrostatic interactions and the release of counterions [2].

Polyelectrolytes are not only of academic interest. They have nowadays several industrial applications; for example, partially hydrolyzed polyacrylamides (PAA) are used by oil companies for Enhanced Oil Recovery (EOR) processes [5, 6] or as flocculants in water treatment plants [7]. PECs and PE-surf complexes are emerging as useful tools for the pharmaceutical and cosmetic industry, given that the complexes can be tailored to have the specific properties. For instance, complexes between sodium dodecyl-sulfate and cationically modified cellulosic polymer are used in formulations for hair conditioning. PE-surf can reduce significantly the surface tension of a system even before reaching the critical micellar concentration (cmc) or the critical aggregation concentration (cac) [8]. In the literature, many developments in the application and uses of PECs are continually emerging. For instance, in the area of pharmacy and medicine it has been discovered that polymeric complexes of insulin can have a more prolonged activity compared to free insulin because of an enhanced resistance to the action of pepsin [9]. One of the major challenges for biological systems is the formation of PECs with DNA to carry out the so-called “gene therapy”.

Gene therapy is defined as the insertion of genetic material into the nucleus of a cell in order to overcome diseases caused by genetic mutations. [10, 11, 12, 13, 14] DNA (Deoxyribose Nucleic Acid) is a negatively-charged polyelectrolyte composed by four repeating units called "bases" and a skeleton of deoxyribose and phosphate groups, which carry the charges of DNA. The order in which the bases are placed determine the structure of the protein to be synthesized in an organism. Some diseases, e.g. hemophilia, are caused by an anomaly either in the structure of the bases or in its order. The addition of a "healthy" gene into a cell may help to cure this type of disease. However, the penetration of DNA into a cell is not a trivial issue. The surface of a cell (cytoplasmatic membrane) consists of phospholipids, which, like DNA, also carry negative charges. As expected, electrostatic repulsions prevents DNA from passing through this cytoplasmatic membrane. Until now, two solutions have been proposed to solve this problem: 1) the use of viruses and 2) the formation of DNA complexes with cationic surfactants or polycations (positively-charged polyelectrolytes). Although the former option has demonstrated to have higher efficiency in terms of DNA insertion into the cell (transfection), some immunological problems may also arise [15, 16, 17, 18, 19, 20]. On the other hand, several surfactants and polymers have been used to form complexes with DNA with unfruitful results, i.e. the efficiency of DNA transfection is low. It has been stated that further physicochemical characterization of these complexes is necessary in order to optimize the cationic agent to be used [21].

The formation of complexes with DNA, and in general with polyelectrolytes, is characterized by multimolecular structures. More than one polyelectrolyte molecule is involved in the final conformation of the "cluster", as a result of a reaction controlled by the kinetics rather than by thermodynamic equilibrium [22, 23, 24]. This issue will be addressed more in detail below. **The main objective of this work is to form DNA complexes consisting of only one polyanion. The complexes are prepared with multivalent cations, monovalent surfactants and polycations under different conditions, i.e. in aqueous and/or organic solvents**. It is important to notice, that DNA was chosen as the polyanion of study because of the potential applications to new and developing concepts within the field in gene therapy. However, it is not the aim of this work to produce complexes to be inserted into a cell.

The physicochemical characterization of DNA complexes is presented in terms of three main topics: topology, conformation, and equilibrium. In some cases, other variables, e.g. the efficiency of complexation are presented. The topology is visualized by means of Atomic Force Microscopy (AFM) and in some cases with Transmission Electronic Microscopy (TEM). In order to verify that the images

given by these techniques are not an artifact depending on the surface-sample interaction (for AFM) or the method of preparation, the average topology of the complexes was determined with Dynamic Light Scattering (DLS) and Static Light Scattering (SLS). With these two last techniques, the z-averaged hydrodynamic radius $\langle Rh \rangle_z$ and the z-averaged radius of gyration $\langle Rg^2 \rangle_z^{1/2}$ can be measured. As explained in chapter 3, the ratio Rg/Rh could be used to estimate the topology of the complexes. The conformation of the DNA within the complexes, e.g. the number of bases and the distance per turn of the helical structure, can be elucidated by means of circular dichroism (CD) spectroscopy. Finally, the equilibrium of the complexes, i.e. the number of bounded and free cationic agent per DNA molecule, is encountered through a detailed analysis of SLS measurements.

The first multivalent cations used to form complexes with DNA were the naturally existing spermidine (3+) and spermine (4+). These molecules condense DNA in the living organisms and play an important role in the normal cell growth [25, 26]. However, the formation of complexes with DNA leads to aggregation and sometimes to precipitation at a charge ratio of positive to negative charges (N+/P-) close to one [27, 28]. Even at lower charge ratios, their complexes with DNA complexes are not composed of only one molecule of the polyanion [29, 30, 31] (see figure 1.2). Furthermore, an excess of cations (polyamines) is required to neutralize all of the DNA charges [32]. The amount of free spermidine or spermine dictated by the equilibrium upon formation of complexes with DNA is larger as desirable. Therefore, in chapter 5 a supercoiled DNA pUC19 is condensed with different spermine derivatives with hydrophilic and hydrophobic groups in order to improve the stability against aggregation and the efficiency in complexing DNA, respectively. Also a polyethylene oxide – polylysine (PEO-PLL) diblock was used to increase the charges of the cation and hence the efficiency.

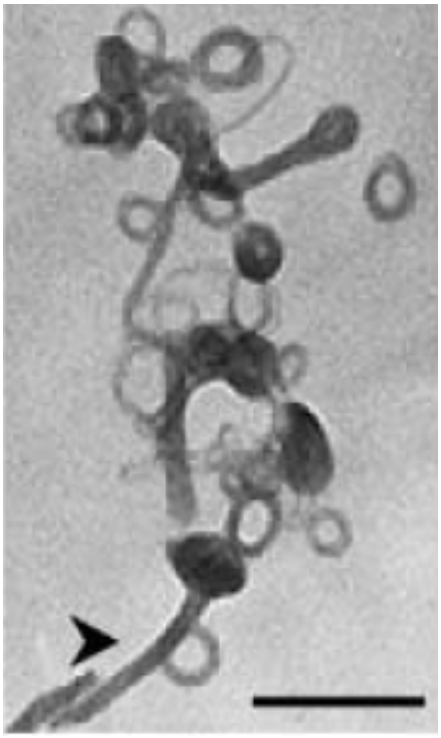

Figure 1.2. Formation of DNA complexes with spermine at a charge ratio of N+/P- = 1.5. [DNA] = 1ug/ml. Bars ~ 200 μm [29].

It is known that in general cations containing at least three charges are required to condense DNA [3, 24, 30]. However, monovalent surfactants, e.g. alkyltrimethylammonium bromide, are also able to neutralize the DNA charges in aqueous solutions, due to the hydrophobic interactions among the tails of the surfactants [33, 34]. The formation of these complexes is the result of a cooperative binding. In other words, once a surfactant interacts electrostatically with DNA, the following surfactants will complex the DNA with a binding constant K*u*, where K is theoretical equilibrium constant for the binding of one single surfactant and *u* is the cooperativity factor. This variable "*u*" accounts for the more efficient binding of free surfactants, due to hydrophobic interactions with other surfactants that are already bound to the DNA. At a charge ratio N+/P- close to one, the complexes may undergo precipitation [34]. Little attention has been paid to the topology of this precipitate, once dissolved in organic solvents. On one hand, hydrophobic interactions disappear, leading to dissolution of the complexes. On the other side, if the solvent used possesses a relative dielectric constant, ε_r, lower than the one for water, the ion-pair interactions are strengthened given that the Bjerrum length (λ_B), defined as the minimum distance for ion-pair formation, increases

$$\lambda_B = \frac{e^2}{4\pi\epsilon_0\epsilon_r k_B T} \quad (1.1)$$

Where e is the elementary charged, ε_0 , the vacuum permittivity, k_B, the Boltzmann constant, and T the temperature.

Furthermore, to the best knowledge of the authors, the formation of complexes between DNA and a polycation in organic solvent has never been reported. It is still not clear, the type of complexes that could be obtained in solvents other than water. An advantage of using organic solvents is that the number of charges of synthetic "hydrophobic" polycations can be drastically reduced, because these charges are responsible for the dissolution of these kind of polyelectrolytes in aqueous solutions and the solubility in this solvent is not longer required. In chapter 6, complexes of supercoiled DNA pUC19 with surfactants and polycations are formed and characterized in organic solvents.

A plasmid (supercoiled) DNA has been used in this work in chapters 5 and 6 and as well as in most of the research found in the literature. However, until now, the only example of DNA complexes consisting of only one molecule of each polyelectrolyte with a topology determined apparently by the thermodynamics has been prepared with linear DNA [35] (see figure 1.3) In chapter 7, the two strands of the supercoiled DNA are cut in one point to generate a linear DNA instead. The molar mass and the number of charges remain constant but the initial topology of the polyanion changes. The influence of the different DNA topology on the final topology of the complexes with surfactants and polycations in organic solvent is examined.

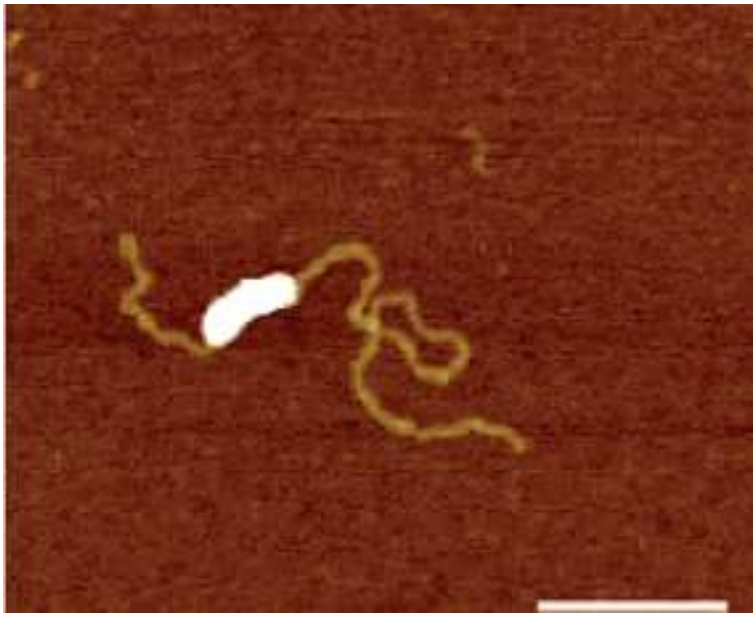

Figure 1.3. High resolution SFM image of linearized DNA pUC19 complex with a dendronized polymer of generation 4 (PG4) at a charge ratio of 1:0.7. [35]

1.1. References

1. Kötz, J.; Kosmella, S.; Beitz, T. Prog. Poly. Sci. 2001, 26, 1199 – 1232.
2. Ankerfors, C. Polyelectrolyte complexes: their preparation, adsorption behavior, and effect on paper properties. Licentiate Thesis. Royal Institute of Technology (KTH): Sweden. 2008.
3. Sennato, S.; Bordi, F.; Cametti, C.; Diociaiuti, M.; Malaspina, P. Biochimica et Biophysica Acta, 2005, 1714, 11 – 24.
4. Reimer, D.; Zhang, Y.; Kong, S.; Wheeler, J.; Graham, R.; Bally, M. Biochemistry, 1995, 34, 12877 – 12883.
5. Moradi-Araghi, A.; in proceedings of the Society Petroleum Engineers International Symposium on Oil Field Chemistry, San Antonio, Texas, 1987. SPE 16273, 1987, 319 – 328.
6. Hernández, C.; Chacón, L.; Anselmi, L.; Baldonedo, A; in proceedings of the Society Petroleum Engineers (SPE) Latinamerican and Caribbean Petroleum Engineering, Buenos Aires, Argentina, 2001. SPE 69544, 2001, 1 – 11.
7. Erciyes, T.; Erim, M.; Hazer, B.; Yagci, Y. Die Angewandte Makromolekulare Chemie, 1992, 200, 163 – 171.
8. Tadros, T. Applied surfactants: principles and applications. Wiley-VCH, 2005.
9. Petrak,K. Journal of bioactive and compatible polymers, 1986, 1, 202 – 219.
10. DeRouchey, J.; Netz, R.; Rädler, R. Eur. Phys. J. E. 2005, 16, 17 – 28.
11. Kuhn, P.; Barbosa, M.; Levin, Y. Physica A, 1999, 278 – 284.

12. Andersson, T.; Aeseyev, V.; Tenhu, H. Biomacromolecules, 2004, 5, 1853 – 1861.
13. Cherstvy, A.; Winkler, R. Journal of Chemical Physics. 2004, 120 (19), 9394 – 9400.
14. Silva, M.; Lucena, L.; Barbosa, M. Physica A: Statistical Mechanics and its Applications. 2004, 331, 42 – 50.
15. Rungsardthong, U.; Deshpande, M.; Bailey, L.; Vamvakaki, M.; Armes, S.; Garnett, M.; Stolnik, S. Journal of Controlled Released, 2001, 73, 359 – 380.
16. Park, S.; Healy, K. Journal of Controlled Released, 2004, 95, 639 – 651.
17. Kircheis, R.; Wightman, L.; Wagner, E. Advanced Drug Delivery Reviews. 2001, 53, 341 – 358.
18. Twaites, B.; de las Heras Alarcón, C.; Cunliffe, D.; Lavigne, M.; Pennadam, S.; Smith, J.; Górecki, D.; Alexander, C. Journal of Controlled Release, 2004, 97, 551 – 566.
19. Sang, M.; Won-Ki, K.; Sun, K.; Jung, M.; Kwang-Hyun, B.; Yu-Kyoung, O. Biochima et Biophysica Acta. 2007, 1770, 747 – 752.
20. Kunath, K.; von Harpe, A.; Fischer, D.; Kissel, T. Journal of Controlled Released. 2003, 88, 159 – 172.
21. Pack, D.; Hoffmann, A.; Pun, S.; Stayton, P. Nature Reviews. Drug Discovery, 2005, 4, 581 – 593.
22. Störkle, D.; Duschner, S.; Heimann, N.; Maskos, M.; Schmidt, M. Macromolecules, 2007, 40 (22), 7998 – 8006.
23. Lai, E.; van Zanten, J. Biophysical Journal, 2001, 80, 864 – 873
24. Bloomfield, V. Biopolymers, 1997, 3, 269-282.
25. Allahryarov, E.; Gompper, G.; Loewen, H. J. Phys: Condens. Matter 2005, 17, 1827 – 1840
26. Shao, Q.; Goyal, S.; Finzi, L.; Dunlap, D. Macromolecules 2012, 45, 3188 – 3196
27. Murayama, Y.; Sakamaki, Y.; Sano, M. Phys. Rev. Lett. 2003, 90(1), 018102 (4 pages)
28. Allahryarov, E.; Gompper, G.; Loewen, H. J. Phys: Condens. Matter 2005, 17, 1827 – 1840
29. Patel, M.; Anchordoquy, T. Biophysical Journal. 2004, 88 (3), 2089 – 2103
30. Bloomfield, V. Biopolymers, 1991, 31, 1471 – 1481.
31. Arscott, P.; Li, A.; Bloomfield. V. Biopolymers, 1990, 30, 619 – 630.
32. He, S.; Arscott, P.; Bloomfield, V. Biopolymers 2000, 53, 329 – 341
33. Matulis, D.; Rouzina, I.; Bloomfield, V. J. Am. Chem. Soc. 2002, 124, 7331 – 7342.
34. Dias, R.S.; Innerlohinger, J.; Glatter, O.; Miguel, M.; Lindman, B. J. Phys. Chem. B 2005, 109, 10458 – 10463
35. Gössl, I.; Shu, L.; Schlüter, D.; Rabe, J. J. Am. Chem. Soc. 2002, 124, 6860 – 6865.

2. Background knowledge on polyelectrolyte complexes

2.1. Complexes between a polyelectrolyte and a surfactant (PE-surf)

Surfactants (abbreviation of SURFace ACTive AgeNT) are molecules able to lower the surface tension of aqueous solutions. They are composed of a hydrophilic part (head) and a hydrophobic part (tail). The main property of the surfactant is that, above a critical concentration, they are able to change abruptly the properties of an aqueous system [1]. This concentration is called the critical micellar concentration. At a lower concentration, surfactants place themselves at the air/water interface to reduce hydrophobic interactions. Once the surface is completely covered (at the cmc), the surfactants aggregate in structures called micelles. At this point, properties such as the turbidity and conductivity start to behave differently.

Surfactants can be ionic or nonionic. In this discussion, the focus will be on ionic surfactants. They are able to form complexes with polyelectrolytes (charged polymers). The main driving forces for the formation of these complexes are the electrostatic interactions and the hydrophobic interactions among the neighboring surfactants.

2.1.1. Equilibrium of formation of PE-surf complexes

At this point, it is important to introduce the definition of cooperative binding [2, 3, 4]. Consider the following equilibria

$$(OO)+D^{+} \overset{K}{\leftrightarrow} (OD)$$

$$(OD)+D^{+} \overset{Ku}{\leftrightarrow} (DD)$$

Given two neighboring sites (charges) in a polyelectrolyte (OO), the binding of an ionic surfactant D+ to one of these sites (O) is dictated by the equilibrium constant K. The binding of another ionic surfactant to a neighboring unoccupied site of the polyelectrolyte is not longer determined by K albeit by K*u* instead [5, 6, 7].

The cooperativity parameter, u, is defined as [5]

$$u = \frac{(DD)(OO)}{(DO)^2} \tag{2.1}$$

Where the parentheses denote concentrations.

If

u>1 the binding is cooperative.

u = 1 the binding is noncooperative

u<1 the binding is anticooperative

The formation of complexes of polyelectrolytes with surfactants is usually a cooperative process, because of the hydrophobic interactions among the tails of neighboring surfactants. Once a surfactant is bound to

one site, the next one will tend to bind the neighboring charge of the polyelectrolyte to lower the free energy by interaction among the hydrophobic parts of surfactants.

The process described above usually includes the release of counterions from the surfactant as well as from the polyelectrolyte. In this case, the reaction is called "metathesis" and it is the most common way of forming PE-surf complexes [8]. The explanation of other routes to obtain the same complexes is out of the scope of this work.

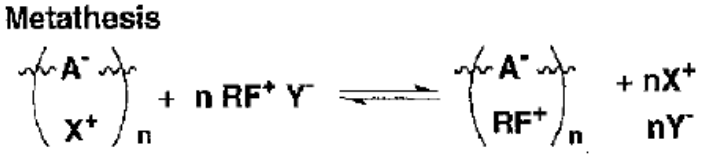

Figure 2.1. Schematic representation of the process of metathesis. In this case, A^- is the polyelectrolyte with its counterion X^+ and RF^+ is a surfactant with a hydrophobic tail R and a functional (charged) group F^+ with with its counterion Y^-. [8]

2.1.2. Mechanism of PE-surf complex formation

Given an aqueous solution containing a constant concentration of a polyelectrolyte being titrated with an oppositely charged ionic surfactant, PE-surf starts forming at a "critical aggregation concentration" (cac). In the case of micelle formation, the hydrophobic forces have to overcome the electrostatic repulsions among the heads of the surfactants and the lost of entropy of the surfactants itself. In contrast, during the formation of PE-surf complexes, electrostatic attractions and the release of counterions from the polyelectrolyte act also as driving forces for the binding of surfactants. Therefore, the cac is typically two orders of magnitudes lower than the cmc [1, 8]. Also, the PE-surf complexes lower significantly the surface tension of an aqueous solution compared to the free surfactants (see figure 2.2.).

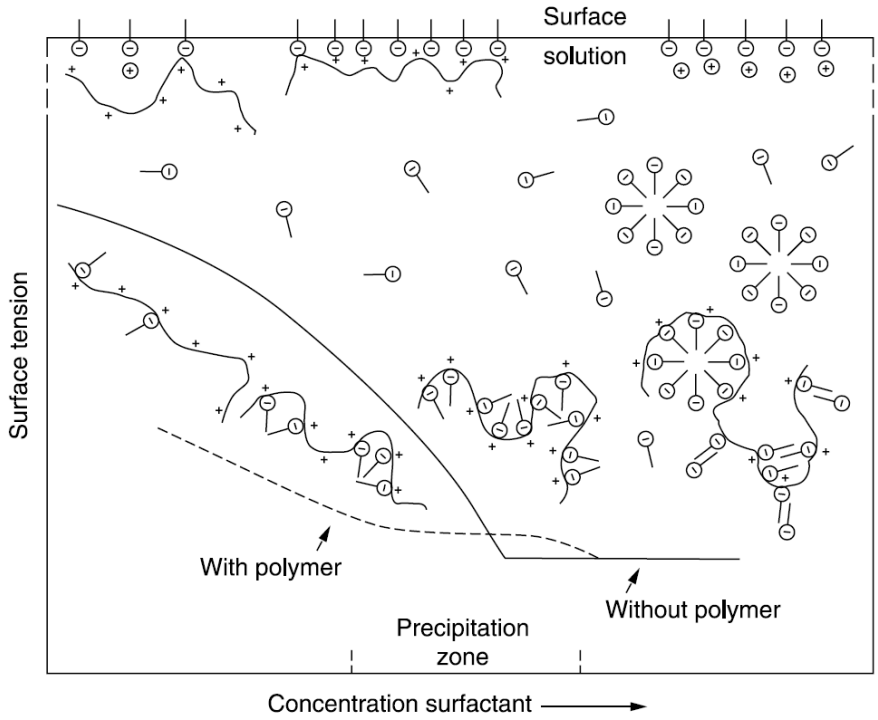

Figure 2.2. Mechanism of formation of PE-surf complexes [1]

When the ratio of positive and negative charges (β) has reached the unity, the PE-surf complexes could precipitate. It has been reported that an excess of the surfactant may cause redissolution of the complexes in aqueous solutions [1].

2.2. Complexes between oppositely charged polyelectrolytes (PECs)

2.2.1. Equilibrium of PECs complex formation

Oppositely charged molecules, e.g. A and B, are attracted due to Coulombic interactions according to the following reaction

$$A + B \text{ ----- } AB$$

For small molecules, the equilibrium constant has a low value.

$$K = \frac{[AB]}{[A][B]} \tag{2.2}$$

However, the binding constant K increases significantly for polymers with positive and negative charges. This increase is explained by the higher probability of interaction of two opposite charges [9]. The binding of free ions requires a large entropic energy, i.e. upon binding, the lost of freedom of motion is significant and the entropy of the ions must be lowered. The charged monomers in a polyelectrolyte have already restriction of motion due to the covalent bonds; hence the decrease of entropy is not significant and can be easier bound.

The formation of polyelectrolyte complexes (PECs) is driven by electrostatic interactions as well as by the augment of entropy due to the release of counterions. A more appropriate description of the formation of complexes between polyelectrolytes is given as follow [10]

$$(A^+a^-)_n.H_2O + (B^-b^+)_m.H_2O \text{ ----- } (A^+B^-)_x + (A^+a^-)_{n-x} + (B^-b^+)_{m-x} + xa + xb + H_2O \tag{2.3}$$

Where A and B are monomers of polyelectrolytes carrying positive and negative charges and their counterions a and b, respectively. The subscripts “n” and “m” denote the number of positive and negative charges in the initial polymers and “x” the number of charges “complexed” or “neutralized”.

Polyelectrolyte complexes (PECs) can be stable against dissociation at a wide range of conditions, i.e. temperature and ionic strength. This stability can be understood in terms of the free energy of the multipoint electrostatic bonding [11].

$$K_n = {K_1}^n = exp\left(-\frac{n\Delta G_1{}^\circ}{RT}\right)$$

The equilibrium of polyelectrolyte complexes is a cooperative process, in which the equilibrium of binding for one monomer K_1 is increased by a factor of "n", where n is the number of charged repeating units.

2.2.2. Topology of PECs complexes

Under relatively low ionic strength PECS are composed of several molecules of the polyelectrolytes while forming kinetically "frozen" structures [12]. At low concentrations, these structures may contain hundreds of polymer chains whereas at high concentrations they could even have thousands of molecules. The structure of PECs with inherently-hydrophobic main chains is shown in figure 2.3. They consist of a hydrophobic core consisting on neutralized polyelectrolytes and some "arms" of the polyelectrolyte in excess forming "flower"like" or "scramble egg" structures [11].

The final structures are usually determined by a kinetically-controlled complexation rather than by a process of equilibrium. At a charge ratio close to 1:1, the complexes aggregate and may undergo subsequent precipitation [10, 11, 12, 13, 14]. The process of aggregation can be explained in three main steps: 1. Formation of primary complexes 2. Intramolecular rearrangement and 3. Intercomplex aggregation (secondary aggregation). [12]. The first process, as mentioned before, it is driven by electrostatic interactions and the entropic energy upon release of the counterions [15]. Next, it is hypothesized that new bonds may be formed within the same molecule. Finally, complexes are aggregated due to the large hydrophobic interactions within the cores of the PECs. [12]

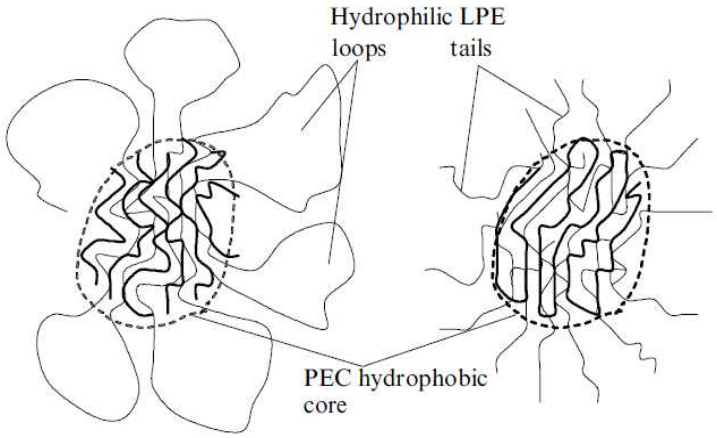

(a) (b)

Figure 2.3. Schematic representation of the structures of PECs with hydrophobic backbones in aqueous solution: (a) flower-like and (b) scramble egg. [11]

Under high concentration of low-molecular weight salts, the PECs are able to undergo a rearrangement process to form more "organized" structures soluble in aqueous solutions. At a even higher concentration of the salts, the complexes could be completely dissociated. It is important to notice that PECs are "living" systems and that a polyelectrolyte could be replaced by other with a larger molar mass or higher charge density [12].

Only a few examples in the literature of "organized" equilibrium structures can be found. For example, Duschner et al. [16] formed complexes of polystyrene sulfonate (PSS) with macromonomers of polyethyleneimine grafted with polyethylene oxide (PMMPEI-PEO) in dimethylformamide (DMF) with rod-like topologies consisting of only one molecule of each polyelectrolyte (see figure 2.4.). The order of mixing did not change the final topology of the complexes.

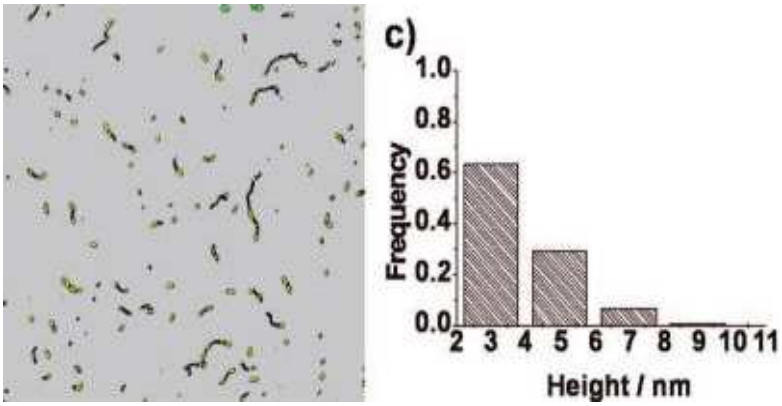

Figure 2.4. AFM pictures (height, left, size: 1.5 x 1.5 μm^2) of complexes of polystyrenesulfonate macromonomer with dodecyltrimethylammonium and slightly charged polyethyleneimine macromonomers (PMMPEI-PEO) and the corresponding high frequencies determined (right). w(PMMPEI-PEO) = 0.70. [16]

2.3. References

1. Tadros, T. Applied surfactants: principles and applications. Wiley-VCH, 2005
2. Hayakawa, K.; Kwak, J. J. Phys. Chem. 1983, 87, 506 – 509.
3. Dias, R.S.; Innerlohinger, J.; Glatter, O.; Miguel, M.; Lindman, B. J. Phys. Chem. B 2005, 109, 10458 – 10463
4. Matulis, D.; Rouzina, I.; Bloomfield, V. J. Am. Chem. Soc. 2002, 124, 7331 – 7342.
5. Hayakawa, K.; Santerre, P.; Kwak, J. Macromolecules, 1983, 16, 1642 – 1645.
6. Wallin, T.; lines, P. Langmuir 1996, 12, 305 – 314
7. Dias, S.; Magno, L.; Valente, A.; Das, D.; Das, P.; Maiti, S.; Miguel, M.; Lindman, B. 2008, 112, 14446 – 14452.
8. Ober, C.; Wegner, G. Adv. Mater. 1997, 9(1), 17 – 31.
9. Petrak,K. Journal of bioactive and compatible polymers, 1986, 1, 202 – 219.
10. Thünemann, A.; Müller, M.; Dautzenberg, H.; Joanny, L.; Löwen, H. Polyelectrolyte complexes. Polyelectrolyte with defined molecular architecture II. Springer, 2004.
11. Izumrudov, V. Russian Chemical Reviews. 2008, 77 (4), 381 – 393.
12. Tsuchida, E. J.M.S. – Pure Appl. Chem. 1994, A31(1), 1 – 15.
13. Michaels, A.; Miekka, R. J. Phys. Chem. 1961, 65, 1765 – 1773.
14. Vasheghani, B.; Rajabi, F.; Ahmadi, M.; Mashhadi, A. Polymer Bulletin. 2008, 61, 247 – 255.
15. Dautzenberg, H.; Jaeger, W. Macromol. Chem. Phys. 2002, 203, 2095 – 2102.
16. Duschner, S.; Störkle, D.; Schmidt, M.; Maskos, M. Macromolecules. 2008. 41, 9067 – 9071.

3. Formation of DNA complexes

3.1. General Background on DNA

DNA is a polyanion with a semi-rigid helical structure formed by two strands. Each of these strands consists of aromatic molecules called "bases", which are hydrophobic at physiological conditions. They are joined by a skeleton of alternating deoxyribose sugar and phosphate groups with negative charges independent of the pH [1 – 4].

3.1.1. Topologies of DNA

DNA can exist in three different topologies: supercoiled, linear and open-circular (nicked-DNA). A supercoiled DNA has a closed-circular topology with twists and writhes. Linear DNA has a "cylindrical-like" conformation with no geometry constraints. DNA can possess an open circular topology, when one strand of the double helix is cut in one point. The three topologies are shown in figure 3.1. [1 – 3, 5]

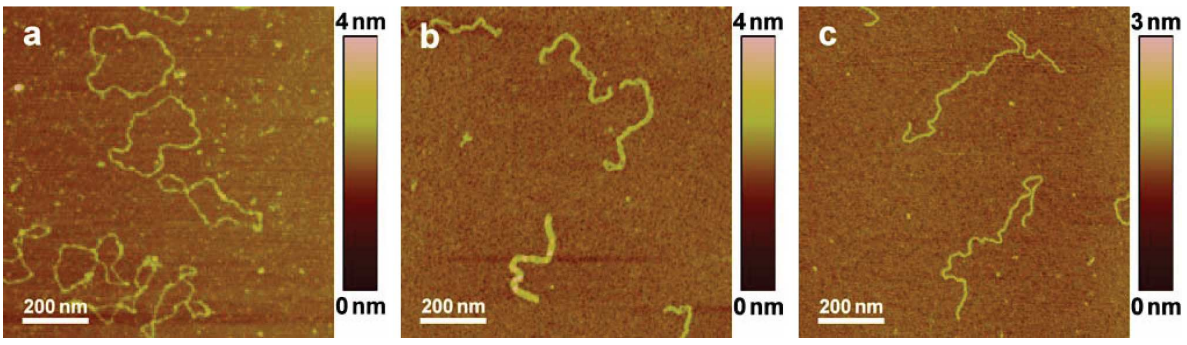

Figure 3.1. DNA topologies: a) open-circular b) supercoiled and c) linear. [5]

The structure of the supercoiled DNA can be better observed in figure 3.2.

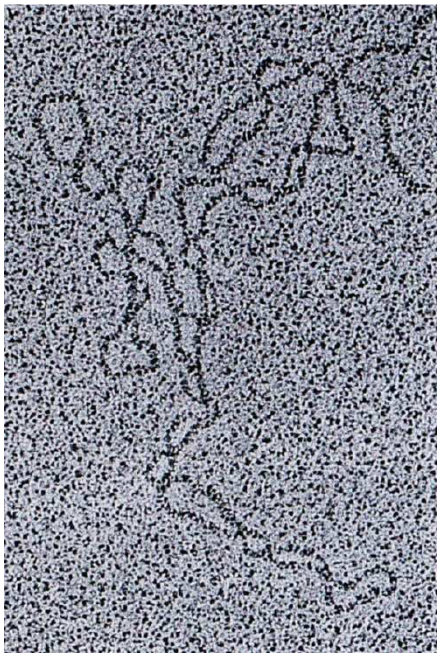

Figure 3.2. Transmission electron microscopy (TEM) image of supercoiled DNA [6].

3.1.2. DNA conformations

The conformation of the double helix, e.g. the number of bases (residues) per turn, the distance between nucleotide bases (axial rise), and the helix sense, can vary under different environments. The most common DNA conformations are presented in table 3.1. [1, 2, 4, 7]

Table 3.1. Conditions and parameters of the different DNA conformations [1 -2].

Parameter	A-DNA	B-DNA	Z-DNA
Conditions for occurrence	Low- humidity environment	Physiological conditions	Under the presence of high salt, certain divalent cations.
Helix sense	Right	Right	Left
Residues per turn	11	10	12
Axial rise (nm)	0.255	0.34	0.37
Diameter of the helix (nm)	0.23	0.20	0.18

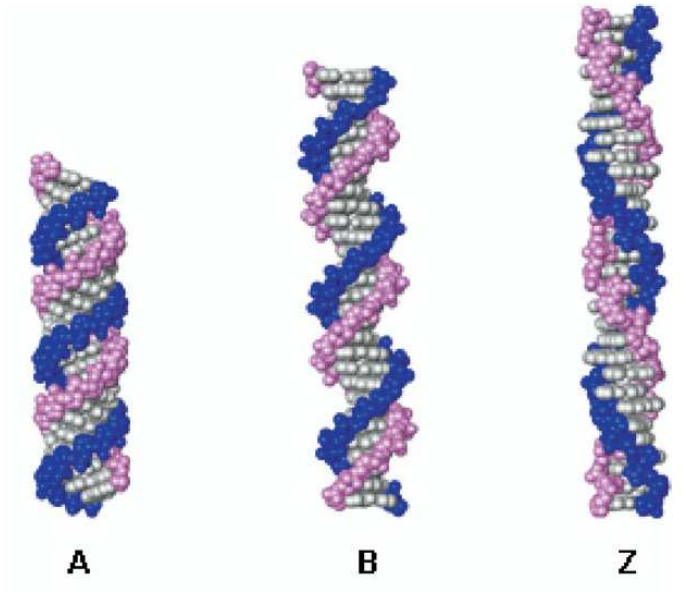

Figure 3.3. A, B and Z- conformations of DNA. In blue and pink each of the strands. The bases are coloured in gray. [7]

DNA conformations can be determined with circular dichroism (CD) spectroscopy [7 – 11]. The explanation of this technique can be read in section 4.2.2. The typical CD spectra for each of these conformations are shown in figure 3.4.

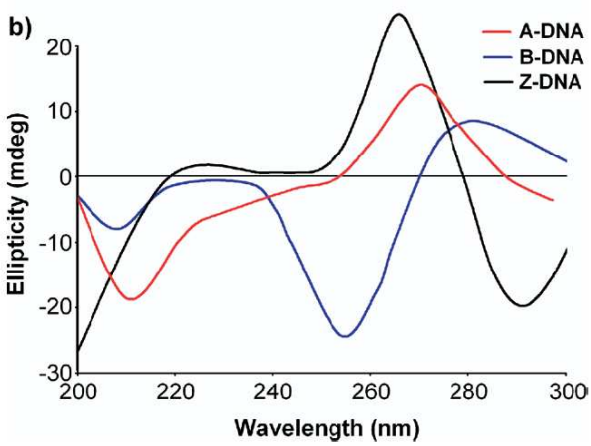

Figure 3.4. CD spectra of A, B and Z-conformations. [7]

Single stranded (denatured) DNA does not have a helix conformation, thereby the intensity measured in CD spectroscopy of a DNA denatured by the action of an organic solvent, i.e. an alcohol, is widely reduced, as observed in figure 3.5.

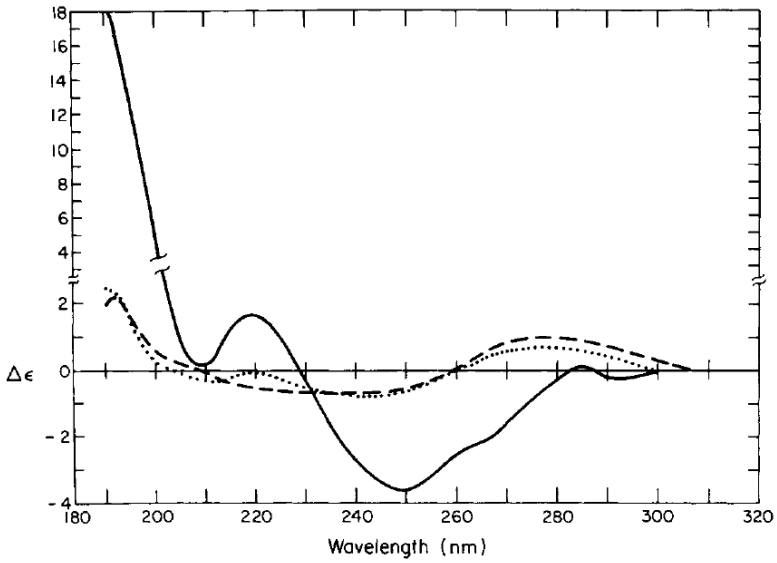

Figure 3.5. CD spectra of double stranded DNA in 95% methanol, 5% water at 8°C (——), of denatured DNA in 95% methanol, 5% water at 33°C (- -), and DNA in 47.5% methanol, 5% water and 47.5% ethanol at 8°C (P-form) (····) [12].

3.2. Formation of DNA complexes in aqueous solution

In aqueous solutions, DNA can interact electrostatically with multivalent cations, mono- or multivalent surfactants and with polycations. Given that the DNA bases (repeating units) are hydrophobic at a pH=7, also hydrophobic interactions may play a role for binding DNA. Following, the structures of the complexes formed with each of the cations mentioned before will be described.

Most of the DNA complexes have been formed in aqueous solutions, mainly due to two reasons: a) DNA is only soluble in water and b) The majority of the complexes have been prepared for transfection. In this work, the complexing agents have been divided into three groups: 1) multivalent cations, 2) surfactants and 3) polycations.

3.2.1. Formation of complexes with multivalent cations

It has been experimentally observed that 89% of the DNA charges must be neutralized in order to condense DNA. Therefore, only cations with at least three charges are used to complex this polyanion [3, 13, 14, 15, 16]. These cations with three or four charges are generally referred as multivalent cations. The first condensing agents used for DNA binding are the polyamines spermidine (3+) and spermine (4+) (see Figure 3.6).

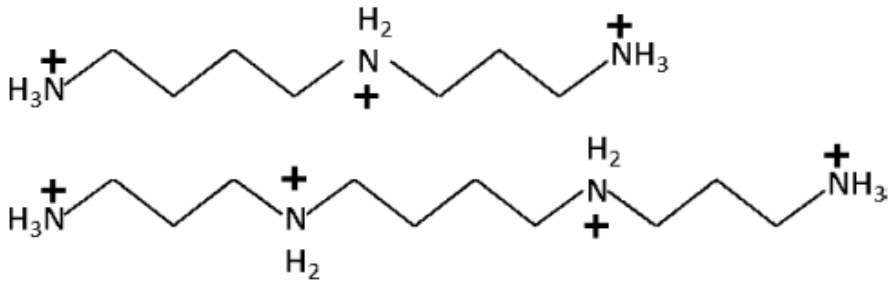

Figure 3.6. Structure of the condensing agents spermidine and spermine. [17]

3.2.1.1. Topology of DNA complexes with multivalent cations

Many studies of the interaction between these multivalent cations and DNA have revealed that toroids are the main structures upon complexation. The size of the toroids seems to be independent of the molecular weight of the DNA, typically between 40 and 50 nm of outer radius and between 14 and 20 of inner radius. Rods are also found within the complexes with dimensions around 230 – 240 nm long and 20 – 30 nm wide [13, 18, 19, 20, 21] (see figure 3.7). These structures are normally not composed of only one but of several DNA molecules. Furthermore, some rods and toroids seem to be connected, forming large structures (see section 1)

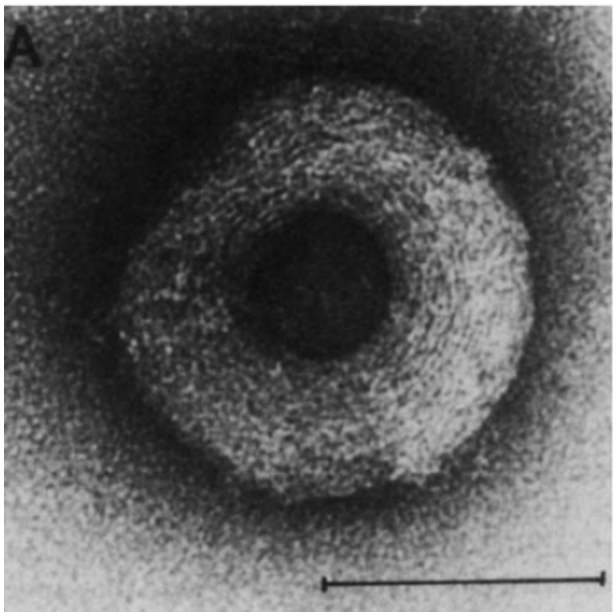

Figure 3.7. Electron micrographs of DNA with 200 μM spermidine at 2 hours [22]. The scale bar corresponds to 100 nm.

Also the inorganic ion hexamine cobalt ($Co(NH_3)_3^{6+}$) has been used as condensing agent. The final topology of the complexes with this trivalent cation is similar to the one for spermidine and spermine [22].

3.2.1.2. Equilibrium of DNA complexes with multivalent cations

Only a part of the polyamines in solution are able to bind DNA. An equilibrium is established with binding constants in the order of $1.9x10^4$ M^{-1} and $6.4x10^4$ M^{-1} for spermidine and spermine, respectively [23]. At a charge ratio (N+/P-) close to one, precipitation takes place. An excess of the polyamines causes of reentrant of the complexes in solution. The reasons for this issue are still a matter of discussion.

3.2.1.3. Conformation of DNA complexes with multivalent cations

As mentioned in section 3.1.2, the DNA helix could have different conformations according to the surrounding environment, i.e. left of right-handed, different amount of bases per turn and distances per base. The most common conformation found in biological systems is the B-conformation composed of 10.4 base pairs per turn and 0.34 nm per base pair. However, for some processes, a shift in DNA conformation is required, for instance to the Z-conformation. The conformation of DNA can be elucidated by means of circular dichroism (CD) spectroscopy.

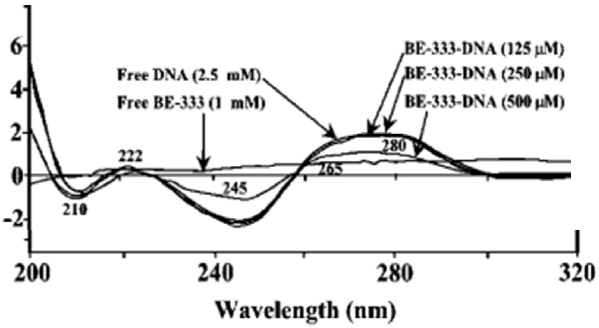

Figure 3.8. Changes of DNA conformation upon formation of complexes with spermine (BE-333). In the y-axis the CD signal is plotted. The concentration of DNA is 2.5 mM and the pH = 7.2. [23]

It has been reported that DNA preserves the B-conformation upon formation of complexes with the polyamines [17]. Nevertheless, some researchers have reported a transition between the A and B conformations of DNA. N'soukpoé-Kossi, C. et al [23] (see figure 3.8).

3.2.2. Formation of DNA complexes with surfactants

As mentioned earlier, multivalent cations with at least three charges are necessary to condense DNA. However, monovalent surfactants can also condense DNA due to hydrophobic interaction among the tails of neighboring bounded surfactants.

3.2.2.1. Topology of DNA complexes with surfactants

3.2.2.1.1. DNA complexes with alkyltrimethylammonium surfactants.

DNA molecules in solution present a linear, open-circular or supercoiled conformation. For sufficiently high concentrations of surfactant, the DNA molecules undergo compaction. In other words, DNA acquires a globular topology. At intermediate concentrations, a mixture of coil and globular conformations can be observed. This compaction arises from the neutralization of the DNA charges, i.e. the intramolecular electrostatic repulsions are diminished, and from the hydrophobic interactions of the bounded surfactants [24].

3.2.2.1.2. DNA complexes with vesicles

Most of the actual commercial cationic agents used for gene transfection are double-tailed surfactants with a low solubility in aqueous solutions. These surfactants form in general vesicles and the formulations recommended by the manufacturers usually imply the interaction of these vesicles with DNA. One of the most studied surfactants in this sense is DOTAP. Researchers have found that the addition of DOTAP to

DNA in aqueous solution results in ill-defined topologies [25]. However, the reversal of the order of mixing results in DNA surrounding DOTAP vesicles at high N+/P- charge ratios (at least N+/P- = 2). [26]. In figure 3.9, the TEM images of DNA after the addition of DOTAP is shown.

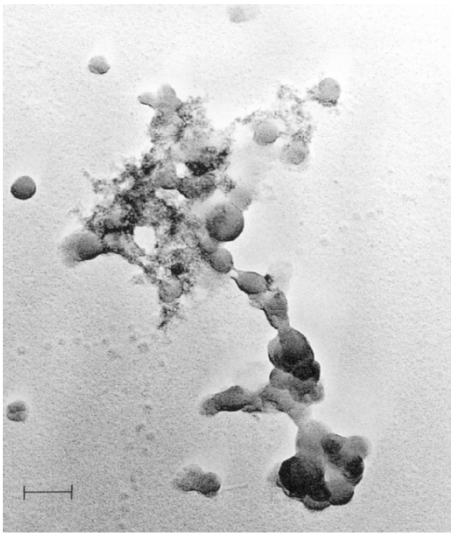

Figure 3.9. Negative stain TEM pictures of (a) DOTAP added to DNA at a charge ratio of N+/P- = 0.7 [25]. Bars represent 100 nm.

3.2.2.2. Equilibrium of DNA complexes with cationic surfactants

As stated in section 2.1.1, the binding of surfactants to an oppositely-charged polyelectrolyte is cooperative, due to hydrophobic interactions. Thereby, the surfactant with longer tail, is more efficient for the DNA binding [27]. This behavior can be observed in figure 3.10. In this work, the conditions under DNA precipitate in aqueous solutions are needed. These precipitates are used as precursor for the formation of DNA complexes in organic solvents

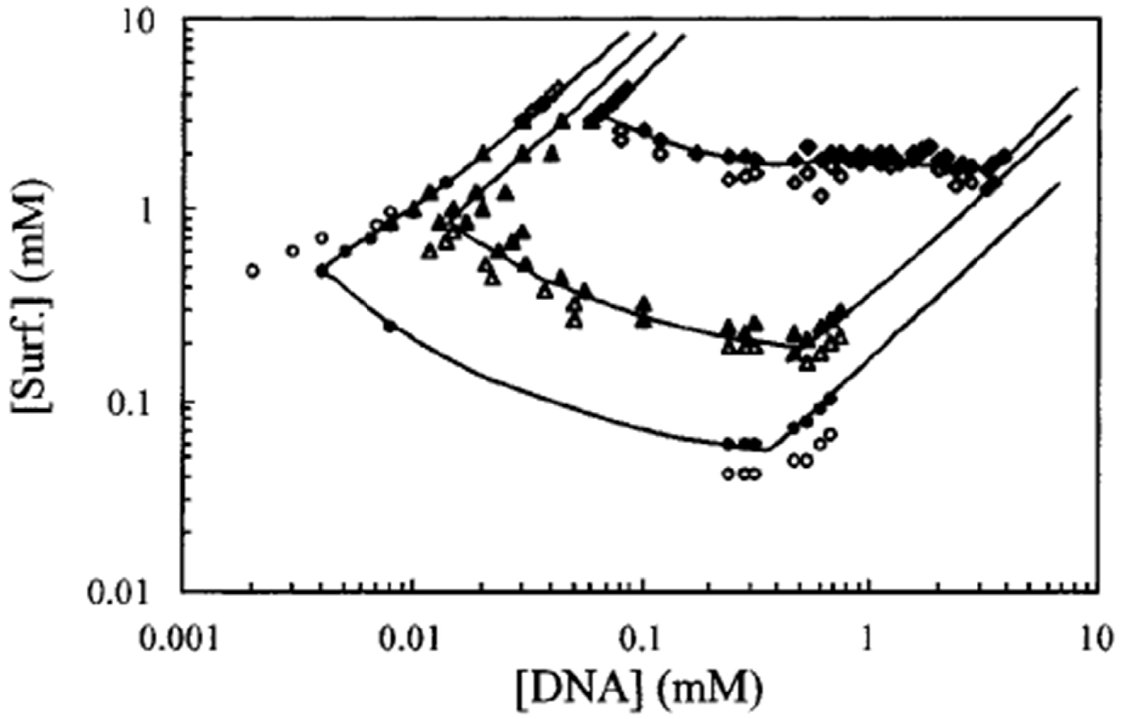

Figure 3.10. Phase diagram of the system DNA-CTAB-water (diamond), DNA-TTAB-water (triangle) and DNA-DTAB-water (circle) systems in the presence of NaBr 0.01 M. Open symbols refer to the clear one-phase solutions and filled symbols to two-phase samples. T = 25 °C. The phase map is represented in logarithmic scale for better visualization [27].

For the system DOTAP (vesicles) and DNA in aqueous solution, it is always assumed that a complete binding of the components take place given the large hydrophobic interactions among the double-tailed surfactants.

3.2.2.3. Conformation of DNA complexes with surfactants.

To the knowledge of the authors, the conformation of DNA upon binding with n-alkyltrimethylammonium surfactants has not been reported. In this work (chapter 6), it is demonstrated that the B-form is preserved in this kind of complexes.

3.2.3. Formation of DNA complexes with polycations.

Several studies have demonstrated that formation of DNA complexes with polycations are driven by a kinetically controlled process [28, 29]. In other words, the rate of complex formation is higher than the rate of formation of equilibrium structures. Störkle et al studied the binding of a supercoiled DNA with polycations with several starting topologies. The complexes were imaged with Atomic Force Microscopy (AFM) and the structures visualized consisted of the typical flower-like or scramble egg structures presented in chapter 2.2. (see figure 3.11).

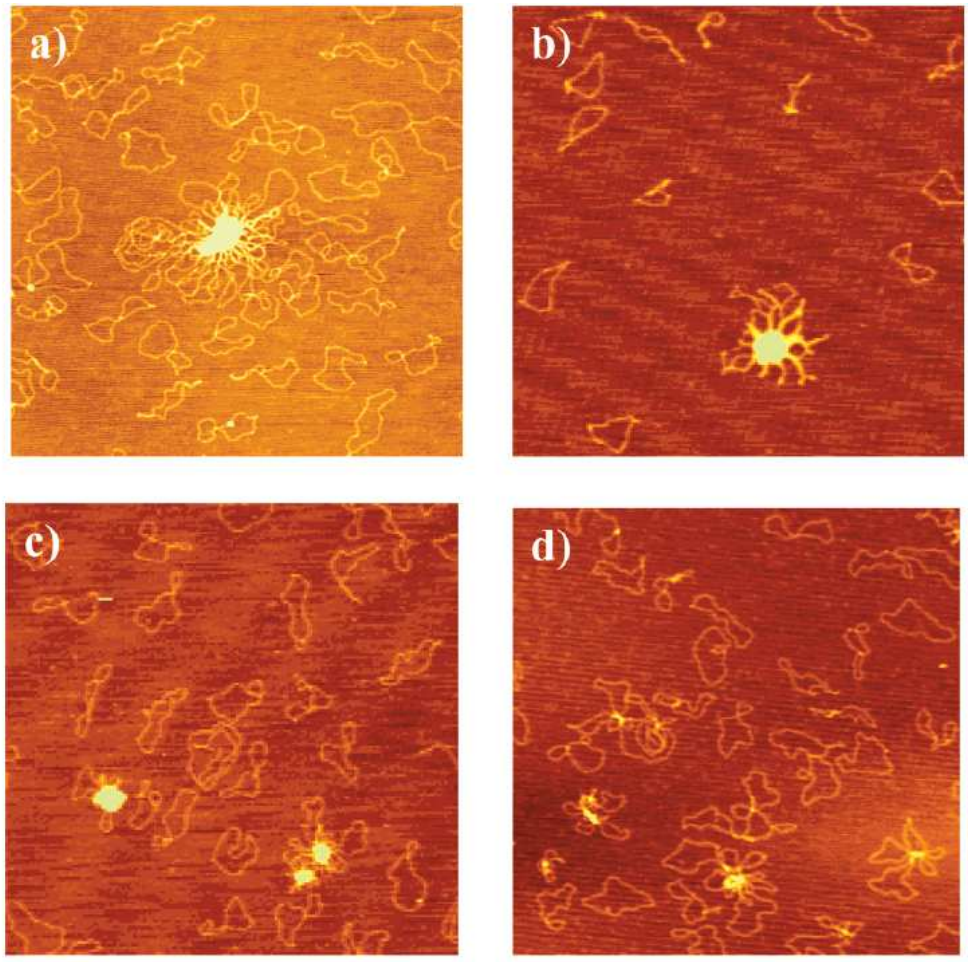

Figure 3.11. AFM pictures of various DNA/polycation complexes: (a) DNA/PVP26 complexes; (b) DNA/ PVP47 complexes; (c) DNA/PEI complexes; (d) DNA/PAMAM complexes. The size of all AFM pictures is 2 x 2um [29]

3.3. Formation of DNA complexes in organic solvents

3.3.1. Topology of DNA-surfactant complexes in organic solvents.

Only very a few studies have addressed the problem of the topology of DNA complexes in organic solvents. In all of the cases, DNA has been bound to surfactants in order to create a polyanion with a hydrophobic surface. Two complementary models about the mechanism of dissolution of DNA-surfactant complexes have been proposed in the literature.

Kabanov et al. [30] prepared complexes between the surfactant dioctadecyldimethylammonium chloride (DODAC) and DNA. Precipitation was observed at charge stoichiometry. The solid was freeze-dried and dissolved in chloroform. The complexes were characterized by means of ultracentrifugation, viscosity measurements, and other techniques. The authors concluded that DNA-DODA complexes are soluble in chloroform and show a compacted topology. In general, PE-surf complexes in organic solvents show an expanded conformation in organic solvents, which is typical polymers (or their complexes) in a good solvent (see figure 3.12). The authors explained that DNA-DODA complexes undergo compaction probably due to the inherent compacted conformation of the DNA despite the rigidity of the helical structure. In order words, DNA is a prestressed elastic rod tending to compaction.

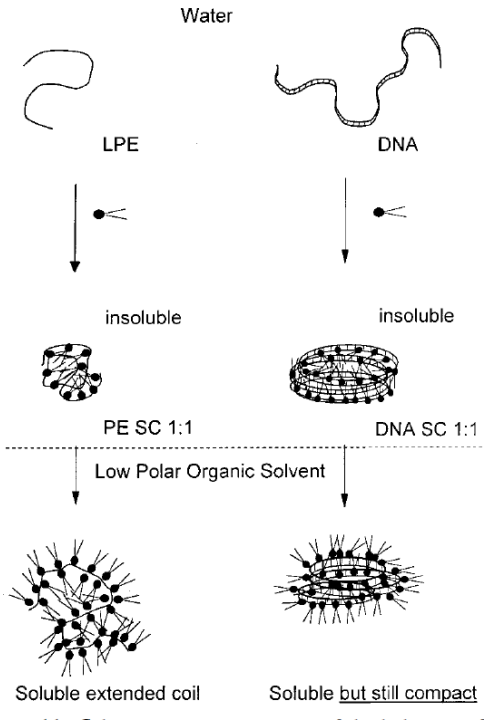

Figure 3.12. Comparison of the behavior of DNA and an ordinary polyelectrolyte after interaction with a surfactant and transfer from water to an organic solvent. [30]

On the other hand, Sergeyev et al. [31] elucidated the mechanism by which alcohol dissolve DNA-cetyldecyltrimethylammonium (CTA) complexes by using mixture of water and ethanol or 2-propanol as solvents. With fluorescent microscopy, the authors visualized globule structures in aqueous solutions, coil structures in mixtures between 40 - 60% v/v water / ethanol and 30 - 50% v/v water / 2-propanol and again globule structures at higher concentration of the alcohols. It was explained that the intermediate mixture of water and alcohol are good solvents for the complexes but an increase of the alcohol content causes the surfactant to partly dissociate and therefore the complexes undergo compaction although they are still in a good solvent (see figure 3.13)

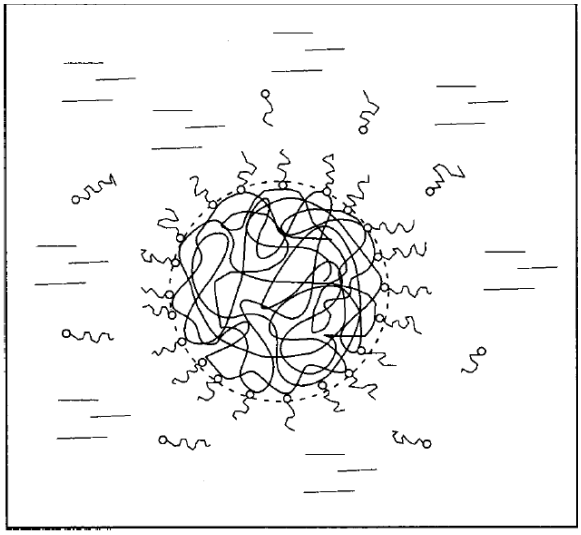

Figure 3.13. Schematic representation of DNA-CTAB complexes in a water/alcohol solution. [31]

3.3.2. Equilibrium of DNA-surfactant complexes in organic solvents

In spite of the indirect observations of partial dissociation of the surfactants in organic solvents by Sergeyev et al. [31], the equilibrium of the surfactants between the bounded and the free states has not been reported.

3.3.3. Conformation of DNA-surfactant complexes in organic solvents.

Kabanov et al. [30] have postulated that DNA-DODA complexes in chloroform possess a C conformation, typical of the dehydrated molecule. However, the CD spectrum was described but not shown. Sergeyev et al. [31] affirmed that the double-helical structure is preserved and that DNA maintain the B conformation at intermediate concentrations of alcohol (35% v/v) but the conformation is shifted towards the A conformation with an alcohol content of 90% v/v (figure 3.14). Tanaka et al. [32] dissolved DNA complexes with lipids consisting of a trimethylammonium head with a radical consisting of blocks of ethylene oxide oligomers and alkyl chains. The CD spectrum after dissolution of complexes in a

mixture of chloroform/ethanol (4:1) revealed a C-conformation. In general, it is accepted that DNA under "dehydration" conditions undergoes a transition from a B to a C or an A conformation.

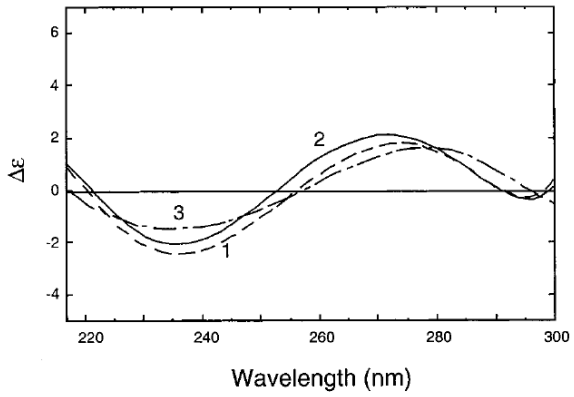

Figure 3.14. CD spectra of (1) DNA in TE buffer, (2) DNA-cetyltrimethylammonium complexes (DNA-CTAB) in 35 % v/v 2-propanol, and (3) DNA-CTAB in 90% v/v 2-propanol [31]

3.4. References

1. Sinden, R. DNA structure and function. Academic Press, 1994.
2. Watson, J.; Baker, T.; Bell, S.; Gann, A.; Levine, M.; Losick, R. Molecular Biology of the Gene. Pearson Education Inc., 2004.
3. Dias, R.; Lindman, B. DNA Interactions with Polymers and Surfactants. John Wiley & Sons, 2008.
4. Berova, N.; Nakanishi, K.; Woody, R. Circular Dichroism. Principles and Applications. Wiley-VCH, 2000.
5. Li, Y.; Yildiz, U.; Muellen, K.; Gorehn, F. Biomacromolecules, 2009, 10, 530 – 540.
6. Boles, T.; White, J.; Cozzarelli, N. J. Mol. Biol. 1990, 213, 931 – 951.
7. Shammel Baker, E.; Bowers, M. J. Am. Soc. Mass. Spectrom., 2007, 18, 1188 – 1195.
8. Kypr, J.; Vorlícová, M. Biopolymers, 2002, 67, 275 – 277.
9. Baase, W.; Johnson, W. Nucleic Acids Research, 1979, 2 (6), 797 – 814.
10. Jaumot, J.; Eritja, R.; Navea, S.; Gargallo, R. Analytica Chimica Acta, 2009, 642, 117 – 126.
11. Brahms, J.; Mommaerts, W. J. Mol. Biol., 1964, 10, 73 – 88.
12. Zhefus, M.; Jhonson, C. Biopolymers, 1981, 20, 1589 – 1603.
13. Bloomfield, V. Biopolymers **1997**, 3, 269-282.
14. Murayama, Y.; Sakamaki, Y.; Sano, M. Phys. Rev. Lett. 2003, 90(1), 018102 (4 pages).
15. Budker, V.; Trubetskoy, V.; Wolff, J. Biopolymers, 2006, 83, 646 – 657.
16. He, S.; Arscott, P.; Bloomfield, V. Biopolymers **2000**, 53, 329 – 341

17. Shao, Q.; Goyal, S.; Finzi, L.; Dunlap, D. Macromolecules **2012**, 45, 3188 – 3196
18. Arscott, P.; Li, A.; Bloomfield, V. Biopolymers, 1990, 30, 619 – 630.
19. Patel, M.; Anchordoquy, T. Biophysical Journal. 2004, 88 (3), 2089 – 2103
20. Grossberg, A.; Zhestkov, A. Journal of Biomolecular Structure and Dynamics, 1985, 3 (2), 515 – 520.
21. Marx, K.; Ruben, G. Journal of Biomolecular Structure and Dynamics, 1986, 4(1), 23 – 39.
22. Plum, G.; Arscott, P.; Bloomfield, V. Biopolymers, 1990, 30, 631 – 643.
23. N'soukpoé-Kossi, C.; Ahmed Ouameur, A.; Thomas, T.; Shirahata, A.; Thomas, T.; Tajmir-Riahi. Biomacromolecules 2008, 9, 2712 – 2718.
24. Dias, S.; Magno, L.; Valente, A.; Das, D.; Das, P.; Maiti, S.; Miguel, M.; Lindman, B. 2008, 112, 14446 – 14452
25. Birchall, J.; Kellaway, I.; Mills, S. International Journal of Pharmaceutics, 1999, 183, 195 – 207.
26. Sennato, S.; Bordi, F.; Cametti, C.; Diociaiuti, M.; Malaspina, P. Biochimica et Biophysica Acta, 2005, 1714, 11 – 24.
27. Dias, R.S.; Innerlohinger, J.; Glatter, O.; Miguel, M.; Lindman, B. J. Phys. Chem. B 2005, 109, 10458 – 10463.
28. Lai, E.; van Zanten, J. Biophysical Journal, **2001**, 80, 864 – 873
29. Störkle, D.; Duschner, S.; Heimann, N.; Maskos, M.; Schmidt, M. Macromolecules, 2007, 40 (22), 7998 – 8006.
30. Sergeyev, V.G.; Pyshkina, O. A.; Lezov, A. V.; Mel'nikov, A.B.; Ryumtsev, E. I.; Zezin, A. B.; Kabanov, V. A. Langmuir, 1999, 15: 4434 – 4440
31. Sergeyev, V. G.; Mikhailenko, S. V.; Pyshkina, O. A.; Yaminsky, I. V.; Yoshikawa, K. J. Am. Chem. Soc, 1999, 121: 1780 – 1785.
32. Tanaka, K.; Okahata, Y. J. Am. Chem. Soc, 1996, 118(44), 10679 – 10683.

4. Techniques for characterization of DNA complexes

4.1. Light Scattering.

4.1.1. Principles of Light Scattering

Matter is composed by atoms. These atoms at the same time consist of protons and electrons carrying positive and negative charges, respectively. Let the light interact with the matter and the cloud of electrons surrounding the nucleus is deformed forming a dipole, meaning that a displacement of the spatial average of the positively charged nuclei with respect to the negatively charged electrons takes place, as shown in Figure 4.1. Since the light consists of electromagnetic waves, the induced dipole oscillates and acts as well as a source of light emission.

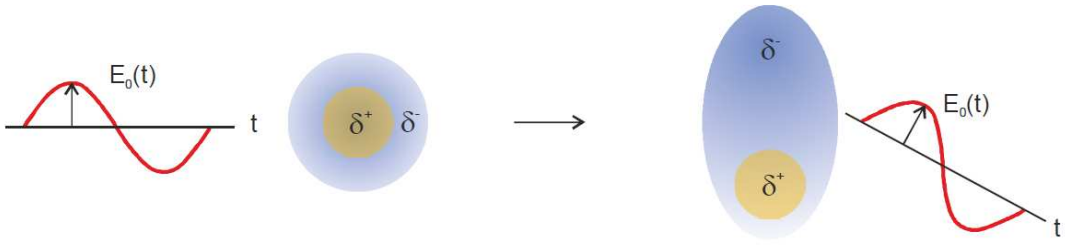

Figure 4.1. Interaction of electromagnetic waves with matter and induction of a dipole [1]

This phenomenon is called light scattering and because it depends on the dynamics and the structure of the molecules, it is used for characterization of nanoparticles. The technique of light scattering can be used in two different ways: 1) In the case that only the average intensity at a given angle is considered, the technique is called Static Light Scattering (SLS) and the weight-averaged molar mass, the so-called radius of gyration and the second virial coefficient (A_2) can be determined; 2) If the fluctuation of the scattering intensity, caused by the Brownian motion of particles in solution, is measured, the diffusion

coefficient and therefore the hydrodynamic radius of these particles can be extracted from the data analysis. This technique is referred as Dynamic Light Scattering (DLS). In Figure 4.2 the intensities measured in each technique is plotted. Following, the two light scattering techniques will be explained in more detail.

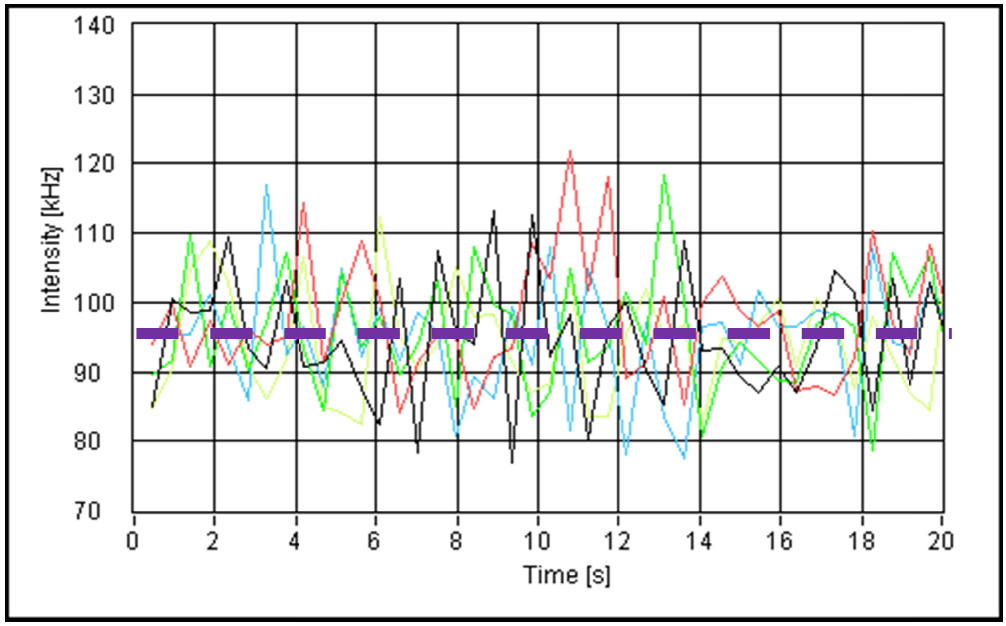

Figure 4.2. Average intensity (purple dashed line) and intensity fluctuations (green, yellow, blue and red straight lines) measured in SLS and DLS respectively for DNA pUC19 c=0.05 g/l in a light scattering equipment using a red laser with λ = 632 nm

4.1.2. Static Light Scattering

As mentioned above, in SLS the average scattering intensity is measured. Since this intensity depends on the molar mass, shape and concentration of the particles in a solution, it allows obtaining information of these particles. Next, the description of this technique will be presented in increasing order of sample complexity

4.1.2.1. SLS of small monodisperse samples

If a particle solution, i.e. a polymer, is considered to be separated by its solvent through a membrane impermeable to the polymer, an osmotic pressure is developed (see Figure 4.3).

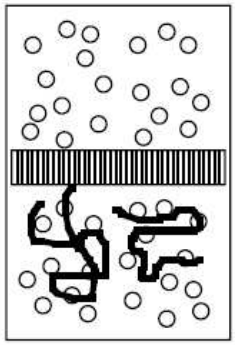

$$\frac{d\Pi}{dc} = RT\left(\frac{1}{M} + 2A_2c + \ldots\right)$$

Figure 4.3. Schematic representation of a nonideal polymer solution separated from the solvent by a semipermeable membrane [2].

Given that n moles of the particle are enclosed in a volume V at a T temperature, the magnitude for the originated osmotic pressure π can be determined by the Van't Hoff's law

$$\pi V = nRT \tag{4.1}$$

If non-idealities are considered a virial coefficient (A_2) must be added into the equation

$$\frac{\pi}{c} = \left(\frac{RT}{M}\right)(1 + A_2cM + \cdots) \tag{4.2}$$

From a thermodynamics point of view, light scattering can be explained in terms of the light scattered by the particles undergoing concentration fluctuations or gradients caused by the thermal energy available. If

the particle is in a good solvent, it is surrounded mainly by solvent and not by other particles, which causes a large osmotic pressure with the surroundings. Thus, the particle "takes" a lot of osmotic pressure to remain in a "not crowded" (not aggregated) state. The magnitude of the $(\partial\pi/\partial c)_T$ modulus is large. Particles that attract to each others, for example, particles in a bad solvent, do not "feel" a large osmotic pressure since they are kept relative together. In other words, particles undergoing large concentration fluctuations, and therefore possessed a large scattering intensity, are responsible for osmotically "stiff" with a low $(\partial\pi/\partial c)_T$. Osmotically compressible molecules, with a large $(\partial\pi/\partial c)_T$, scattered the light weaker. From this relationship, it can be concluded that the static scattering intensity of small particles in a very dilute solution (in order to avoid intermolecular scattering) depends on the contrast factor K, their mass concentration c and the osmotic pressure π, as follow:

$$I \sim KkT \frac{c}{\left(\frac{\partial \pi}{\partial c}\right)_{T,N}} \tag{4.3}$$

The factor "K" is related to the Rayleigh mechanism of scattering. All of the scattering techniques depend on a contrast factor K, which account for the difference in a certain property with respect to the solvent. In the case of light scattering, a difference in the refractive index between the sample and the solvent is required. Mathematically, the contrast factor K is expressed as

$$K = \frac{4\pi^2}{{\lambda_0}^4 N_L} {n_{D,0}}^2 \left(\frac{\partial n_D}{\partial c}\right)^2 \tag{4.4}$$

Where

λ_0 is the wavelength of the incident light.

$n_{D,0}$ is the refractive index of the solvent

N_L is the Avogadro number

$\left(\frac{\partial n_D}{\partial c}\right)$ is the change of refractive index of the solution with the concentration of the solute

It is important to notice that if the refractive indexes of the solvent and the solute are identical, the factor $\left(\frac{\partial n_D}{\partial c}\right)$ gets equal to 0.

The intensity of the light scattered (I) varies according to the equipment used, since parameters, for instance the sample-detector distance, may be different. In order to avoid ambiguity and to be able to compare measurements being carried out with different experimental set-up the Rayleigh ratio, R, instead the scattered intensity is used. The solvent also contributes to the total scattered intensity, and therefore it must be subtracted from the intensity of the solution. By substituting the values of contrast factor K and the osmotic pressure π (for ideal solutions), a final equation for R is given by

$$R = KcM = \frac{4\pi^2}{{\lambda_0}^4} {n_{D,0}}^2 \left(\frac{\partial n_D}{\partial c}\right)^2 \frac{cM}{N_L} = (I_{solution} - I_{solvent}) \frac{{r_D}^2}{V} \qquad (4.5)$$

Where

r_D: sample-detector distance

V: scattering volume

In practice, the intensity of a standard solvent I_{std}, usually toluene, is measured and renormalized by the absolute intensity of this standard $I_{std,abs}$.

$$R = (I_{solution} - I_{solvent}) \frac{I_{std,abs}}{I_{std}} \qquad (4.6)$$

Finally, for non ideal solutions with $A_2 \neq 0$, equation 4.2 is substituted in equation 4.3 and equation 4.5 can be rewritten to yield the basic equation for static light scattering experiments on solutions of small particles:

$$\frac{Kc}{R} = \frac{1}{M} + 2A_2 c + \cdots \qquad (4.7)$$

In expression 4.7, it is assumed that every particle acts as one and only one scattering center and therefore its validity is restricted to particles smaller than λ/50. For larger particles, the scattering intensity I depends on the angle of measurement and therefore a factor to account for the different scattered centers within a molecule (and hence its topology) must be included, as explain in the next section.

4.1.2.2. SLS of large monodisperse samples.

For particles with a radius larger than λ/20, more than one scattering center is found within a molecule, as demonstrated in Figure 4.4.

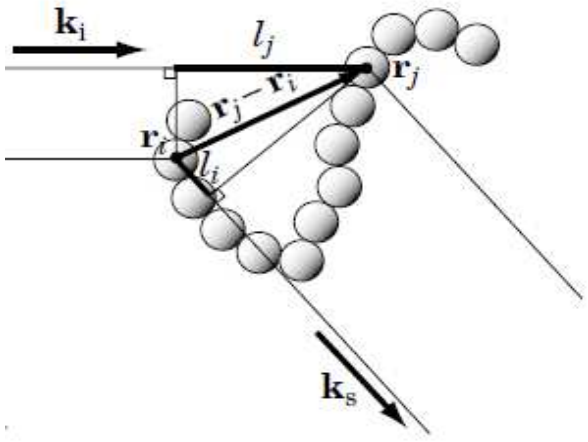

Figure 4.4. Interference of scattering centers. Note that "k" instead of "q" is used to denote the scattering vector [3].

In this case, the scattering intensity depends on the angle of measurement, θ, i.e. the angle between the incoming light and the detector (see Figure 4.5). The length scale of this technique is then defined by the vector q, which is given by the subtraction of the incident and the scattered light vectors.

(4.8)

$$\boldsymbol{q} = \boldsymbol{k_s} - \boldsymbol{k_i}$$

The magnitude of q can be calculated as

$$q = \frac{4\pi n_{sol}}{\lambda} sin\frac{\theta}{2} \quad (4.9)$$

q scattering vector

k propagation of vector (s) scattered and (i) incoming light

n_{sol} index of refraction of the solvent

θ scattering angle

λ wavelength of incoming light

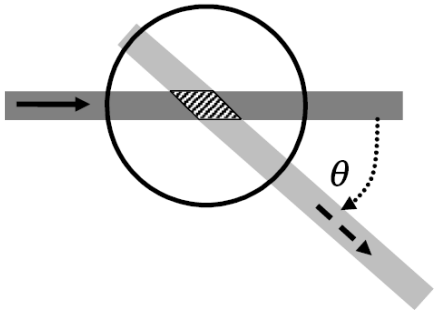

Figure 4.5. Definition of the scattering angle [4].

The vector q allows defining a factor, P(q), which considers the multiple scattering centers within a molecule.

$$P(q) = 1 - \frac{1}{3}\langle s^2 \rangle q^2 + \cdots \quad (4.10)$$

Its demonstration is beyond the scope of this work, but could be found elsewhere [4]. Since this for factor is derived from a series of Taylor interrupted after the second term, it can only be used for particles with a radius smaller than 50 nm. For larger particles, specific form factors according to the examined topology (i.e. sphere, disk, and so on) can be used. In the case of lack of information with respect to the possible topology of the particles, different form factor should be fitted and the best fit will give an idea of the shape of the molecules.

Note that $\langle s^2 \rangle$ is squared average of the so-called radius of gyration and represents squared the distance vector between the center of mass and each of the "i" scattering centers within a particle, normalized by total amount of scattering centers Z.

$$< s^2 >= \frac{1}{Z} \sum {s_i}^2 \tag{4.11}$$

The form factor P(q) is introduced in equation 4.7 as follows

$$\frac{Kc}{R} = \frac{1}{MP(q)} + 2A_2 c + \cdots \tag{4.12}$$

which gives the so-called Zimm equation

$$\frac{Kc}{R} = \frac{1}{M}\left(1 + \frac{1}{3}\langle s^2 \rangle q^2\right) + 2A_2 c \tag{4.13}$$

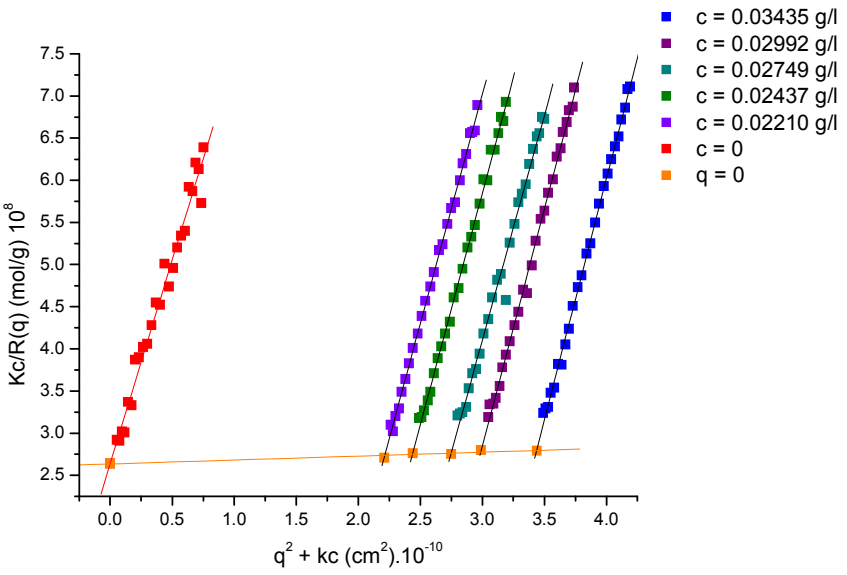

Figure 4.6. Example of the Zimm Plot of DNA-DTA complexes in DMF measured at angles from 30 to 150° in steps of 5° at 20°C

If the concentration is extrapolated to c→0, the equation 4.13 is transformed to

$$\frac{Kc}{R} = \frac{1}{M}\left(1 + \frac{1}{3}\langle s^2\rangle q^2\right) \tag{4.14}$$

From the intercept 1/M, the molecular weight could be obtained and from the slope, the radius of gyration "s" (also called Rg), can be calculated.

If q^2 is extrapolated towards zero, the Zimm equation takes the form

$$\frac{Kc}{R} = \frac{1}{M} + 2A_2c \tag{4.15}$$

And the intercept should also give 1/M. In practice the intercepts of the expressions 4.14 and 4.15 should be equal and this condition is taken as one of the criteria for the validity of the static light scattering measurements. The slope gives information about the second virial coefficient A_2. (see Figure 4.6)

4.1.2.3. SLS of polydisperse samples

Until now, it has been discussed how to obtain information from "small" and "large" monodisperse samples with static light scattering. This information is useful, for instance, for DNA pUC19, a monodisperse DNA used in this work. However, synthetic polymers or DNA-complexes, like the ones prepared in this research, are usually polydispersed. In this case, the molar mass obtained by static light scattering is a weight-averaged molecular weight.

If c→0 and q→0, Zimm equation is given by

$$\langle M \rangle = \frac{R}{Kc} \tag{4.16}$$

Since the total static intensity R is given by the sum of the intensities of each of the "i" particles and the total concentration is also given by the sum of all of "n" the particles, then

$$\langle M \rangle = \frac{\sum_{i=1}^{n} R_i}{K \sum_{i=1}^{n} c_i} \tag{4.17}$$

The contribution of each of the "i" particles to the total scattering intensity can be expressed as

$$R_i = K c_i M_i \tag{4.18}$$

Rearranging equation 4.17 it can be shown that

$$\langle M \rangle = \frac{\sum_{i=1}^{n} K c_i M_i}{K \sum_{i=1}^{n} c_i} = \frac{\sum_{i=1}^{n} m_i M_i}{\sum_{i=1}^{n} m_i} = \frac{\sum_{i=1}^{n} n_i {M_i}^2}{\sum_{i=1}^{n} n_i M_i} = Mw \quad (4.19)$$

Where m_i is the mass of each particle and is equal to $m_i=n_iM_i$. In static light scattering a weight-average molecular weight "Mw" is measured.

Similarly it can be proven, that the form factor $P_z(q)$ and radius of gyration Rg obtained for polydisperse samples with light scattering is a z-averaged.

$$P_z(q) = \frac{\sum n_i {M_i}^2 P_i(q)}{\sum n_i {M_i}^2} \quad (4.20)$$

$$\langle s^2 \rangle_z = \langle {R_g}^2 \rangle_z = \frac{\sum n_i {M_i}^2 \langle {s_i}^2 \rangle}{\sum n_i {M_i}^2} \quad (4.21)$$

In the case of a polymer, $P_z(q)$ and $<s^2>_z$ does not represent only an average over the different chains with different degree of polymerization but also an average over the conformation.

4.1.3. Dynamic Light Scattering (DLS)

The concentration of a solute varies microscopically in the solution, therefore the intensity of the light scattered fluctuates with the time I(t). These fluctuations can give information about the diffusion of the particles in solution and the technique of Dynamic Light Scattering (DLS) is based on this principle, as demonstrated below.

4.1.3.1. DLS of small monodisperse samples

A typical DLS measurement can be seen in Figure 4.7. In order to obtain information about the dynamics of a particle in solution, it is necessary to use a function that describes its movement, i.e. the probability of finding this particle at a position **r** at a time t+τ, if at a time t the same particle was located at a position of reference **0**. This function is called the van Hove self correlation G_s

$$G_s(\boldsymbol{r},\tau) = \langle n(\mathbf{0},t)n(\boldsymbol{r},t+\tau)\rangle \tag{4.22}$$

Here, n(**r**,t) is the local number density of scattering particles at a given time t.

For a particle undergoing a "random walk" motion, caused by concentration fluctuations in a solution due to the thermal density fluctuations of the solvent, the analytical solution is given as

$$G_s(r,\tau) = \left[\frac{2\pi}{3}\langle\Delta R(\tau)^2\rangle\right]^{3/2} exp\left(-\frac{3r(\tau)^2}{2\langle\Delta R(\tau)^2\rangle}\right) \tag{4.23}$$

Note that the vector r was replaced by the distance r. $\langle\Delta R(\tau)^2\rangle$ the mean square displacement of the scattering particle and it is given by

$$\langle\Delta R(\tau)^2\rangle = 6D_s\tau \tag{4.24}$$

The van Hove self correlation can be related to the fluctuation of the scattered light measured in DLS by its Fourier Transformation F_s

$$F_s(q,\tau) = \exp\left(-\frac{q^2\langle\Delta R(\tau)^2\rangle\tau}{6}\right) = \exp\left(-D_s q^2\tau\right) \tag{4.25}$$

$F_s(q,\tau)$ is indeed the autocorrelation function of the electric field

$$F_s(q,\tau) = \langle E_s * (q,t).E_s(q,t+\tau)\rangle \quad (4.26)$$

That means that the fluctuations of the electric field during a DLS measurement are correlated to each other through the equation 4.26. In other words, the electric field at given angle (or scattering angle q) and at a given time t is multiplied by itself but at a time t+τ. This τ is a variable and can take any value, from nanoseconds to seconds, within the time of measurement. These products are averaged over the whole measurement time and $F_s(q,\tau)$ can be obtained for each angle.

Unfortunately the electric field E(q,τ) cannot be directly measured with a light scattering equipment, only the fluctuations in the intensity of the scattered light can be detected through a detector (typically a photomultiplier). For this reason, the intensity and not the electric field is correlated.

$$I(q,\tau) = \langle I(q,t).I(q,t+\tau)\rangle \quad (4.27)$$

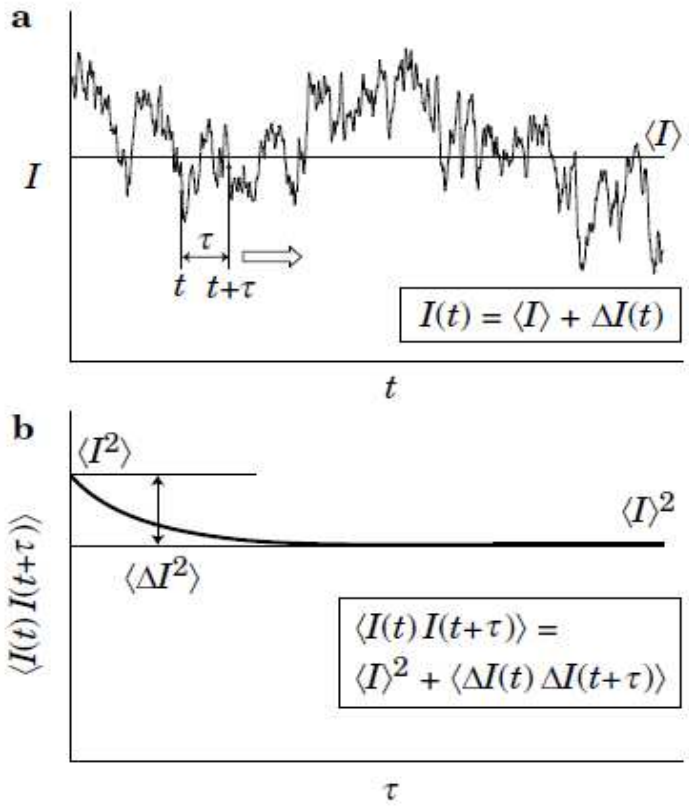

Figure 4.7. Example of (a) fluctuations of the intensity and (b) the corresponding autocorrelation function of the intensity [3].

The limits of this intensity autocorrelation function are given by

a. Upper limit: Full correlation. $\tau=0$

$$I(q,\tau) = \langle I(q,t).I(q,t)\rangle = \langle I^2\rangle \tag{4.28}$$

b. Lower limit: No correlation. $\tau\rightarrow\infty$

$$I(q,\tau) = \langle I(q,t).I(q,t)\rangle = \langle I\rangle^2 \tag{4.29}$$

In order to calculate the electric autocorrelation function *Fs(q, τ)* and subsequently the diffusion coefficient of the particles D_s, from the intensity autocorrelation function I(t), the following equation is used

$$F_s(q,\tau) = \exp(-D_s q^2 \tau) = \langle E_s * (q,t).E_s(q,t+\tau)\rangle = \sqrt{\frac{\langle I(q,t).I(q,t+\tau)\rangle}{\langle I(q,t)\rangle^2} - 1} \qquad (4.30)$$

This equation is called the Siegler relation and it is based on the fact that I=E.E*. *Fs(q, τ)* can be evaluated with different models, e.g. the exponential models used in this work.

By using the Stokes-Einstein, which describes the ratio between thermal and frictional forces, it is possible to calculate the hydrodynamic radius (Rh) of a particle

$$D_s = \frac{kT}{6\pi\eta R_H} \qquad (4.31)$$

Rh represents the radius of a spherical particle that "feels" the same friction than the particles measured with DLS. In other words, Rh is only an equivalent radius. Only by spherical particles represents Rh the actual radius of the particle with its hydration shell.

For small particles ($R < \lambda/20$), Ds and therefore Rh are independent of q.

It is important to notice that in this section the self-diffusion coefficient (Ds) has been derived. However, in light scattering this coefficient can only be measured for very dilute solutions. In general, in DLS the cooperative diffusion coefficient, Dc, which takes into account the "restrictions" or interactions with other molecules in the solution, is determined.

4.1.3.2. DLS of large and/or polydisperse samples

So far, we have only considered small and monodisperse particles. As in SLS, if the radius of the particles is larger than λ/20 or if the polydispersity cannot be neglected, the form factor P(q) needs to be taken into account. Hence Ds and Rh become q dependent, according to equation 4.32.

$$D_{app}(q) = \frac{\sum n_i {M_i}^2 P_i(q) D_i}{\sum n_i {M_i}^2 P_i(q)} \tag{4.32}$$

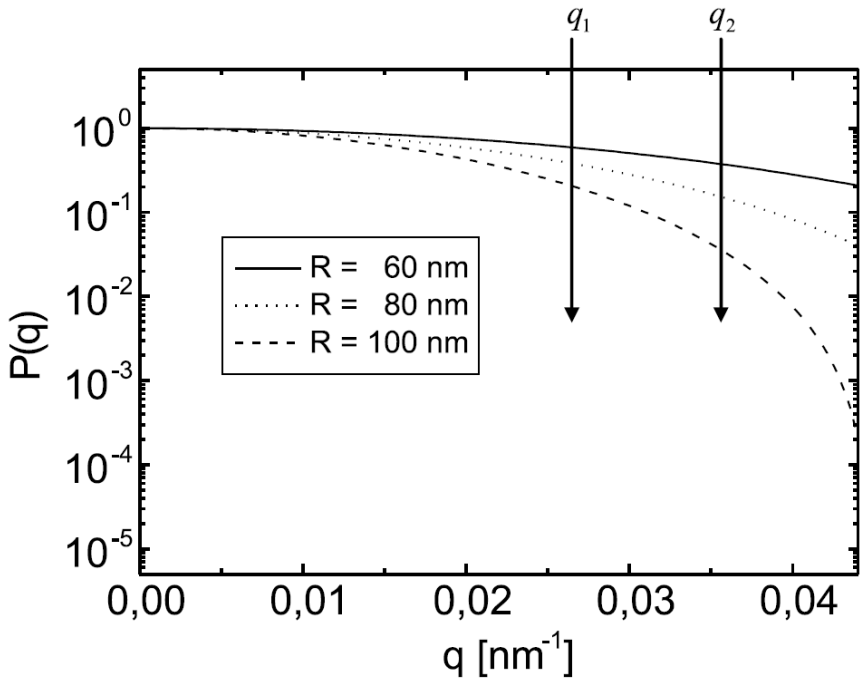

Figure 4.8. Decay of P(q) with the scattering vector q

Light scattering works as an "inverse" microscope. The length scale of the technique increases with a decrement of the vector q. In other words, details of the structure of a particle can be seen at high q while the overall particle can be seen at low q. The form factor P(q) decreases monotonically with q. The occurrence of interference leads to a weakening of the scattering intensity with increasing angle (see

Figure 4.8). For the same reason, the change of P(q) with the scattering vector q is more pronounced for larger particles.

The decrement of P(q) leads to an increment of Ds with q. As mentioned above, only at q→0, P(q)→1 and the true z-averaged diffusion coefficient can be obtained, as shown in Figure 4.9.

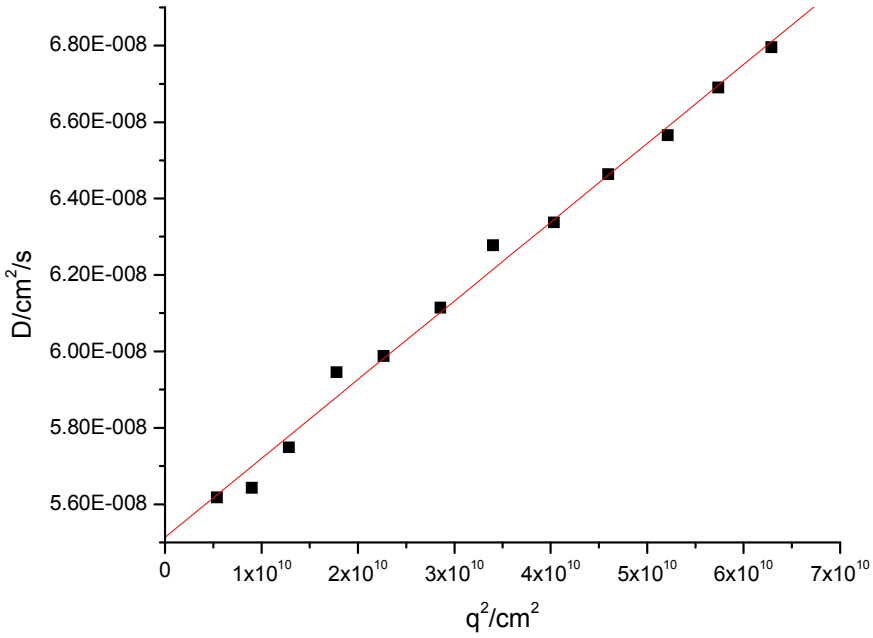

Figure 4.9. Example of angle dependency of the diffusion coefficient of a polydisperse polylysine brush in DMF measured at angles from 30° to 157° with a multiangle LS equipment composed of 8 detectors separated by 17° each.

Not only the polydispersity of a particle causes a q-dependency of Ds. The internal motions, i.e. the fluctuations without a displacement of the center of mass, of even monodisperse but large particles also produce a variation of the diffusion coefficient with the scattering angle, as in the case of the DNA pUC19 used in this work.

4.1.4. Investigation of the topology of a particle with light scattering

It is possible to determine the topology of a particle, e.g. sphere, disc, rod-like, among others, with SLS by fitting the form factor P(q) and selecting the best fit. However, if the sample is very complex or a lack of information does not permit the correct fitting of P(q), an estimation of the topology may be obtained with the ρ-ratio.

$$\rho = \frac{R_g}{R_h} \tag{4.33}$$

The different topologies are tabulated according to the ρ-ratio in Table 4.1.

Table 4.1. ρ-ratio for the most typical particle topologies[40]

Topology	ρ-ratio theory
Homogeneous sphere	0.775
Hollow sphere	1
Ellipsoid	0.775 – 4
Random coil, monodisperse, θ conditions	1.505
Random coil, polydisperse, θ conditions	1.73
Random coil, monodisperse, good solvent	1.78
Random coil, polydisperse, good solvent	2.05
Cylinder of length l, diameter D	$\frac{1}{\sqrt{3}}.ln\left(\frac{l}{D}-0.5\right)$

4.2. Circular dichroism (CD) spectroscopy

The CD spectroscopy is based on the same principles than UV-vis spectroscopy. The difference between these two techniques relies on the type of polarization of the source light. Whereas in UV-vis spectroscopy a linear polarized light is used, in CD spectroscopy a circular polarized light as light source is required.

A sample is irradiated with left and right circular polarized light and if the sample is optically active, the absorption will be difference for each of the direction of polarization. A different extinction coefficient is also expected and therefore the following equation holds

$$\Delta A = A_L - A_R = (\varepsilon_L - \varepsilon_R)cl \qquad (4.35)$$

with L and R denoting the left and right direction of the polarization. The circular dichroism is defined in terms of the difference in extinction coefficient ε_L-ε_R.

The circular dichroism is expressed in terms of the ellipticity. A ray of light entering in the sample is circular polarized. Since one of the directions will be absorbed stronger than the other one, it causes that the exiting ray of light is not longer circular but forms an ellipse. The light has been elliptically polarized. An ellipse is mathematically characterized by the angle θ = arctan (b/a), where b and a are the two axes of the ellipse (figure 4.11). This angle is defined as the "ellipticity" and it can be demonstrated that

$$\theta = 33\Delta A \qquad (4.36)$$

Most of the new instruments measured the difference in absorbance and contain an internal calibration for the ellipticity.

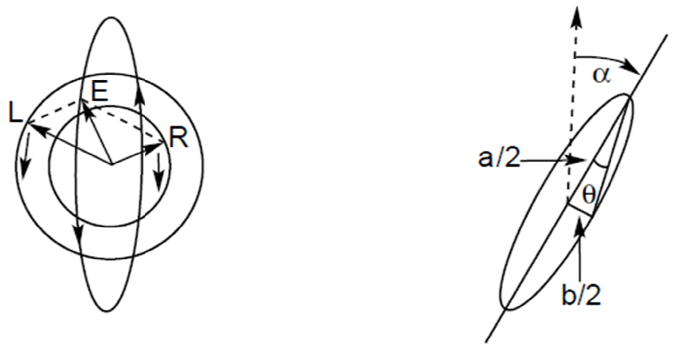

Figure 4.11. (a) Elliptically (E) polarized light due to the differences in absorption of left (L) and right (R) polarized lights. (b) Graphical representation of the ellipticity, θ. [5]

4.3 Theory of electrophoresis

Electrophoresis is defined as the migration of ions under the effect of an electric field. It is clear that ions with different charge densities migrate with different velocities but in some cases even ions with the same amount of charges have different migration velocities. The electrophoresis phenomenon is used to develop techniques for ions separation and quantification, as explained below.

An ion under the effect of an electric field experiences two opposite forces: an electric force towards the electrode of opposite sign and a frictional force on the opposite direction. Given that the ion moves at a constant velocity, the condition of equality of forces must be fulfilled

(4.37)

The electrical force is proportional to the charges per ion, q, and the electric field, E. On the other hand, the frictional forces are dependent of the velocity *v* of the ions and their hydrodynamic radius Rh.

$$qE = v.6\pi R_H \eta \tag{4.38}$$

where η is the viscosity of the solution. In capillary electrophoresis, the comparison of the migration velocities of ions is of great interest. Since this velocity is proportional to the electric field applied, normalization becomes necessary

$$\mu = \frac{v}{E} = \frac{q}{6\pi R_H \eta} \tag{4.39}$$

μ is the so-called electrophoretic mobility. This term is a measure of the intrinsic velocity of each ion and it constitutes the base of any electrophoresis technique. Two ion species are "easy" to be separated, if their electrophoretic mobilities differ widely from each other.

In this work, capillary as well as gel electrophoresis were used for DNA separation. The difference between both techniques will be explained as follow.

4.3.1. Capillary Electrophoresis

Capillary electrophoresis is a technique analogous to SEC (Size Exclusion Chromatography) except that the stationary phase is no longer a gel matrix but a current induced in the capillary. In the case of free solution capillary electrophoresis, this leads to a stempel instead of a parabolic elution profile which leads to a better resolution of the elugrams. A typical capillary electrophoresis equipment is sketched in Figure 4.12.

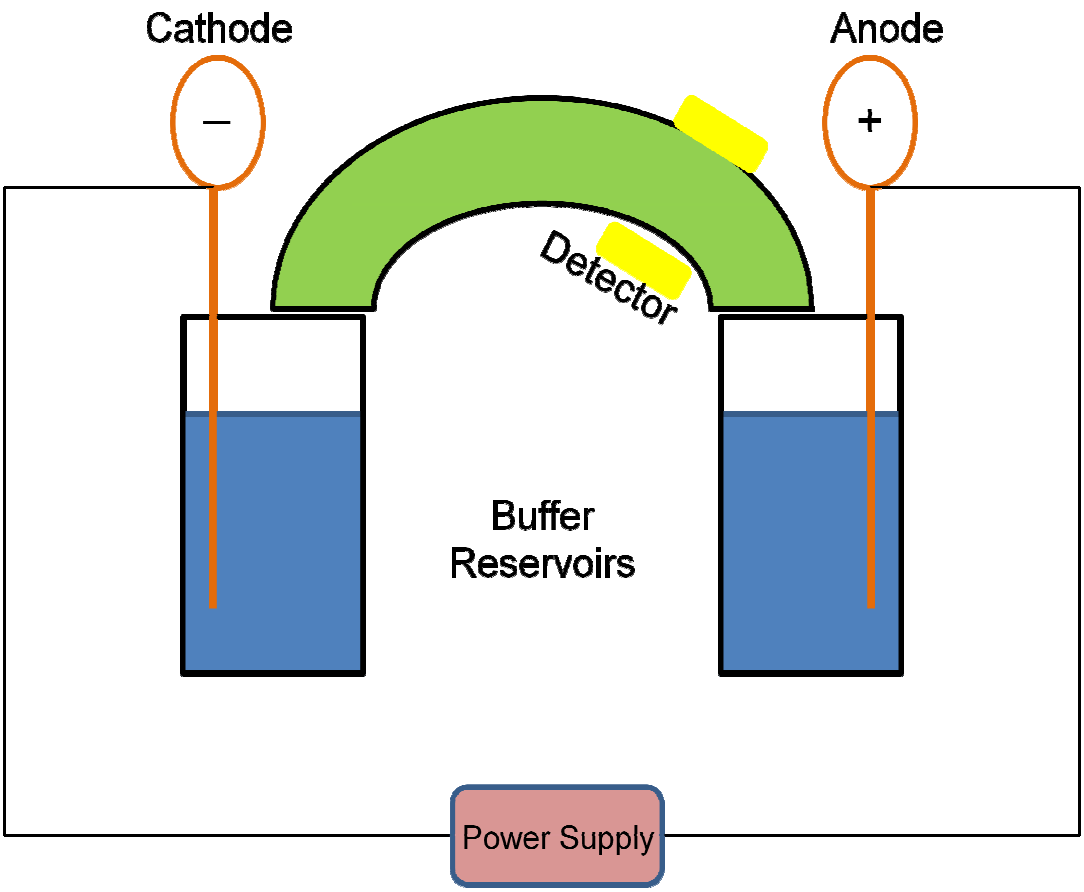

Figure 4.12. Scheme of the typical capillary electrophoresis equipment

Capillary electrophoresis equipment consists of two electrodes, each of them in contact with an electrolyte reservoir and connected by one capillary, typically made of quartz with a coating of polyacrylamide. A sample can be injected into the capillary by replacing one of the electrolytes reservoirs (usually the one in the cathode) by the sample reservoir and applying then a pressure (or vacuum).

During the operation mode, a voltage is applied across the capillary which causes the ions to migrate at different velocities. A capillary with a small inner diameter (d) (typically around 50 μm) is required in order to minimize the Joule heating effect.

When a voltage (V) is applied while using a capillary of length L_t and cross-sectional area A and containing a buffer of conductivity, κ, the rate of heat generation could be approximated as [6]

$$\frac{dH}{dt} = \frac{IV}{L_t A} \tag{4.40}$$

Where the current I is given by

$$I = V\kappa \frac{d^2\pi}{4L_t} \tag{4.41}$$

The lower the rate of heat generation is reached by using capillaries of small diameters. Furthermore, the heat dissipation system with air on the outside of the capillary becomes more efficient with lower d.

A variety of detection systems is used for quantification. The most common used is a UV-vis detector. In this case, the samples must absorbed light at the wavelength between 200 – 900 nm or a dye absorbing in the UV-vis region must be employed as a buffer, in order to register negative peaks of the non-absorbing sample (indirect detection). Other types of detectors include a conductivity, fluorescence and mass spectrometer detectors.

The standard capillary used for CE is a silica capillary with silanol groups on the surface. At a pH higher than 2, these groups are deprotonized which leads to a capillary with a negatively charged surface. In order to satisfy the electroneutrality condition, positively charged counterions are placed in the neighboring areas of the silanol groups. Under the influence of an electric field, the counterions will migrate towards the cathode, dragging the liquid with them, which translates to an overall migration of the system to the cathode. This is an important phenomenon that appears in capillary electrophoresis and it is called "electroosmotic flow" (EOF). In the presence of EOF, the ions will migrate at an effective electrophoretic mobility μ_{eff}

$$\mu_{eff} = \mu + \mu_{EOF} \tag{4.42}$$

Equation 4.42 indicates a vectorial sum of the electrophoretic mobilities.

The electroosmotic flow increases with the pH. At a pH=7, the electroosmotic flow becomes strong enough to force all of the ions, independent of their charges, to migrate towards the cathode, which could give an advantage because simultaneous analysis of anions and cations is possible. The order of migration is shown in figure 4.13.

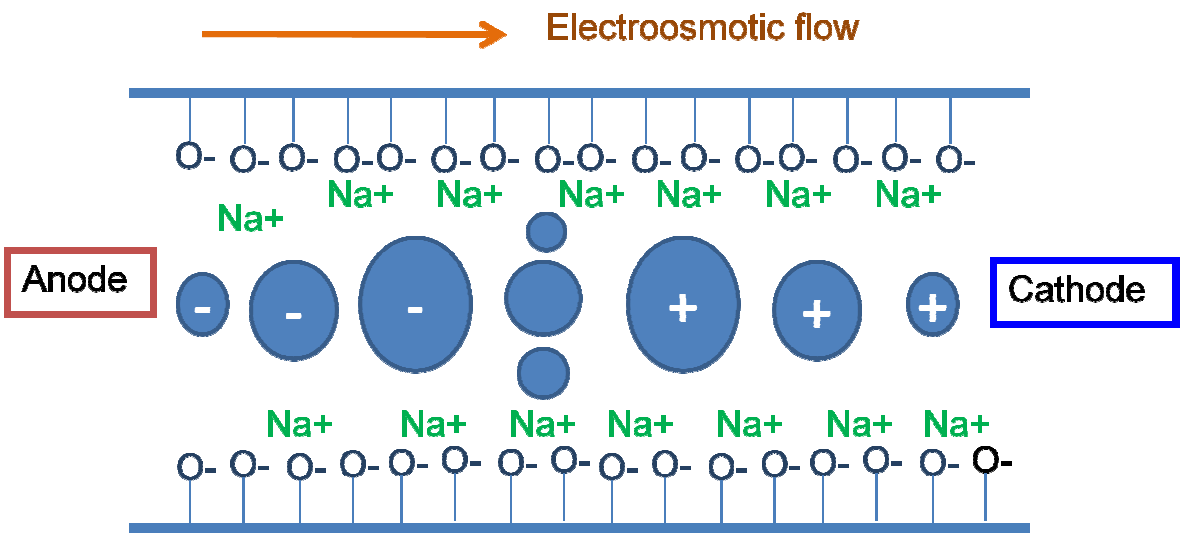

Figure 4.13. Order of migration of molecules in CE pushed by the electroosmotic flow.

In practice, the velocity of the ion can be estimated by dividing the effective length of the capillary, l_d, (distance from the inlet to the detector) with the migration time (t_m) of the ion. The electric field is given by the voltage V distributed in the capillary with total length L_t. The electrophoretic mobility of the EOF is determined by injecting a neutral molecule, i.e. acetone, whose migration time, t_{EOF}, only depends on the EOF. The electrophoretic mobility of the sample can be calculated as

$$\mu = \frac{L_d L_t}{V}\left(\frac{1}{t_{EOF} +/- t_m}\right) \tag{4.43}$$

The symbol + / - corresponds to cations or anions respectively. Cations migrate in the same direction of the EOF whereas anions migrate to the opposite direction.

Equation 4.39 presented in the previous section is not valid for polyelectrolytes, since the interactions with the counterions are neglected. Muthukumar [7] developed a theory to calculate the electrophoretic mobilities of polyelectrolytes

$$\mu = \frac{z_i}{6\pi\eta R_g} M(\chi R_g) \tag{4.44}$$

As it can be notice from equation 4.44, the electrophoretic mobility of a polyelectrolyte could be calculated as μ of an ion with an additional correction factor M(χRg) depending on the inverse of the Debye length, χ, and introducing the radius of gyration Rg instead of the hydrodynamic radius. For polyelectrolytes at a high ionic strength, the correction factor is given by

$$M(\chi R_g) = \frac{1}{(\chi R_g)^{\frac{1}{\nu}-1}} \tag{4.45}$$

where *ν* is the so-called molar mass-radius exponent for a defined architecture, $M = k_2 {R_g}^{1/\nu}$.

Given that for a polyelectrolyte, the number of charges increases with the molar mass, $z_i = k_1 M$, the electrophoretic mobility of a polyelectrolyte can be expressed as

$$\mu = K \frac{e}{6\pi\eta\chi^{\frac{1}{\nu}-1}} \tag{4.46}$$

As consequence of the clouds of counterions surrounding a polyelectrolyte, the separation by molar mass is not possible with CE. Cottet et al [8] after experimental work with polystyrene sulfonate also concluded that the mobility of polyelectrolytes with the same topology is independent of the degree of polymerization. This behavior is called "free draining regime" of polyelectrolytes.

In this work, the separation of DNA according to its molar mass was not possible with free solution CE. However, the separation of linear and supercoiled DNA was successful, since the molar mass-radius exponent *v* is different for these two architectures.

4.3.2. Agarose gel electrophoresis

In the previous section, it was shown that with free solution CE, polyelectrolytes cannot be separated according to their molar mass. Hence, agarose gel electrophoresis has become a powerful tool for DNA analysis. The principles dominating this technique and SEC are similar; however in agarose gel electrophoresis the application of a pressure is not necessary. Instead a voltage V needs to be applied in order to "force" the DNA to pass through a stationary phase, which in this case consists of a matrix gel of agarose. The larger DNA fragments will more easily become entangled with the matrix and will, therefore, migrate slower. The main advantage of this technique relies on the separation of DNA according to the number of bases and the conformation. Supercoiled DNA will migrate faster than the single strand nicks (open circular) and linear DNA due to the lower friction against the agarose matrix. The order of migration can be better visualized in figure 4.14.

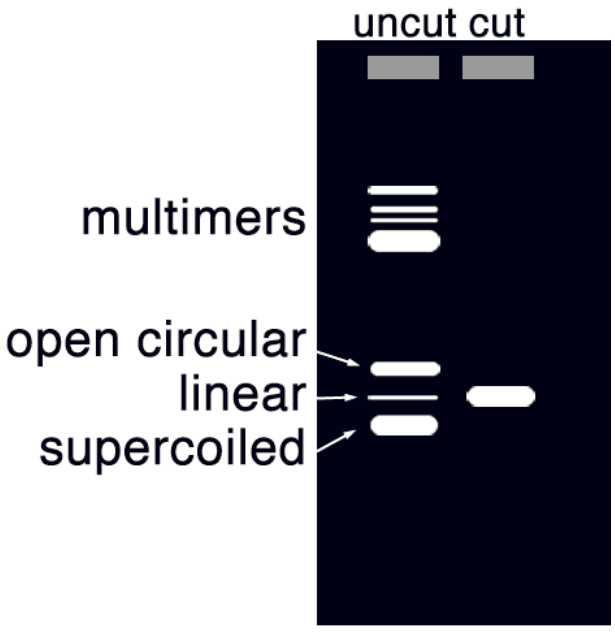

Figure 4.14. Migration of the different conformations of DNA in an agarose gel electrophoresis. [6]

A disadvantage of agarose gel electrophoresis is that the joule heating effect becomes stronger and the heat dissipation is less efficient compare to CE, which limits the maximum possible applied voltage. Due to the reasons mentioned before, a poorer resolution is to be expected than in CE. Besides that, quantification of the DNA fragments becomes difficult and less precise.

4.4. Atomic Force Microscopy (AFM)

Atomic Force Microscopy belongs to the family of Scanning Probes Microscope (SPM), instruments used to image and measure some properties of different materials. In AFM, the forces between a tip and a sample are measured and a map of the sample is generated in three dimensions. A scheme of the instrument is presented in Figure 4.15.

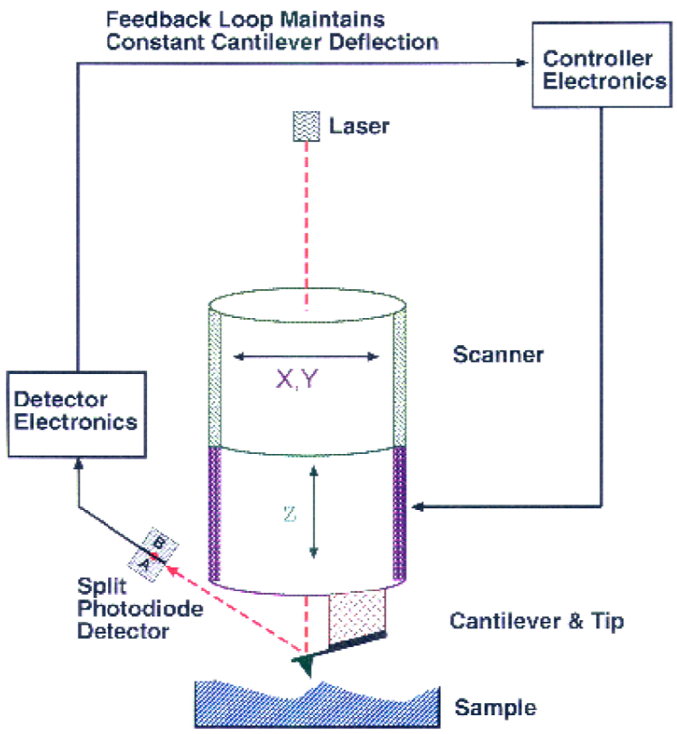

Figure 4.15. Schematic representation of equipment for Atomic Force Microscopy (AFM) measurements [9]

The equipment consists of a tip, a cantilever, a detection system to quantify the inflection of the cantilever and a feed-back system. Briefly, the tip experiences forces with the sample as a result of tip-sample interactions. The tip is attached to a spring (a cantilever), which is deflected according to the magnitude of the tip-sample forces. This deflection can be measured with a detection system based typically on a laser and a photodiode detector. A feedback loop is also used in some AFM modes, i.e. constant force measurements. Following, each part of the AFM equipment will be explained in detail.

The tip could be made of different materials, such as silicon or quartz. It contains the "probe" molecule, used to interact with the sample. As a results of this interaction, certain forces are generated, i.e. Pauli exclusion, van der Waals forces, electrostatic interactions among others. The specific types of forces experienced by the tip depends on the material of this tip, on the sample and on the AFM mode used for the measurements (see below).

For quantification of the forces, a spring with a given spring constant k is attached to the tip. This "spring" must have a low k in one direction and a high one in the other two directions, therefore a cantilever is chosen as the best option. The inflections of the cantilever due to the forces between the tip and the sample are typically detected by a laser beam aimed at the back of the cantilever and a photodiode detecting the reflected light. This system was employed in this research in the image DNA complexes. There are other detection systems such as an interferometer or a STM tip attached to the back of the cantilever but they will not be covered in this work.

AFM can be used in two different modes: the static and the dynamic modes.

In the static mode, a tip is rastered towards the sample at a constant height or a constant force. In the former mode, mainly repulsive interactions are measured. In latter mode, attractive forces are also measured and a feed-back loop is required in order to vary the tip-sample distance. These two modes are relatively easy to employ but the tip or the sample may suffer some damage. An alternative to avoid this problem is to work with AFM in a dynamic mode. In this case, the cantilever-tip system is oscillated to a given amplitude A and frequency f. If the tip contacts the sample, then the type of measurement is called tapping mode. It is important to notice that tip is not being dragged anymore along the sample but it is "touching" the sample at one point at a time and therefore, damages of the tip or the sample are avoided. Again, the tapping mode could be used at a constant height or at constant amplitude. An advantage of this mode is that delicate samples, such as DNA (see Figure 4.16) can be imaged with AFM, as in the case of this work. The dynamic AFM mode can also be non-contact, i.e. frequency modulated. The explanation of this mode goes beyond the scope of this work but it is important to mention that atomic resolution with AFM is only achievable with this frequency modulated mode.

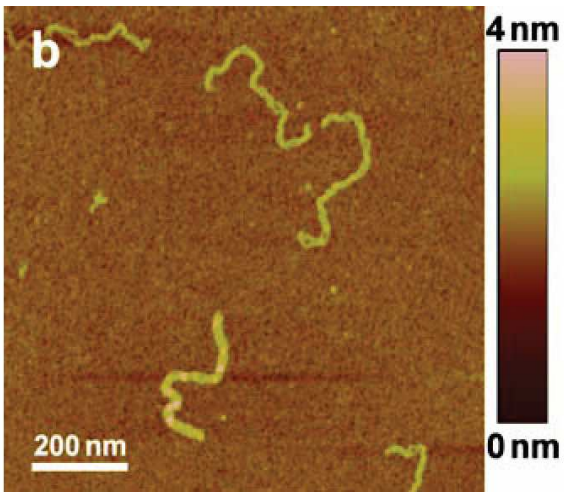

Figure 4.16. supercoiled DNApUC19 imaged with AFM in tapping mode [10]

4.5. References

1. Pecora, R. Dynamic Light Scattering: applications of photon correlation spectroscopy, Plenum Press, 1985.
2. Poche, D.; Russo, P.; Fong, B.; Temyanko, E.; Ricks, H. Journal of Chemical Education. 1999, 76(11), 1534 – 1538.
3. Teraoka, I. Polymer Solutions. Introduction to physical properties. John Wiley & Sons, 2002.
4. Schärtl, W. Light Scattering from Polymer Solutions and Nanoparticle Dispersions. Springer, 2007.
5. Bondesen, B.; Schuh, M. Journal of Chemical Education, 2011, 78 (9), 1244 – 1247.
6. Introduction to capillary electrophoresis. Beckman Coulter.
7. Muthukumar, M. Electrophoresis. 1996, 17, 1167 – 1172.
8. Cottet, H.; Gareil, P.; Theodoly, O.; Williams, C. Electrophoresis, 2000, 21, 3529 – 3540.
9. Blanchard, C. The Chemical Educator, 1996, 1(5), 1-8.
10. Li, Y.; Yildiz, U. Müllen, K.; Gröhn, F. Biomacromolecules, 2009, 10(3), 530 – 540.

5. Formation of complexes between a plasmid DNA pUC19 and positively charged spermine and polylysine derivatives.

DNA is a biological molecule, which contains the genetic information in all living organisms. It consist of two strands, each of them composed by an array of aromatic molecules with heteroatoms, like nitrogen (N) and oxygen (O), called "bases". These two strands are kept together due to hydrogen bonding, hydrophobic and base-stacking interactions. The bases in one strand are joined through a backbone of sugar (deoxyribose) and phosphate groups which confer the DNA a negatively charged surface. In some biological processes *in vivo*, the charges of DNA are screened by positively charged biomolecules, what induces a compaction of the DNA into smaller particles, since electrostatic repulsions within the DNA decrease. This process is called "DNA condensation" [1]. The forces leading to the DNA condensation can be summarized in coulombic interactions and hydration forces [1]. From a biological, physical, and chemistry point view, it is important to elucidate the mechanism by which DNA is being compacted by multivalent cations. Among other advantages, the gaining of knowledge in this problematic helps scientist to find the most adequate vector for "gene therapy" (defined as the insertion of a healthy gene into the cells of a patient with a disease caused by a genetic mutation). Due to its low cytotoxicity, biomolecules have been widely used to form complexes with DNA. However, this is not the only requirement. It is known that the minimum amount of charges that a cation must possess in order to condense DNA is 3+ [1].

A good candidate to complex DNA is, for instance, spermine. This cation is known to be involved in several biological processes, such as the normal cell growth [2,3], gene transcription and activation of DNA synthesis [3] and contains four amine groups, which are protonated at a pH=7 (pK_as of amine groups within spermine are 10.9, 10.1, 8.9 and 8.1 [4]). In spite of its attributes, spermine cannot be directly used as a DNA condensing agent, since hydrophobic regions are formed due to the charge neutralization of the phosphate backbone. Thereby these complexes may aggregate and even precipitate at a sufficient high concentration and at a charge ratio close to one. [5,6]. Although under certain conditions, i.e. low concentration of DNA, precipitation of the complexes is avoided, they are rarely composed of one DNA molecule [1]. The aim of this work is to form complexes with spermine derivates which consist of only one DNA molecule even after neutralization of 100% of the charges.

One possibility to prepare soluble DNA complexes with spermine is the addition of an excess of cation. The reentrant of DNA precipitate given that the solution contains a large excess of polyamines has been widely studied but it is still not fully understood. Several hypotheses have been proposed to explain this phenomenon, for example, the increased binding of polyamine (spermine, in this case) after precipitation causes the complexes to be hydrophilic enough to be redissolved [2]. This option is, nevertheless, not suitable for biomedical applications. The "ideal" condensing agent should screen 100% of the charges with no excess of the cation in the solution, while keeping the DNA complexes stable.

Three spermine derivatives were synthesized by Chai, W. [7] to be used as condensing agent of DNA. Their structure are shown in Figure 5.1.

In the first structure (EG-SP) an oligomer based on ethylene glycol moiety was included in order to give the DNA complexes stability in aqueous solution. Polyethylene glycol (or polyethylene oxide) is a water soluble molecule and it has been used in many studies to improve the stability of polyelectrolyte complexes (PECs) for biomedical applications [8 – 17]. Hietala et al [18] achieved to prepare polyelectrolyte complexes between a polyanion, polymethacrylic acid (PMAA) with a hydrophilic polyethylene oxide (PEO) block, PEO-b-PMAA, and a polycation, poly(methacryloyl oxymethyl trimethyl ammonium chloride) (PMOTAC) stable in aqueous solutions. The complexes possessed approximately the same size independent of the method or concentration of preparation. The authors claimed to have prepared complexes undergoing a thermodynamic equilibrium. Cavallaro et al [19] also formed water-stable PECs by employing a copolymer consisting of polyaspartylhydrazide (PAHy) and PEO blocks as polycation.

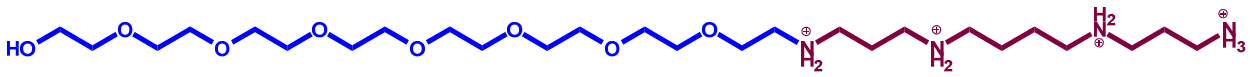

(a)

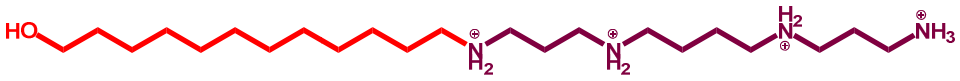

(b)

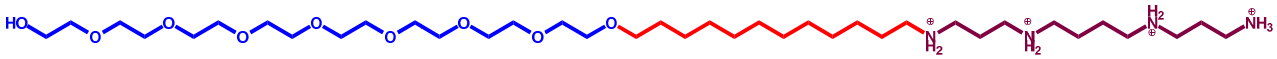

(c)

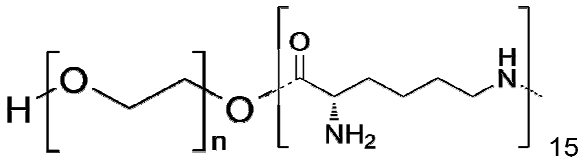

(d)

Figure 5.1. Multivalent cations used to form complexes with DNA in aqueous solutions: (a) polyethylene glycol – b – spermine (EG-SP), (b) dodecylspermine (C12-SP), (c) polyethylene glycol – b – dodecylspermine (EG-C12-SP), (d) block copolymer of polyethylene oxide and polylysine (EG-PLL). Mw_{EG}=12000 g/mol and DP_{PLL}=15

The condensation of DNA with EG-SP does not guarantee 100% of charge neutralization upon addition of the spermine derivative until a charge ratio N+/P- = 1. An excess of the multivalent cation may be required in order to shield all of the charges carried by the phosphate groups. Therefore, a spermine derivative with a hydrophobic moiety consisting of a hydrocarbon with 12 carbons has been synthesized. It has been already reported that monovalent cationic surfactants can condense DNA due to hydrophobic interactions among the tails. However, stability may be compromised. In order to ameliorate the efficiency of formation of DNA complexes (defined by the ratio of positive charge screening the DNA charges to the total amount of positive charges in solution) and to maintain the DNA complexes soluble in aqueous solutions, two approaches were taken: the first one consists on synthesizing a spermine derivative containing a hydrophobic and a hydrophilic moieties (see Figure 1c); the second approach

consists in increasing the charges of the condensing agent instead of including a hydrophobic tail but keeping the PEG block. Because a block copolymer of polyethylene glycol and polylysine (EG-PLL) was already available in the group of Prof. Kataoka, University of Tokio, a new polyamine with a larger amount of charges was not synthesized but the EG-PLL was used instead.

In this chapter the formation of complexes between DNA and spermine- and lysine-based multivalent cations with different moieties are characterized in terms stoichiometry, equilibrium, efficiency, topology and conformation in the search for the "ideal" condensing agent: 1) able to neutralize 100% of the DNA charges with no excess in solution and 2) capable of forming unimolecular DNA complexes.

5.1. Preparation of DNA complexes with spermine and polylysine derivatives.

The DNA used is pUC19-supercoiled DNA, which contains 2686 base pairs. Its characterization is shown in Table 1.

Table 5.1. Light Scattering characterization of pUC19-Supercoiled DNA

Polymer	Solvent	(dn/dc) (ml/g)	Mw (g/mol)	A_2 (mol.ml/g^2)	Rg (nm)	Rh (nm)	Rg/Rh
DNA pUC19	5mM phosphate buffer	0.17	1.7×10^6	6.7×10^{-4}	65.6	43.6	1.5

The radius of gyration of pUC19 was also measured by Lai and van Zanten [20]. However, the measured a value of 169 nm, more than two times higher than the values reported in this work. The authors of reference 10 did not measure dynamic light scattering (DLS) but if the value of 43 nm is taken, the ρ-ratio of DNA pUC19 would be around 3. This value is too high for a polymer with a coil conformation. Not even the linear DNA with an extended conformation has such a high Rg/Rh ratio (see chapter 7). Our values are in agreement with Li et al. [21]

Complex formation. An aqueous solution of DNA c=0.05 g/l (unless otherwise stated) was titrated directly in a light scattering cuvette with one of the multivalent cations shown in Figure 2.1. Concentration of the stock solutions are shown in Table 2.1. All of the solutions contained 5 mM of phosphate buffer pH= 7 to screen electrostatic interactions. After each addition of the cations, samples were equilibrated for 30 minutes. After this time, changes of the molar mass or size of the sample were not detected with dynamic and static light scattering. Also He et al [22] reported that stopped-flow measurements of DNA condensation with spermidine and spermine suggested that a fast intramolecular condensation takes places in 1 ms and a slow intermolecular condensation occurs within the next 100 s. A time of 30 min seems to be enough for equilibration of the complexes.

Table 5.2. Conditions for the formation of complexes between DNA and multivalent cations

	EG-SP	C12-SP	EG-C12-SP	EG-PLL
Stock solution concentration (g/l)	0.1	0.15	0.15	0.32

Circular Dichroism spectroscopy. Circular Dichroism (CD) spectra were measured on a Jasco J-815 Spectrometer. Spectra were recorded between 200 and 320 nm (data pitch: 1 nm, scan mode: continuous, sensitivity: 10 mdeg, speed: 50 nm m-1, response: 4 s, bandwidth: 1nm, five accumulations) using a Hellma quartz cell with pathlength of 10 mm.

Static and Dynamic Light Scattering. The complex solutions were typically measured from 30 to 150° in steps of 5° (SLS) or with a multiangle light scattering apparatus consisting of eight detectors separated by an angle of 17° each. For each sample, two measurements were performed: one positioning the first of the eight detectors at 30° and another one placing this detector ar 39° (DLS). Samples were filtered through a: GHP filter 200 nm for DNA and the spermine derivatives (a, b and c from Figure .2.1) and GS filter 220 nm for EG-PLL. Cuvettes were cleaned with distilling acetone.

The evaluation of the data is not trivial. Even assuming an ideal solution (A_2=0), i.e. no concentration dependency and after extrapolation towards q→0 (form factor P(q) = 1), the Zimm equation gives two incognita for the complexes (see equation 5.1)

Since the exact stoichiometry of the complexes is unknown, both the concentration and the weight-averaged molecular weight (Mw) are yet to be found. In order to solve this problem, in this work a model is generated under the assumption that complexes consists of only one DNA molecules and several multivalent cations as shown in Figure 5.2.

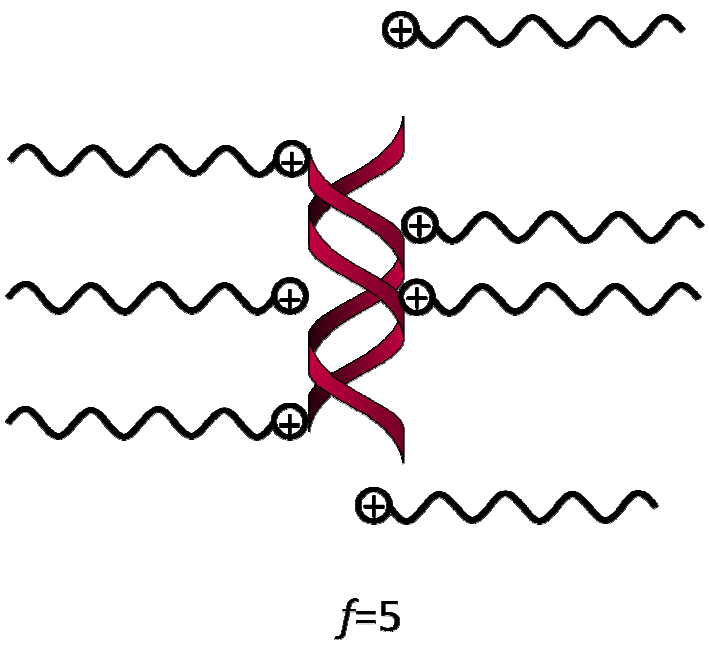

Figure 5.2. Schematic representation of DNA complexes with multivalent cations. DNA is represented in red and the cations in green. Complexes consist of only one DNA molecule with several cations attached to it. In this picture, the number of cations/ DNA (*f*) is equal to 5.

$$\frac{Kc_{complex}}{R} = \frac{1}{M_{complex}} \quad (5.1.)$$

The molar mass of the complex is given by the sum of the DNA molar mass and the number of surfactants bound to DNA (represented in this work with the letter "*f*") times the molar mass of each cation.

$$M_{complex} = M_{DNA} + fM_{cation} \quad (5.2)$$

At a given value V, the total concentration of complexes is given by the sum of the DNA concentration and the total concentration of surfactants bounded to DNA. This last concentration is given by the DNA concentration times the weight fraction of surfactant bounded to DNA (=$f.M_{cation}/M_{DNA}$).

$$c_{complex} = c_{DNA}\left(1 + f\frac{M_{cation}}{M_{DNA}}\right) \quad (5.3)$$

Substituting equations 5.2 and 5.3 in 5.1

$$\frac{Kc_{DNA}}{R} = \frac{1}{\left(\frac{M_{cation}{}^2}{M_{DNA}}f^2 + 2M_{cation}f + M_{DNA}\right)} \quad (5.4)$$

$$\frac{Kc_{DNA}}{R} = \frac{1}{M'} \quad (5.5)$$

The static light scattering (Kc/R) is determined using the DNA concentration (c_{DNA}) and the number of cations bound to DNA (*f*) is calculated with equation 5.4. In this way, the data could be evaluated in a reliable way. Notice that no assumption is being made with respect to the topology or type of complexes. Equations 5.2 and 5.3 are valid for any kind of complex formation, as long as they are formed by only one polyelectrolyte and small cations. The static light scattering intensity was taken from the extrapolation q→0 but samples were measured at only one concentration. It is therefore assumed that the samples are

very diluted and concentration-dependent measurements are not required. It is also important to notice that the scattering intensity of the free multivalent cation is neglected. This assumption is based on the fact that the intensity scales with M_i and the difference between the molar masses of DNA / DNA complex and the free cations is three orders of magnitudes. In other words, the scattering intensity of DNA complexes is around three orders of magnitude higher than the intensity of the free cations.

The refractive index increment (dn/dc) of the spermine-derivatives is unknown, therefore the dn/dc of the DNA pUC19 (equals to 0.17) was used. For the complexes with EG-PLL, dn/dc is calculated with the following relation

$$\left(\frac{dn}{dc}\right)_{complex} = \sum_{i=1}^{n} w_i \left(\frac{dn}{dc}\right)_i = w_{DNA}\left(\frac{dn}{dc}\right)_{DNA} + w_{cation}\left(\frac{dn}{dc}\right)_{cation} \quad (5.6)$$

Where w_i is the weight fraction of each component. The (dn/dc) of the EG-PLL was obtained from Kataoka et al. [23]. Experimental and calculated values with equation 5.4 were compared for DNA complexes with EG-PLL and the results were identical within experimental error [24].

5.2. Stoichiometry of DNA complexes with spermine and polylysine derivatives.

As previously mentioned, the complexes between DNA and multivalent cations are prone to precipitation when the ratio of charges neutralized approach the unity (N+/P- = 1). In general, it could be stated that "intrinsically"-hydrophobic polyelectrolytes become usually water insoluble when all of their charges are shielded by an oppositely-charged molecule. In other words, the charges of a polymer are responsible for its dissolution in aqueous solution. Furthermore, it has already been reported that the formation of complexes between DNA and multivalent cations with 3 or 4 positive charges, i.e. spermine, is a process controlled by the kinetics and that very seldom they are composed of one DNA molecule per complex [1, 12].

In this work, we study the complex formation between DNA and spermine derivatives with hydrophobic and hydrophilic moieties with respect to their stability and number of DNA molecules per complex. Figure 5.2 shows the results of static light scattering measurements (SLS) after the stepwise addition of the multivalent cations shown in Figure 5.1. The data was evaluated as described in the experimental section and with the correct molecular weight, the number of cations in the complexes and therefore, and the charge stoichiometry, are calculated. To calculate the percentage of neutralized DNA charges (%N+/P- complexed) plotted in figure 5.3, the number of cations per DNA molecule was multiplied with the number of charges per molecule, i.e. for spermine %N+/P.- complexed = 4**f**100%. For the polylysine block copolymer a factor of 15 instead of 4 was used in the calculations. It could be observed that, except for the cation C12-SP, only one DNA is presented within the complexes. When looking into other works, mainly multimolecular DNA complexes have been obtained with spermine [2, 22] and polylysine [20]. The mechanism of a single-molecule DNA condensation has only been elucidated with techniques like optical tweezers [3, 4, 5, 25, 26]. It is evident that the presence of hydrophilic units like EG within the cations (and therefore in the surface of the complexes) stabilizes the DNA even if all of the charges are screened.

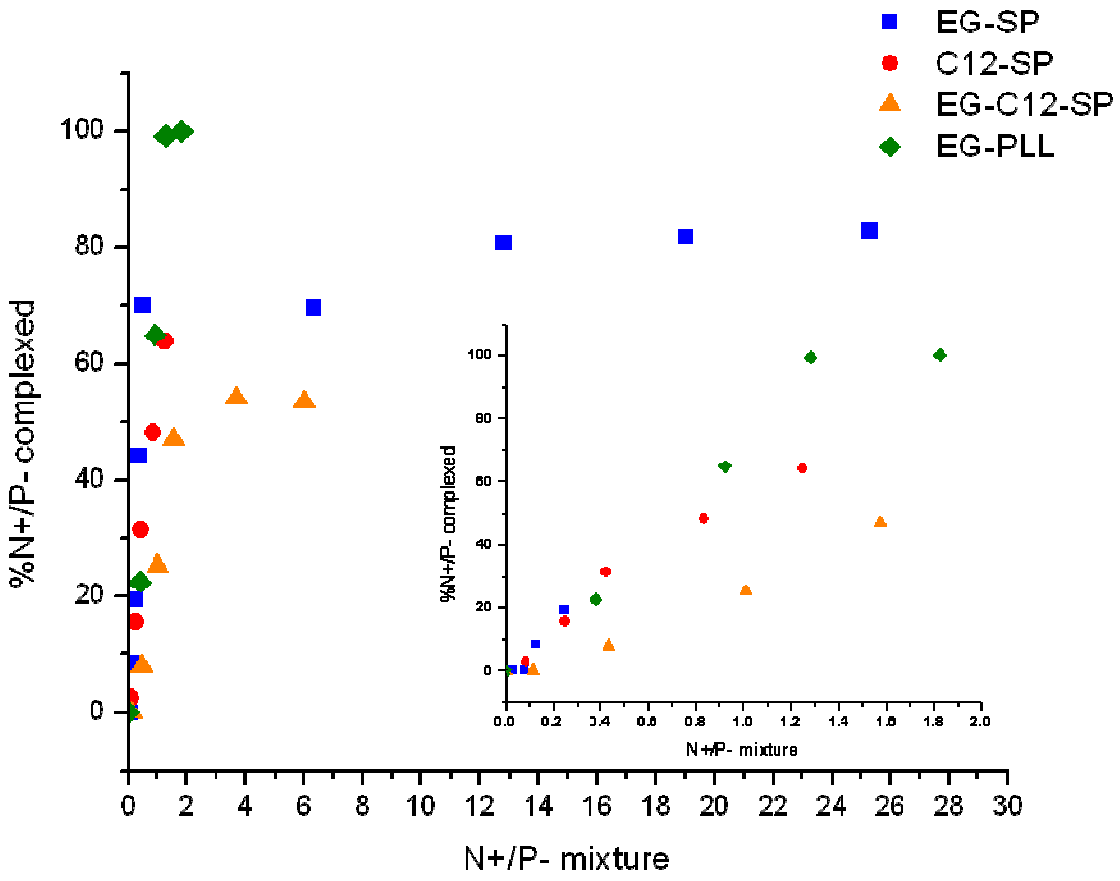

Figure 5.3. Stoichiometry of complexes (percentage of charges neutralized) with respect to the charge ratio in solution. The positive charges are given by the multivalent cations shown in Figure 5.1. and also shown in the legend of this plot. The starting concentration of DNA was c=0.05 g/l in all of the cases at 20°C in 5 mM phosphate buffer pH=7 aqueous solution. Titration of DNA proceeded until a plateau was observed, except in the case of C12-SP because the complexes undergo precipitation.

The use of EG units to improve solubility and stability of DNA complexes is not a novel approach. Several researchers have successfully used block copolymers with PEG or PEO (especially with PLL) to maintain the DNA complexes in solution [9, 24, 27, 28]. It has been claimed that the PEG chains are oriented to the outer surface of the complexes and interact with the aqueous solution [27]. This issue could explain why the complexes do not precipitate after condensation of 100% of the polyanion charges but it does not make clear the lack of interbridging of the complexes until they reach a critical mass and

precipitate (secondary aggregation). It is indeed reported the ion-pair formation between DNA and the block copolymer PEO-PLL block requires a large excess of positive charges (N+/P- = 2) in order to achieve a complete condensation of the DNA [24, 27]. Although the two works are independent from each other, they both concluded that presumably steric hindrance effects were responsible for this phenomenon.

The formation of complexes with a spermine derivative with a hydrophobic moiety (C12-SP) resulted in an abrupt precipitation of the complexes. When 65% of the DNA charges were condensed (at a charge ratio of mixing N+/P- = 1.6), the complexes were still soluble in water. Subsequent addition of the cation, increased hydrophobic forces among the complexes (due to screening of the charges and the further insertion of hydrophobic groups on the surface of the complexes) and a rapid precipitation could be noticed. This observation is in accordance with the work of Cavallaro et al. [19]. They attached hydrophilic (PEG) and hydrophobic (C16) groups to polyaspartylhydrazide (PAHy) and after mixing with the DNA, they concluded that while PEG gives stability to the complexes, the hydrophobic moiety induces aggregation.

It is interesting to notice that the spermine derivate with hydrophobic and hydrophilic moieties (see Figure 5.1. c) does not undergo precipitation. Even if some hydrophobic interactions among neighboring cations could be present, the stability of the complexes is not compromised since the hydrophilic groups are oriented towards the surface of the complexes upon DNA condensation.

It should be noticed in Figure 5.3 that only with PEO-PLL 100% of the charges are condensed. An excess of spermine is required in order to neutralize of all of the charges from the DNA. Furthermore, as already mentioned, the steric hindrance due to the addition of the EG units can hinder the complete condensation of DNA. The insertion of a hydrophobic group instead of a hydrophilic moiety improves only slightly the ratio of positive charges neutralizing in DNA to the total positive charges added. The complexes formed with hydrophilic-hydrophobic moieties (figure 5.1.c) are stable in the aqueous solution but only around 50% of the charges could be neutralized even after an excess of 6 in terms of charges. The reasons for this deviation from the expected behavior will be discussed in section 5.6. In general, the multivalent cation undergoes equilibrium between the free and bound state, and therefore an excess of surfactant is needed to reach a plateau, which does not always indicate complex formation. The EG-PLL polycation has a

larger number of charges, (15+ charges compared to 4+ of the spermine derivatives) which leaded to a complete neutralization of the DNA (without aggregation) after the addition of the polycation only until a charge ratio of 1.2. This binding equilibrium and the efficiency of formation of complexes will be discussed in section 5.3 and 5.4, respectively.

It is important to mention that for the spermine derivatives a dn/dc of 0.17 cm^3/g, equals to the one of DNA, was used to determine the molecular weight and the effective charge ratio. Given that the dn/dc of the multivalent cations is lower than the given value for DNA, the refractive index increment is expected to be lower as well, which would lead to a higher molar mass and a higher effective charge ratio.

5.3. Equilibrium of DNA complexes with spermine and polylysine derivatives.

As mentioned before, two observations could be extracted from Figure 5.3:

1. An addition of cation until reaching a charge ratio of N+/P- = 1 is not equivalent to neutralization of 100% of the DNA charges. An excess of multivalent cations is usually required in order to reach a plateau.

2. Even after reaching a plateau, the fraction of DNA charges forming an ion pair with the positive charges of the amines from the multivalent cations is not always equal unity.

The first and partly the second point can be explained in terms of a binding equilibrium. At the concentration of study (see section 5.1), the multivalent cations are fully soluble in the aqueous solution. In the presence of a polyanion, only a fraction of these cations will condense the DNA charges whereas another part will remain in solution. The hydrogen bonding that the species with EG units may form with water and the partial screening of the charges by the dipole in the water molecules favor the free (not bound) state of the condensing agents.

DNA condensation is favored by forces coming from the coulombic interactions (ΔG_{elect}). However, DNA must be bent during condensation, which contributes negatively to the formation of complexes (ΔG_{bend}) and an entropic cost is to be expected if DNA is compacted due to restrictions of motion, what is called entropy of mixing (ΔG_{mix}). Furthermore, the hydration forces must be also taken into account and they could be either attractive or repulsion (ΔG_{hyd}). If only the forces acting on the DNA are considered, the sum of all of the forces just mentioned determines the total free energy [1].

$$\Delta G_{total} = \Delta G_{bend} + \Delta G_{mix} + \Delta G_{elect} + \Delta G_{hyd} \quad (5.7)$$

If the complex formation reaches the equilibrium (which is not always the case)

$$\Delta G_{total} = -RTlnK_{binding} \quad (5.8)$$

The more negative the total free energy, ΔG_{total} , the higher the equilibrium constant of binding $K_{binding}$.

In this research, we observed that the system undergoes the following equilibrium

DNA+Spermine ----- DNA-spermine

The equilibrium constant, $K_{binding}$, should be given by

$$K_{binding} = \frac{[DNA-SP]}{[DNA]_{uncomplexed}[SP]_{uncomplexed}} \quad (5.9)$$

In Figure 5.4, the equilibrium constants for the different multivalent cations are presented. Instead of giving the value of a global equilibrium constant until an added charge ratio of N+/P- = 1, it was decided to report a $K_{binding}$ for each of the steps, i.e. for each N+/P-. It should be noticed that the exponent of the cation (4 for the spermine and 15 for the polyysine block copolymer) is not taking into account, since the

equilibrium constants reported by other authors do not consider as well these exponents and it is desired to compare the results in this work with others encountered in the literature. It is also important to mention that in the equilibrium reaction, the counterions are omitted.

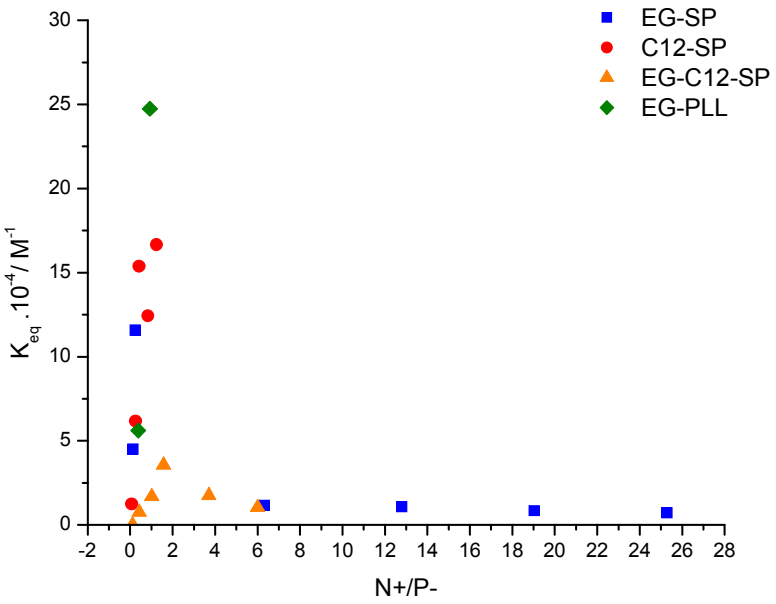

Figure 5.4. Equilibrium constant of the binding of DNA with multivalent cations calculated for each step during the titration of DNA (initial concentration 0.05 g/l) with multivalent cation at 20°C in 5 mM phosphate buffer pH=7 aqueous solution. $K_{binding}$ of EG-PLL was plotted only for the first two charge ratios N+/P-. The equilibrium constants for further addition of this agent diverges.

The equilibrium constant is usually reported for 90% of charge neutralization [1]. As shown in Figure 5.3, this value could be misleading. $K_{binding}$ is only a function of temperature (and slightly of pressure) for reactions of small molecules in solution. However, for polyelectrolytes this constant is also dependent on the sites available and on interactions among neighboring molecules. For instance, equilibrium constants of the complex formation between DNA and the spermine derivates with hydrophilic and hydrophobic moieties, EG-SP and C12-SP, at low charge ratio N+/P- < 0.5, are similar (see Figure 5.4.) At higher ratios, a cooperative binding of C12-SP can be observed, as a result of hydrophobic interactions between neighboring surfactants. Therefore K increases by a factor of *u* (introduced in section 2.1.1) with respect

to the binding constant of EG-SP (or to the pure spermine) [6]. Different $K_{binding}$ for spermine and DNA have been reported in the literature. Patel et al [6] determined $K=3.5*10^5\ M^{-1}$ employing the technique of isothermal titration calorimetry. A similar binding constant ($K=2.3*10^5\ M^{-1}$) was found by Ouameur et al while using affinity capillary electrophoresis [31]. A small discrepancy exists with the results from N'soukpoé-Kossi et al [32]. These authors differentiate biogenic and analogues polyamine. After UV measurements at different spermine/DNA charge ratios, they concluded that biogenic spermine binds stronger to DNA ($K_{binding} = 1.4*10^5\ M^{-1}$) than its analogue ($K_{binding} = 6.4*10^4\ M^{-1}$). The order of magnitude of experimental $K_{binding}$ for DNA with the spermine derivatives examined in this work agree within experimental error with the constants found by other researchers. The binding mode of spermine is therefore not affected by the moieties attached to it. This aspect will be discussed in detail in section 5.6.

As expected, the equilibrium constant of EG-SP decreases with the increment of the charge ratio. The reduction of unbound phosphate groups is responsible for this behavior. Figure 5.3 shows exceptionally low values for the binding constant of DNA with EG-C12-SP. The reason for these values is not fully understood. It could be hypothesized that steric hindrance play an important role in the formation of these complexes, however, the binding of DNA with EG-PLL concludes in 100% neutralization of the DNA charges, although one block is composed of polyethylene glycol Mw=12000. It is also important to notice that these two condensing agents, EG-C12-SP and EG-PLL cannot be directly compared. The positive charges are given by different groups and the amount of charges in EG-PLL is more than 3 times higher than in EG-C12-SP. This difference in the charges increases the electrostatic interactions, which are partly responsible for the higher binding constants of EG-PLL with DNA.

Kataoka et al. [24] formed complexes with EG-PLL block copolymer similar to the one used in this work. Only the degree of polymerization (DP) of the PLL block was different: DP = 48 instead DP = 15. It would be expected that the polymer used by Kataoka neutralizes 100% of the DNA charges at a charge ratio approximately one. However, the authors claimed that at a charge ratio of two (N+/P-=2) not all of the DNA charges were complexed. They never stated the concentrations of the polycation but it is known that the formation PECs depend on the concentration of the polyelectrolytes [33] and other conditions i.e. pH and ionic strength.

5.4. Efficiency of DNA complexes with spermine and polylysine derivatives.

As it has been shown throughout this work, not all of the added positive charges neutralize the negative charges from the phosphate groups. We have defined an "efficiency of complexation" as the ratio between the positive charges forming part of the DNA complexes ($N+_{complexed}$) with respect to the total added amount of charges ($N+_{mixture}$)

$$\text{Efficiency of complexation} = \frac{N+_{complexed}}{N+_{mixture}} \qquad (5.10)$$

This definition is only valid until 100% neutralization of DNA charges. Further addition of the surfactant would lead to a lower efficiency of complexation, which is erroneous because there are not more negative charges available and therefore complex cannot longer be formed.

In general, it could be stated that the amount of free phosphate groups diminish with the addition of more positive charges to the solution. Thus, for a multivalent cation with no hydrophobic moieties, a monotonic decrease of the efficiency of complexation is to be expected. Clearly, formation of DNA complexes with EG-SP (see figure 5.5) follows this trend. If a hydrophobic tail is attached to the multivalent cation, two effects appear: 1) the decrement of the vacancy sites just mentioned and 2) hydrophobic interactions between neighboring surfactants. In monocationic surfactants, a cooperative binding has been already reported. For the case of multivalent cations, however, the hydrophobic forces may be weaker since the average distance between two neighboring tails is larger and the total amount of hydrophobic groups in a complex at a given charge ratio is reduced (by a factor of 4 in the case of spermine). In Figure 5.5, a non-monotonic behavior for the system DNA+C12-SP and DNA+EG-C12-SP is observed. At lower N+/P- ratios, the efficiency of complexation increases in accordance to the theory of cooperative binding due to hydrophobic interactions. At mixing ratios around N+/P – = 0.9 for C12-SP and N+/P- = 1.2 for EG-C12-SP, the efficiency starts to decrease. The effect of lower vacancy charges may be more pronounced than the hydrophobic interactions. The formation of complexes between DNA and EG-PLL also follows this non-monotonic behavior. Nevertheless, the rise of the efficiency is not fully understood. Interactions among the PEG chains may be one explanation but further studies need to be done to clarify this issue.

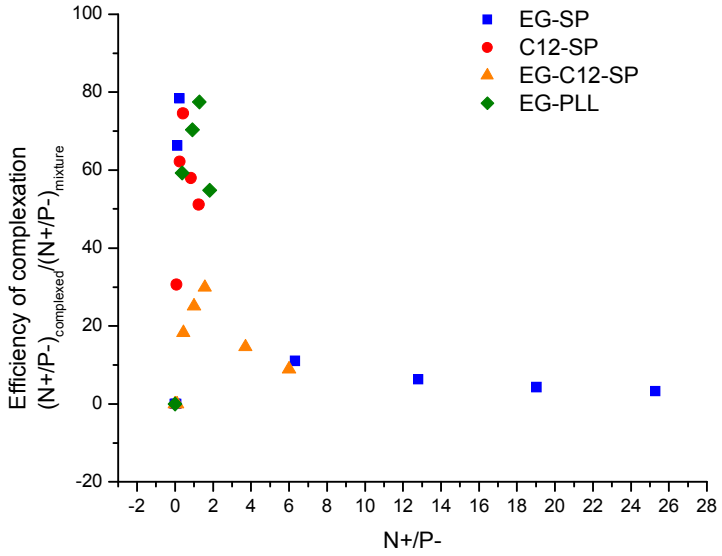

Figure 5.5. Efficiency of complexation of DNA with multivalent cations calculated for each step during the titration of DNA (initial concentration 0.05 g/l) with multivalent cations at 20°C in 5 mM phosphate buffer pH=7 aqueous solution

There may be other effects that are not being considered in this discussion. For instance, Toncheva et al [27] worked with different block copolymers of PEO-PLL and attributed the low efficiency of complexation to steric effects due to the large PEO chains.

5.5. Topology of complexes between a plasmid DNA pUC19 and spermine and polylysine derivatives

The formation of complexes between DNA and spermine or PLL derivatives does not lead to appearance of aggregates (see Figures 5.7 and 5.8). The variations of the radius of gyration (Rg) are in the order of 30%, whereas the change of hydrodynamic radius of the DNA complexes with respect to the pure DNA is approximately 20%. For kinetically controlled processes, in which aggregates are formed, for instance, during the formation of DNA with polycations, Rg and Rh increase drastically, i.e. more than 100%, especially at a charge ratio close to unity [20, 32]. Furthermore, the data in figure 5.3 support the idea of

unimolecular DNA complexes. The increment of Rg and Rh observed in figure 5.6 may be due to the expansion of the supercoiled structure of the DNA.

To discuss further the specific topology of the DNA complexes with spermine and PLL derivatives, the possible structures must be considered. DNA adopts usually (but not always) a donut-like (toroids) structure upon formation of complexes with multivalent cations, such as polyamines and the trivalent metal ion complex hexaammine cobalt (III), $Co(NH_3)_6^{3+}$ [1,3,4,5,22,28]. The theory developed by Grossberg and Zhestkov [29] explains that the toroidal structures are the result of the sum of compressive, repulsive and elastic energy. The compressive energy is caused by a poor solvent or certain non-ionic condensation agents, i.e. PEG. The repulsive term is given by the excluded volume of the DNA and the elastic energy is related to the bending of the DNA. In general, DNA is a stiff polyelectrolyte (persistence length of 50 nm) with a coiled conformation [5] and once it its charges are neutralized; it has the tendency of undergoing compaction. Other topologies, i.e. rod-like structures have been also observed [1]. Sphere-like structures have been reported by Toncheva et al. [27] for complexes between DNA and PEG-PLL. Divalent and tetravalent dyes induce flower-like aggregates [21]. Atomic Force Microscopy (AFM) pictures of complexes with polycations exposing several topologies showed flower-like and scramble eggs aggregates consisting of several molecules of the polyelectrolytes, as the result of a kinetically controlled process [30]. Complexes with a lipospermine, with a dioctadecylamidoglycyl pendant group, were imaged by TEM. Tubular structures with a dense core in the inner part (presumably corresponding to the hydrophobic part) were observed [6].

The topology of a polymer (or its complexes) can be estimated with light scattering techniques by means of the ρ-ratio (=Rg/Rh). Compacted topologies, such as sphere-like structures, are characterized by a ρ-ratio lower than one, whereas extended topologies, i.e. rod-like structures showed higher ratios. In figure 5.6 the ρ-ratio of the different condensing agents are compared. The DNA complexes with EG-SP and C12-SP are composed of more extended particles than the complexes with EG-PLL. Similar results are reported by Plum et al. [34]. These authors visualized by TEM the topologies of DNA complexes with the trivalent cations hexamine cobalt (III), spermidine, and a fully methylated spermidine. These first two cations were more efficient in condensing DNA and formed a larger number of compacted structures (toroids) than the complexes with methylated spermidine. More than 50% of the structures obtained upon complex formation with this last cation possessed a rod-like shape. The kinetics of condensation was also determined and the methylated spermidine not only had a lower efficiency of complexation but also

showed the slowest kinetics. It was hypothesized that DNA spends positive free energy in order to be bent and in order to form more compacted structures like toroids. This energy is compensated by the negative free energy resulting from the binding of the cation (see equation 5.7). Given that the methylated spermine has the lower efficiency of complexation, it cannot provide the sufficient energy to effectively bend the DNA and hence rod-like structures are mainly formed. In this study, it was also stated that the formation of rods requires tighter bending than the formation of toroids, therefore a mechanism taking place at a lower rate could be expected for the formation of more extended structures. Due to the slow kinetics of the methylated spermine, the complexes with DNA are more probable to present a more elongated conformation. The explanation given by Plum et al. could also be valid to explain the results in figures 5.9. EG-PLL is the multivalent cation with the highest complexation efficiency and also seems to form the most compacted structures with DNA. However, further studies need to be done in order to corroborate this statement.

It is also important to notice that even if EG-PLL contains polyethylene glycol with the highest degree of polymerization (DP=300), it also provides a lesser amount of non-ionic chains. At the same percentage of charge neutralized, DNA complexes with EG-SP, and EG-C12-SP possess five times more EG chains than EG-PLL. This may contribute to stronger intramolecular steric hindrance of complexes form with spermine derivatives. Furthermore the condensation of spermine and polylysine cannot be directly compared. For instance, to the knowledge of the author, it is still unclear which cation is more efficient in condensing DNA under the constraint that they possess the same amount of charges.

The ρ-ratio of DNA bound to EG-C12-SP is almost identical to C12-SP. This may suggest that even if electrostatics plays an important role in the initial process of complex formation, neighbor-neighbor interactions are determinant in the final structure of the complexes. However, after a mixing charge ratio of N+/P- = 1.5, DNA complexes with C12-SP precipitates whereas compaction of the structures could be observed with EG-C12-SP. Hydrophobic forces may have reached a critical point and since the EG groups stabilize the DNA complexes with EG-C12-SP, they undergo compaction and not precipitation. This hypothesis needs nevertheless to be proven with the appropriate design of further experiments, for example, by including AFM pictures and by extending light scattering studies to DNA complexes with hydrophilic/hydrophobic spermine derivatives with different size of the hydrocarbon chain.

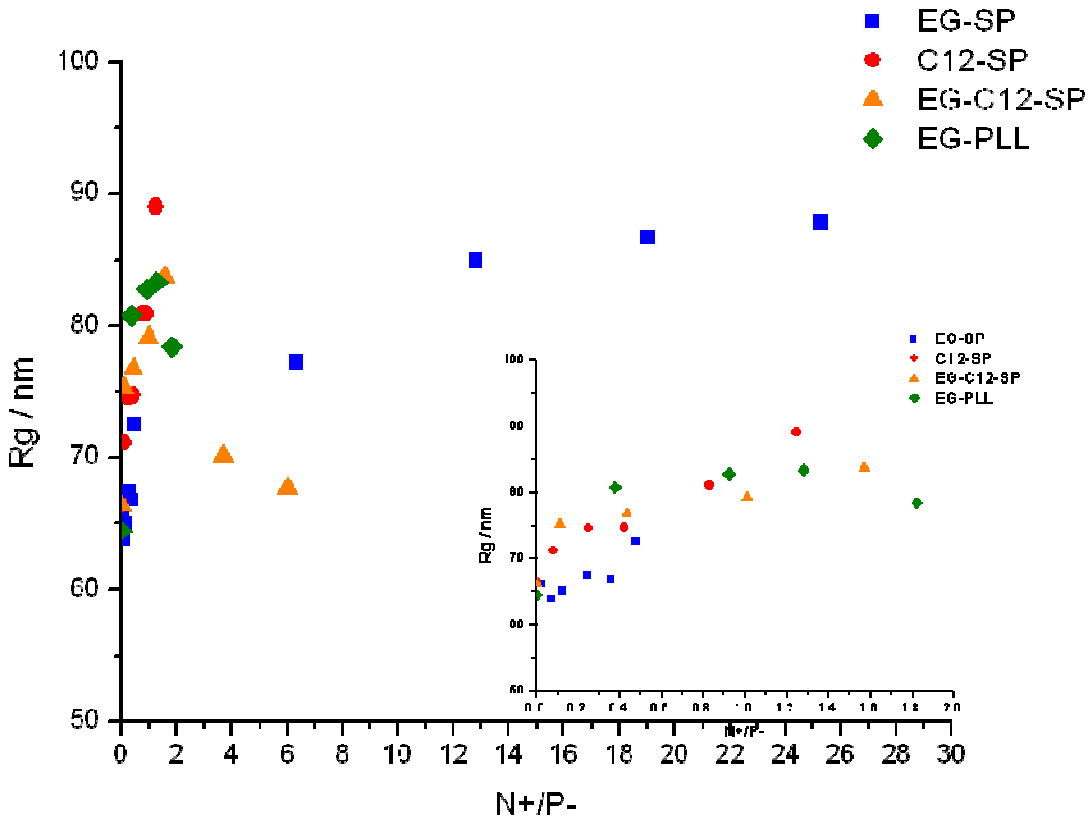

Figure 5.7. (a) Radius of gyration of DNA complexes with multivalent cations determined from SLS and DLS measurements at angles from 30° to 150° in steps of 5°. DNA initial concentration is 0.05 g/l. Measurements were performed at 20°C in 5 mM phosphate buffer pH=7 aqueous solution

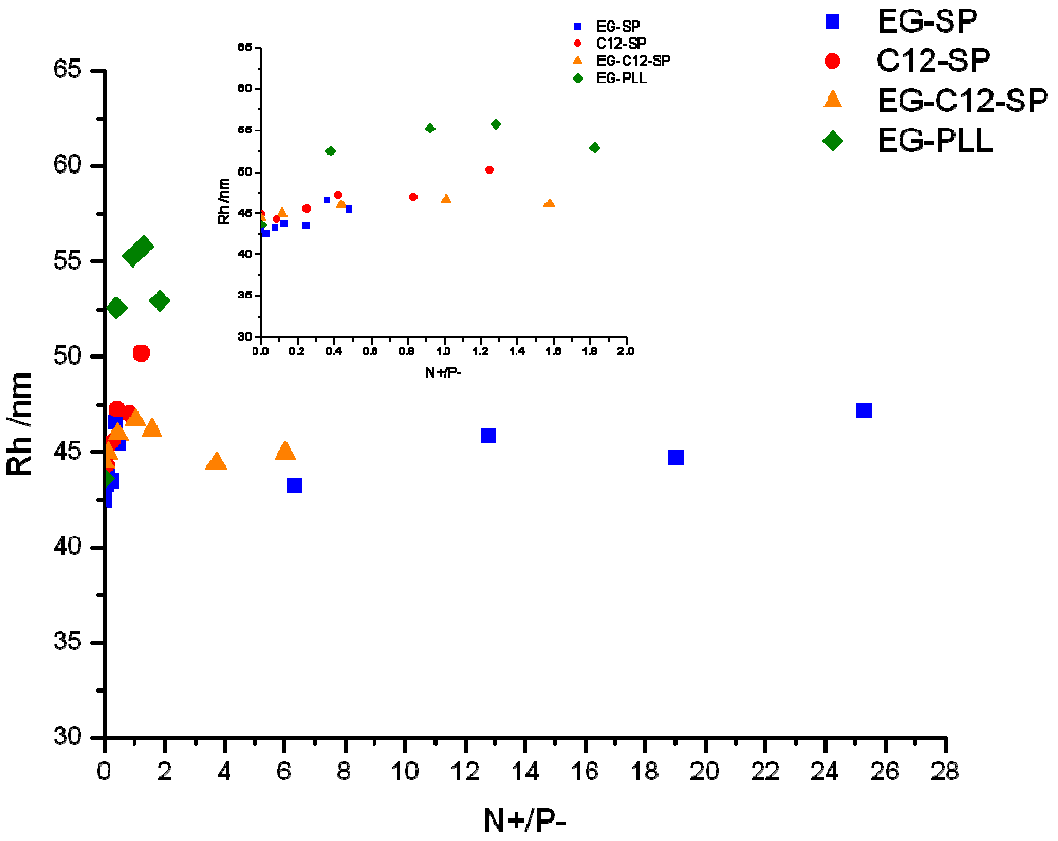

Figure 5.8. Hydrodynamic radius of DNA complexes with multivalent cations determined from SLS and DLS measurements at angles from 30° to 150° in steps of 5°. DNA initial concentration is 0.05 g/l. Measurements were performed at 20°C in 5 mM phosphate buffer pH=7 aqueous solution

An intriguing behavior is presented by the complexes with EG-PLL. The ρ-ratio seems not to vary. There are two possible explanations: 1) the supercoiled conformation of DNA is not altered upon formation of complexes or 2) Extended and compacted structures are formed, in such a way that the Rg/Rh ratio does not experience an abrupt change. The first explanation is not very probable. Neutralization of the charges given by the phosphate groups reduces intramolecular and intermolecular electrostatic repulsions. Hence, compaction and aggregation are expected. Also the large PEG block in the EG-PLL structure may generate steric hindrance within the complexes and therefore extension of the supramolecular structure. In order to explore the second possibility, and because the EG-PLL appears to be the "ideal" condensing agent, AFM measurements of the complexes were performed (see figure 5.10). As mentioned before, rod-

like (extended) and toroids (compacted) structures are observed in Figure 5.10. It should be noticed that light scattering only measures a z-averaged Rg and z-average diffusion coefficient.

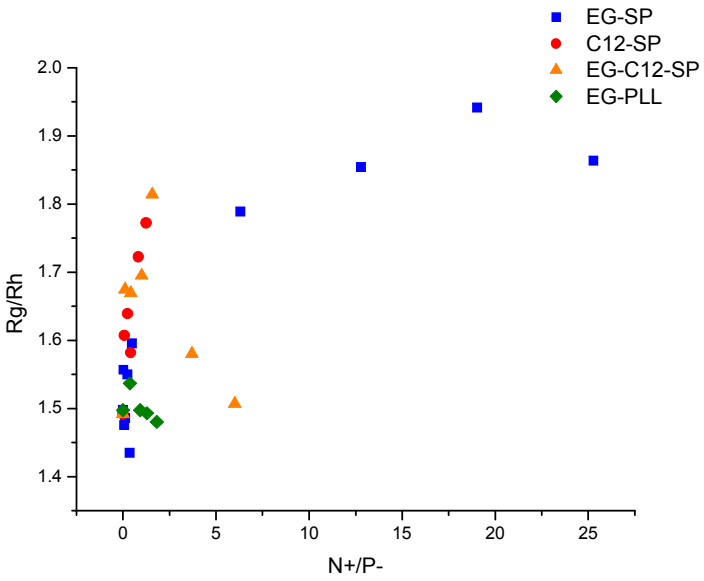

Figure 5.9. ρ-ratio (Rg/Rh) of DNA complexes with multivalent cations determined from the data in Figures 5.5 (a) and (b).

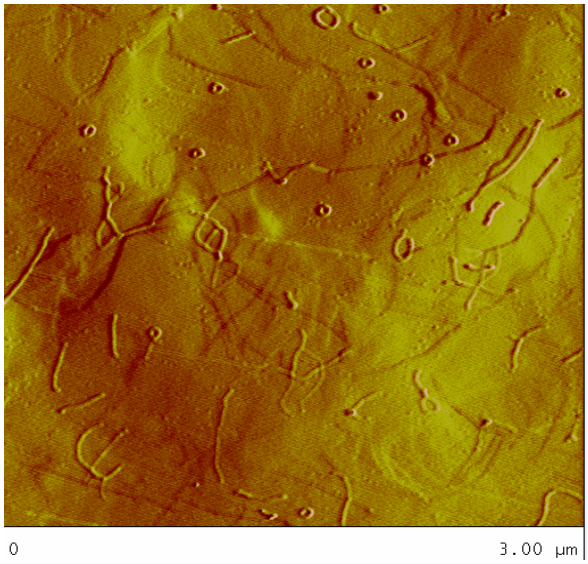

Figure 5.10. AFM pictures of DNA complexes with EG-PLL (N+/P- = 1.3) imaged on mica treated with magnesium after spin casting. The minimum and maximum diameters of the toroids are between 80 and 150 nm. The rod-like structures have a length between 190 and 250 nm.

5.6. Conformation of DNA complexes with spermine and polylysine derivatives.

DNA has a B-conformation under physiological conditions. In a circular dichroism (CD) spectrum, this conformation of DNA is characterized by a maximum at wavelength around 280 nm and a minimum at approximately 250 nm [35] (see figure 5.11). The stabilization of this conformation upon the binding of spermine has been already reported [3].

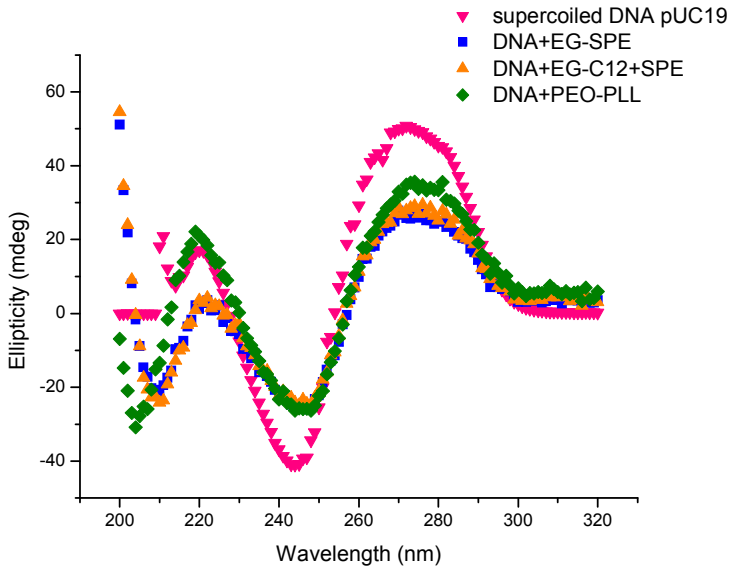

Figure 5.11. CD spectra of DNA pUC19 complexes with EG-SP, C12-SP, EG-C12-SP and EG-PLL at charge ratios of 25.3, 1.25, 6.0, 1.3 respectively at 20°C and pH=7.

In figure 5.8 it is shown that spermine and polylysine derivatives do not preserve the B-conformation of DNA (CD spectra do not superimpose with pure DNA). Similar results were found by N'soukpoé-Kossi et al [32]. These authors also observed a decrease in negativity at λ=245 nm without major shift of the maximum and minimum at the different wavelengths. The authors attributed these changes in the CD spectra to a partial B – to A-DNA conformation upon complex formation with spermine. (see A-conformation spectrum in section 3.1.2). They validated their supposition by observing the changes in the bands of infrared spectra (IR). Also theoretical calculations [36] predicted a change of the DNA B-conformation after the binding of spermine. It was postulated that the most favorable interactions of spermine with DNA takes place in the major groove and that the interstrand distance is shortened due to sugar puckering. Interactions with the minor groove of DNA are also possible [1].

5.7. Conclusions

In this chapter, DNA complexes with several spermine- and lysine-based multivalent cations have been characterized. All of the complexes formed consisted of only one DNA molecule. Only the complex with the hydrophobic moiety (C12-SP) is unstable and precipitates at a charge ratio higher than 1.5. Rod-like structures were measured with SLS and DLS whereas toroids and rod-like structures can be observed by AFM for the lysine-based cation (EG-PLL). In terms of stoichiometry and efficiency, EG-PLL was the only condensing agent able to neutralize 100% at a high efficiency of complexation. **In conclusion, the EG-PLL seems to be "ideal" condensing agent for DNA. The requirements of formation of complexes with 100% of DNA charges neutralized with a very high efficiency (more than 80%) and consisting of only one DNA molecule were fulfilled in aqueous solutions.**

5.8. References

1. Bloomfield, V. Biopolymers **1997**, 3, 269-282.
2. Allahryarov, E.; Gompper, G.; Loewen, H. J. Phys: Condens. Matter 2005, 17, 1827 – 1840
3. Shao, Q.; Goyal, S.; Finzi, L.; Dunlap, D. Macromolecules **2012**, 45, 3188 – 3196
4. van den Broek, B.; Noom, M.; van Mameren, J.; Battle, C.; MacKintosh, F. Biophysical Journal, **2010**, 98, 1902 – 1910.
5. Murayama, Y.; Sakamaki, Y.; Sano, M. Phys. Rev. Lett. 2003, 90(1), 018102 (4 pages)
6. Patel, M.; Anchordoquy, T. Biophysical Journal. 2004, 88 (3), 2089 – 2103
7. Chai, W. Work in progress. Johannes Gutenberg Universität-Mainz, PhD thesis.
8. Wakebayashi, D.; Nishiyama, N.; Itaka, K.; Miyata, K.; Yamasaki, Y.; Harada, A.; Koyama, H.; Nagasaki, Y.; Kataoka, K. Biomacromolecules, 2004, 5, 2128 – 2136.
9. Osada, K.; Christie, J.; Kataoka, K. J. Roy. Soc. Interface, 2009, 6, 325 – 339.
10. Otsuka, H.; Nagasaki, Y.; Kataoka, K. Advanced Drug Delivery Reviews. 2003, 55, 403 – 419.
11. Park, S.; Healy, K. Journal of Controlled Release, 1995, 95, 639 – 651.
12. Petersen, H.; Fechner, P.; Martin, A.; Kunath, K.; Stolnik, S.; Roberts, C.; Fischer, D.; Davies, M.; Kissel, T. Bioconjugate Chem. 2002, 13, 845 – 854.
13. Rungsardthong, U.; Deshpande, M.; Bailey, L.; Vamvakaki, M.; Armes, S.; Garnett, M.; Stolnik, S. Journal of Controlled Release. 2001, 73, 359 – 380.
14. Katayose, S.; Kataoka, K. Bioconjugate Chem. 1997, 8, 702 – 707.
15. Fu, C.; Sun, X.; Liu, D.; Chen, Z.; Lu, Z.; Zhang, N. Int. J. Mol. Sci. 2011, 12, 1371 – 1388.

16. Kabanov, A.; Vinogradov, S.; Suzdaltseva, Y.; Alakhov, V. Bioconjugate Chem. 1995, 6, 639 – 643.
17. Luo, L.; Tam, J.; Maysinger, D.; Eisenberg, A. Bioconjugate Chem. 2002, 13, 1259 – 1265.
18. Hietala, S.; Parviainen, H.; Andersson, T.; Tenhu, H. Proceeding of the 8th Polymers for Advanced Technologies International Symposium. Budapest, Hungary, 13 – 16 September 2005
19. Cavallaro, G.; Licciardi, M.; Mandracchia, D.; Pitarresi, G.; Giammona, G. Polym Int 2008, 57, 708-713
20. Lai, E.; van Zanten, J. Biophysical Journal, **2001**, 80, 864 – 873
21. Li, Y.; Yildiz, U.; Muellen, K.; Gorehn, F. Biomacromolecules, 2009, 10, 530 – 540.
22. He, S.; Arscott, P.; Bloomfield, V. Biopolymers **2000**, 53, 329 – 341
23. Osada, K.; Oshima, H.; Kobayashi, D.; Doi, M.; Enoki, M.; Yamasaki, Y.; Kataoka, K. J. Am. Chem. Soc., 2010, 132 (35), 12343 – 12348.
24. Itaka, K.; Yamauchi,K.; Harada, A.; Nakamura, K.; Kawaguchi, H.; Kataoka, K. Biomaterials. 2003, 24, 4495 – 4506.
25. Husale, S.; Grange, W.; Karle, M.; Buergi, S.; Hegner, M. Nucleic Acid Research, **2008**, 36(5), 1443 – 1449
26. Pelta, J.; Livolant, F.; Sikorav, J. The Journal of Biological Chemistry, 1996, 271, 5656 – 5662.
27. Toncheva, V.; Wolfert, M.; Dash, P.; Oupicky, D.; Ulbrich, K.; Seymour, L.; Schacht, E. Biochimica et Biophysica Acta **1998**, 1380, 354 – 368.
28. Osada, K.; Oshima, H.; Kobayashi, D.; Doi, M.; Enoki, M.; Yamasaki, Y.; Kataoka, K. J. Am. Chem. Soc., 2010, 132 (35), 12343 – 12348.
29. Grossberg, A.; Zhestkov, A. J. Biomol. Struc. Dynam, 1985, 3, 515 – 520.
30. Störkle, D.; Duschner, S.; Heimann, N.; Maskos, M.; Schmidt, M. Macromolecules, 2007, 40 (22), 7998 – 8006.
31. Ouameur, A., Tajmir-Riahi, H. J. Bio. Chem., 2004, 279 (40), 42041 – 42054.
32. N'soukpoé-Kossi, C.; Ahmed Ouameur, A.; Thomas, T.; Shirahata, A.; Thomas, T.; Tajmir-Riahi. Biomacromolecules 2008, 9, 2712 – 2718.
33. Thünemann, A.; Müller, M.; Dautzenberg, H.; Joanny, L.; Löwen, H. Polyelectrolyte complexes. Polyelectrolyte with defined molecular architecture II. Springer, 2004.
34. Plum, G.; Arscott, P.; Bloomfield, V. Biopolymers, 1990, 30, 631 – 643.
35. Berova, Nakanishi, Woody. Circular Dichroism: Principles and applications. Second Edition. Wiley-vch.
36. Feuerstein, B.; Pattabiraman, N.; Marton, L. Proc. Natl. Acad. Sci. USA. **1986**, 83, 5948 – 5952.

6. Formation of complexes with a plasmid (supercoiled) and DNA pUC19 in organic solvents

The formation of complexes between a polyelectrolyte and an oppositely charged molecule, i.e. a surfactant or another polyelectrolyte, in aqueous solution has been extensively studied. It has been reported that the interpolyelectrolyte complexes, meaning from a polycation and a polyanion, have usually a "disordered" structure described mainly by two models: ladder-like and scramble-egg. The final topology is typically defined by a mixture of these two models [1]. On the other hand, complexes between a polyelectrolyte and a surfactant tend to form mesophases with a high level of order [2].

Only a few researchers have succeeded in obtaining topologically-controlled structures of interpolyelectrolyte complexes. Duschner et al. demonstrated that under certain conditions, i.e. by using aprotic organic solvents (for example, DMF), the complex formation of PAMAM dendrimers with polystyrene sulfonate (NaPSS) leads to thermodynamically controlled complexes even though they exhibited a kinetically frozen structure in aqueous solution. Because NaPSS is not soluble in DMF, first complexes between NaPSS and a surfactant were formed [3,4].

As mentioned in the previous chapter, the polyelectrolyte chosen in this work to study the complex formation with surfactants and oppositely-charged polyelectrolytes is DNA. One of the reasons for this selection is that DNA complexes are viewed as future vectors for gene delivery into the nucleus of cells, which could lead to a successful gene therapy. Only very a few studies have addressed the issue of the final topology of the complexes in aqueous solutions, e.g. Störkle et al. demonstrated that independent of the topology of the polycation, DNA complexes always showed a "flower-like" or "scramble-egg" topology in aqueous solutions as a result of a kinetically controlled complexation [5, 6]. Nevertheless the nature is capable of producing complexes of DNA with greatly defined structures. A typical example of this is, for instance, the DNA packaging in chromatin and chromosomes. Chromosomal DNA is thousand times longer than the diameter of the nucleus of a cell; therefore DNA is compacted through some proteins to form chromatin, a well-defined supramolecular structure [7].

In the last chapter we succeeded in neutralizing 100% of the DNA charges with almost no excess of the multivalent cation PEG-PLL while forming unimolecular DNA complexes. The positive charges were given by the polylysine block with a degree of polymerization of 15. The objective of this chapter is to obtain these "ideal" complexes, via a "topologically" or "thermodynamically" controlled process with a polycation. For this purpose, the approach of Duschner et al is followed. Briefly, the DNA is bound with a cationic surfactant in order to generate a hydrophobic shell, which allows the dissolution of these complexes in organic solvents. A polycation with low charge density is then used to form complexes with DNA while displacing the surfactant. Details will be presented as follow.

The binding of surfactants into a polyelectrolyte, i.e. DNA, it is usually a cooperative process due to interactions between neighboring surfactants, for example, hydrogen bonding. In this respect, the behavior of alkyltrimethylammonium surfactants was studied by Dias et al [8]. A phase diagram for DNA complexes with hexadecyl-, tetradecyl- and dodecyltrimethylammonium in aqueous solution was postulated. The difference in the phase boundaries were attributed to the cooperative binding due to hydrophobic interactions. However, if precipitates from these complexes are dissolved in organic solvents, the hydrophobic interactions weaken or may even disappear leading probably to different structures to the ones in aqueous solutions. The structure of the polyelectrolyte complexes in any of the cases is not widely understood when an organic compound instead of water is used as a solvent. Several questions arise, i.e. the solubility of the complexes in this kind of medium and the new topology that these complexes may acquire. The first attempt to answer these questions was made by Ijiro and Okahata [9] with the dissolution of complexes between double-chain surfactants and DNA in hydrophobic solvents like benzene, chloroform and diethyl ether. Since then, several authors have tried to vary the system, e.g. the length of DNA, the type of surfactant and the solvents. In all of the cases, compacted structures were obtained [10, 11, 12, 13]. Cationic dialkyl amphiphiles, due to their higher hydrophobicity, were used in order to dissolve DNA in low-polar solvents, like chloroform, whereas single-chain cationic surfactants, for example, dodecyl- and cetyldecyltrimethylammonium surfactants were used to obtain complexes of DNA soluble in more polar solvents, mainly in alcohols. Nevertheless many incognitos are yet to be answered: Do the complexes consist of only one DNA molecule? Is there a partial dissociation of the surfactants in organic solvents since hydrophobic interactions are not longer present? Until now it has always been claimed that the DNA remained intact, meaning that the double helical structure of the DNA is not altered in organic solvents, but is this condition always satisfied?.

Our approach consists on adding alkyltrimethylammonium bromide surfactants, C_nH_{2n+2}- $(CH_3)_3N^+$ Br^-, with a hydrophobic tail consisting of n=12 and 14 atoms of carbon, to DNA until precipitation. After isolation, DNA-surfactant complexes were dissolved in different organic solvents. Positively-charged cylindrical brushes, that are not soluble in aqueous solutions due to their low charge density, are then added to the DNA in organic solvents.

In the biological field, it is accepted that a deeper physical chemical characterization of DNA complexes is necessary [14]. We believe that with our methodology we could gain a better understanding of the behavior of DNA complexes with surfactants and polycations. Furthermore, the study of DNA-surfactant complexes in organic solvents could be used as a model for the transfer of the complexes into "liquid membranes" [10]

The objective of this chapter is to determine the topology of DNA complexes, with surfactants and with polycations, in organic solvents.

6.1. Experimental section

The DNA used is pUC19-supercoiled DNA, which contains 2686 base pairs. Its characterization was shown in Table 5.1. (Chapter 5).

Complex formation. DNA is complexed with a series of surfactants and polycations according to figure 6.1. After precipitation with the trialkyltrimethylammonium surfactants, DNA complexes are isolated and dissolved in organic solvents. Next, polycations with low charged density were added and the topologies of the complexes were investigated. Details are given in the following sections.

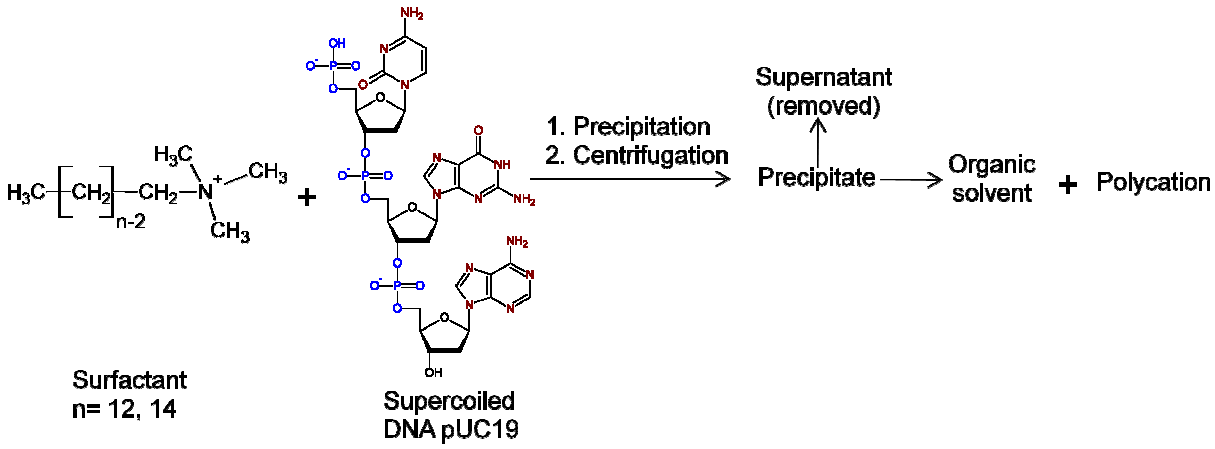

Figure 6.1. Procedure for DNA-polycation complex formation in organic solvents.

Surfactant-DNA Complex preparation. A stock solution of the surfactant was mixed with pUC19-Supercoiled DNA (c = 1 g/l) at ratios and with final concentrations listed in Table 6.2. The precipitates were centrifuged for 30 min at 4000 rpm and the supernatant was removed. The solids were freeze-dried for at least 24 h. After that, different organic solvents were added and the mixtures were gently agitated for one day. For light scattering experiments, solvents contained 1 mM of salt (typically NaBr). For AFM pictures the use of salt in the solvent was avoided.

Table 6.1.. Conditions for the formation of precipitates between DNA and different surfactants.

	DTAB	TTAB
Stock solution concentration (mM)	7.30	2.97
Critical Micellar Concentration (cmc) (mM)	16 [15]	3.6 [16]
N+/P-	5	9.53
Final concentration after mixing (mM)	5	2.71
Final DNA concentration (mM)*	1	0.28

*Concentrations expressed in terms of nucleotide bases.

DTAB: dodecyltrimethylammonium bromide, TTAB: tetradecyltrimethylammonium bromide, Concentrations and N+/P- for DTAB and TTAB were selected from Dias et al [8].

The transfer of the complexes to organic solvents immiscible in water was avoided, since it is already reported that usually this method does not lead to a successful dissolution of the complex in organic solvents [10]. The authors explained that both, DNA and the headgroup of cationic surfactants, are highly hydrated even after the formation of complexes. Sergeyev et al also pointed out that traces of water in the complexes may hinder their solubility in organic solvents; therefore the complexes need to be completely dry. [11]. However, Reimer et al. [17] succeeded in the transfer of DNA to an organic solvent (chloroform/methanol) in a biphasic system. The addition of an excess of commercial liposomes for gene transfection, i.e. lipofectine, lipofectamine and transfectam, was necessary.

Polycation-DNA formation of complexes. DNA-surfactant was complexed with three polymers positively charged: a linear polyvinylpyridine with 10% of quaternization (l-PVP-etBr), a non-quaternized polyvinylpyridine brush (b-PVP) and a polylysine brush (b-PLL). The characterization of the polyelectrolytes can be found in Table 3.

Table 6.2. Light Scattering characterization of investigated polymers

Polymer	Solvent	(dn/dc) (ml/g)	Mw (g/mol)	A_2 (mol.ml/g^2)	Rg (nm)	Rh (nm)	Rg/Rh
l-PVP-etBr**	Methanol	0.254	7.60×10^5	4.5×10^{-6}	88.8	23.5	3.8
b-PVP*	DMF	0.17	2.4×10^6	4.3×10^{-8}	42	28	1.5
b-PLL*	HFIP	0.23	1.3×10^7	-3.4×10^{-8}	78.8	45	1.75
PNIPAM*	Methanol	0.1754	3500	8.6×10^{-7}	< 5	1.6	-

- *Synthesis details of this polymer are given in [18], [19], and [20] for the b-PVP, b-PLL and the PNIPAM. The structure of these polymers can be found in the Appendix. The PNIPAM contains a trialkylammonium end-group, which provides it with one positive charge per polymer.

** The l-PVP-etBr was quaternized with ethylbromide. Details in ref [21]

Static and Dynamic Light Scattering. The equipments and conditions under SLS and DLS are described in section 5.1. Samples were filtered through a: GHP filter 200 nm (for DNA and surfactants in aqueous

solutions) and LG filter 200 nm (for complexes in organic solvents). Cuvettes were cleaned with distilling acetone. The sample solutions contained 1 mM of salt (LiBr) in order to screen electrostatic interactions.

Atomic Force Microscopy (AFM). 12 μL of the desired complex was placed on freshly cleaved mica, followed by spin casting. For imaging, a Multimode AFM instrument (Nanoscope IIIa instrument, Digital Instruments, Santa Barbara, CA) in the tapping mode was used.

Circular Dichroism spectroscopy. Circular Dichroism (CD) spectra were measured on a Jasco J-815 Spectrometer. Spectra were recorded between 200 and 320 nm (data pitch: 1 nm, scan mode: continuous, sensitivity: 10 mdeg, speed: 50 nm m-1, response: 4 s, bandwidth: 1nm, five accumulations) using a Hellma quartz cell with pathlength of 10 mm.

6.2. Dissolution in organic solvents

A direct complexation of DNA with polycations is not possible. Since DNA is mainly soluble in aqueous solutions, the prior complexation with a surfactant is necessary in order to create a "hydrophobic shell" that could allow dissolution of DNA into other solvents different from water. The advantage of using a polycation with a low charge density for DNA complexation is that coulombic interactions are reduced, which could increase the probability of internal rearrangement of the polyelectrolytes within the complex. On the other hand, the charges of a polyelectrolyte are responsible for its solubility in water. By reducing the amount of charges in a polymer, it becomes less soluble in aqueous solution**;** therefore the use of organic solvents becomes almost mandatory for the complex formation. Since DNA shows almost no solubility in other solvents but water [9], surfactants are used as a medium to dissolve DNA in organic solvents by "hydrophobizing" the DNA surface. These results are in agreement with the work of Leal et al. These authors claim that the solubility of DNA-DTA complexes increase with the decrement of the tail length of the alcohol used as solvent.

Two surfactants were used to bind DNA: tetradecyl- (TTA) and dodecyltrimethylammonium (DTA) bromide. The conditions for precipitation were found according to Dias et al. [8] to then dissolve the

complex of DNA with TTA in methanol and with DTA in DMF at final concentrations of 0.165 and 0.315 g/l, respectively. Several solvents were used for DNA-surfactant complexes (DNA-surf) dissolution (see table 6.3), however only the solvents reported here gave macroscopically homogeneous solutions. Ethanol and 1-propanol could visually dissolve DNA-TTA complexes but during light scattering measurements, adhesion to the walls was observed, even after hydrophobizing the interior of the cuvettes with a chloromethylsilane/toluene solution (2/98 v/v).

The dissolution of DNA-surf complexes in alcohols has been previously reported [12, 13]. The property of alcohols of acting as good solvents for DNA-alkytrimethylammonium surfactant is explained by means of its Gordon parameter (defined as the ratio between the surface tension and the cubic root of the molar volume of a liquid). Surfactants have the tendency of forming micelles in low-polar or highly-polar solvents, e.g. solvents with a Gordon parameter higher than 1.3 J/m^3. Alcohols show typical Gordon parameters lower than 0.6 J/m^3, therefore the hydrophobic tails of the surfactants forming complexes with DNA do not show the tendency of aggregation [12]. On the other hand, to the knowledge of the authors, the dissolution of DNA-surf in DMF has not yet been reported. Only the work of Mok et al [22] showed DNA nanogels encapsulated with crosslinked PEG soluble in methanol and DMF. The Gordon parameter of DMF is around 0.83 J/m^3, also below the established limit of 1.3 J/m^3 for the formation of micelles and Graciani et al indeed showed that the cmc of DTAB and TTAB increases around four times more in a solution of DMF-water 20% compared to pure water [23]. It is known, that the critical association concentration (cac) could be even an order of magnitude lower than the cmc, since the electrostatic repulsions do not play a role, therefore the Gordon parameter could be useful only for a qualitative explanation of the dissolution of the DNA-surf complexes in organic solvents. It is important to notice that this dissolution also depends on specific interactions between the solvents and the complexes mentioned before and the Gordon parameter alone cannot explain the solubility of the complexes in organic solvents.

The results in Table 6.3 are in agreement with the work of Leal et al [12]. These authors observed that the dissolution of DNA-DTA complexes increases with the decrement of the length of the tail of the alcohol used as solvent.

Neither DNA-DTA nor DNA-TTA were soluble in low-polar organic solvents, which is in accordance to results of Mel'nikov and Lindman. These authors showed that only complexes formed with double-tail surfactants can be dissolved in low-polar organic solvents like chloroform; nevertheless surfactants like CTAB are not hydrophobic enough to favor the dissolution in this kind of solvents [10]. The electrostatic interactions are responsible for the binding between surfactants and DNA. However, the hydrophobicity of the tail determines the solvents in which the complexes are soluble [9] and its supramolecular structure [17]. For instance, DNA complexes with surfactants containing aromatics moieties, i.e. carbazole and triphenylamine are soluble in chloroform, methanol and ethanol but also insoluble in THF, n-hexane and toluene [24]. It is also very important to notice that simple neutralization of the charges by multivalent cations without a hydrophobic part does not lead to complexes soluble in organic solvents. Reimer et al [17] could not dissolve DNA complexes with lysine (1+), magnesium (2+), and polylysine (polycation) whereas these authors obtained complexes soluble in chloroform with liposomes.

The complexes are only soluble, if the procedure described in figure 6.1 is followed. In this work, it has been observed that variations of this methodology, i.e. formation of complexes with a charge ratio of mixing N+/P- 1:1 (with no precipitation observed) after either freeze-drying or standard drying does not lead to complexes, which are able to be dissolved in neither of the organic solvents mentioned before.

Table 6.3. Solubility of DNA -Tetradecyltrimethylammonium bromide(DNA-TTA) and DNA -Dodecyltrimethylammonium bromide (DNA-DTA) precipitate in organic solvents

Solvent	Solubility DNA-TTA	Solubility DNA-DTA
Dimethylformamide	X	√
Nitromethane	X	X
Methanol	√	X
Ethanol	X*	
1-propanol	X*	
1,1,1,3,3,3-hexafluoro-2-propanol	X	X
Tetrahydrofurane	X	X
Hexane	X	
Toluene	X	

X* It could visually dissolved DNA-TTA complexes (macroscopically homogeneous solutions) but adhesion to the walls the cuvette for light scattering was observed, even after hydrophobizing the interior of the cuvettes with a chloromethylsilane/toluene solution (2/98 v/v) as described in ref [21].

6.3. Characterization of complexes in organic solvents

6.3.1. Topology of DNA-surf complexes in organic solvents

Characterization of the DNA-surf complexes is shown in Table 6.4 and their respective AFM pictures are shown in Figure 6.2

Table 6.4. Light scattering characterization of DNA-surfactant complexes

Complex	Solvent	(dn/dc) (ml/g)	Mw (g/mol)	A_2 (mol.ml/g^2)	Rg (nm)	Rh (nm)	Rg/Rh
DNA-TTA	Methanol	0.17	1.20×10^6	1.4×10^{-7}	40.6	29.0	1.4
DNA-DTA	DMF*	0.071	2.93×10^6	1.9×10^{-7}	75.3	62.1	1.2

- Concentration lost due to filtration was unavoidable.

The molar mass of the complexes in table 6.4 is determined by light scattering using the DNA concentration without considering the gain of mass due to the bounded surfactant. Hence, the molar mass reported here is higher than the true molar mass. Complexes between DNA-TTA in methanol show a topology that is more compacted compared to the supercoiled DNA pUC19 in aqueous solution, i.e. the hydrodynamic radius (Rh) is reduced from 43 nm to 29 nm in methanol and the radius of gyration goes from 65.6 to 40.6 nm. Nevertheless the ρ-ratio (Rg/Rh) remains relatively constant around 1.4. The AFM picture (Figure 6.2a) shows two coexisting populations: compacted spheres and more elongated rod-like structures. It is important to emphasize that the radius of gyration of the DNA-TTA complexes in methanol may depend on their concentration (see Zimm Plot of the DNA-TTA complexes in Appendix A13), therefore the radius of gyration reported here is only an average over the Rg at different concentrations. This dependency of Rg with the concentration of the complexes in methanol is reproducible and not an artifact

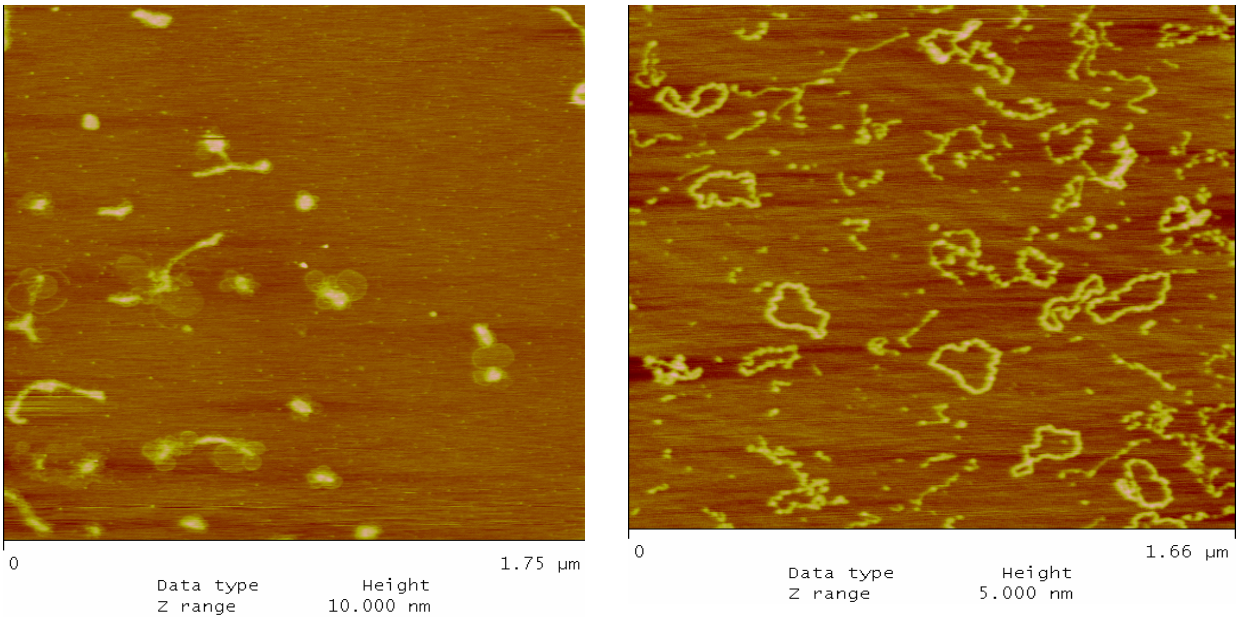

(a) **(b)**

Figure 6.2. AFM pictures of a) DNA-TTA complexes in methanol and b) DNA-DTA complexes in DMF

The results shown in table 6.4 are in agreement with several studies of DNA-surf complexes in organic solvents, in which a compacted topology was always obtained [10, 11, 13]. Sergeyev et al [11] studied the formation of complexes of two DNA of different lengths with dioctadecyldimethylammonium bromide in organic solvents like chloroform and concluded that DNA is a pre-stressed molecule showing an extended conformation in aqueous solutions due to repulsions of the negative charges on the surface; however if the charges are screened, DNA has the tendency to be in a compacted conformation. On the other hand, Sergeyev et al. [13] elucidated the mechanism of dissolution of DNA-CTA complexes in alcohols by analyzing the complexes dissolved in an alcohol-water mixture at different ratios with fluorescent microscopy and they presented a model of DNA with a globular conformation surrounded by surfactant molecules attracted due to electrostatic interactions.

Surprisingly, a surfactant with only two carbons less on the tail (DTAB) forms complexes with DNA exhibiting a complete different topology, i.e. an expanded circular conformation with a ρ-ratio of 1.2. It is known that the charges of a surfactant promote the formation of complexes with DNA but the hydrophobic part defines the solubility and topology of the complexes [9]. Although it could be argued that the interaction between neighboring surfactants is stronger in the case of DNA-TTA, the difference of

hydrophobicity does not account for the large change of conformation. In the next sections, the reasons for the different topologies will be analyzed in detail.

Some authors have identified a shift of the conformation of DNA complexes (measured with CD spectroscopy) in organic solvents with the addition of water[9, 12, 13]. This dependency of the topology with respect the amount of water is out the scope of this work and does not seem to represent an issue since the complexes are hydrophobic and therefore the absorption of humidity after the process of freeze-drying is unlikely. Furthermore the content of water of the organic solvents used for dissolution of the complexes is lower than 44 mmol/dm^3 (0.792 g/l) and 40% water (7.2 g/l), concentrations at which the conformation of DNA complexes starts to change in chloroform [9] and in alkyl alcohols with low carbon chains [13], respectively.

6.3.2. Possible causes for the low molar mass of the complexes

The values of the molar masses of the complexes in organic solvents presented in Table 6.4 are smaller than the molar mass of DNA pUC19. There are three possible explanations: 1. DNA denatures in the presence of organic solvents in spite of the surfactants bound to it, 2. the complexes are being degraded, and 3. the surfactants dissociate from the DNA in organic solvents

6.3.2.1. Denaturation of DNA-surf complexes in organic solvents.

For the DNA-TTA in methanol, the first explanation seems to be appropriate. UV measurements of these complexes gave an extinction coefficient of 9163 l/mol.cm (see Appendix A17), corresponding to the value of a single-stranded DNA in aqueous solution. It is known that extinction coefficients cannot be compared in different solvents. However, Sergeyev et al. [13] obtained a similar result for denatured DNA in alcohols. Also Sorokin et al [25] observed an increase of the extinction coefficient during the denaturation of DNA with the addition of glycerol and Sergeyev et al [11] determined approximately the same extinction coefficient (6600 mol^{-1}cm^{-1}) of DNA in buffer and non-denaturated DNA-surf complexes

in organic solvents. Figure 6.3 shows that DNA in aqueous solution has a B-conformation characterized by a minimum at a wavelength λ=254 nm and a maximum around λ=280 nm. A comparison of the CD spectroscopy spectra of DNA in aqueous solution and the complexes in methanol demonstrates a pronounced change of DNA conformation, e.g. a dramatic decrease of the ellipticity, also shown to correspond to single stranded DNA [26] or a P conformation of DNA [27, 28]. These two conformations are essentially indistinguishable. However, a displacement of the spectra with a maximum at 280 nm to the right (towards 300 nm) is mainly only seen in the "typical" denatured DNA and not in the P-conformation. The ellipticity of DNA in methanol is very difficult to determine experimentally, because pure DNA is insoluble in this solvent. Nevertheless, Qu et al [24] measured the CD spectrum of the DNA- triphenylamine complex in methanol and the ellipticity is only slightly reduced (approximately 10%). Thus, it could be speculated that DNA-TTA complexes in methanol denature. It is known that pure DNA denatures in organic solvents. Sorokin et al [25] stated that organic solvents usually increase the electrostatic repulsion between the two strands of the DNA due to the decrease of the dielectric constant and the hydrophobic interactions among the bases also tend to disappear. After having measured the denaturation temperature of DNA and DNA complexes with polycations in several organic solvents, Schindler et al [29] concluded that organic solvents lower the denaturation temperature but it is not correlated with the dielectric constant of the solvent. Even if the denaturation of unbound DNA has been widely studied, from a experimental and a theoretical point of view [30] our results are still striking since until now, it has been always reported that DNA retains its double stranded nature in organic solvents when bound to surfactants [9, 10, 13, 24]. One reason for the observed denaturation of DNA in this work may be related to dissociation of the surfactants from the complexes. This issue will be discussed in section 6.3.

For the case of DNA-DTA, spectroscopic measurements were not possible since the cut-off wavelength of DMF with UV light is around 270nm. However, CD spectra until this wavelength could demonstrate also some changes in the conformation. Also the AFM picture in Figure 6.2 shows some degradation products of theses complexes in DMF (in the dried state after spin casting).

In order to prove that the denaturation of the DNA is caused by the organic solvent and not during the formation of the complexes with the surfactants, mixtures of the DNA and alkyltrimethylammonium compounds were prepared at concentrations closed to precipitation. In case of disruption of surfactant into

the helical structure of the DNA, changes of the conformation of DNA (and therefore of the CD spectra) should be observed. However, figure 6.3 shows that the conformation of DNA remains almost unchanged after the addition of the amphiphiles.

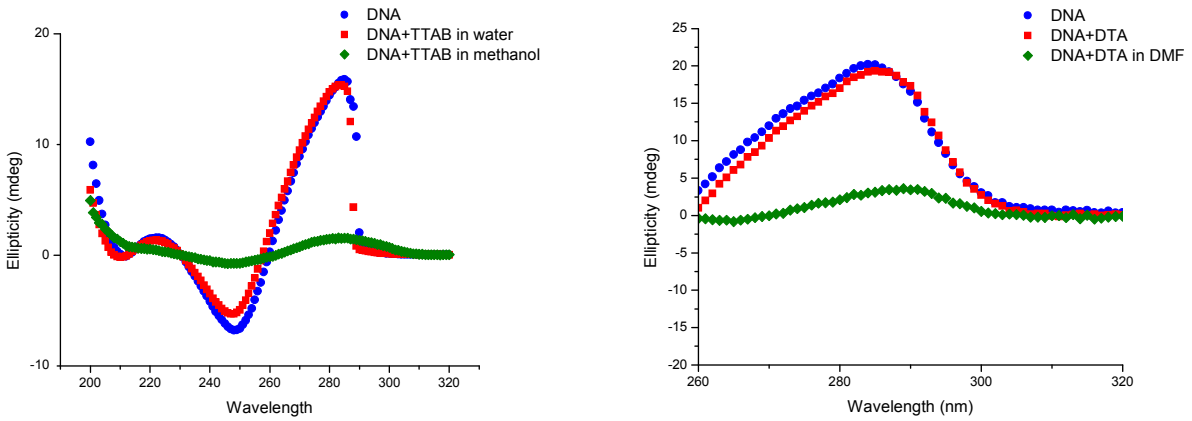

(a) (b)

Figure 6.3. CD Spectroscopy of DNA pUC19 and DNA complexes with (a) TTAB and (b) DTAB in aqueous solution and in organic solvents, methanol and DMF respectively. The concentration of DNA is kept constant in all of the cases and equals to c=0.165 g/l in the case of methanol and c=0.315 g/l for DMF.

The molar mass expected for a denatured and fully-neutralized DNA with TTA in methanol is 1.75×10^6. However, the measured value with light scattering is only 1.20×10^6. The low molar mass of the complexes in methanol and the appearance of small degraded chains in the AFM pictures of the complexes in DMF (see figure 6.2) suggests that the complexes are being at least partially degraded. This topic will be covered in the next section.

6.3.2.2. Degradation of DNA-surf complexes in organic solvents

To investigate whether degradation of the DNA complexes in organic solvents has taken place, two approaches were taken: 1) The values of static light scattering intensity were analyzed with equation 5.4

(see section 6.3.2.3) and 2) DNA was isolated and characterized through light scattering techniques (described in this section). For this reason, DNA-TTA complexes in methanol were dialyzed against an aqueous solution of 0.7 M NaCl with a clear cellulose ester dialysis membrane with a molecular weight cut off between 8000 – 10000 g/mol. These conditions were found ideal to dissociate the polycations from DNA in aqueous solutions [30]. Monovalent cations at such high concentration debilitate the electrostatic interactions between the surfactant and the DNA. The amphiphilic cation leaves the complexes and the DNA is unbound and can be characterized by means of light scattering. The results are shown in Table 6.5

Table 6.5. Light Scattering characterization of pUC19-Supercoiled DNA after dissociation DNA-TTA complexes in methanol solution.

Polymer	Solvent	(dn/dc) (ml/g)	Mw (g/mol)	A_2 (mol.ml/g^2)	Rg (nm)	Rh (nm)	Rg/Rh
dialyzed dsDNA pUC19	0.7M NaCl	0.17	9.86×10^{5} (a) 1.18×10^{6} (b)	4.64×10^{-8} (a) 4.43×10^{-8} (b)	91.2	58.8	1.55

(a) Concentration determined spectrometrically assuming that the complete amount of DNA has been renatured.

(b) Concentration determined spectrometrically assuming that 39% of DNA is renatured.

The molar mass of the dialyzed DNA is lower than the molar mass of DNA (see table 6.5). To explain this result, two scenarios are considered: 1. DNA is completely renatured after being transferred to aqueous solutions during the dialysis and the low molar mass is attributed to degradation of the DNA. 2. DNA is not degraded but its renaturation is only partial. It is important to mention that the difference in the molar mass depending on the scenario (see table 6.5) is a consequence of using a different concentration for each of the cases. To determine the weight-averaged molecular weight of with SLS, the concentration of the sample must be known. The concentration of DNA was measured with a UV-vis spectrometer. Nevertheless, to determine the concentration in this manner, a value of the extinction coefficient must be given. For the first case, i.e. complete DNA renaturation is assumed, the value of double stranded DNA (6600 l/mol) is utilized to determine the concentration. In the case that DNA is only partially renatured (second scenario), the concentration cannot be directly determined, since the extinction

coefficient is unknown. The measured absorbance is the result of the addition of the single-stranded (ssDNA) and double-stranded DNA (dsDNA). Therefore, an iteration process is applied in which 1. An initial DNA concentration is assumed and the concentrations after further dilutions are calculated. 2. The weight-averaged molecular weight is determined and since the molar mass of each of the components (ssDNA and dsDNA) is known, the weight fraction of each of the component is found and 3. The concentrations of each component and the total absorbance are calculated. The iteration finishes, when the calculated absorbance matches the measured absorbance. With this procedure, a weight fraction of 0.389 for dsDNA was calculated and a weight-averaged molecular weight of 1.18×10^6 (see table 6.5) was obtained with the Zimm plot.

In the case that DNA is 100% renatured and hence, the low molar mass measured is caused by degradation, DNA fractions in average with 50% of the original molar mass are expected. The two strands of the DNA must be cut at least in two points. Thus, the geometrical restrictions disappear and the DNA presents a linear topology, instead of a supercoiled one. The radius of gyration of the degraded DNA can be determined. In section 7.1 the radius of gyration of a linear DNA with the same molar mass than the original DNA pUC19 (1.7×10^6 g/mol) is measured (Rg=139.7 nm). Since the degraded DNA has only approximately half of the molar mass than the original DNA, the fractions must have a radius of gyration of 70 nm. Notice that for rod-like structures the molar mass is proportional to the length (M~L) and the radius of gyration is proportional to the length of the cylinder $Rg = L/\sqrt{12}$. A reduction of 50% of the molar mass causes the radius of gyration of a cylinder to be also reduced to 50% of the original Rg. The radius of gyration of the dialyzed sample measured with SLS is 23% higher than the theoretical Rg for a rod-like structure. The reason for this discrepancy can be explained in terms of polydispersity. The degradation of DNA very likely produces fractions with different sizes. It is known that polydispersity increases the radius of gyration of sample containing the same weight-averaged molar mass (or length in the case of cylinders) [31]. Furthermore, because the DNA is randomly cut, nicked-DNA (open circular) could be also present. Supercoiled DNA adopts this open circular topology, if only of the strands is cut in one point. The radius of gyration for this structure is equal to the radius of the ring. The contour length of DNA pUC19 is 910 nm, therefore $R = Rg = \frac{L}{2\pi} = \frac{910nm}{2*3.1416} = 144.8nm$. A small percentage of open circular DNA could also lead to an increase in the radius of gyration.

In the second scenario, it is assumed that DNA is only partially renatured. In this case, single (ssDNA) and double-stranded DNA coexist in solution. This scenario is not likely to happen because when supercoiled DNA is denatured, i.e. upon dissolution in organic solvents, the two strands remain "anchored" and therefore under adequate conditions, for instance, after it has been transferred into aqueous solution, renaturation is complete. Also renatured supercoiled DNA maintains its topology and the radius of gyration should be only 43 nm (see table 5.1). On the other hand, denatured DNA loses its helix conformation; hence it has a persistence length of 1.5 nm [32] and acquires a globular structure. Single stranded DNA is more hydrophobic because the bases are exposed to the aqueous solutions, thereby it has a compacted topology. A radius of gyration of 91 nm cannot be explained under this scenario.

The conformation of the dialyzed DNA was determined with CD spectroscopy. Results are shown in figure 6.4. Linear DNA has a lower intensity than supercoiled DNA and denatured DNA has even a lower intensity and the maximum at λ=280 nm is shifted to higher values (~290 nm). The CD spectra of the dialyzed and the linear DNA are almost identical within experimental error. The results seem to confirm that DNA complexes in methanol are degraded into smaller linear fractions and that DNA is entirely renatured after dialysis against an aqueous solution. The CD spectrum of denatured DNA (DNA-TTA in methanol) is plotted for comparison reasons. It can be observed, that the intensity of DNA in methanol is even lower than linear double-stranded DNA.

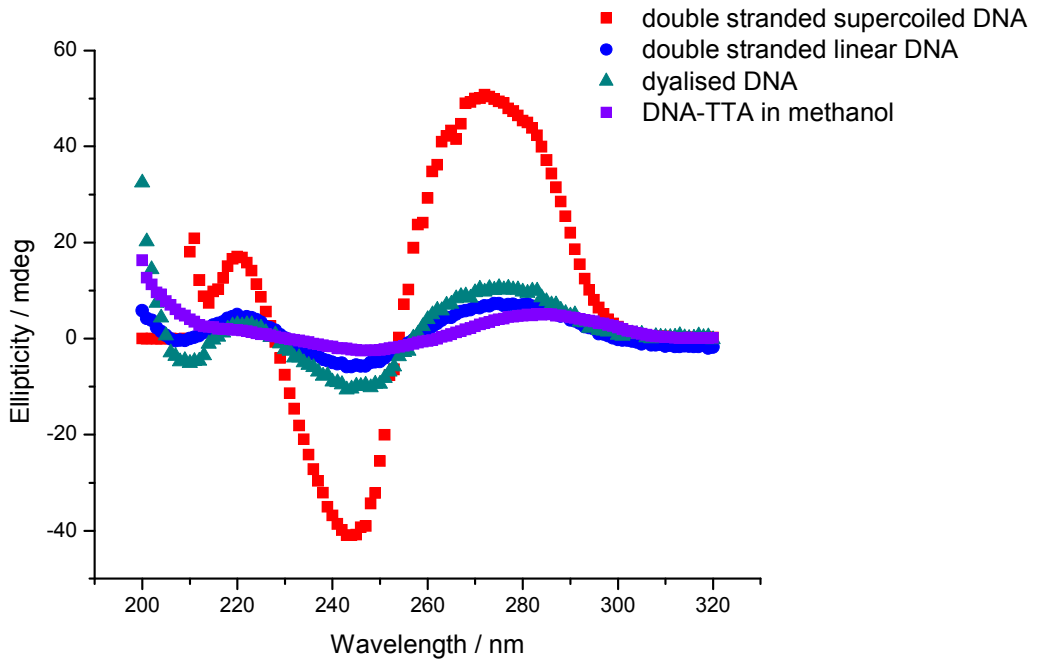

Figure 6.4. CD Spectroscopy of supercoiled DNA pUC19 (red squares), linear double stranded DNA (blue circles) and DNA-TTA complexes after dialysis against 700 mM NaCl aqueous solution (green triangles). All the spectra were normalized to a concentration of 1 g/l.

It must be taken into account, that in the first scenario (DNA degradation) there could be a fraction of DNA, which is partially denatured. It is not very likely that such a long DNA with 2686 base pairs per strand renatures 100% after having been randomly cut.

The dialysis and the subsequent light scattering measurements were only carried out for DNA-TTA in methanol, because of the difficulty in finding commercial dialysis membranes adequate to work with DMF. The reasons for the degradation of DNA-surf complexes in organic solvents is yet to be found, however, it has been already reported that DNA is degraded after it has been emulsified in an oil phase and then re-emulsified in aqueous solution. The degradation was attributed to the shear stress conditions to prepare the emulsions. [33]

6.3.2.3. Dissociation of the surfactants from the complexes in organic solvents. Addition of free surfactant to the DNA complexes: An equilibrium study.

As DNA-surf complexes are macroscopically dissolved in organic solvents, equilibrium of dissociation may take place, in which the surfactants distribute themselves between the free and the bounded (to DNA) states. It is well known that monovalent cations cannot condense DNA. Cationic surfactants with only one charge are able to bind DNA in aqueous solutions due to the hydrophobic interactions of neighboring surfactants. However, these interactions disappear in organic solvents; therefore partial dissociation of the surfactant is expected [11]. For instance, Leal et al [12] found out that DTA is partly dissociated in a mixture of water/decanol. It is also important to mention that electrostatic interactions are increased since water is replaced by solvents with lower dielectric constants. Sorokin et al. [25] applied the following relationship to calculate the equilibrium constant K of monovalent cations with no hydrophobic tails upon a change of solvent from water to organic solvents as a function of the dielectric constants ε.

$$\frac{logK_{organic\ solvent}}{logK_{water}} = \frac{\varepsilon_{water}}{\varepsilon_{organic\ solvent}} \qquad (6.1)$$

Rearranging the equation 6.1.

$$K_{organic\ solvent} = (K_{water})^{a} \qquad (6.2)$$

Where a = 2.4 for methanol and a= 2.1 for DMF. According to equation 6.2, dissociation of the surfactant from the DNA complexes is not to be expected; however, as stated before, the total disappearance of the hydrophobic interactions is not taken into account.

To corroborate the hypothesis of partial dissociation of the surfactant in organic solvents, the complexes are titrated with a concentrated solution containing only the surfactant.

The addition of free surfactant to a solution of the complexes increased the static light scattering intensity (figure 6.5). Since this intensity is proportional to the molecular weight of the sample, free surfactants must be binding the initial complex. The following equilibrium is then proposed.

After dissolution in organic solvents

$$\text{DNA-(n) surf} \text{ ----- } \text{DNA-(n-x)surf} + \text{(x) surf}$$

Through the addition of free surfactant

$$\text{DNA-(n-x) surf} + \text{(m) surf} \text{ ---- } \text{DNA-(n-x+y)} + \text{(m-y) surf}$$

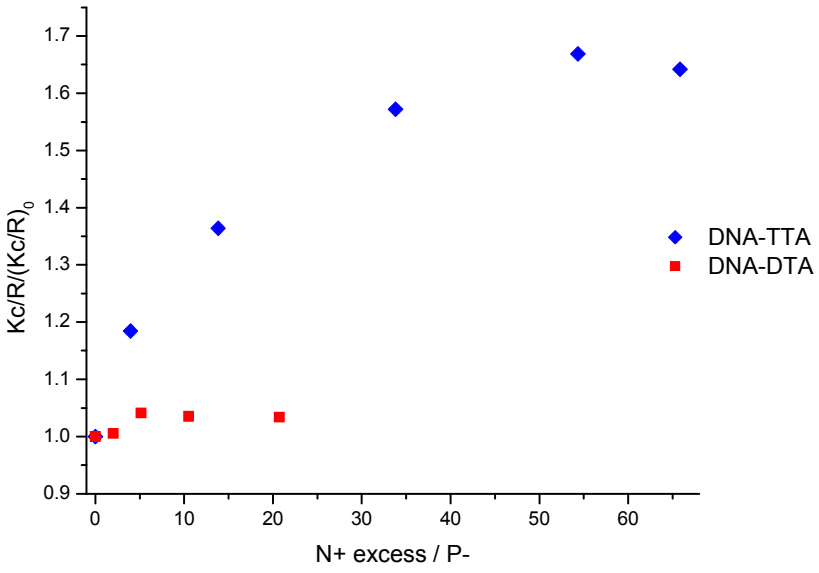

Figure 6.5. Static light scattering intensity ratio (extrapolated to q = 0) as a function of the concentration of excess of surfactant. $(Kc/R)_0$ refers to the complexes in organic solvents before the addition of surfactant. DNA concentration (without surfactant) is used to calculate the static light scattering intensity (Kc/R)

For DNA-TTA a pronounced dissociation is demonstrated in figure 6.5. The SLS intensity increases approximately 70%. The exact molecular weight of the complexes cannot be determined, because their concentration in unknown and depends directly on the molar mass. Two methodologies are taken to find the molar of the complexes after dissociation of the surfactant (Mdiss). In the first methodology an apparent molar mass ($M_{w,app}$) is determined by using the concentration of non-dissociated complexes ($c_{non-dis}$), in other words, under the assumption that all of the charges of DNA are neutralized by the surfactant and dissociation does not take place.

$$\frac{Kc_{non-dis}}{R_{diss}} = \frac{1}{Mw,_{app}} \tag{6.3}$$

The complexes scatter the light with intensity R_{diss}. If the concentration of the complexes after dissociation (c_{diss}) is used instead, the true molar mass (M_{true}) can be calculated

$$\frac{Kc_{diss}}{R_{diss}} = \frac{1}{Mw,_{diss}} \tag{6.4}$$

Dividing equation 6.3. and 6.4

$$\frac{c_{non-dis}}{c_{diss}} = \frac{Mw,_{diss}}{Mw,_{app}} \tag{6.5}$$

Hence,

$$Mw,_{app} = Mw,_{diss}\left(\frac{c_{diss}}{c_{non-dis}}\right) \tag{6.6}$$

It can be demonstrated that

(6.7)

$$\frac{Mw,_{diss}}{Mw,_{non-dis}} = \frac{c_{diss}}{c_{non-dis}}$$

The apparent molar mass can be then expressed as

$$M,_{app} = Mw_{non-dis}\left(\frac{c_{diss}}{c_{non-dis}}\right)^2 \qquad (6.8)$$

With equation 6.8 the concentration of the complexes after dissociation (c_{diss}) can be determined and with equation 6.6 the true molar mass can be calculated. Results are shown in figure 6.6.

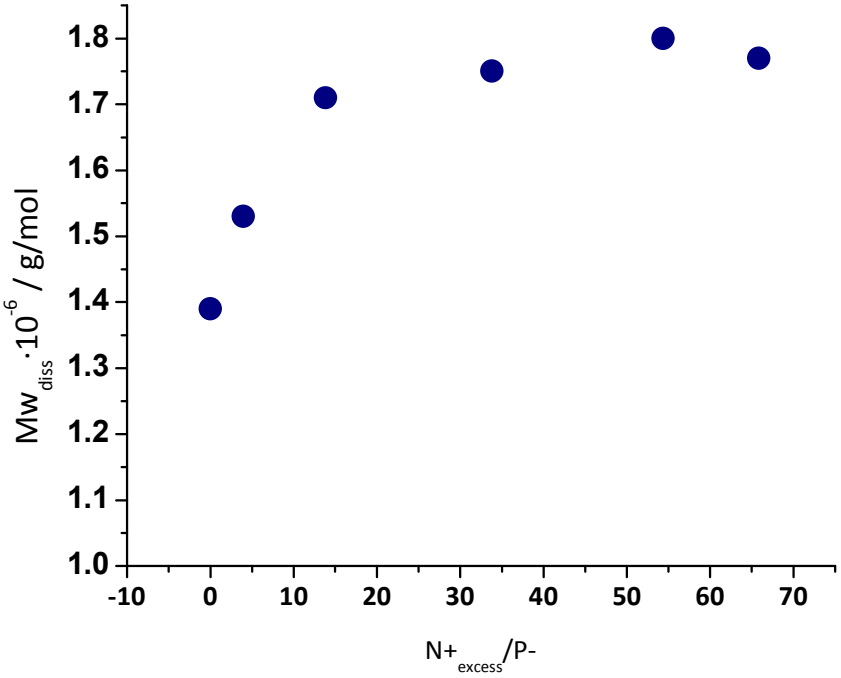

Figure 6.6. Calculated true molar mass of DNA-TTA complexes in methanol upon dissociation. $Mw_{non-dis}$ used for the calculations is $3.5x10^6$ g/mol. This value corresponds to a double stranded DNA with 100% of the charges neutralized with TTAB.

It is important to mention that the formulas above only apply at the limit of $c \rightarrow 0$ (very dilute solutions). The term "Mw_{diss}" does not mean that the concentration dependency was taken into account during the SLS measurements.

The maximum molar mass of DNA-TTA complexes (calculated at $N+_{excess}/P-=54.3$) is $1.77x10^6$. This molar mass is in agreement with the molar mass of a degraded DNA into fractions with a molar mass 50% lower (in average) with 100% of the charges neutralized with the surfactant. However, if the DNA is denatured in organic solvents, the molar mass should be lower.

In the second methodology, it is assumed that the plateau in figure 6.5 is reached after 100% neutralization of the DNA charges. In this case, the number of surfactants bound to the DNA (*f*) would be the equal to the number of DNA bases

$$M_{w,DNA} = M_{base} * \text{number of DNA bases} = M_{base} * f \quad (6.9)$$

To find "*f*", equation 5.4 is used. In this case, the apparent molar mass is not defined in terms of the static light scattering evaluated using the concentration of a fully-complexed DNA. Instead, the apparent molar mass Mw,app is defined as the molar mass obtained with SLS when only the DNA concentration is employed for data evaluation.

$$M_{w,app} = R/Kc_{DNA} \quad (6.10)$$

From equation 5.4, the following expression can be obtained

$$M_{w,app} = \left(\frac{M_{cation}{}^2}{M_{base} f} f^2 + 2M_{cation} f + M_{base} f \right) \quad (6.11)$$

Rearranging this equation

$$M_{w,app} = \left(\frac{M_{cation}{}^2}{M_{base}} + 2M_{cation} + M_{base} \right) f \tag{6.12}$$

Hence

$$f = \frac{M_{w,app}}{\left(\frac{M_{cation}{}^2}{M_{base}} + 2M_{cation} + M_{base} \right)} \tag{6.13}$$

At the saturation point $N+_{excess}/P-=54.3$ (asymptote) $M_{w,app} = 1.9x10^6$ g/mol

$$f = \frac{1.9 * 10^6}{\left(\frac{256^2}{315} + 2 * 256 + 315 \right)} \tag{6.14}$$

$$f = 1836$$

In other words, the DNA forming the complexes has 1836 bases. The molar mass of the DNA must then be 578340 g/mol. This molar mass is clearly lower than the molar mass of the dialyzed DNA determined in section 6.3.2.2 ($M_{w,DNA}$ = . $9.86x10^5$). Since the molar mass calculated with this last approach is approximately the half of the molar mass of the dialyzed DNA, it might be deduced that the DNA is denatured in organic solvents and upon dialysis a large fraction of it renatures.

With the DNA molar mass of 5.8 $x10^5$ g/mol the percentage of the DNA charges neutralized by surfactants can be obtained as shown in figure 6.7.

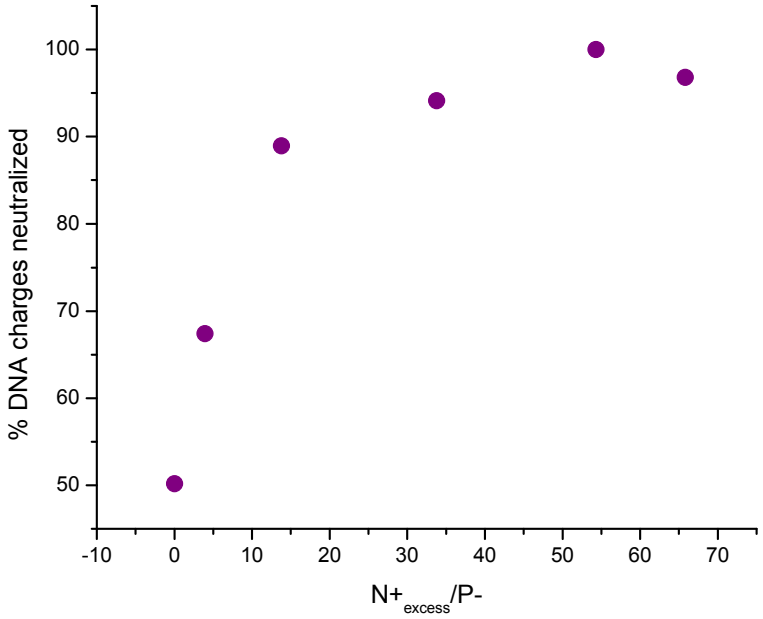

Figure 6.7. Fraction of DNA charges neutralized by TTAB in methanol after addition of an excess of surfactant.

In figure 6.8, it is shown that the z-average radius of gyration and the hydrodynamic radius of both complexes, DNA-TTA in methanol and DNA-DTA in DMF do not increase dramatically. There is no indication of aggregation, even after 100% of the negative charges are complexed. The ρ-ratio remains relatively constant. The equilibrium constant calculated for the dissociation of the surfactant TTAB from the complexes in methanol at 20°C (293 K) is $K_{diss} = 1.913 \times 10^{-3}$ M.

On the contrary, DTA barely leaves DNA. As for the case of DNA-TTA, the values of Rg and Rh do not show significant variations. The differences between the theoretical molar mass (3.35×10^6) and the determined by SLS, 2.23×10^6 (see table 6.4) could be attributed to degradation (observed by AFM in figure 6.2) assuming that the DNA is not partly denatured.

The difference in the dissociation degree of TTA and DTA from DNA may explain the differences in the topologies. A more "naked" DNA could acquire a more compacted conformation in order to reduce the surface exposed to a "bad" solvent.

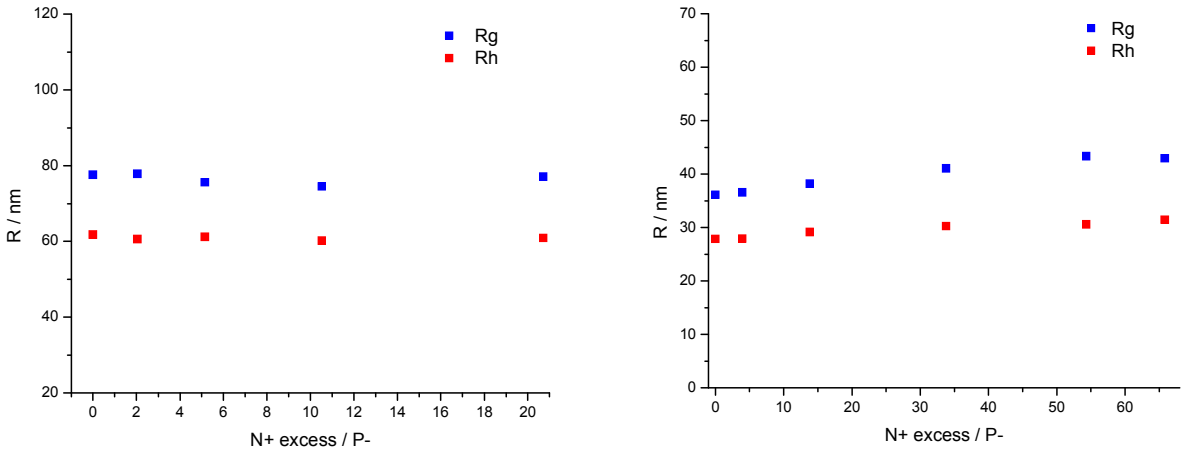

(a) (b)

Figure 6.8 Hydrodynamic radius and radius of gyration of (a) DNA-TTA complexes in methanol after the stepwise addition of TTA and (b) DNA-DTA complexes in DMF after the stepwise addition of DTA

The polydispersity of the complexes upon the addition of the free surfactant was evaluated by fitting the correlation function of the complexes at 90° (see figure 6.9). A limit of u_2=0.05 is usually taken to consider a sample "monodisperse". DNA-TTA complexes are less polydisperse than the DNA-DTA complexes in DMF. These last complexes consist of rings, and degraded and non-degraded rod-like structures (see AFM pictures in figure 6.2), therefore it is expected that they show a larger polydispersity than DNA-TTA complexes in methanol.

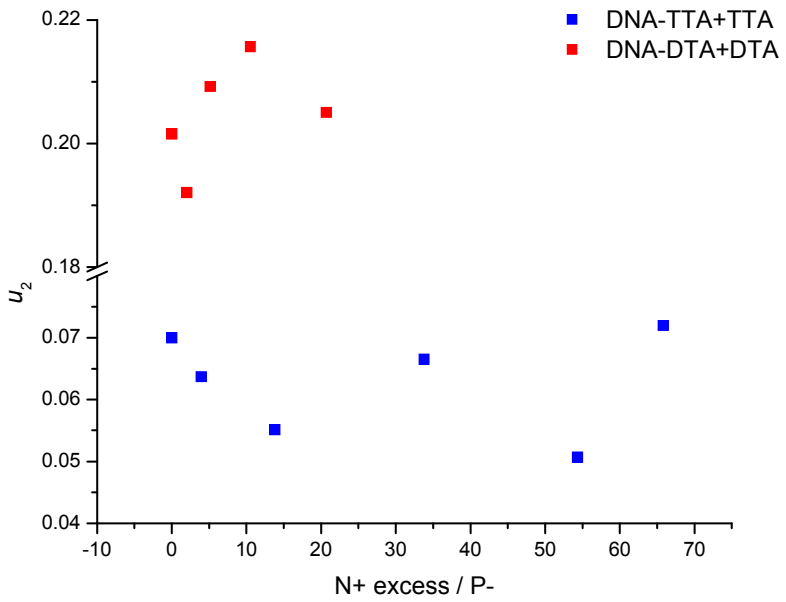

Figure 6.9 Polydispersity coefficient u_2 given by the second term of a Cumulant fit of DNA-surf complexes after the stepwise addition of surfactant (same conditions as in figures 6.4 and 6.5).

Upon addition of the surfactant, the UV-vis signal the ellipticity (with CD spectroscopy) of the DNA-surf + free surfactant were measured to investigate the role that plays the increment of electrostatic repulsions between the two DNA strands in organic solvents. We speculated that the complete neutralization of the negative charges from the phosphate groups could lead to renaturation of DNA. The results show that the DNA does not undergo any change in conformation after free surfactant was added (see Appendix A22 and A23).

6.3.2.3.1. Additional studies on the equilibrium of the surfactants between bounded and free state in organic solvents

6.3.2.3.1.1. Effect of temperature on the dissociation of DNA-TTA in methanol

In section 6.3.2.3 it has been demonstrated that DNA-TTA complexes undergo an equilibrium in which the surfactant is found in the bound as well as in the free states. It is interesting to evaluate the effect of the temperature in this equilibrium. Figure 6.10 shows the temperature dependency of the molar mass and the Rg and Rh of the complexes.

After increasing the temperature from 288 to 303 K, the molar mass of the complexes remains constant. The equilibrium is not affected by the changes of temperature in this range. In other words, the equilibrium proposed in section 6.3.2.3 is not shifted to any side of the reactions. By analyzing equation 6.15, the change of the equilibrium constant K_2/K_1 with the temperature T is exponentially proportional to the change of enthalpy

$$ln\left(\frac{K_2}{K_1}\right) = \frac{-\Delta H}{R}\left(\frac{1}{T_2} - \frac{1}{T_1}\right) \quad (6.15)$$

By substituting the two extreme values of the temperature from figure 6.16, the ratio of the equilibrium constants from K_1 at T_1=288 K to K_2 at T_2=303K is given by

$$\frac{K_2}{K_1} = e^{(2.068x10^{-5})\Delta H} \quad (6.16)$$

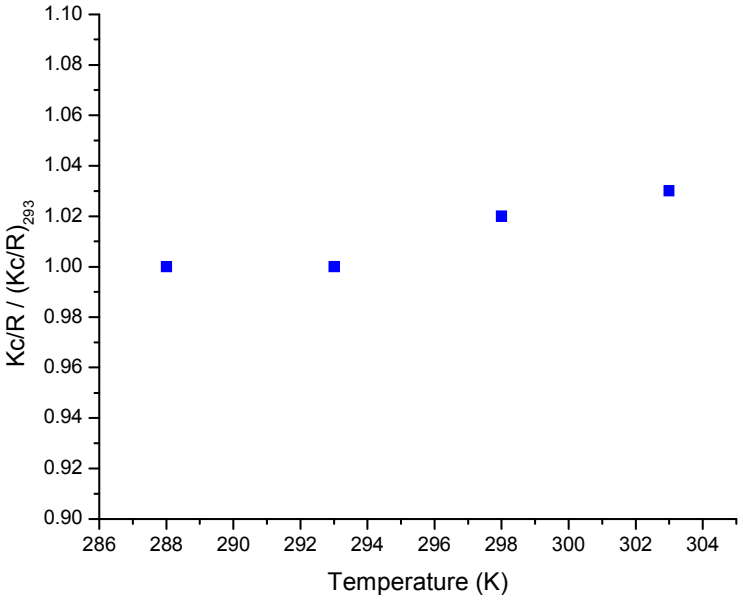

(a)

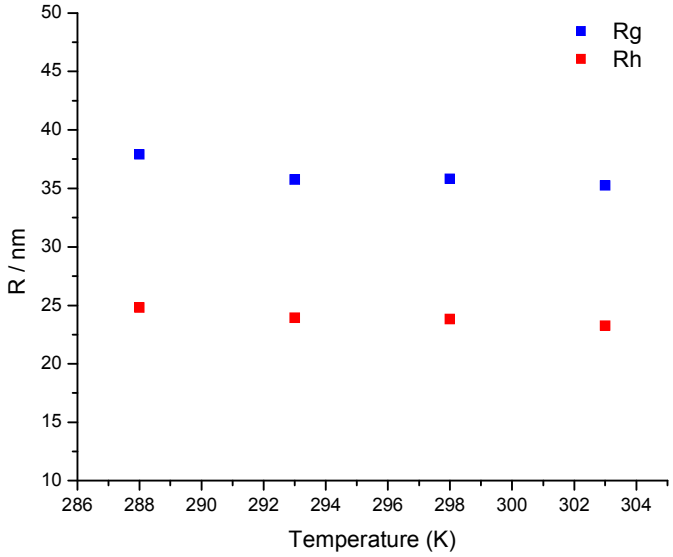

(b)

Figure 6.10. Temperature dependence of the DNA-TTA complexes in methanol c=0.165 g/l: a) static light scattering intensity ratio Kc/R / $(Kc/R)_{293}$ and b) radius of gyration and hydrodynamic radius.

The change of enthalpy must have a high value in order to increase significantly the equilibrium constant. To the knowledge of the author, the enthalpy of association/dissociation of surfactants from DNA-surf complexes in organic solvents has not yet been reported. However, given the behavior presented by the system in figure 6.16, it can be postulated that the change of enthalpy for such a process is low, and therefore the system is insensitive to the temperature. In order to determine the enthalpy of formation of DNA complexes in organic solvents, Isothermal Titration Calorimetry (ITC) measurements could be carried out, but the use of this technique is beyond the scope of the present work.

6.3.2.3.1.2 Dissolution of DNA complexes in organic solvents containing pre-dissolved surfactant

The interaction of trialkylammonium surfactants with DNA in organic solvents leads to a very subtle equilibrium, as shown in Table 6.6. If solutions of a surfactant with the corresponding solvent are added to the dried complexes, their dissolution is not possible. Only if the amount of pre-dissolved excess of surfactant is equal or lower than 0.1 mM the complexes become soluble again.

Table 6.6. Dissolution of DNA-surf complexes in organic solvents with pre-dissolved surfactants

DNA-TTA Methanol		DNA-DTA DMF	
Conc of predissolved TTA in methanol (mM)	Soluble	Conc of predissolved DTA in DMF(mM)	Soluble
0.1	√	0.1	√
1	**X**	1	**X**
10	**X**	10	**X**

Possible causes for the non-solvency of the complexes in organic solvents with the pre-dissolved surfactants could be either crystallization of the neighboring surfactants or a “salting-out” effect. The first one is discarded since the complexes remain soluble even after their saturation. Besides that, another experiment was performed, in which complexes of DNA were formed with 1-2 dioleoyl-3-

trimethylammonium-propane (DOTAP). Because this surfactant has double bonds in its tail, crystallization should be hindered. We achieved to dissolve the DNA-DOTAP complexes in chloroform, if precipitates in water with a charge ratio of N+/P-=1 were prepared, nevertheless they were not soluble anymore if a solution of 1 mM DOTAP instead of pure chloroform was used as the solvent (see section 6.3.4.1).

6.3.2.3.1.2.1. Formation of complexes with non-crystallizing surfactants

1-2 dioleoyl-3-trimethylammonium-propane (DOTAP) is an amphiphile with a limited solubility in aqueous solutions (cmc = $7x10^{-5}$ mol/l or 0.049 g/l). At concentrations above the cmc, DOTAP forms filled vesicles or spheres in aqueous solutions (see figure 6.11) with a molar mass of $6.32x10^{6}$ (table 6.7), which corresponds to 9050 DOTAP monomers per vesicle (a single DOTAP molecule has a molar mass of 698.5). As expected, DOTAP above the cmc has a negative second virial coefficient ($A_2<0$) and the vesicles are stable along all of the concentrations above the cmc (see appendix A28).

Table 6.7. Characterization of DOTAP vesicles with DLS and SLS

Surfactant	Solvent	(dn/dc) (ml/g)	Mw (g/mol)	A_2 (mol.ml/g^2)	Rg (nm)	Rh (nm)	Rg/Rh
DOTAP	1mM NaCl aqueous solution	0.17	$6.318x10^{6}$	-3.23×10^{-7}	229.3	392	0.584

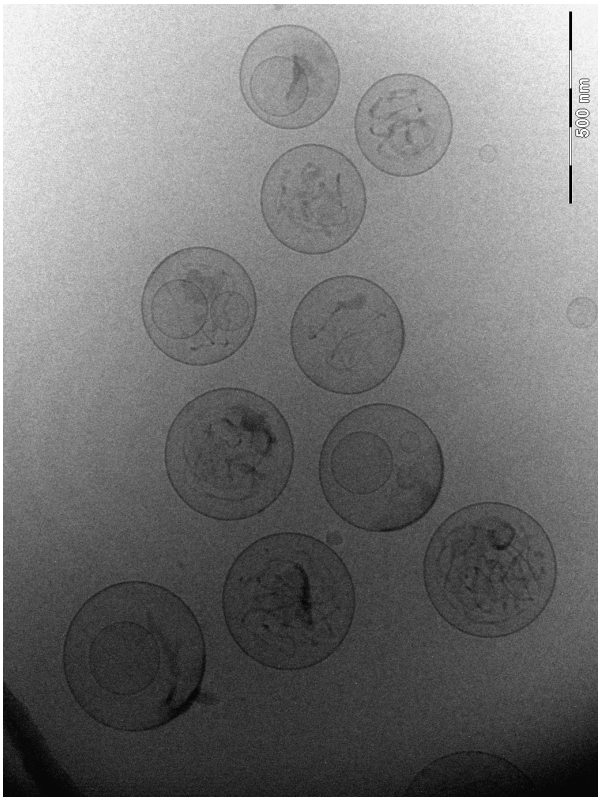

Figure 6.11. Cryo-TEM image of DOTAP at c=0.2214 g/l in mili-Q water. N+/P- = 1.82 stained with uranyl acetate. DLS measurements were performed upon addition of uranyl acetate to the solution and no effect was observed (see Appendix A29)

As previously mentioned, the formation of DNA complexes with DOTAP may give us some hints in terms of the mechanism of how the surfactants bind the DNA and the reasons for the subtle equilibrium of DNA complexes. First complexes were formed in aqueous solutions changing the order of mixing, i.e. adding DOTAP to a DNA solution and vice versa. The results are shown in figure 6.12. In the first case, when DNA is titrated with a DOTAP solution, the hydrodynamic radius increases steadily. Other studies [35, 36] have proved that the DNA formed clusters of aggregated vesicles. DNA acts as a fusogenic agent for the filled vesicles and the liposomes collapses the DNA. The fusogenic character of the DNA can be understood, if it is considered, that the electrostatic repulsions between vesicles are shielded DNA layers. Furthermore, DNA can bridge more or several vesicles and hence induce aggregation. The steadily increment of Rh could be explained by the aggregation of DNA-vesicles complexes. If DOTAP is titrated with a DNA solution, a constant Rh can be identified in figure 6.12. Sennato et al. [37] observed the same behavior with dynamic light scattering (only at 90°) and with Transmision Electron Microscopy (TEM).

They imaged intact spherical isolated DNA-coated vesicles at N+/P- from 14.3 to 4. At N+/P- between 4 and 1 the vesicles were still distinguishable but they looked "glue together". Aggregates were formed at this stage of the formation of complexes. The results shown in figure 6.12 are consistent with the images from Sennato et al. The hydrodynamic radius remains constant at a value of close to the Rh of a single vesicle until a N+/P- of around 2. A sudden aggregation becomes evident at lower charge ratios.

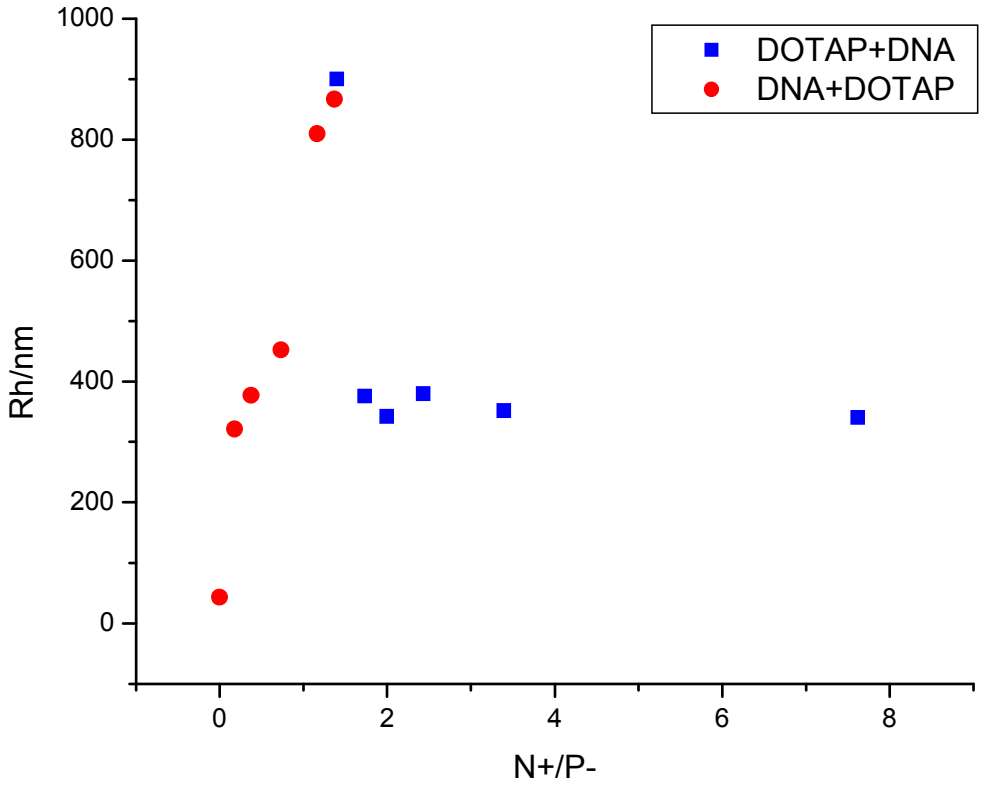

Figure 6.12. Hydrodynamic radius of DNA complexes with DOTAP vesicles determined from DLS measurements at angles from 30° to 157°. DNA initial concentration is 0.05 g/l. Measurements were performed at 20°C in an aqueous solution with 1 mM NaCl

A Cryo-TEM DNA image of the complexes at a charge ratio of N+/P- of 1.82 is presented in figure 6.13. A vesicle surrounded by a layer of the polyanion, as described by Sennato et al. [37] cannot be visualized anymore. Instead ill-defined complexes consisting of aggregating vesicles are shown. Similar images

were also shown by Birchall et al. [36] which described semi-fused, disrupted liposomes forming complexes with DNA. They also found other not well-defined structures of different size at the same charge ratio and demonstrated the heterogeneity of the complexes within a single lipid-DNA formulation.

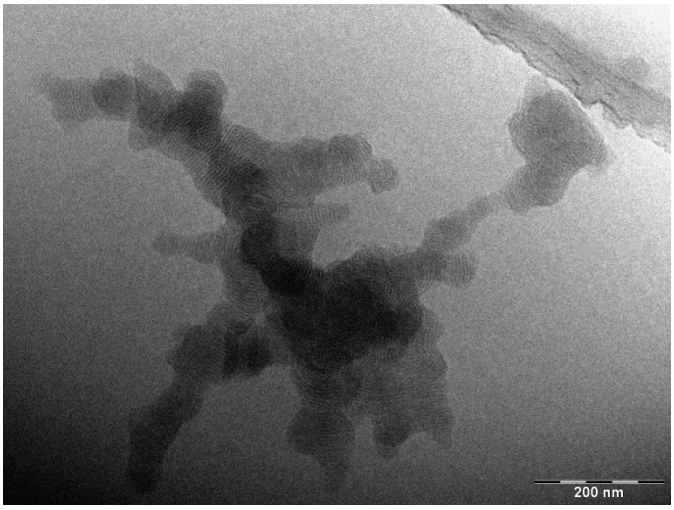

Figure 6.13. Cryo-TEM image of DOTAP at c=0.7 g/l titrated with DNA c=0.158 g/l at a charge ratio of N+/P- = 1.82 in mili-Q water. The complexes were stained with uranyl acetate for better visualization.

The final purpose of using DOTAP to form complexes with DNA is to gain some knowledge on the mechanism of precipitation of DNA-surf complexes when dissolve in solvents containing already free surfactant at a concentration higher than 0.1 mM. Therefore, complexes with a charge ratio of N+/P-=1 were prepared in order to induce precipitation (see table 6.8 for conditions of precipitation). Subsequent dissolution of the DNA precipitate in chloroform was possible. The dissolution of DNA bound to double-tail surfactants, i.e. dioctadecyldimethylammonium bromide [11] and didodecyldimethylammonium bromide [10] has been already reported. The precipitates of DNA-DOTAP were as well not soluble in solution of chloroform with free DOTAP dissolved at concentrations higher than 0.1 mM (see table 6.9). Since DOTAP cannot crystallize due to the double bonds in its structure, it is concluded that crystallization is not the mechanism responsible for the insolubility of the DNA complexes in solvents containing pre-dissolved free surfactants.

Table 6.8. Conditions for the formation of precipitates between DNA and DOTAP

	DOTAP
Stock solution concentration (mM)	1.00
Critical Micellar Concentration (cmc) (mM)	0.07 [11]
N+/P-	1.0
Final concentration (mM)	1.0
Final DNA concentration (mM)*	1

*Concentration expressed in terms of base pairs.

Table 6.9. Dissolution of DNA-DOTAP complexes in chloroform

DNA-DOTAP Chloroform	
Conc of predissolved DOTAP in aqueous solution (mM)	Soluble
0.1	√
1	X
10	X

Due to the large heterogeneities of the ill-defined of DNA-DOTAP complexes, further characterization was not possible.

6.4. Formation of complexes between DNA-surf and polycations in organic solvents.

The formation of polyelectrolyte complexes in aqueous solution results in kinetically controlled processes, usually with a globular compacted topology that becomes less defined while the stoichiometry charge ratio (N+/P-) approaches the unity [38, 39]. Depending on the system, macroscopic precipitation may occur. IPECs of DNA and polycation in organic solvents resulting from pre-complexes with surfactants do not show a different behavior. With this approach, two opposite effects take place: a) The

Bjerrum length is diminished by a factor higher than 2, due to the differences in the dielectric constants of water and the two organic solvents used in this work and b) the effective charge of the DNA is widely reduced, since it is already complexed with a surfactant and because the charges of the polycations are not fully dissociated in organic solvents. The former effect increases the probability of ion pair formation while the other two have an influence on the other direction since the Debye length is reduced. Furthermore, in organic solvents there is the possibility of using polyelectrolytes of low charge density, with the subsequent decreaset of the columbic interactions. When a linear polyvinylpyridine (l-PVP-etBr) with 10% of quaternization was added to DNA-TTA complexes in methanol, large aggregates were formed (figure 6.14). For the characterization of the l-PVP-etBt see table 6.2.

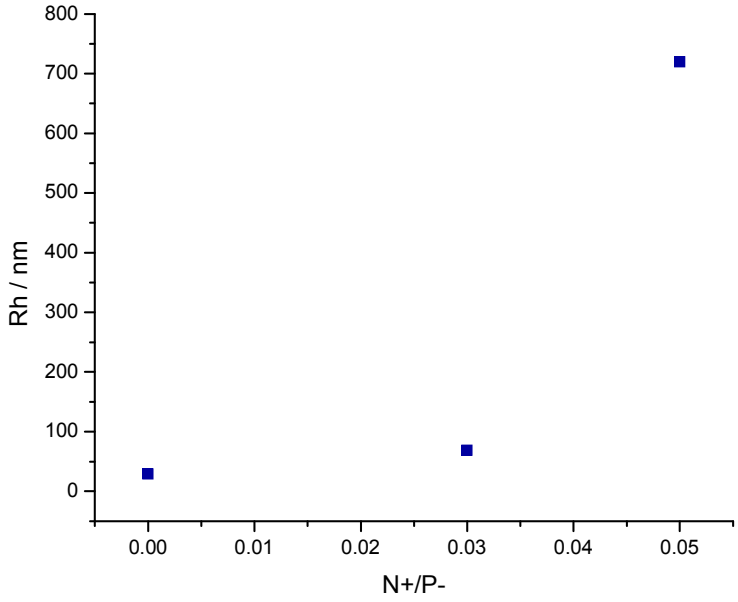

Figure 6.14. Hydrodynamic radius of DNA-TTA complexes (initial c = 0.60 g/l) in a methanolic solution upon the stepwise addition of a linear polyvinylpyridine (l-PVP-etBr) with 10% of quaternization in methanol at 20°C ([LiBr = 0.001 M)]. DLS measurements were performed with a multiangle light scattering equipment described in the experimental section.

In order to reduce the charges of the polycation, a separate experiment took place in which a non-quaternized Polyvinylpyridine brush (b-PVP) with only a few residual charges (not possible to quantify)

was added to DNA-TTA complexes in methanol. Through the formulas described in reference [5] it was demonstrate that no complexes were formed due to the lack of positive charges.

$$\left(\frac{dn}{dc}\right)_{mixture} = w_{complex}\left(\frac{dn}{dc}\right)_{complex} + w_{PVP}\left(\frac{dn}{dc}\right)_{PVP} \tag{6.17}$$

$$Mw_{mixture}\left(\frac{dn}{dc}\right)^2_{mixture} = w_{complex}Mw_{complex}\left(\frac{dn}{dc}\right)^2_{complex} + w_{PVP}Mw_{PVP}\left(\frac{dn}{dc}\right)^2_{PVP} \tag{6.18}$$

$$\begin{aligned}\langle Rg^2\rangle_{z,mixture}Mw_{mixture}\left(\frac{dn}{dc}\right)^2_{mixture} &= w_{complex}\langle Rg^2\rangle_{z,complex}Mw_{complex}\left(\frac{dn}{dc}\right)^2_{complex} \\ &+ w_{PVP}\langle Rg^2\rangle_{z,PVP}Mw_{PVP}\left(\frac{dn}{dc}\right)^2_{PVP}\end{aligned} \tag{6.19}$$

$$\begin{aligned}\langle Rh^{-1}\rangle_{z,mixture}Mw_{mixture}\left(\frac{dn}{dc}\right)^2_{mixture} &= w_{complex}\langle Rh^{-1}\rangle_{z,complex}Mw_{complex}\left(\frac{dn}{dc}\right)^2_{complex} \\ &+ w_{PVP}\langle Rh^{-1}\rangle_{z,PVP}Mw_{PVP}\left(\frac{dn}{dc}\right)^2_{PVP}\end{aligned} \tag{6.20}$$

Here "PVP" stands for the non-quaternized polyvinylpyridine brush (b-PVP) described in the experimental section (section 6.1) and "complex" refers to the DNA-TTA complexes in organic solvents.

The formation of complexes increases the molar mass to higher values than the addition of the single components. In figure 6.15 values of the molar mass, Rg and Rh lower or equal to the corresponding values for a mixture of both components (b-PVP and DNA-TTA) can be observed.

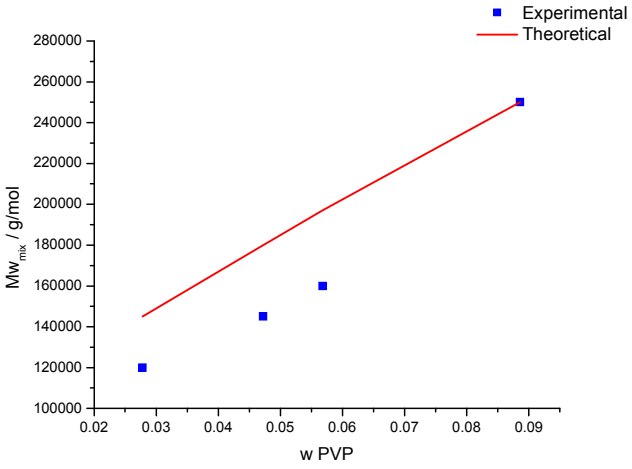

(a)

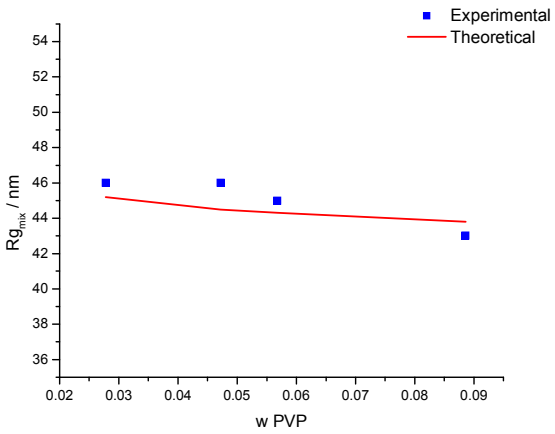

(b)

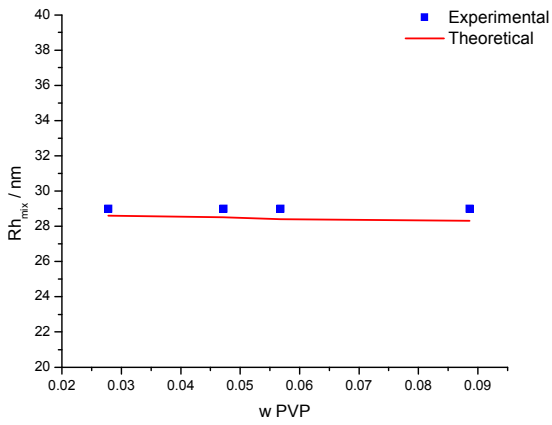

(c)

Figure 6.15. Comparison of measured and calculated (considering mixture of homopolymers) (a) molar masses, (b) radii of gyration and (c) hydrodynamic radii for the system: DNA-TTA complex in methanol + non-quaternized polyvinylpyridine at 20°C ([LiBr = 0.001 M)]

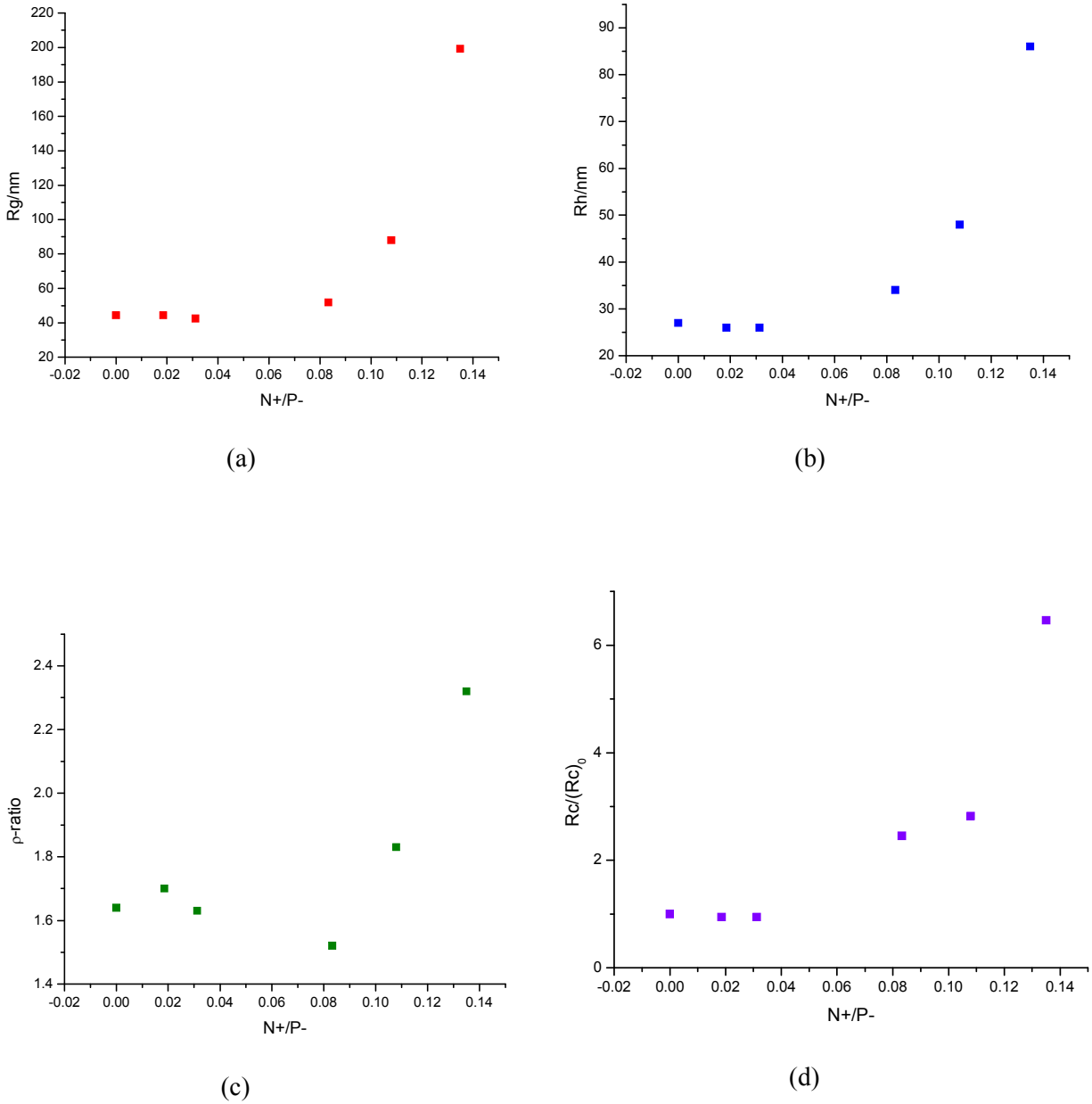

Figure 6.16. SLS and DLS measurements of a methanolic solution of DNA-tetradecyltrimethylammonium complex (initial c = 0.94 g/l) and non-quaternized polyvinylpyridine brushes after the stepwise addition of a solution of HCl in methanol at 20°C ([LiBr = 0.001 M)]. (a) Rg vs. N+/P- (b) Rh vs. N+/P- (c) ρ-ratio of N+/P- and (d) $Rc_0/(R_0c)$

Subsequent addition of methanolic hydrochloric acid (m-HCl) in order to charge the b-PVP shows qualitatively a similar behavior than the one described for DNA-polycation complexes in aqueous solutions. At charge ratios close to N+/P- = 0.1 an abrupt increase of the Rh, Rg and the light scattering intensity could be observed with the addition of more m-HCl (see figure 6.16), suggesting the formation of complexes containing several molecules of both components. It was demonstrated that the kinetics dominates the process of complex formation by modifying the history of preparation of the complexes. For example, changes in the order of mixing at a N+/P- of 0.108 resulted in different structures, e.g. different hydrodynamic radii (see Appendix A33). Other possible reasons like the formation of insoluble complexes in methanol are discarded for the system DNA-DTA + b-PVP + m-HCl. The stability of DNA-TTA complexes and of the b-PVP against the m-HCl was investigated by means of DLS (see Appendix A35). The mixtures between two of the three components of the system seem to be stable and compatible with each other. In other words, aggregates are only formed when the three components (polyanion, polycation and acid) are mixed together.

The conditions for aggregation and precipitation depend greatly on the starting polyelectrolyte. Krohne et al. [40] used a polystyrene sulfonate macromonomer complexed to DTA in order to form IPECs in DMF with a protected polylysine brush (b-PLL). In this case, the addition of triethylamine up to 20% v/v seemed to help in the formation of IPECs of well defined topologies. Under the same conditions (i.e. polycation, solvent and volume fraction of triethylamine) the same b-PLL was complexes with DNA-DTA in DMF. Results showed that aggregates with larger sizes are formed and at lower charge ratios with the addition of triethylamine (see Fig 6.17). The formation of topologically controlled complexes depends greatly on the topology of the starting materials. By changing one of the polyelectrolytes, complexes with different topologies are formed. Another explanation for this behavior could be related to the stability of the complexes in the solvents. It is not clear whether the final complexes are soluble in the solvents already mentioned (DMF and DMF with 20% v/v triethylamine). Duschner et al [3] could obtain of topologically-controlled complexes of PSS using as polycation a PEI grafted with PEO in order to improve the solubility of the PEI. The same PEO may have also improved the solubility of the whole complex in DMF.

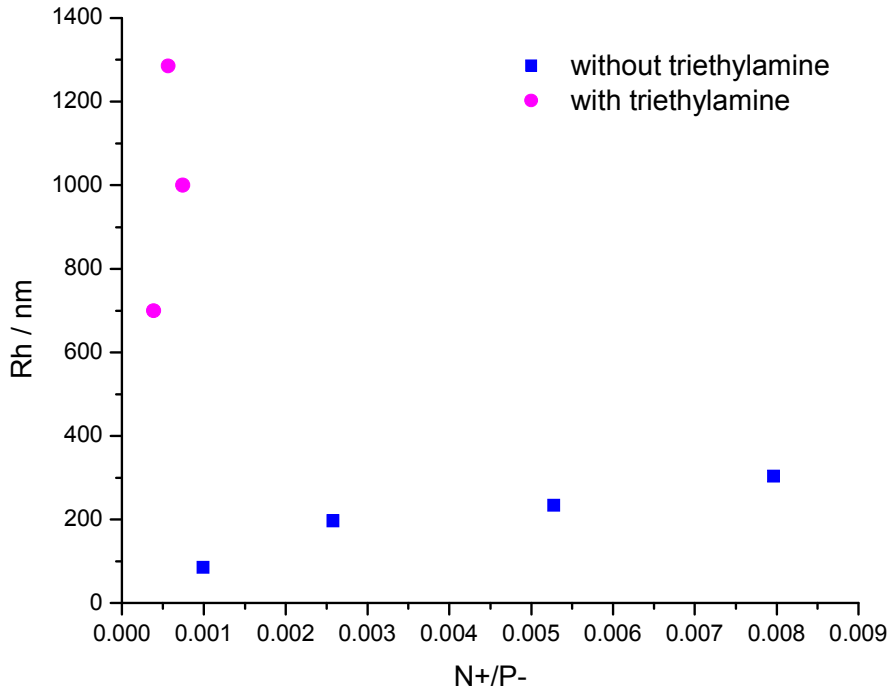

Figure 6.17. Variation of the hydrodynamic radius at 20°C of DNA-DTA complexes in DMF after the stepwise addition of a protected polylysine brush. Experiments were carried out with and without the presence of triethylamine (20%v/v)

6.5. Formation of complexes in aqueous solution vs in organic solvents.

In this section the formation of DNA complexes in organic solvents (methanol) and aqueous solution are qualitatively compared. PNIPAM with one charge per polymer given by the end group (a trialkylammonium radical) and with common solubility in these two solvents was used for this purpose. The results are summarized in table 6.10.

Whereas complexes are not formed in aqueous solutions at increasing charge ratios until N+/P- = 3, which was expected since monovalent cations cannot condensate DNA. At a charge ratio close to the unity, complexes of DNA-TTA with PNIPAM precipitate. Two possible reasons may be responsible for

the differences in complex formation among the two solvents: electrostatics or interactions with single stranded DNA. Hydrophobic interactions are excluded because they disappear in organic solvents like methanol. The negative free energy given by the release of counterion could be comparable in aqueous solutions and in organic solvents. The sodium counterions in the buffer have the same or slightly higher freedom of motion as the TTAB surfactant in the methanol. Electrostatics attractions are definitely increased in methanol by a factor of 2 as mentioned before. Also the partial dissociation of double stranded conformation proved in 6.3.2 and 6.4.1 may lead to other kind of interactions not possible in water, for instance, hydrogen bonding. PNIPAM is well known to form hydrogen bonding with water. It could also be possible that these interactions are also possible between the PNIPAM and the bases of the single stranded DNA, which are also known to form hydrogen bonding among each other. However, these are only speculations and other measurements, i.e. H-NMR should be carried out to demonstrate this hypothesis.

Table 6.10. Comparison of formation of complexes of DNA with PNIPAM in methanol and in aqueous solutions

Polyanion	Solvent	N+/P-	Result
DNA	5 mM Buffer	3	No formation of complexes
DNA-TTA	Methanol +1 mM LiBr	0.979	Precipitation

Not in every case a change of solvent causes differences in the properties or conformation of the DNA. Ganguli et al [41] showed AFM pictures and CD spectra of DNA complexes with methoxy poly(ethylene glycol) monomethacrylate (MePEGMA) and (3-(methacryloylamino)propyl)trimethylammonium chloride (MAP-TAC). The topology and the conformation of DNA complexes with MAP-TAC in common solvents like water, benzene, DMSO and THF were similar in all of the cases.

6.6. Conclusions

DNA complexes with n-alkyl-trimethylammonium surfactants, i.e. dodecyl- and tetradecyltrimethylammonium bromide (DTAB and TTAB, respectively) were prepared and dissolve in organic solvents. These complexes were only soluble in methanol (for DNA-TTA) and in DMF (for DNA-DTA). The topologies of these two complexes differ considerably. Whereas the DNA-TTA complexes show a compacted conformation, the DNA-DTA complexes in DMF are encountered as open rings. In both cases, a lower molar mass than expected was measured. DNA is denatured and degraded in methanol. In DMF, AFM pictures also show degradation of DNA. These two complexes also possess different properties: DNA-TTA complexes in methanol undergo an equilibrium in which the surfactant is distributed between a free and a bounded state. This equilibrium is not observed for DNA-DTA in DMF. This is a very subtle equilibrium and the addition of solvent containing a concentration higher than 1mM of free surfactant leads to precipitation of the complexes. The further formation of complexes of this "hydrophobic" DNA with polycations, i.e. PVP brush and a polylysine brush in methanol and DMF respectively, resulted in the formation of kinetically controlled topologies and subsequent precipitation at low charge ratios.

6.7. References

1. Michaels A.S., Miekka, R. J. Phys. Chem 65: 1765 – 1773.
2. Antonietti, M.; Conrad, J.; Thünemann, A. Macromolecules, 1994, 27: 6007 – 6011.
3. Duschner, S.; Störkle, D.; Schmidt, M. Macromolecules, 2008, 41: 9067 – 9071.
4. Krohne, K.; Duschner S.; Störkle, D.; Schmidt, M.; Maskos, M. Macromolecules, 2010, 43: 8645 – 8650.
5. Störkle, D; Duschner, S.; Heimann, N.; Maskos, M.; Schmidt, M. Macromolecules. 2007, 40: 7998 – 8006.
6. Lai, E.; van Zanten, J. Biophysical Journal, 2001, 80(2): 864 – 873.
7. Pollard, T.; Earnshaw, W. Cell Biology. Spektrum Akademischer Verlag. 2007.
8. Dias, R.; Mel'Nikov, S.; Lindman, B.; Miguel, M. Langmuir, 2000, 16: 9577 – 9583.
9. Ijiro, K.; Okahata, Y. J. Chem. Soc., Chem Commun., 1992, 1339 – 1341.
10. Mel'nikov, S. M.; Lindman, B. Langmuir, 1999, 15: 1923 – 1928.
11. Sergeyev, V.G.; Pyshkina, O. A.; Lezov, A. V.; Mel'nikov, A.B.; Ryumtsev, E. I.; Zezin, A. B.; Kabanov, V. A. Langmuir, 1999, 15: 4434 – 4440.
12. Leal, C.; Bilalov, A.; Lindman, B. J Phys. Chem. B, 2006, 110: 17221 – 17229.

13. Sergeyev, V. G.; Mikhailenko, S. V.; Pyshkina, O. A.; Yaminsky, I. V.; Yoshikawa, K. J. Am. Chem. Soc, 1999, 121: 1780 – 1785.
14. Pack, D.; Hoffmann, A.; Pun, S.; Stayton, P. Nature Reviews, 2005, 4: 581 – 593.
15. Schick, M. J Phys Chem. 1963, 67, 1796.
16. Venable, R., Nauman, R. J Pohys Chem. 1964, 68, 3498.
17. Reimer, D.; Zhang, Y.; Kong, S.; Wheeler, J.; Graham, R.; Bally, M. Biochemistry, 1995, 34, 12877 – 12883.
18. Stephan, T. Amphypolare zylindrische Bürsten. Darstellung und Charakterisierung von Copolymakromonomeren. PhD Thesis. Thesis. Johannes Gutenberg Universität-Mainz: Germany. 2002.
19. Sahl, M. Synthese und Charakterisierung von zylindrischen Bürsten mit Polypeptidseitenketten. PhD Thesis. Johannes Gutenberg Universität-Mainz: Germany. 2011.
20. Franz, M. α,ω-Funktionalisierung von Polymeren mittels neuartigem RAFT-Reagenz. Diplomarbeit. Johannes Gutenberg Universität-Mainz: Germany. 2010.
21. Loh, P. The collapse of linearpolyelectrolyte chains in a poor solvent: when does a collapsing polyelectrolyte collect its counter ions?. PhD Thesis. Johannes Gutenberg Universität-Mainz: Germany. 2008.
22. Mok, H.; Gwan Park, T. Bioconjugate Chem., 2006, 17(6), 1369 – 1372.
23. Graciani, M.; Muñoz, M.; Rodríguez, A.; Moyá, M. L. Langmuir, 2005, 21: 3303 – 3310.
24. Qu, J.; Morita, R.; Ashitaka, H.; Ogata, N.; Masuda, T. Polymer, 2008, 49, 3663 – 3670.
25. Jaumot, J.; Eritja, R.; Navea, S.; Gargallo, R. Analytica Chimica Acta, 2009, 642: 117 – 126.
26. Sorokin, V.; Gladchenko, G.; Valeev, V.; Sysa, I.; Petrova, L.; Blagoi, Y. Journal of Molecular Structure, 1997, 408/409, 237 – 240.
27. Zehfus, M.; Johnson, C. Biopolymers, 1981, 20, 1589 – 1603.
28. Zehfus, M.; Johnson, C. Biopolymers, 1984, 23, 1269 – 1281.
29. Schindler, T.; Nordmeier, E. Polymer, 1999, 40, 7019 – 7027.
30. Breslauer, K.; Bodnar, C.; McCarthy, J. Biophysical Chemistry, 1978, 9, 71-78.
31. Schmidt, M.; Stockmayer, W. Macromolecules. 1984, 17, 509 – 514.
32. Tinland, B.; Pluen, A.; Sutrm, J.; Weill, G. Macromolecules, 1997, 30, 5763 – 5765.
33. Kühn, F. Polykation-DNA-Komplexe: Eigenschaften und Anwendung in der Gentransfektion. PhD Thesis. Johannes Gutenberg Universität-Mainz: Germany. 2010.
34. Mok, H.; Gwan Park, T. European Journal of Pharmaceutics and Biopharmaceutics, 2008, 68, 105 – 111.
35. Gershon, H.; Ghirlando, R.; Guttman, S.; Minsky, A. Biochemistry, 32, 1993, 7143 – 7151.
36. Birchall, J.; Kellaway, I.; Mills, S. International Journal of Pharmaceutics, 1999, 183, 195 – 207.
37. Sennato, S.; Bordi, F.; Cametti, C.; Diociaiuti, M.; Malaspina, P. Biochimica et Biophysica Acta, 2005, 1714, 11 – 24.
38. Thünemann, A.; Müller, F.; Dautzendberg, H.; Goanny, J.; Löwen, H. Adv. Poly. Sci. 2004, 166: 113 – 117.
39. Dautzenberg, H.; Jaeger, W. Macromol. Chem. Phys. 2002, 203: 2095 – 2012.

40. Krohne, K. Topologisch kontrollierte Interpolyelektrolytkomplexe aus kettensteifen Polyelektrolyten. Einfluss von Polykation, Lösungsmittel und Protonierungsgleichgewicht. PhD Thesis. Johannes Gutenberg Universität-Mainz: Germany. 2011
41. Ganguli, M.; Jayachandran, K.; Maiti, S. J. Am. Chem. Soc, 2004, 126, 26 – 27.

7. Influence of the topology of the initial polyanion (DNA pUC19) on the topology and equilibrium of DNA complexes: use of a cut (linear) DNA.

In the last chapter, complexes between supercoiled DNA pUC19 stabilized with surfactants and polycations in organic solvents were characterized. It was concluded that the topology of the complexes is determined by a kinetically controlled process. Aggregates were formed and further precipitation took place. In this chapter, the supercoiled structure is modified by the specific digestion (cut) of the DNA with an enzyme specific to a given sequence of nucleotides encountered only once in the DNA pUC19. The result is a linear DNA with the same molar mass but with a more "organized" structure. In this chapter, it is assumed that the supercoiling introduces a certain level of disorder to the polyelectrolyte and therefore to the formation of complexes. Furthermore, as shown in section 7.4, in the linear conformation the number of charges per volume (~Rh^3) is lowered due to a reduction of the DNA density as a consequence of a more extended conformation. The decrease of charges per volume unit may weaken the electrostatic interactions between the two oppositely-charged polyelectrolytes, which would favor the rearrangement of the complexes until reaching a thermodynamic equilibrium. This hypothesis is investigated in this chapter.

The objective of this chapter is to compare the topologies and efficiency of complex formation between the supercoiled and the linear DNA pUC19 under the same conditions (described in chapter 6). Therefore, the experimental section of this chapter will be skipped. For any details, refer to section 6.1.

7.1. Enzymatic digestion (cut) of supercoiled DNA pUC19.

As mentioned in the introduction, the two strands of the DNA are cut with an enzyme at same point to untwist the supercoiled structure. The procedure for DNA digestion is given by the manufacturer. Briefly,

5 ug of DNA is incubated in a commercial buffer adequate for the enzyme and dilute in a relation of 1:10 and 1 ul of the enzyme at 37°C for the time recommended by the manufacturer. The order of addition must be: 1. Water, 2. Buffer, 3. DNA and 4. Enzyme. For purification, the DNA is then precipitated with pure ethanol and a concentrated solution of sodium acetate (CH_3COONa) 3 M at -20°C overnight. After centrifugation for 30 min at 14000 rpm, the supernatant is removed and the salt is eliminated by addition of a cold mixture 70% ethanol. Again the sample is centrifuged and the supernatant removed. The clean linear DNA is then dissolved in water and the concentration is determined with a UV-vis spectrometer.

The selection of the enzyme is not trivial. The results after the measurement of the molar mass of digested DNA with different enzymes is shown in table 7.1.

Table 7.1. Characterization of pUC19-Supercoiled after digestion with different enzymes

Enzyme	Solvent	(dn/dc) (ml/g)	Mw (g/mol)	A_2 (mol.ml/g^2)	Rg (nm)	Rh (nm)	Rg/Rh
SpI	5mM phosphate buffer	0.17	-*	-*	-*	59.6	-*
BamHI Fast Digest	5mM phosphate buffer	0.17	2.34×10^6	2.5×10^{-6}	167.0	55.8	3.0
BamHI	5mM phosphate buffer	0.17	2.34×10^6	2.5×10^{-6}	167.9	42.5	3.9
EcoRI	5mM phosphate buffer	0.17	2.40×10^6	1.9×10^{-7}	105.3	58.8	1.8
SamI	5mM phosphate buffer	0.17	1.7×10^6	7.7×10^{-7}	139.7	69.6	2.0

- Values not measured because incomplete digestion of the DNA was observed in electropherograms with capillary electrophoresis (see Appendix A38).

The two strands of DNA are only cut in one point. A change in the topology but not in the molar mass is expected. However, the measured molar mass of the DNA after digestion with most of the enzymes presented in table 7.1 (BamHI Fast Digest, BamHI and EcoRI) is higher than the theoretical molar mass of $1.7x10^6$. These enzymes leave the so-called "sticky-ends", i.e. small fractions of single stranded DNA, at both ends. Given that the "sticky-ends" are complementary stranded, the formation of rings or of junctions with other DNA chains is possible. The probability of obtaining these "unwanted" topologies increases with the use of a buffer (which is necessary in light scattering measurements to screen the electrostatic interactions). The digestion with the enzyme SpI was incomplete (see electropherogram obtained with capillary electrophoresis in appendix A38). The enzyme SamI is able to completely cut DNA (see gel electrophoresis with Bioanalyser in appendix A39) without the formation of sticky-ends. Hence, the molar mass of the DNA digested with SamI is equal to the molar mass of the supercoiled DNA pUC19.

To compare the two topologies of the DNA pUC19, the characterization of linear and supercoiled DNA are shown in Table 7.2. From now on, the enzyme is not longer specified. It is assumed that DNA was digested with SmaI.

Table 7.2. Characterization of supercoiled and linear DNA pUC19.

Polymer	Solvent	(dn/dc) (ml/g)	Mw (g/mol)	A_2 (mol.ml/g^2)	Rg (nm)	Rh (nm)	Rg/Rh (ρ-ratio)
DNA pUC19	5mM phosphate buffer	0.17	1.7×10^6	6.7×10^{-4}	65.6	43.6	1.5
Linear DNA pUC19	5mM phosphate buffer	0.17	1.7×10^6	7.7×10^{-7}	139.7	69.6	2.0

The supercoiled DNA has a closed circular topology with twists and writhes characterized by the linking number Lk. This constant Lk, describes the total amount of twists and writhes on the supercoiled system

[1]. Therefore, it is usually represented as a supercoiled polymer. On the other hand, linear DNA does not have these constrains of Lk, therefore develops a more extended conformation usually visualized as a charged cylinder. For a quantitative comparison between the two topologies, the ρ-ratio (=Rg/Rh) is analyzed. It is known that the ρ-ratio of supercoiled DNA is around 1.505 [2]. On the other hand, the ρ-ratio of a cylinder with length *l* and diameter *D* must be determined.

$$\rho - ratio = \frac{1}{3} ln\left(\frac{l}{D} - 0.5\right) \tag{7.1}$$

As mentioned in chapter 5, the contour length of DNA pUC19 is approximately 910 nm and the DNA diameter measured by different techniques is around 2 nm. With this values, the theoretical ρ-ratio can be calculated

$$\rho - ratio = \frac{1}{3} ln\left(\frac{910nm}{2nm} - 0.5\right) = 2.0 \tag{7.2}$$

Again, this value is in accord with the experimental ρ-ratio measured with dynamic and static light scattering.

The topologies here reported are in agreement with the light scattering measurements of DNA pUC19 with the two topologies already mentioned from Yi et al [3]. However, these results are in contrast with the topologies deduced by de Carmejane et al. [4]. These authors performed separations of linear and supercoiled DNA with a capillary electrophoresis and determined different slopes from the plots of ln (*u*) vs ln (*N*) (*u* is the electrophoretic mobility and N is the amount of base pairs). The authors concluded that linear DNA migrates as a random coil whereas supercoiled DNA migrates as an elastic rod. The differences between results in table 7.2 and the findings of de Carmejane et al may be related to the deformation of polyelectrolytes under an electric field.

7.2. Characterization of the linear DNA-surf complexes in organic solvents

7.2.1. Topology of linear DNA-surf complexes in organic solvents

Complexes with linear DNA were formed according to the procedure described in the experimental section of chapter 6, section 6.1. Results are shown in table 7.3 and table 7.4. The characterization of complexes with supercoiled DNA is again presented for comparison purposes.

Table 7.3. Light scattering characterization of linear and supercoiled DNA-surfactant complexes in methanol

Complex	Solvent	(dn/dc) (ml/g)	Mw (g/mol)	A_2 (mol.ml/g^2)	Rg (nm)	Rh (nm)	Rg/Rh
Supercoiled DNA-TTA	Methanol	0.17	1.01×10^6	1.4×10^{-7}	40.6	29.0	1.4
Linear DNA-TTA*	Methanol	0.17	9.36×10^5	-1.37×10^{-7}	67.4	26.5	2.2

- Aggregates were observed in the Zimm Plot

Table 7.4. Light scattering characterization of linear and supercoiled DNA-surfactant complexes in dimethylformamide.

Complex	Solvent	(dn/dc) (ml/g)	Mw (g/mol)	A_2 (mol.ml/g^2)	Rg (nm)	Rh (nm)	Rg/Rh
Supercoiled DNA-DTA	DMF	0.071	2.23×10^6	1.9×10^{-7}	75.3	62.1	1.2
Linear DNA-DTA	DMF	0.071	1.21×10^6	-6.42×10^{-7}	74.1	59.4	1.25

Complexes with linear DNA in methanol exposed a more expanded conformation compared to the supercoiled conformation, demonstrated by the increase of the ρ-ratio. The results for linear DNA-TTA may be biased due to the formation of aggregates (see Zimm Plot in Appendix A41). This issue and the partial denaturation of the DNA in methanol (see figure 7.1) can explain the low molar mass measured with light scattering (table 7.3). The topology of the complexes with TTAB using linear DNA as precursor is definitely different than the compacted DNA-TTA complexes formed with supercoiled DNA in methanol. The differences could be attributed to the large cost of entropy to bend the linear DNA into more less extended structures.

Bloomfield [5] proposed that condensation must overcome the cost of the energies of bending (ΔG_{bend}) and mixing entropy (ΔG_{mix}), due to the lost of entropy while going from a random coil to a more compacted conformation. The free energy of bending depends on the total length of the DNA (L), the persistence length (a_p), and the radius of curvature (r_c) of the condensed structure.

$$\frac{dG_{bend}}{kT} = \frac{La_p}{2{r_c}^2} \tag{7.3}$$

The cost of entropic energy for DNA depends also on the contour length (L = 0.34 nm x number of base pairs) and on the persistence length

$$\frac{dG_{mix}}{kT} = \frac{L}{a_p} \tag{7.4}$$

DNA pUC19 contains 2686 base pairs. Given that the persistence length of the DNA is approximately 50 nm, the total cost of energy of compaction ($\Delta G_{compact}$) is given by

$$\frac{dG_{compact}}{kT} = 18.3 + \frac{22831}{{r_c}^2} \tag{7.5}$$

It is important to notice that the energy of compaction is inversely proportional to the square of the radius of the final structure. In other words, the cost of energy to obtain complexes with a compacted topology is very high.

On the other hand, theoretical calculations of the cost of energy to go from an open circular to a supercoiled configuration (ΔG_s) have been reported [1, 6, 7]. For instance, Lahiri et al [6] derived an expression for the enegy of supercoiling by adding the contributions of the entropic cost (ΔG_{ent}), the bending (ΔG_{bend}), and the twisting (ΔG_{twist}) of the DNA to form a supercoiled structure.

$$dG_s = dG_{ent} + dG_{bend} + dG_{twist} \quad (7.6)$$

Only the difference between the energy of compaction and the energy of supercoiling is needed by the DNA with a supercoiled conformation to form compact complexes. Given that the linear DNA must overcome ΔG_s during the process of compaction, it can be deduced that the cost of energy to acquire a compact conformation is higher than that for the supercoiled DNA. Therefore, the linear DNA adopts an extended conformation and prefers to aggregate instead.

Results shown in table 7.3 for the complexes DNA-DTA in DMF confirm the explanation given previously for the complexes in methanol. Independent of the initial conformation of the polyanion, the complexes with DTA in DMF possess similar expanded structures with respect to the Rg and Rh. This may be explained in terms of low cost of free energy to form the complexes, since compaction does not take place. Interestingly, the molar mass of the complexes with supercoiled DNA is two times higher than the one of the complexes formed with linear DNA in DMF. Two explanations are possible: 1) The degree of degradation is higher for linear DNA and 2) Complexes with linear are completely denatured in DMF whereas complexes with supercoiled DNA are only partially or even not at all denatured, as discussed in sections 6.32 and 6.4.1. The second possibility will be discussed in section 7.2.2. It is also important to notice that complexes with linear DNA are characterized by a negative second virial coefficient (A_2).

Several examples in the literature show that complexes with linear DNA have a different size and topology than the supercoiled. Arscott et al [8] formed complexes with linear and supercoiled DNA using

hexamine cobalt (III) as condensing agent. After the visualization of the complexes with TEM and the proper statistical treatment, their results demonstrate that supercoiled DNA pUC12 (also with around 2700 base pairs) yielded particles 25-30% smaller (average radius of 34 nm) than particles from linear DNA (average radius of 44 nm). It was explained that even a small amount of supercoiling could introduce enough stress to make the plasmid more susceptible to tighter curvatures. Also von Groll et al [9] observed by atomic force microscopy (AFM) two completely different morphologies of complexes with a cut and an uncut plasmid DNA. The authors intended to explain the differences in transfection efficiency of complexes formed with linear and supercoiled DNA (being the supercoiled DNA the more efficient one) upon binding of the commercial liposome, lipofectamine. They found out that if supercoiled DNA is used as precursor, the complexes possess sphere-like structures with diameters between 100 and 500 nm (a more compacted structure) whereas the complexes with linear DNA were not able to be condensed but they showed pearl-necklace morphologies with pearls varying from 250 to 400 nm. Ma et al [10] proved that magnesium (Mn2+) can induce condensation of supercoiled DNA into toroids, while it only yields thin, fibrous structures with no definite morphology, described as aggregates, with linear DNA. All of these results are in perfect agreement with results shown in table 7.3.

7.2.2. Conformation of linear DNA-surf complexes in organic solvents

The B-conformation of the linear DNA in methanol is not entirely preserved. The band at around 250 nm looses negativity and the band at 280 nm is shifted to 290 nm. These changes were also observed by Girod et al [11] upon the addition of methanol to an aqueous solution of DNA. The spectrum seems to correspond to a change from a helical structure to a random coil conformation. This is an indication of partial DNA denaturation. The low molar mass of lDNA-TTA complexes in table 7.3 cannot only be attributed to this phenomenon. This point will be treated in detail in section 7.3.

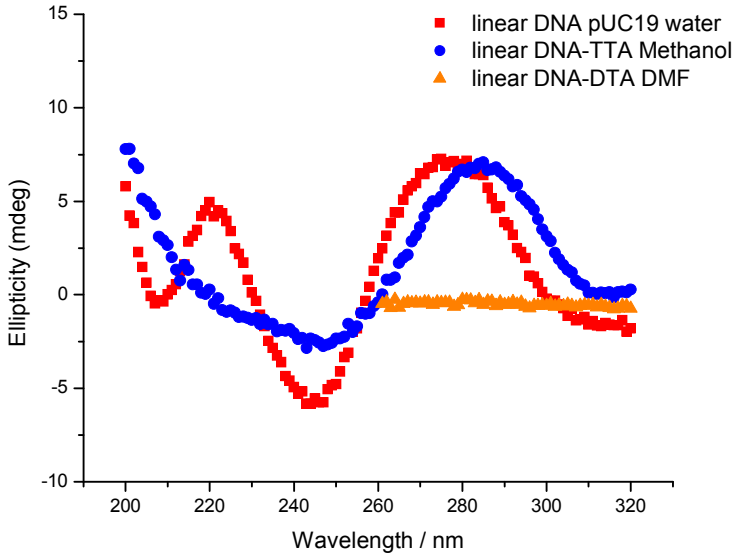

Figure 7.1. CD Spectroscopy spectra of the normalized ellipticity of linear DNA pUC19 and linear DNA complexes with TTAB in methanol and with DTAB in DMF.

From figure 7.1 it is evident that the complexes with linear DNA in DMF are completely denatured. In contrast, the double stranded structure of the "hydrophobic" supercoiled DNA in DMF remains at least partially intact. It is known that supercoiled DNA is more stable against denaturation than linear or nicked DNA [12]. The hydrogen bonding interactions maintaining the helical structure weaken or disappear during the process of denaturation. This leads to a separation of the strands. However, in supercoiled DNA remaining anchor of the base pairs and sterical stabilization as a result of supercoiling prevent the complete separation of the complementary strands [12]. Frerix et al. developed indeed a method for separation of supercoiled DNA from its linear and open circular analogues based on this principle. Hence, it is not surprising that only the linear DNA is completely denatured in DMF.

The ellipticity of the linear DNA and its complex with tetradecyltrimethylammonium in methanol is almost identical. Therefore, The CD spectra of the complexes with linear and supercoiled DNA in methanol are compared in figure 7.2.

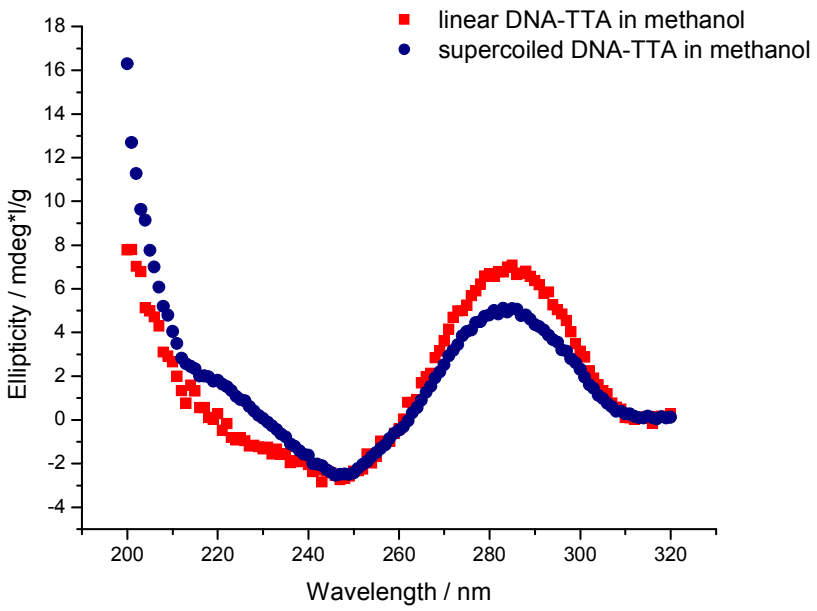

Figure 7.2. CD Spectroscopy spectra of the normalized ellipticity of DNA-TTA complexes prepared with linear and supercoiled DNA pUC19 in methanol.

In both cases the maximum at λ=280 nm is shifted to higher wavelengths and the maximum at λ=220 nm disappears. Since the denaturation of DNA was demonstrated for the complexes with supercoiled DNA, it can be also argued that the complexes with linear DNA are also denatured.

7.3. Equilibrium in complexes between linear DNA and n-alkyltrimethylammonium surfactants in organic solvents.

Upon addition of a solution of the corresponding free surfactant for each complex, except for the supercoiled DNA in methanol (DNA-TTA), the static light scattering (SLS) intensity of the complexes remain relatively constant (see figure 7.3). A slight increase of the SLS intensity of maximum 20% is observed for the complexes between linear DNA and DTAB (lDNA-DTA). For these complexes at a charge ratio of excess of surfactant N+excess/P- = 2.5 an abrupt increase of the intensity and the radius of gyration (see figure 7.4) is observed. It could be hypothesized that aggregates are being formed due to the

low solubility of the complexes in DMF (A_2<0). lDNA-TTA also shows a slight rise of the scattering intensity which corresponds to a monotonic increase of the radius of gyration. The hydrodynamic radius remains constant, hence large aggregates (with an increasing ρ-ratio) could be formed. As stated before, only DNA-TTA shows a clear trend with respect to an increasing SLS intensity. This issue leads to the open question: Is the compaction of the supercoiled DNA responsible for the dissociation of the surfactant in methanol and therefore the further increase of the SLS intensity upon addition of free surfactant in this solvent?

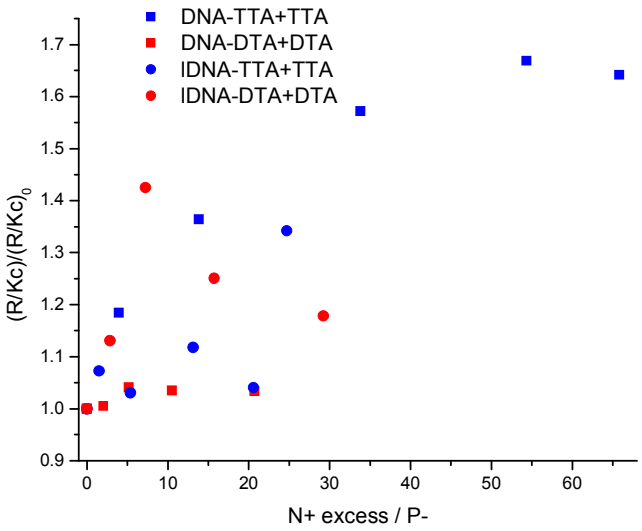

Figure 7.3. Static light scattering intensity ratio (extrapolated to q = 0) as a function of the concentration of excess of surfactant. $(Kc/R)_0$ refers to the complexes in organic solvents before the addition of surfactant. The letter "l" was added to the complexes with linear DNA (circles). The data for supercoiled DNA was replotted for comparison purposes. DNA concentration (without surfactant) is used to calculate the static light scattering intensity (Kc/R)

If the same methodology as in section 6.3.2.3 is used (equation 6.13), the number of DNA bases forming complexes in organic solvents after degradation and/or denaturation can be calculated. In table 7.5 these values are summarized for all of the complexes investigated in this work. It is clearly observed that supercoiled DNA has a lower tendency towards degradation.

Table 7.5. Calculated number of bases of DNA forming complexes with surfactants in organic solvents.

Complexes	Number of DNA bases (*f*)
DNA-TTA + TTA	1836
DNA-DTA + DTA	3213
lDNA-TTA + TTA	1202
lDNA-DTA + DTA	1174

With the number of bases (or molar mass) of the DNA forming these complexes, the fraction of surfactants bounded to the DNA at every charge after the addition of the excess of surfactant can be determined. Results showed the same trend discussed in figure 7.3.

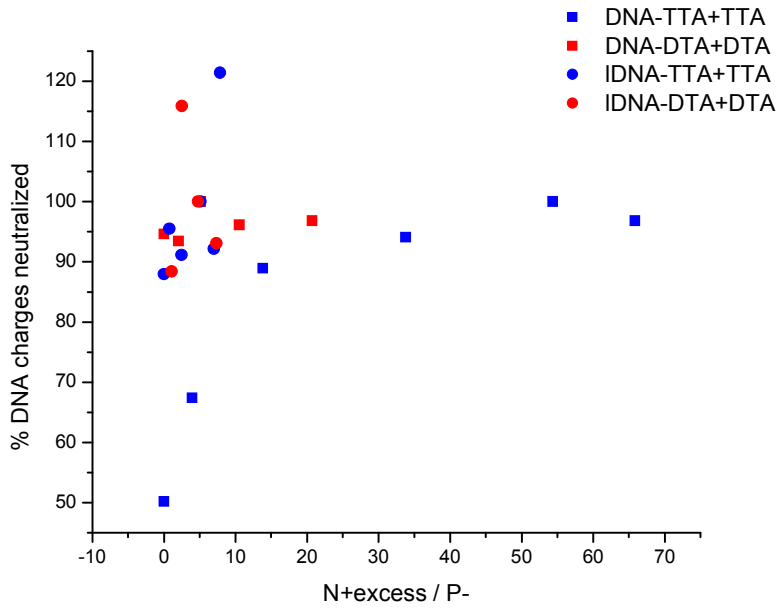

Figure 7.4. Fraction of DNA charges neutralized by surfactants after the addition of an excess of surfactant to the solution. A 100% of bounded DNA was chosen arbitrarily at a charge ratio where the complexes showed the "largest logical" molar mass. Molar masses out of the trend were not taken into account for this selection, therefore there are %DNA charged neutralized higher than one.

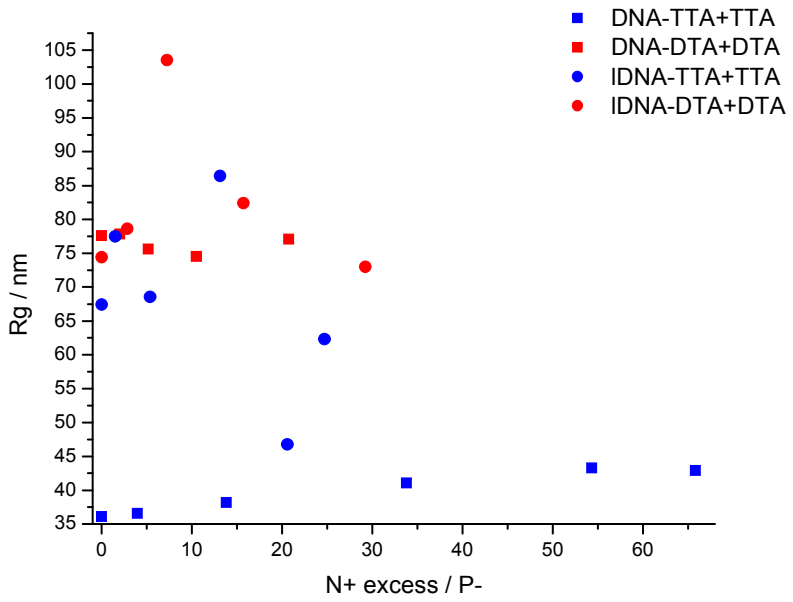

(a)

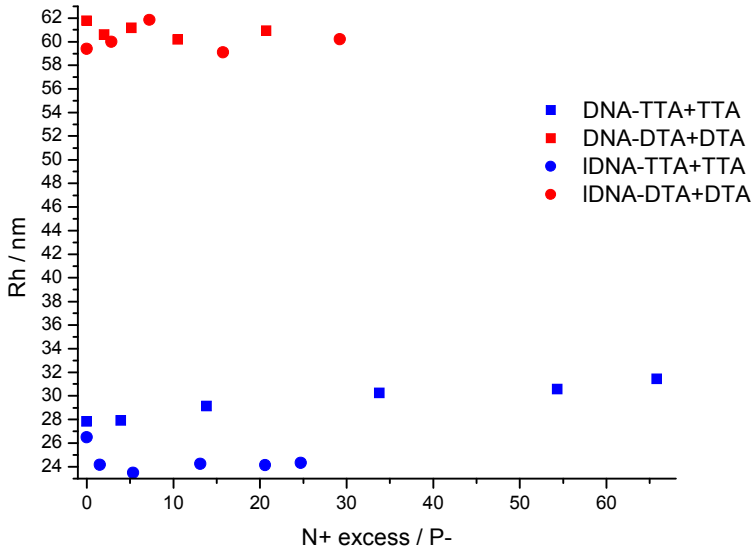

(b)

Figure 7.5 Radii of gyration (a) and hydrodynamic radii (b) of DNA-TTA complexes in methanol and DNA-DTA in DMF for linear and supercoiled DNA after the stepwise addition of TTA and DTA, respectively.

Figures 7.5 a and b confirm the statements given before. Except for the complexes with supercoiled DNA in methanol (DNA-TTA), an increase of the SLS intensity, and thus the molar mass, is always associated with an increase of the radius of gyration, whereas the hydrodynamic radius remains constant in all of the cases. Therefore, if the solutions are free of impurities, aggregates of a more extended conformation are sometimes formed.

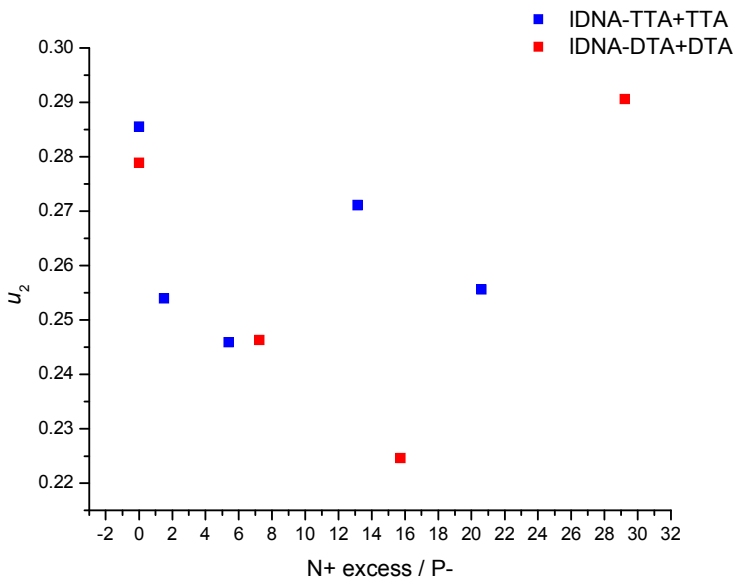

Figure 7.6 Polydispersity coefficient u_2 given by the second term of a Cumulant fit of DNA-surf complexes after the stepwise addition of surfactant (same conditions as in figures 7.2 and 7.3).

The polydispersity coefficient u_2 of the complexes with linear DNA was evaluated with a cumulant fit of the autocorrelation functions measured with DLS. It is important to notice that u_2 is different to the polydispersity index Mw/Mn measured, for instance, by gel permeation chromatography (GPC). The upper limit of u_2 to consider a sample monodisperse is 0.05. In figure 7.6 the complexes with linear DNA has a mean polydispersity coefficient of approximately 0.26. As expected, DNA complexes with linear DNA are widely polydispersed in organic solvents. The formation of some aggregates, as seen in the Zimm plots (appendix A41 and A43) may be partially responsible for the high polydispersity.

7.4. Characterization of complexes between linear DNA-surf and polycations

As stated in the introduction, the main goal of this chapter is to observe the differences in the process of formation of DNA complexes with polycations in organic solvents when a linear instead of a supercoiled DNA is employed as polyanion. It is hypothesized that a less disordered initial topology of the polyanion, i.e. the linear DNA, would lead to the formation of complexes with a controlled topology. In this section, several experiments are carried out in other to accept or reject this assumption.

7.4.1. Formation of lDNA-TTA complexes with polycations in methanol

In order to modulate the charges of the polycation and to compare the complex formation between the two different topologies of DNA in organic solvents, a non-quaternized polyvinylpyridine brush (b-PVP) is first mixed with lDNA-TTA and a methanolic HCl is added afterwards. The experimental conditions in terms of concentration, temperature and other variables are identical to the formation of complexes with supercoiled DNA described in chapter 6.

The PVP is non-quaternized, which means that except for some residual charges, it does not contain quaternary amines carrying a positive charge. However, these residual charges, although not quantified, could yield the formation of complexes with lDNA-TTA. In the case of real formation of complexes, the SLS intensity must be higher than the theoretical intensity of the mixture of the components without interaction (see equations from 6.17 to 6.20 for the calculations). In figure 7.7 theoretical calculations and experimental values after the formation of complexes with a PVP brush are shown. In effect, SLS intensities and radii of gyration higher than the predicted values for mixtures are observed. It could be postulated that complexes are indeed being formed. Nevertheless, the experimental values approach the theoretical ones for a mixture of components at a high mass fraction of the PVP. The SLS intensity is dominated by the PVP at concentrations of this polymer. In the case of complex formation, the addition of PVP at each step should lead to an increasing intensity difference between the two components. In other

words, the difference between the measured and calculated values should be larger at higher weight fractions of PVP. The experimental behavior is not clear.

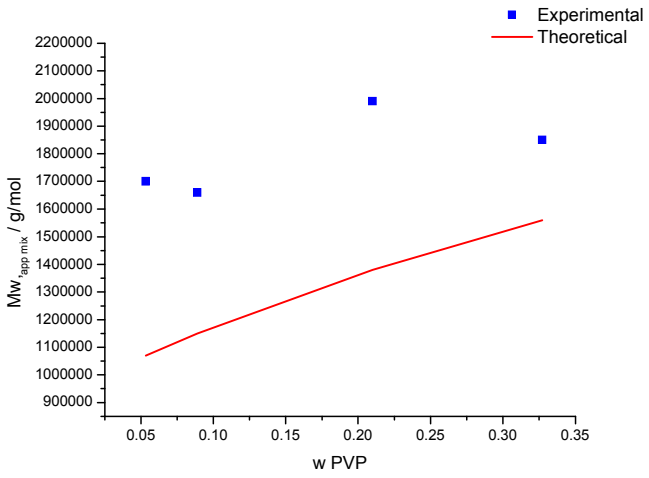

(a)

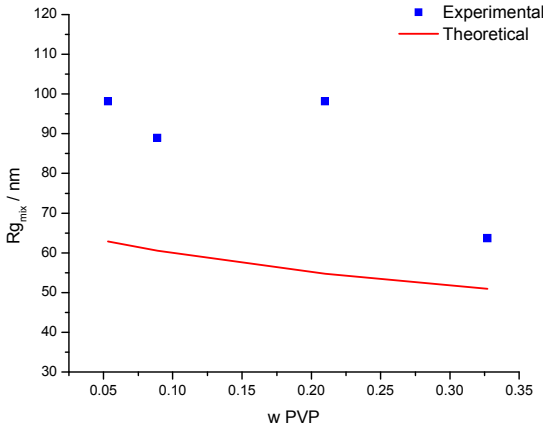

(b)

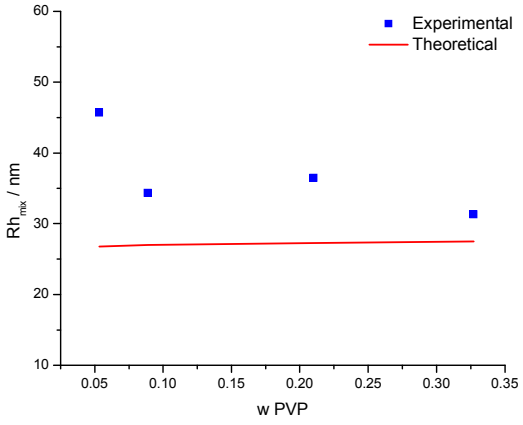

(c)

Figure 7.7. Comparison of measured and calculated (considering mixture of homopolymers) (a) molar masses, (b) radii of gyration and (c) hydrodynamic radii for the system: lDNA-TTA complex in methanol + non-quaternized polyvinylpyridine at 20°C ([LiBr = 0.001 M)]

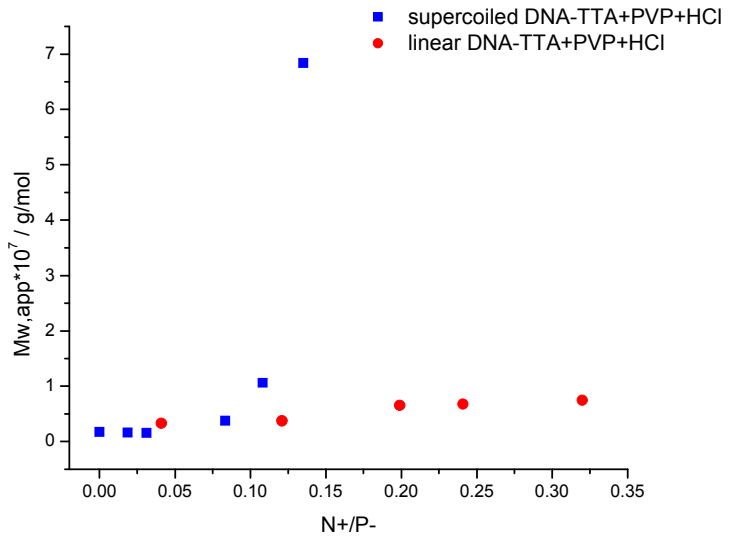

(a)

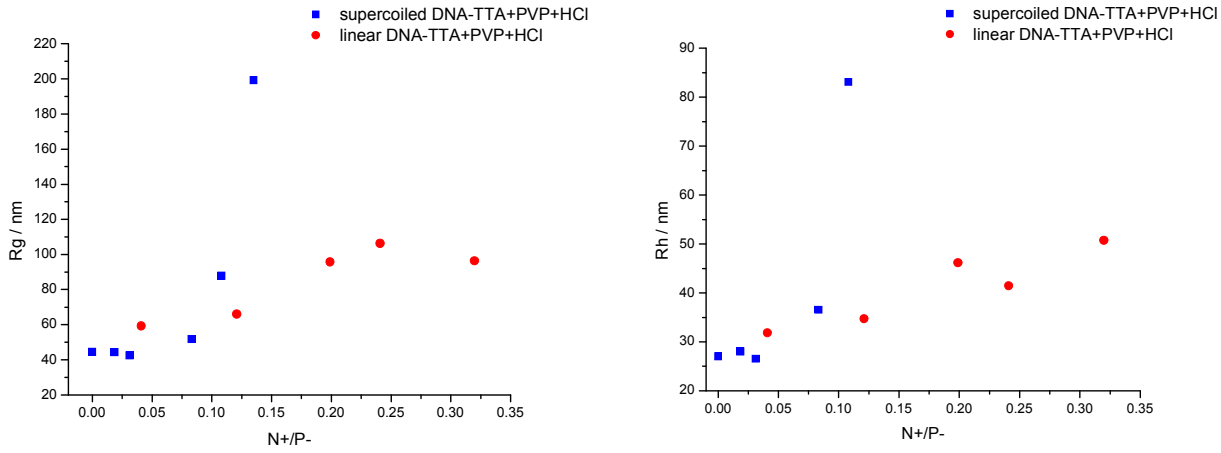

(b) (c)

Figure 7.8. (a) Apparent molar mass ($Mw_{,app}$), (b) radius of gyration and (c) hydrodynamic radius of complexes between DNA-tetradecyltrimethylammonium complex and non-quaternized polyvinylpyridine brushes in a methanolic solution after the stepwise addition of a solution of HCl in methanol at 20°C ([LiBr = 0.001 M)]. At charge ratios (N+/P-) higher than the plotted in this figure, the complexes undergo precipitation.

Upon titration of the lDNA-TTA + b-PVP with methanolic HCl 1 mM, complexes are formed as indicated by the increase of molar mass in figure 7.8. Surprisingly, complexes prepared with linear and supercoiled DNA differ significantly in the way the molar mass varies with an increment of the positive charges. For the supercoiled DNA-TTA, the molar mass remains constant until a critical charge ratio of N+/P- ≈ 0.08. Addition of more acid resulted in a large increase of the molar mass until precipitation at a charge ratio of N+/P- = 0.15. Assuming that polyelectrolyte aggregates are formed in the same manner in aqueous solutions and in organic solvents, the aggregation of supercoiled DNA can be attributed to interbridging of polyelectrolytes and of "primary complexes" as described in other works [13]. For linear DNA, the critical charge ratio at which a molar mass increase starts to be evidenced is around N+/P- =0.12, higher than for supercoiled DNA. Also precipitation of complexes with linear DNA takes place at a higher charge ratio (N+/P- > 0.32). Whereas the molar mass of the complexes increases exponentially for supercoiled DNA, the molar mass of lDNA-TTA increases only slightly until a sudden precipitation takes place.

Several researchers have already reported that supercoiled DNA forms complexes at lower charge ratios than linear DNA. Ma et al [10], for instance, prepared complexes with magnesium (Mn^{2+}) using DNA with these two topologies. Whereas the SLS intensity for the linear DNA remain unchanged after the addition of 2 mM of Mn, the SLS of the supercoiled DNA with the same concentration of the divalent cation increased about threefold. The authors pointed out that negative supercoiling of plasmid DNA facilitate condensation because with this topology long stretches of DNA can be brought into close proximity with a roughly parallel orientation. This conformation may be viewed to produce a "pressure" pushing the helices together, similar to the osmotic stress caused by high concentration of neutral polymers. On the contrary, linear DNA cannot make long DNA stretches come together in parallel position, which lead to a loss of the contribution to nucleation of DNA. In other words, in the supercoiled structures, the charges are "forced" to be closer and therefore the intramolecular electrostatic repulsions are higher than in linear DNA. These repulsions make supercoiled DNA more susceptible to complexation. Ma et al also claimed that the supercoiling stress cooperates in producing and stabilizing localized distortions of the double helix, important to produce or increase attractive forces between DNA chains. Itaka et [14] al and Li et al [3] also observed that formation of complexes with linear DNA required a higher charge ratio under the same conditions. It is also well known that supercoiled DNA is

more efficient and faster in the process of transfection [9, 15, 16, 17], presumably in some cases due to the higher efficiency of complexation of supercoiled DNA.

It is important to consider that supercoiled DNA is more densed than linear DNA. Then density, ρ, of a particle can be estimated as [13],

$$\rho = \frac{Mw/N_L}{(\frac{4}{3})\pi Rh^3} \qquad (7.8)$$

Where

Mw: molar mass

N_L: Avogadro's number

Rh: hydrodynamic radius

For supercoiled DNA ρ = 0.0085 g/cm^3 whereas for the linear conformation ρ = 0.0052 g/cm^3. In other words, DNA pUC19 augment its density (and hence the number of charges per unit volume) by 40% in its negative supercoiled conformation. Given that the number of charges of the DNA remains unchanged upon enzymatic cut in one point, an increment of the density also represents a rise of the number of charges / volume. This variation of the density can be interpreted as lower electrostatic forces with the linear DNA.

7.4.2. Formation of DNA-DTA complexes with polycations in DMF

The non-quaternized PVP brush was also titrated to the complexes lDNA-DTA in DMF. For Rg and Rh the deviations of the experimental data from the calculated values are low. However, measured molar mass is significantly higher than the theoretical for a mixture of the components. From these results, it can

be deduced that complexes are being formed. Because an abrupt change of Rg and Rh cannot be observed in figure 7.9 b and c, it can be also inferred that aggregates are not present.

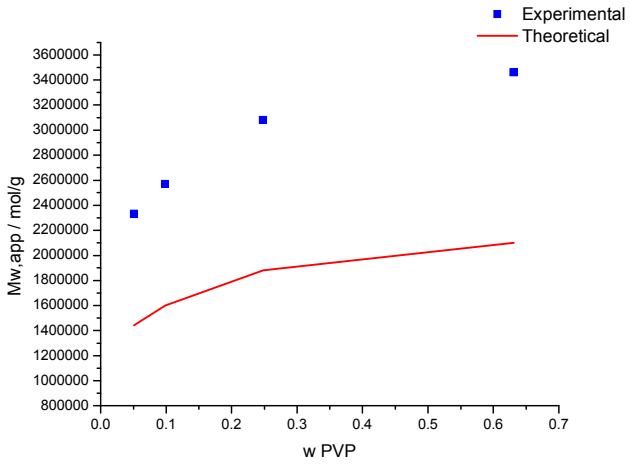

(a)

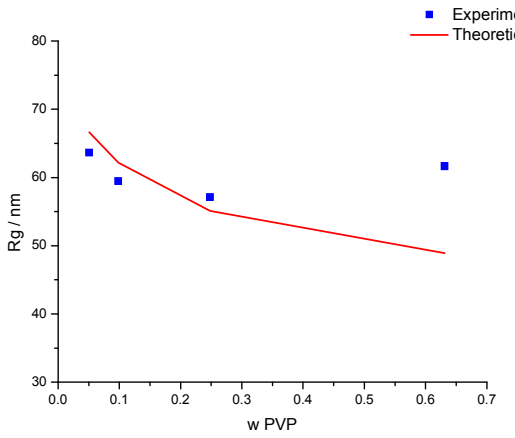

(b)

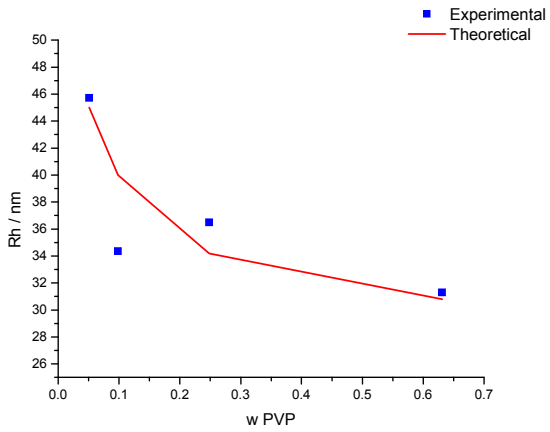

(c)

Figure 7.9. Comparison of measured and calculated (considering mixture of homopolymers) (a) molar masses, (b) radii of gyration and (c) hydrodynamic radii for the system: lDNA-DTA complex in DMF + non-quaternized polyvinylpyridine at 20°C ([LiBr = 0.001 M)]

Complexes with linear DNA in DMF were also formed with the same polylysine brush (b-PLL) introduced in chapter 6.1. At low concentrations of the b-PLL c=0.02 g/l no formation of complexes was evidenced. The concentration of the polycation was then increased to c=10.75 g/l. The results after the increase of the concentration are shown in figures 7.10 a – c. Since the polylysine is charged (approximately 900 charges / polymer), the variables Mw, Rg and Rh are plotted not only against the weight fraction (wPLL) but also against the charge ratio. The molar mass of the complexes at low charge ratios differs widely from the calculated for a mixture of the components. However, the experimental molar mass decreases with the increment of the concentration and at higher weight fraction of PLL (wPLL=0.985). This result is meaningless. The molar mass cannot decrease under these conditions. At high weight fraction of the polylysine, the light scattering intensity is dominated by the polycation, i.e. the SLS intensity becomes significantly higher than the intensity of the complexes and the calculated and experimental results tend to converge.

Next, the order of mixing was inverted. The lDNA-DTA c=0.315 g/l was added to a solution containing the polylysine brush at a concentration of c=10.75 g/l. Given that the ratio of Mw PLL / Mw lDNA-DTA is approximately 10 and the concentration of b-PLL is higher by a factor of 34, the SLS intensity is expected to be dominated by the polylysine. In figure 7.11a the molar mass of the mixture is calculated using the apparent molar mass of the PLL at each concentration. Under this condition, the calculated and experimental molar masses are similar. Hence, it is concluded that complexes are not formed. It is important to notice that at such high concentration, the polylysine could be in a semidilute instead of a dilute regime.

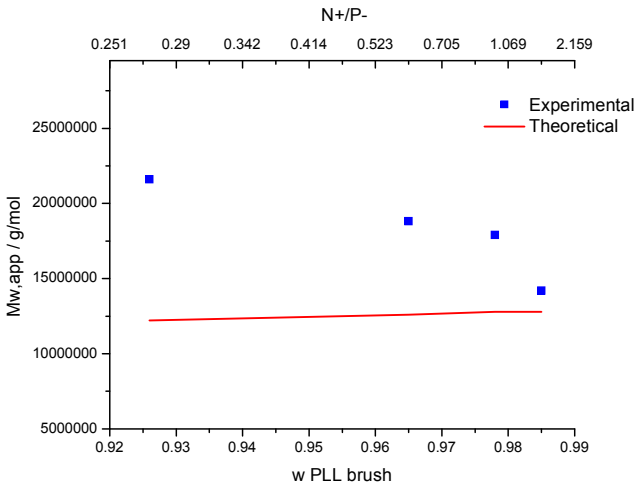

(a)

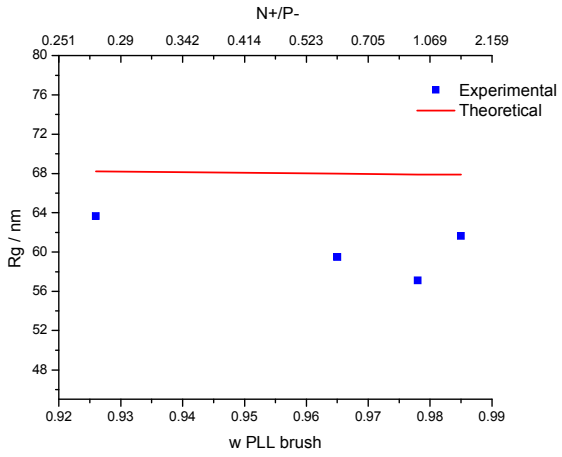

(b)

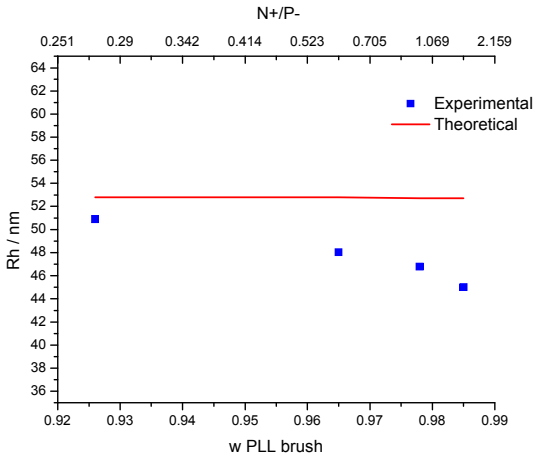

(c)

Figure 7.10. Comparison of measured and calculated (considering mixture of homopolymers) (a) molar masses, (b) radii of gyration and (c) hydrodynamic radii for the system: lDNA-DTA complex in DMF $c_{initial}$ = 0.315 g/l + polylysine brush c_{stock}=10.75 g/l at 20°C ([LiBr = 0.001 M)]

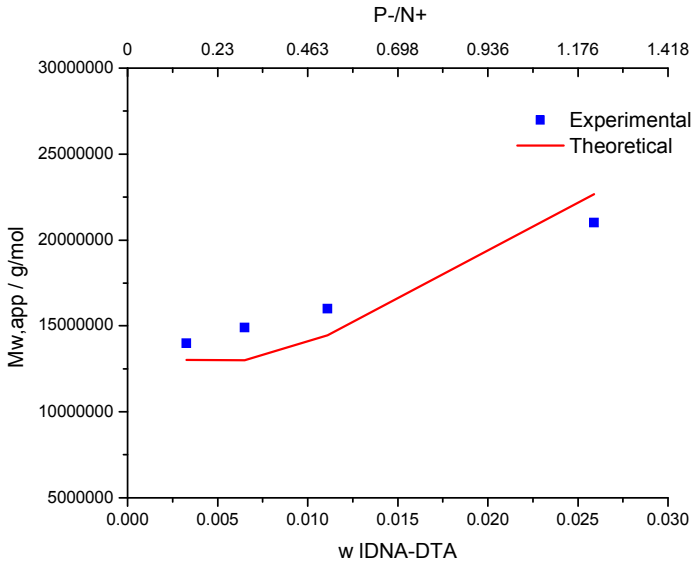

(a)

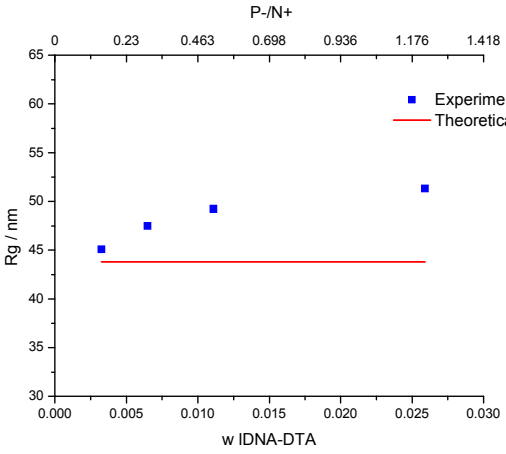

(b)

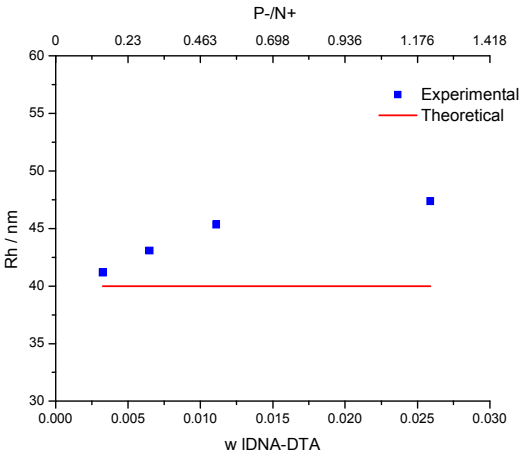

(c)

Figure 7.11. Comparison of measured and calculated (considering mixture of homopolymers) (a) molar masses, (b) radii of gyration and (c) hydrodynamic radii for the system: polylysine brush $c_{initial}$=10.75 g/l + lDNA-DTA complex in DMF c_{stock}=0.315g/l at 20°C ([LiBr = 0.001 M)]

To determine the regime of concentration for the polylysine at c=10.75 g/l, the overlap polymer concentration (c*) is calculated assuming a coiled polymer in a good solvent[18].

$$c^* = \frac{3M}{4\pi N_L Rg^3} \tag{7.9}$$

In table 6.1 (chapter 6, section 6.1) the values of Mw and Rg for the polylysine brush are given. The calculated overlap concentration has a value of 10.5 g/l. Even if equation 7.9 is just an approximation, since the polylysine is a brush with a ρ=1.75, which corresponds to the value of polydisperse flexible coil, it shows that this polymer is close or in a semidilute regime. In this case, the properties of the polymer vary vastly. Furthermore, at such high concentrations, not only a form factor P(q) has to be utilized in the Zimm equation (see section 4.2) but also a structure factor S(q) must be considered to account for the intermolecular scattering [19]. During the dilution of the polymer, S(q) increases until a limit value of 1. Hence the results in figure 7.9 cannot be directly interpreted as the formation of complexes with linear DNA in DMF. A comparison of a Zimm plot (by only diluting the polylysine brush) and the results in figure 7.8 revealed that, in fact, complexes are not formed and the increment of the light scattering intensity, and therefore the molar mass, is only an artifact due to the high concentration of the polylysine (see appendix A56).

7.5. Conclusions

The topology of complexes with surfactants and polycations using a linear and a supercoiled DNA as precursors was compared. In DMF, DNA complexes showed similar sizes whereas in methanol expanded structures were measured with light scattering for linear DNA and compacted conformations for supercoiled DNA. It could be postulated that linear polyanions could have a tendency of forming more expanded complexes given the high cost of entropic energy of compaction. It could be also affirmed that the initial topology of the polyanion has an influence on the final size of the complexes, only if the formation of final compacted structures is favored. The solubility of the complexes is slightly changed with respect to the initial conformation of the DNA. Whereas methanol and DMF turned out to be good solvents (A_2>0) for DNA-TTA and DNA-DTA complexes, respectively; the measured second virial

coefficient is always negative for linear DNA complexes. Upon formation of complexes with polycations in methanol, linear DNA complexes are more stable (aggregates are formed at a higher charge ratio N+/P-) than supercoiled DNA. Surprisingly, under different conditions and polycations it was not possible to form complexes with polycations for linear DNA in DMF. These results are in contrast to the formation of precipitates with the supercoiled DNA-DTA complexes in DMF after the addition of a polylysine brush.

7.6. References

1. Boles, C.; White, J.; Cozzarelli, N. J. Mol. Biol., 1990, 213, 931 – 951.
2. Schärtl, W. Light Scattering from Polymer Solutions and Nanoparticle Dispersions. Springer, 2007.
3. Li, Y.; Yildiz, U.; Muellen, K.; Gorehn, F. Biomacromolecules, 2009, 10, 530 – 540.
4. de Carmejane, O.; Schwinefus, J.; Wang, S.; Morris, M. Journal of Chromatography, 1999, 849, 267 – 276.
5. Bloomfield, V. Biopolymers, 1991, 31, 1471 – 1481
6. Lahiri, A. Biopolymers, 1994, 34, 799 – 804.
7. Vologodskii, A.; Levene, S.; Klenin, K.; Frank-Kamenetskii, M.; Cozzarelli, N. J. Mol. Biol, 1992, 227, 1224 – 1243.
8. Arscott, P.; Li, A.; Bloomfield. V. Biopolymers, 1990, 30, 619 – 630.
9. von Groll, A.; Levin, Y.; Barbosa, M.; Ravazzolo, A. Biotechnol. Prog, 2006, 22, 1220 – 1224.
10. Ma, C.; Bloomfield, V. Biophysical Journal, 1994, 67, 1678 – 1681.
11. Girod, J.; Johnson, C.; Huntington, S.; Maestre, M. Biochemistry, 1973, 12 (25), 5092 – 5096.
12. Frerix, A.; Geilenkirchen, P.; Müller, M.; Kula, M.; Hubbuch, J. Biotechnology and Bioengineering, 2007, 96, 57 – 66.
13. Störkle, D.; Duschner, S.; Heimann, N.; Maskos, M.; Schmidt, M. Macromolecules, 2007, 40 (22), 7998 – 8006.
14. Itaka, K.; Yamauchi,K.; Harada, A.; Nakamura, K.; Kawaguchi, H.; Kataoka, K. Biomaterials. 2003, 24, 4495 – 4506.
15. Tabuchi, H.; Hirose, S. The Journal of Biological Chemistry, 1988, 263 (30), 15282 – 15287.
16. Cherng, J.; Schuurmans-Nieuwenbroek, N.; Jiskoot, W.; Talsma, H.; Zuidam, N.; Hennink, W.; Crommelin, D. Journal of Controlled Release, 1999, 60, 343 – 353.
17. Remaut, K.; Sanders, N.; Fayazpour, F.; Demeester, J.; De Smedt, S. Journal of Controlled Release, 2006, 115, 335 – 343.
18. Lodge, T.; Muthukumar, M. J. Phys. Chem. 1996, 100, 13275 – 13292.
19. Teraoka, I. Polymer Solutions. Introduction to physical properties. John Wiley & Sons, 2002.

8. General Conclusions

Polyelectrolyte complexes with oppositely charged multivalent ions, surfactants and polyelectrolytes were formed in aqueous solutions as well as in organic solvents. In the literature, it has been reported that complexes typically consist of several molecules of the polymer(s). In this work, we achieve to prepare complexes containing only one polyanion (DNA). From a physical chemistry perspective, the "ideal" polyelectrolyte complexes fulfill the following conditions: 1) Complex stability with varying charge ratio and 2) 100% charge neutralization without the need for an excess of any of the components. During the course of our investigations we found four systems which form complexes with DNA but only one system that meets these ideal conditions for complex formation, DNA complexes with the block copolymer polyethylene glycol – b – polylysine.

It was also demonstrated that polyelectrolytes complexes in organic solvents have different characteristics than those reported in aqueous solutions. Dried precipitates of supercoiled DNA complexes with alkyltrimethylammonium bromide surfactants containing 12 (DTAB) and 14 (TTAB) carbons were dissolved in DMF and methanol, respectively. The main differences between complexes in aqueous solutions and in organic solvents are:

1. Dissociation of the surfactants can take place. Monovalent cations cannot condense DNA. However, alkyltrimethylammonium surfactants have the ability to condense DNA due to the hydrophobic interactions among neighboring surfactants within a given complex. These hydrophobic interactions disappear in organic solvents. Thus, the surfactants can "easily" leave the DNA complex.

2. DNA denatures partially or totally. The two strands of DNA are held together because of the hydrogen bonding and hydrophobic interactions among the nucleotide bases. The repulsive electrostatic interactions of the negative charges in the DNA backbone oppose the formation of the double strand. All these opposing forces described are in balance in aqueous solutions.

However, in organic solvents with a lower dielectric constant with water, not only the hydrophobic interactions disappear but also the electrostatic repulsions increase. Therefore, the repelling forces dominate within DNA dominate and the double helix denatures, i.e. the two strands dissociate. It has been reported, that surfactants can protect DNA against denaturing in organic solvents. However, in our studies, it was observed that DNA denatures completely in methanol. This can be explained in terms of the surfactant dissociation. Once the surfactant "leaves" the complex, DNA is unprotected and denatures.

3. DNA complexes in organic solvents are degraded (some bonds from the DNA are being broken). The cause of degradation remains still as an open question.

It is important to notice, that the characteristics of DNA complexes depend on the specific cation used to neutralize the charges. For example, the complexes with the surfactant containing 12 carbons (DNA-dodecyltrimethylammonium) are only soluble in DMF, whereas the complexes with a similar surfactant, containing only two additional carbons on the tail (DNA-tetradecyltrimethylammonium) are soluble in methanol. The conformation of DNA complexes with these two surfactants is significantly different. In DMF, the DNA-surfactant complexes form stiff rings with some additional degradation products. In methanol, the complexes have a compacted conformation, consisting of a mixture of sphere-like and rod-like structures.

The complex formation between DNA and polycations is controlled by the kinetics. As a consequence of this kinetically controlled process, the final structure of the complexes consists of several molecules (aggregate), which eventually precipitate.

The initial topology of the polyelectrolytes also plays a decisive role in the properties of the complexes. The supercoiled structure of the DNA was linearized while keeping the molar mass constant in order to study the influence of how different DNA topologies affect the structures of the resultant complexes in organic solvents. There were 2 main differences observed between the linear and supercoiled DNA complexes:

1. Complexes prepared with linear DNA have a greater tendency to aggregate than those prepared with supercoiled DNA. As previously mentioned, DNA complexes in methanol form compacted structures to minimize contact with the solvent. The formation of compact structures requires a high entropic energy, i.e. the molecule looses conformational degree of freedom. This cost of entropy is higher for linear DNA, because the "supercoiled" structure is already partially compacted. Hence, to avoid contact with the solvent, complexes with linear DNA preferred to aggregate rather than to form more compact structures.

2. Supercoiled DNA in organic solvents forms complexes with polycation at lower charge ratios than linear DNA under the same conditions. Whereas precipitation at a charge ratio as low as 0.12 was observed with supercoiled DNA in DMF, complexes did not form under the same conditions, e.g. using the same polycation (a protected polylysine brush). In methanol precipitation is observed with both topologies, but linear DNA requires a polycation (polyvinylpyridine) with a charge density five times higher than for supercoiled DNA.

9. Appendix

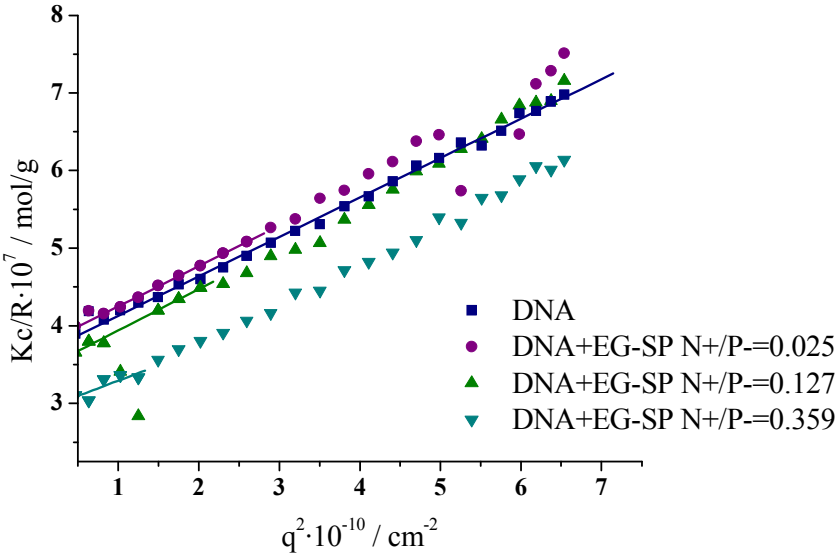

(a)

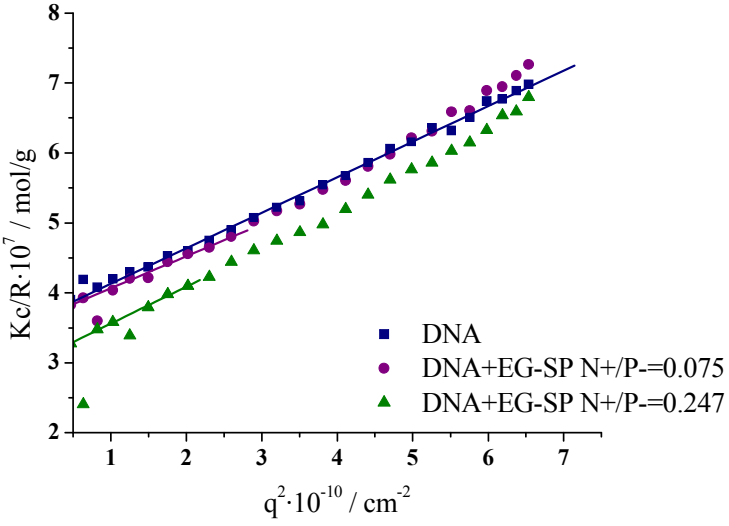

(b)

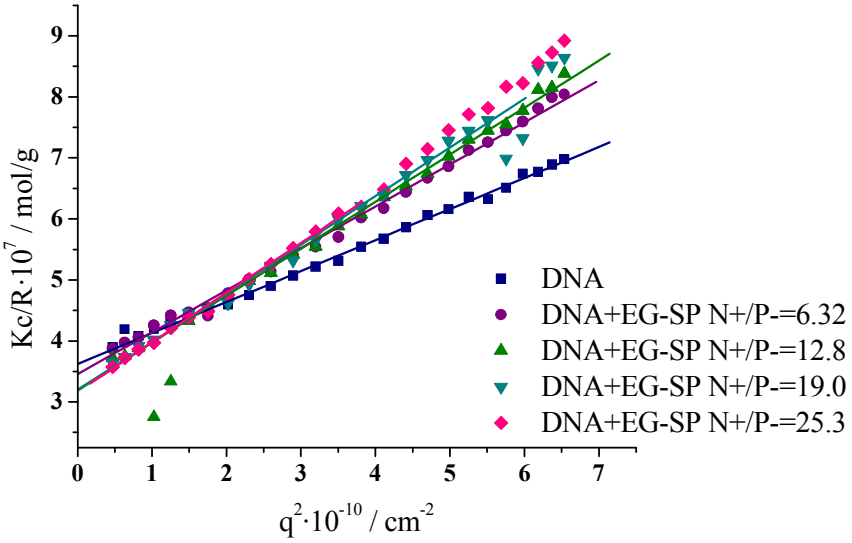

(c)

Figure A1. Static light scattering intensity (Kc/R) vs. the scattering vector (q^2) of DNA titrated with a spermine derivatives containing a block of seven repeating units of ethylene glycol (EG-SP) in a 5 mM phosphate buffer pH = 7, at T=20°C. The static light scattering (SLS) measurements were performed at amgles from 30° to 150° in steps of 5°. The total measurements were generated in two different titrations: the first titration was done until a charge ratio of N+/P- =0.479 at a concentration of EG-SP c=0.025 g/l (divided in plots (a) and (b) for better illustration); the second titration was done from N+/P- = 6.32 to N+/P- = 25.3 (c). The concentration of EG-SP was c=2.25 g/l. The initial concentration of DNA was in the two titrations c=0.05 g/l.

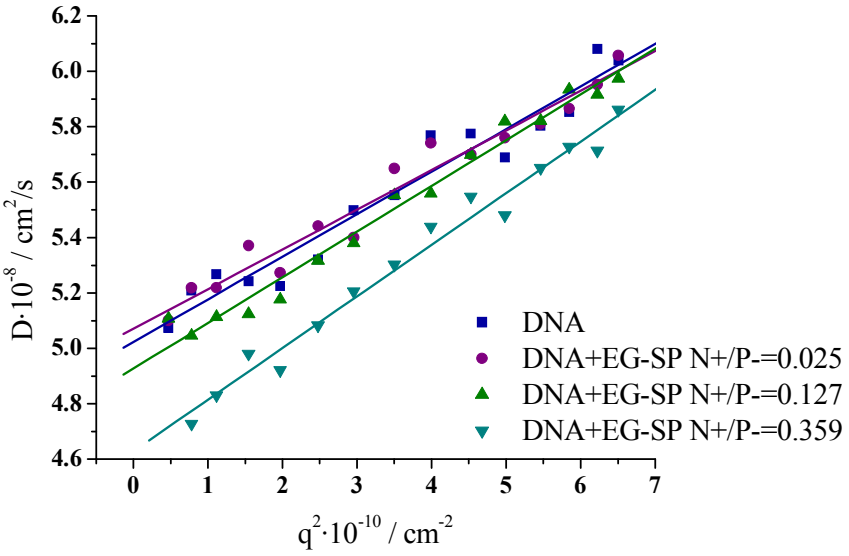
6.2
6.0
5.8
5.6
5.4
5.2
5.0
4.8
4.6
D·10^-8 / cm^2/s
0
1
2
3
4
5
6
7
q^2·10^-10 / cm^-2
DNA
DNA+EG-SP N+/P-=0.025
DNA+EG-SP N+/P-=0.127
DNA+EG-SP N+/P-=0.359

(a)

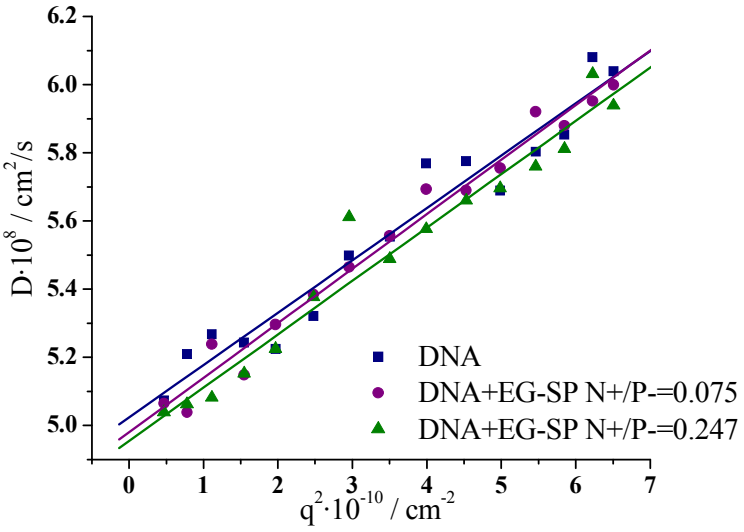
6.2
6.0
5.8
5.6
5.4
5.2
5.0
D·10^8 / cm^2/s
0
1
2
3
4
5
6
7
q^2·10^-10 / cm^-2
DNA
DNA+EG-SP N+/P-=0.075
DNA+EG-SP N+/P-=0.247

(b)

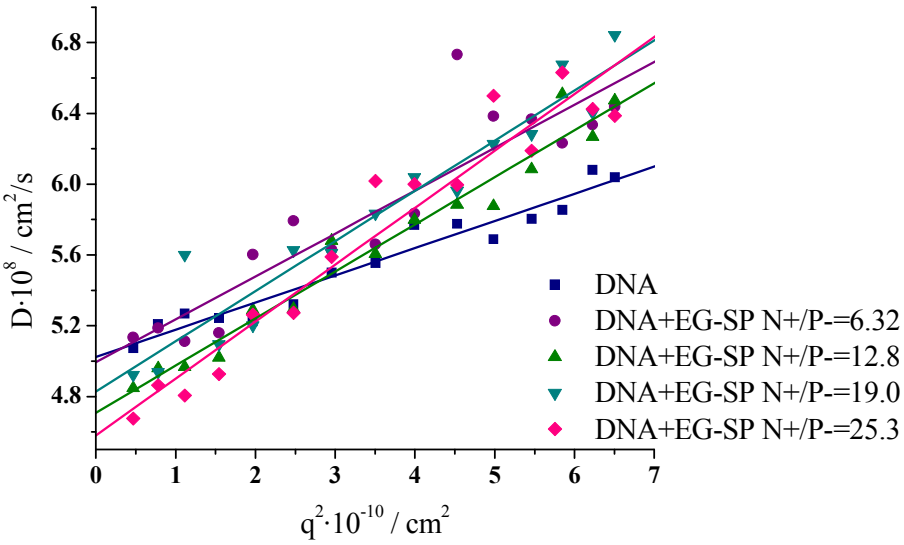

(c)

Figure A2. Diffusion coefficient (D) vs. the scattering vector (q^2) of DNA titrated with a spermine derivatives containing a block of seven repeating units of ethylene glycol (EG-SP) in a 5 mM phosphate buffer pH = 7, at T=20°C. The dynamic light scattering (DLS) measurements were performed with a multiangle light scattering having 8 detectors, separated by an angle of 17° each. The first detector was placed at an angle of 30° and 39°. The total measurements were generated in two different titrations: the first titration was done until a charge ratio of N+/P- =0.479 at a concentration of EG-SP c=0.025 g/l; (divided in plots (a) and (b) for better illustration) the second titration was done from N+/P- = 6.32 to N+/P- = 25.3 (plot (c)). The concentration of EG-SP was c=2.25 g/l. The initial concentration of DNA was in the two titrations c=0.05 g/l.

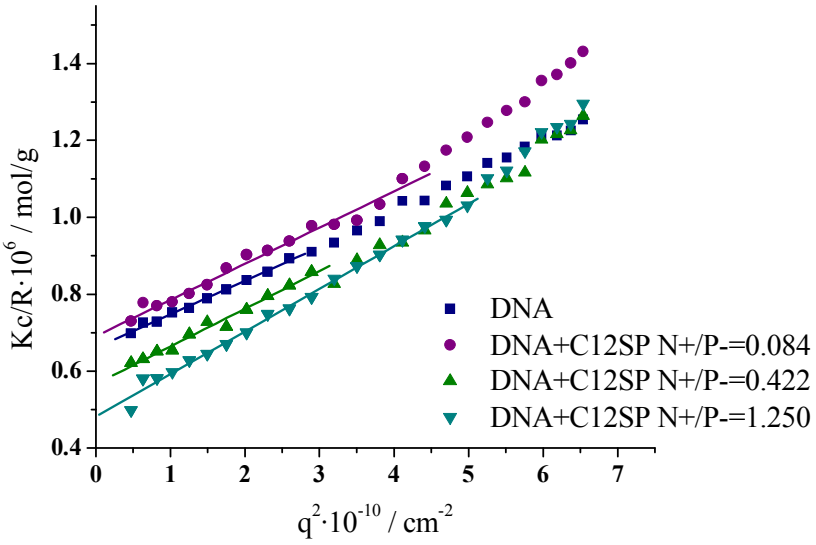
Kc/R·10^6 / mol/g
q^2·10^-10 / cm^-2
DNA
DNA+C12SP N+/P-=0.084
DNA+C12SP N+/P-=0.422
DNA+C12SP N+/P-=1.250

(a)

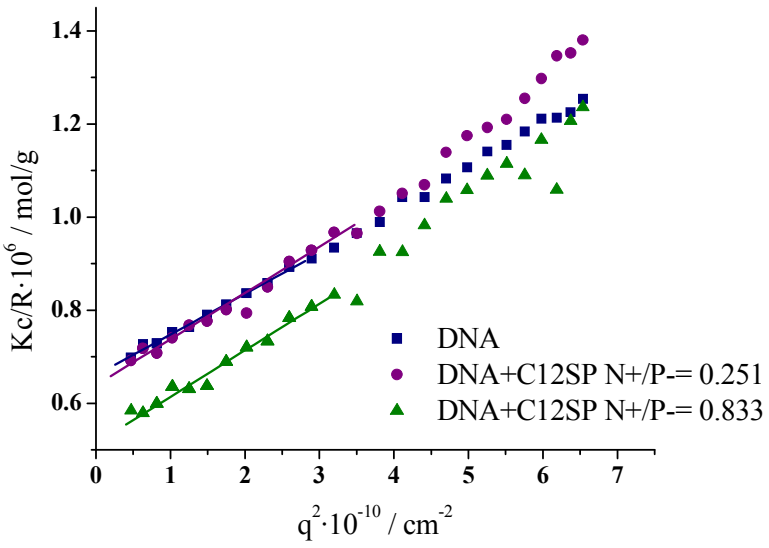

(b)

Figure A3. Static light scattering intensity (Kc/R) vs. the scattering vector (q^2) of DNA titrated with a dodecylspermine in a 5 mM phosphate buffer pH = 7, at T=20°C. The static light scattering (SLS) measurements were performed at amgles from 30° to 150° in steps of 5°. The concentration of the dodecylspermine stock solution is 0.015 g/l. The initial concentration of DNA was c=0.05 g/l. The scattering ratio at N+/P- = 1.663 was omitted because there were aggregates. The plots were divided in (a) and (b) for better illustration.

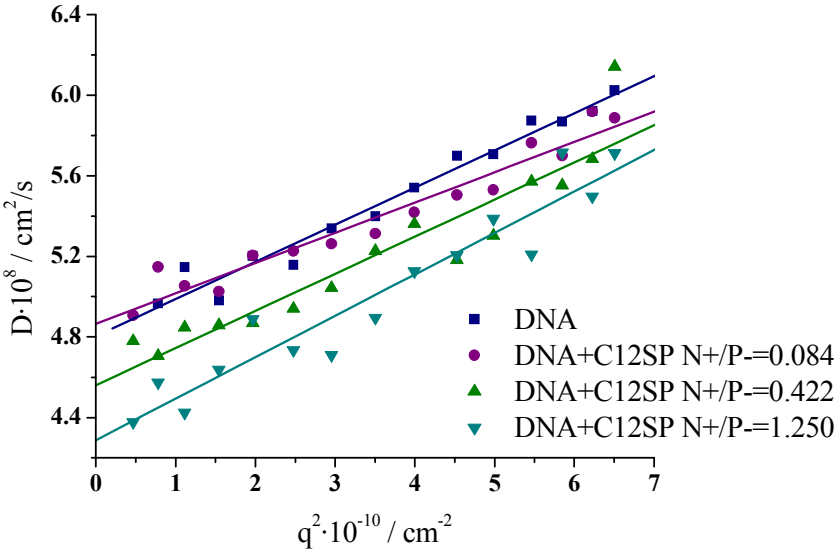
6.4
6.0
5.6
5.2
4.8
4.4
0
1
2
3
4
5
6
7
D·10^8 / cm^2/s
q^2·10^-10 / cm^-2
DNA
DNA+C12SP N+/P-=0.084
DNA+C12SP N+/P-=0.422
DNA+C12SP N+/P-=1.250

(a)

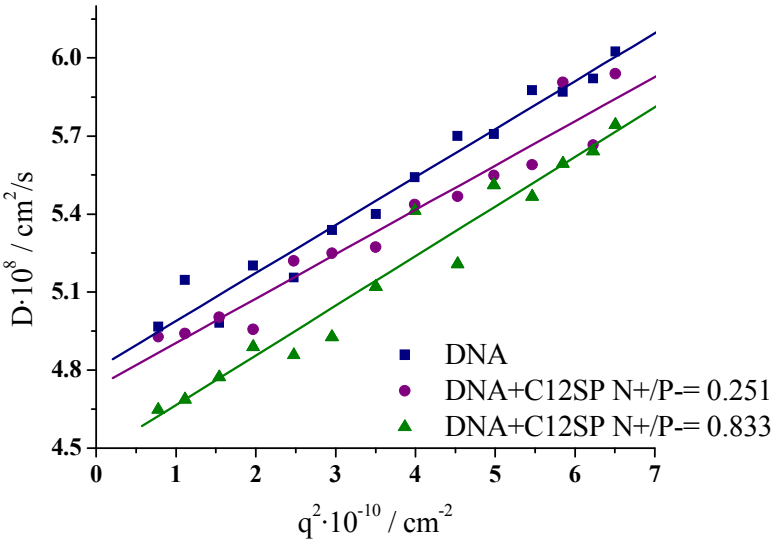

(b)

Figure A4. Diffusion coefficient (D) vs. the scattering vector (q^2) of DNA titrated with a dodecylspermine in a 5 mM phosphate buffer pH = 7, at T=20°C. The dynamic light scattering (DLS) measurements were performed with a multiangle light scattering having 8 detectors, separated by an angle of 17° each. The first detector was placed at an angle of 30° and 39°. The concentration of the dodecylspermine stock solution is 0.015 g/l. The initial concentration of DNA was c=0.05 g/l. The plots were divided in (a) and (b) for better illustration.

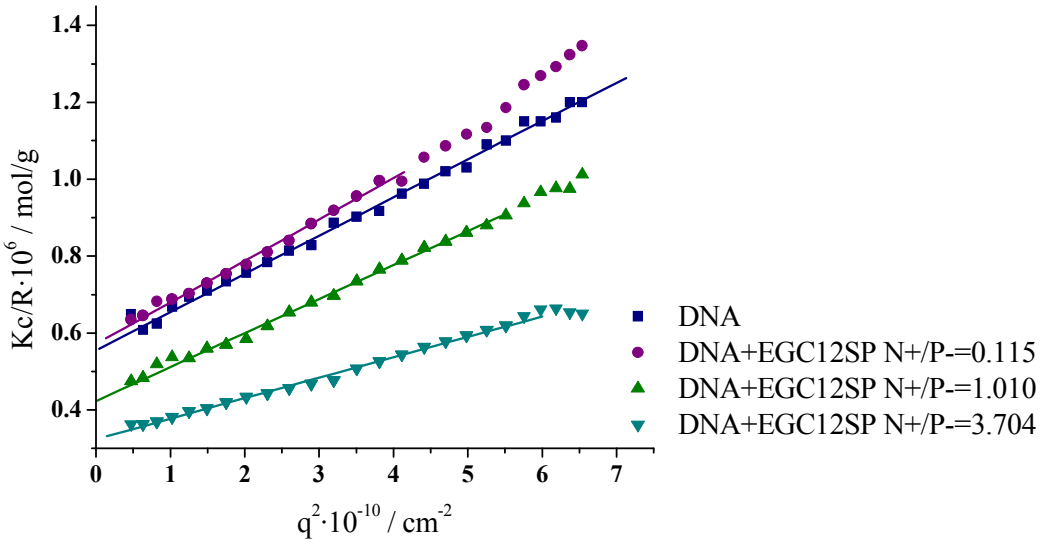
1.4
1.2
1.0
0.8
0.6
0.4
Kc/R·10^6 / mol/g
0
1
2
3
4
5
6
7
q^2·10^-10 / cm^-2
DNA
DNA+EGC12SP N+/P-=0.115
DNA+EGC12SP N+/P-=1.010
DNA+EGC12SP N+/P-=3.704

(a)

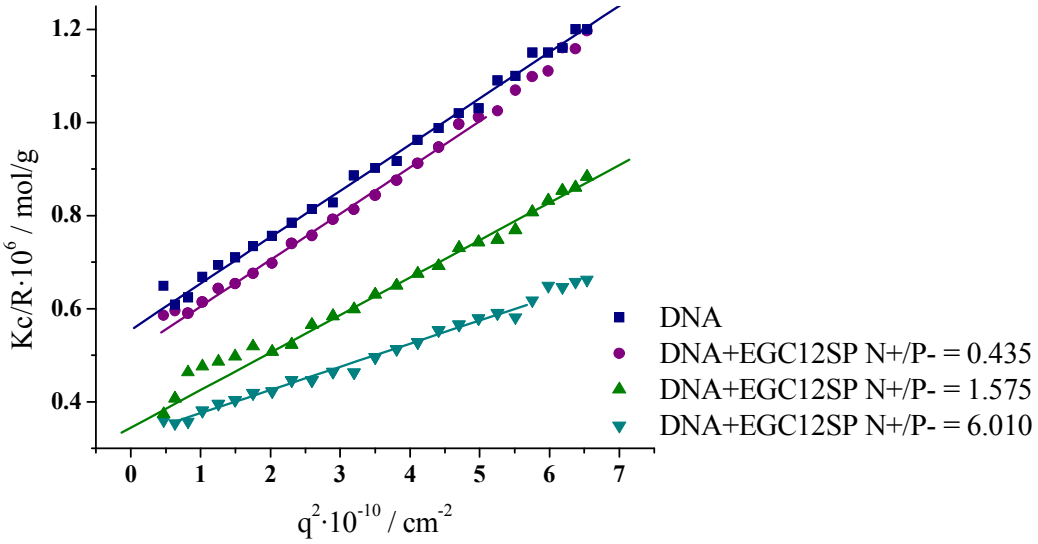

(b)

Figure A5. Static light scattering intensity (Kc/R) vs. the scattering vector (q^2) of DNA titrated with a spermine derivatives containing a block of seven repeating units of ethylene glycol and another block of a dodecyl- radical (EG-C12-SP) in a 5 mM phosphate buffer pH = 7, at T=20°C. The static light scattering (SLS) measurements were performed at amgles from 30° to 150° in steps of 5°. In the the measurements until a charge ratio of N+/P- =1.575, the concentration of the EG-C12-SP stock solution was 0.1 g/l. From N+/P- = 3.704 to N+/P- = 6.01. The concentration of EG-C12-SP was c=1 g/l. The initial concentration of DNA was c=0.05 g/l. The plots were divided in (a) and (b) for better illustration.

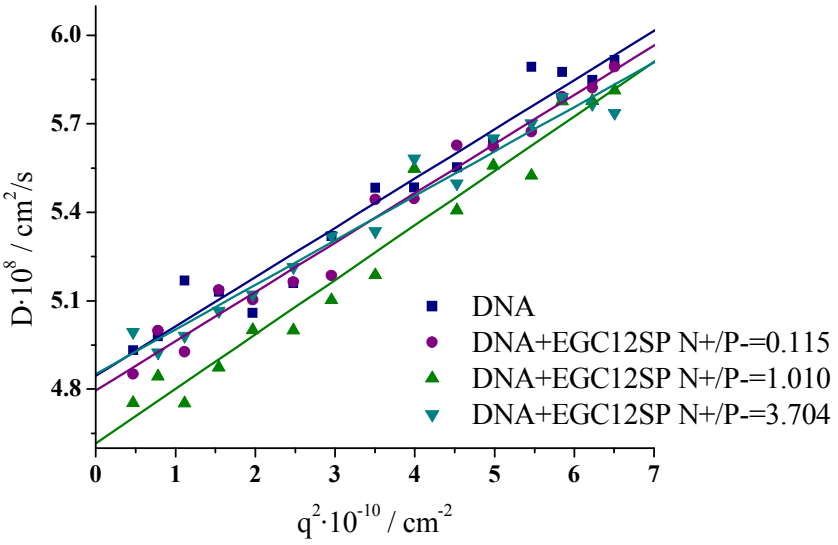
6.0
5.7
5.4
5.1
4.8
D·10^8 / cm^2/s
0
1
2
3
4
5
6
7
q^2·10^-10 / cm^-2
DNA
DNA+EGC12SP N+/P-=0.115
DNA+EGC12SP N+/P-=1.010
DNA+EGC12SP N+/P-=3.704

(a)

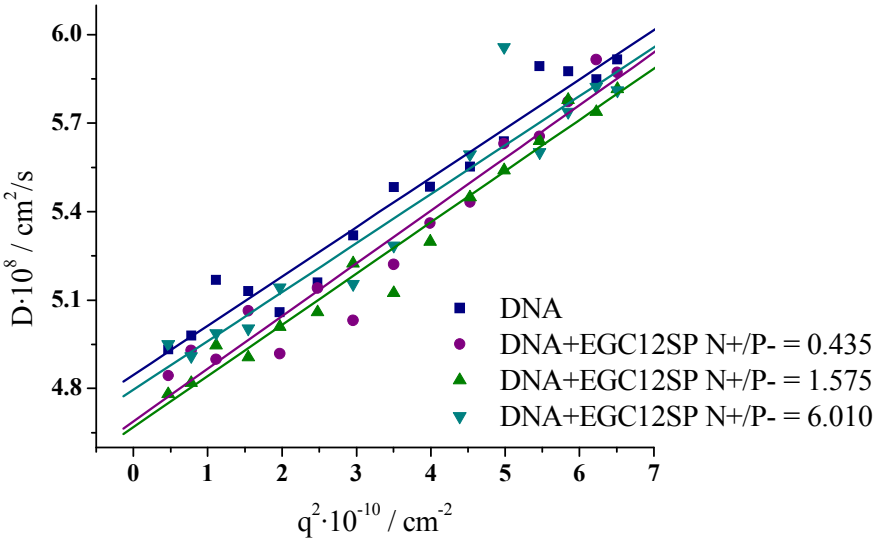

(b)

Figure A6. Diffusion coefficient (D) vs. the scattering vector (q^2) of DNA titrated with a spermine derivatives containing a block of seven repeating units of ethylene glycol and another block of a dodecyl-radical (EG-C12-SP) in a 5 mM phosphate buffer pH = 7, at T=20°C. The dynamic light scattering (DLS) measurements were performed with a multiangle light scattering having 8 detectors, separated by an angle of 17° each. The first detector was placed at an angle of 30° and 39°. In the the measurements until a charge ratio of N+/P- =1.575, the concentration of the EG-C12-SP stock solution was 0.1 g/l. From N+/P- = 3.704 to N+/P- = 6.01. The concentration of EG-C12-SP was c=1 g/l. The initial concentration of DNA was c=0.05 g/l. The plots were divided in (a) and (b) for better illustration

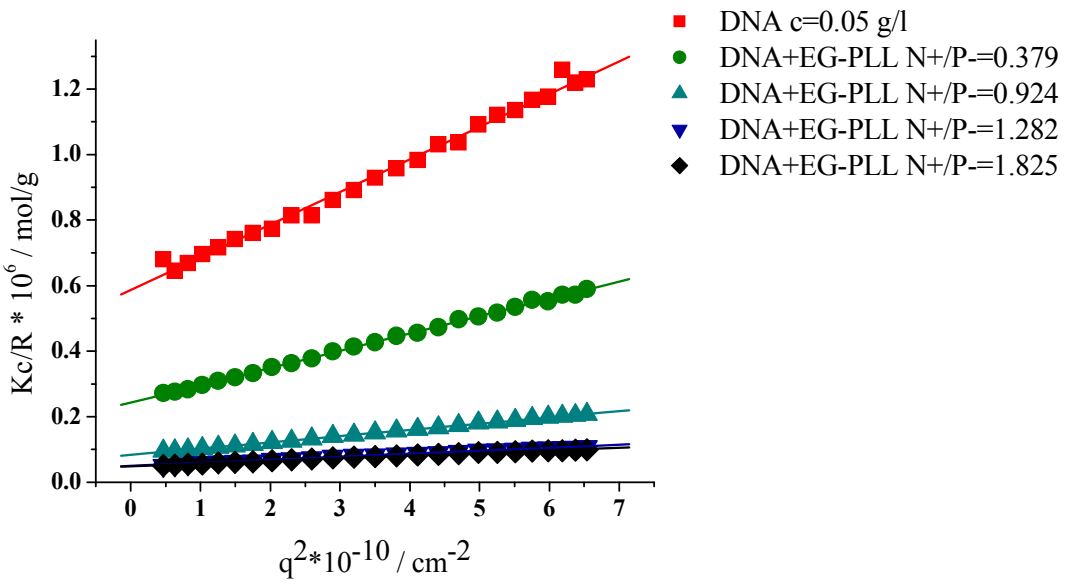

Figure A7. Static light scattering intensity (Kc/R) vs. the scattering vector (q^2) of DNA titrated with a block copolymer of polyethylene glycol (Mw=12000) – b – polylysine (DP=15) (EG-PLL) in a 5 mM phosphate buffer pH = 7, at T=20°C. The static light scattering (SLS) measurements were performed at angles from 30° to 150° in steps of 5°. The total measurements were generated in two different titrations: the first titration was done until a charge ratio of N+/P- =0.28 at a concentration of EG-PLL c=0.032 g/l; the second titration was done from N+/P- = 0.38 to N+/P- = 1.83. The concentration of EG-PLL was c=0.32 g/l. The initial concentration of DNA was in the two titrations c=0.05 g/l.

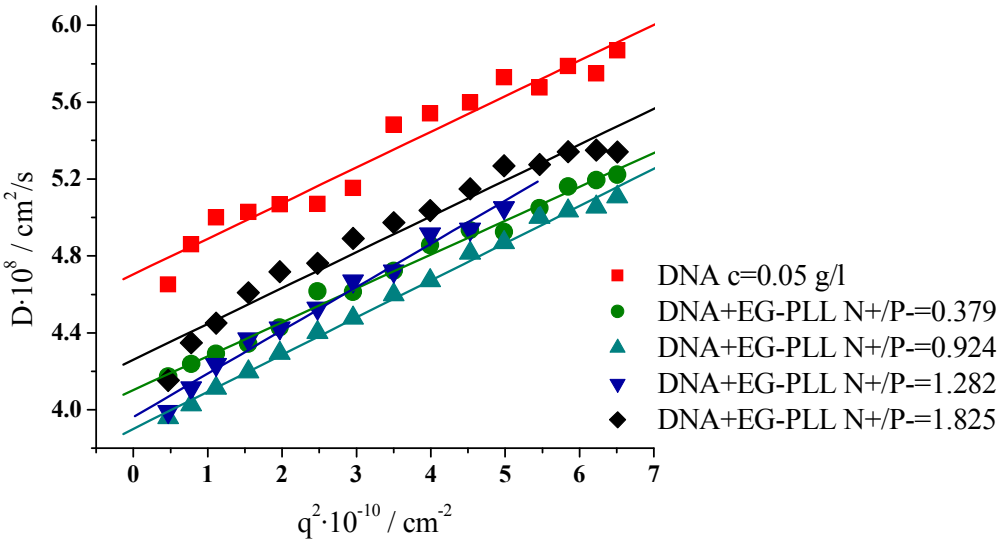

Figure A8. Diffusion coefficient (D) vs. the scattering vector (q^2) of DNA titrated with a block copolymer of polyethylene glycol (Mw=12000) – b – polylysine (DP=15) (EG-PLL) in a 5 mM phosphate buffer pH = 7, at T=20°C. The dynamic light scattering (DLS) measurements were performed with a multiangle light scattering having 8 detectors, separated by an angle of 17° each. The first detector was placed at an angle of 30° and 39°. The total measurements were generated in two different titrations: the first titration was done until a charge ratio of N+/P- =0.28 at a concentration of EG-PLL c=0.032 g/l; the second titration was done from N+/P- = 0.38 to N+/P- = 1.83. The concentration of EG-PLL was c=0.32 g/l. The initial concentration of DNA was in the two titrations c=0.05 g/l.

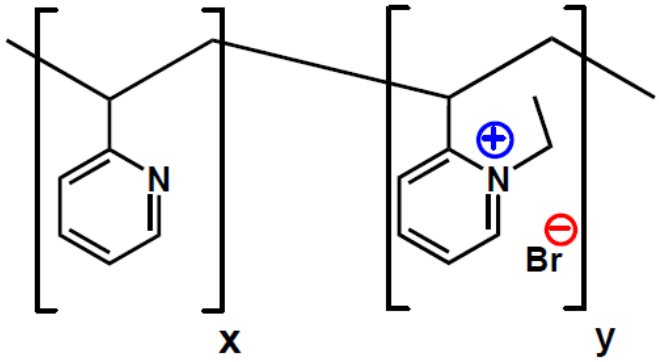

Figure A9. Structure of a linear Polyvinylpyridine (PVP) quaternized with ethyl bromide. In this work, A PVP with 10% quaternization was used, e.g. x = 90% and y = 10%.

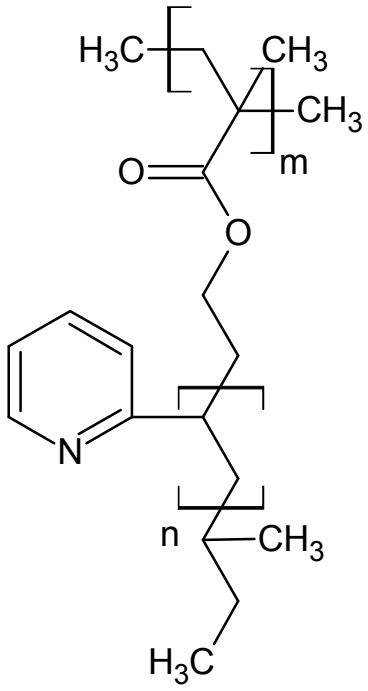

Figure A10. Structure of a brush with poly (methyl methacrylate) as a backbone and side chains of poly (vinylpyridine) with degree of polymerization DP=47.

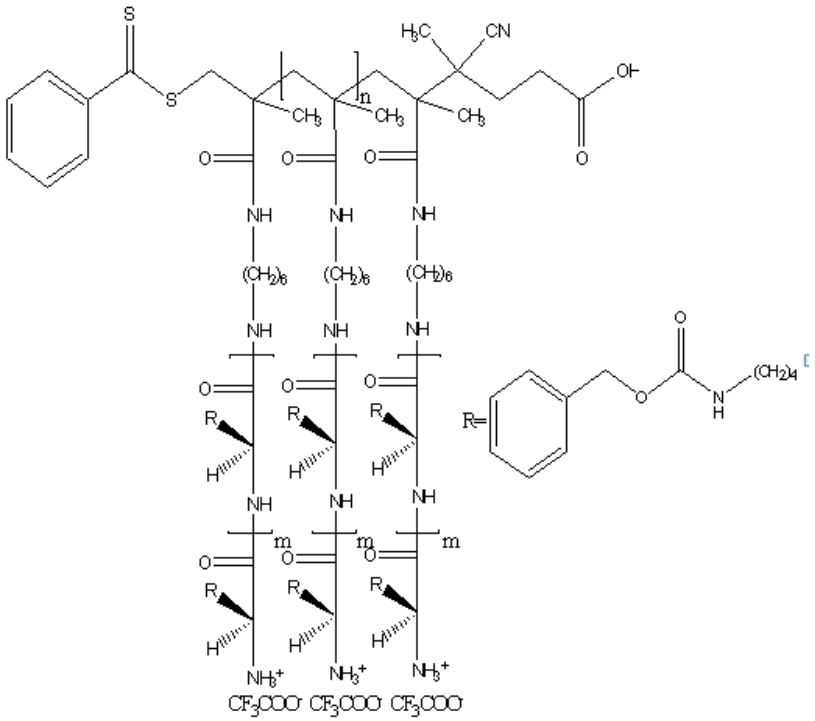

Figure A11. Structure of a protected polylysine brush (b-PLL)

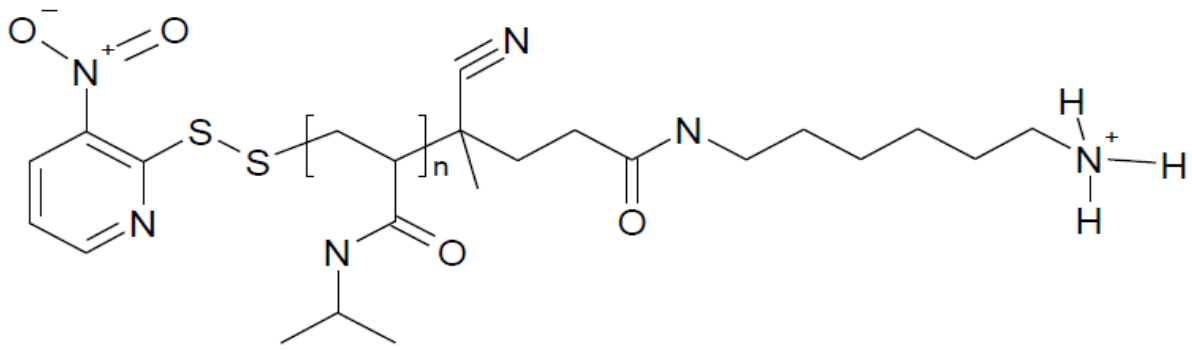

Figure A12. Structure of a poly(N-isopropylacrylamide) with one positive charge (PNIPAM)

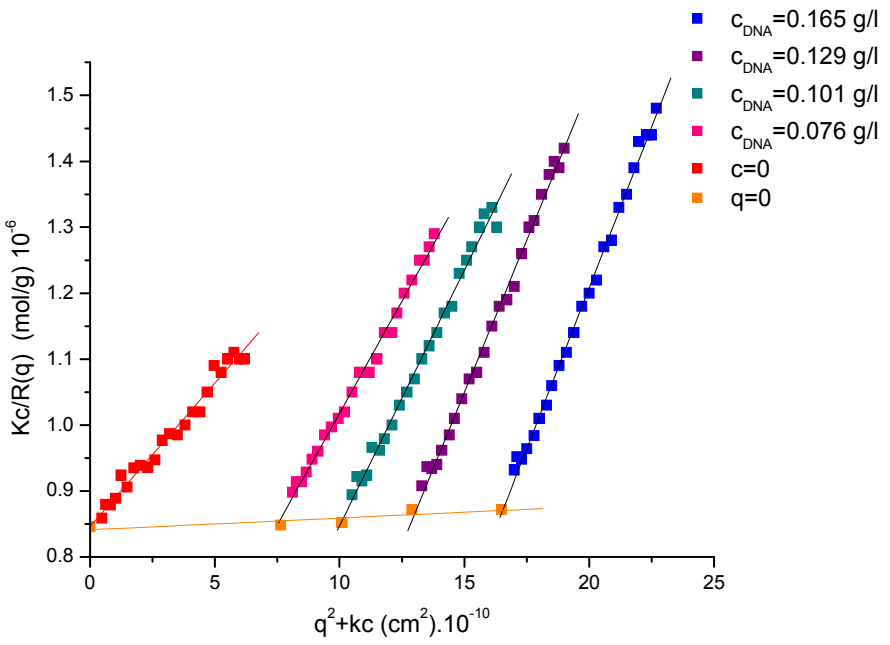

Figure A13. Zimm plot of DNA-tetradecyltrimethylammonium (DNA-TTA) in methanol [LiBr]=1mM. SLS measurements were done from 30° to 150° with steps of 5°. T = 20°C.

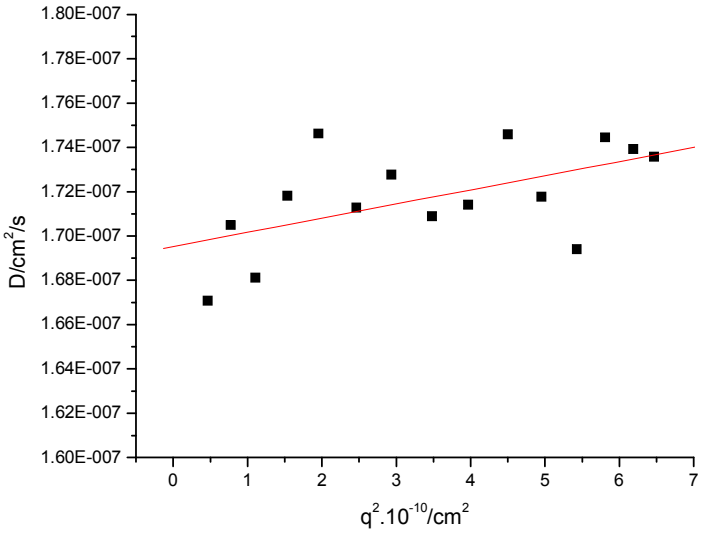

Figure A14. Diffusion coefficient vs. scattering vector q^2 of DNA-tetradecyltrimethylammonium bromide complex in methanol c=0.165 g/l at T=20°C. The salt LiBr at a concentration of 1mM was used to screen electrostatic interactions.

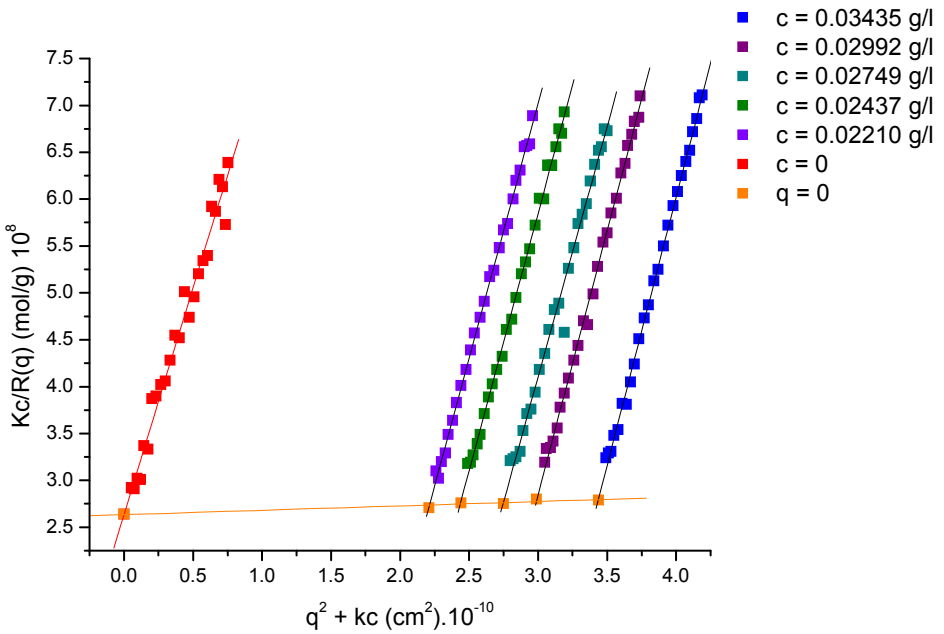

Figure A15. Zimm plot of DNA-dodecyltrimethylammonium (DNA-DTA) in DMF [LiBr]=1mM. SLS measurements were done from 30° to 150° with steps of 5°. T = 20°C.

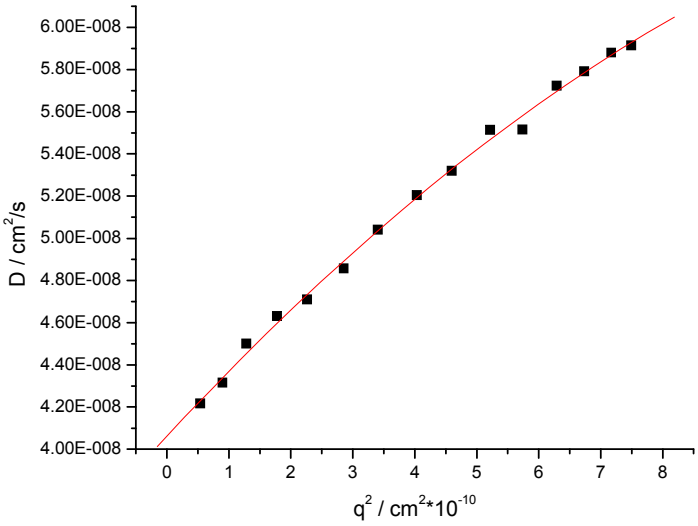

Figure A16. Diffusion coefficient vs. scattering vector q^2 of DNA-dodecyltrimethylammonium complex in DMF c=0.315 g/l at T=20°C. The salt LiBr was used at a concentration of 1mM to screen electrostatic interactions

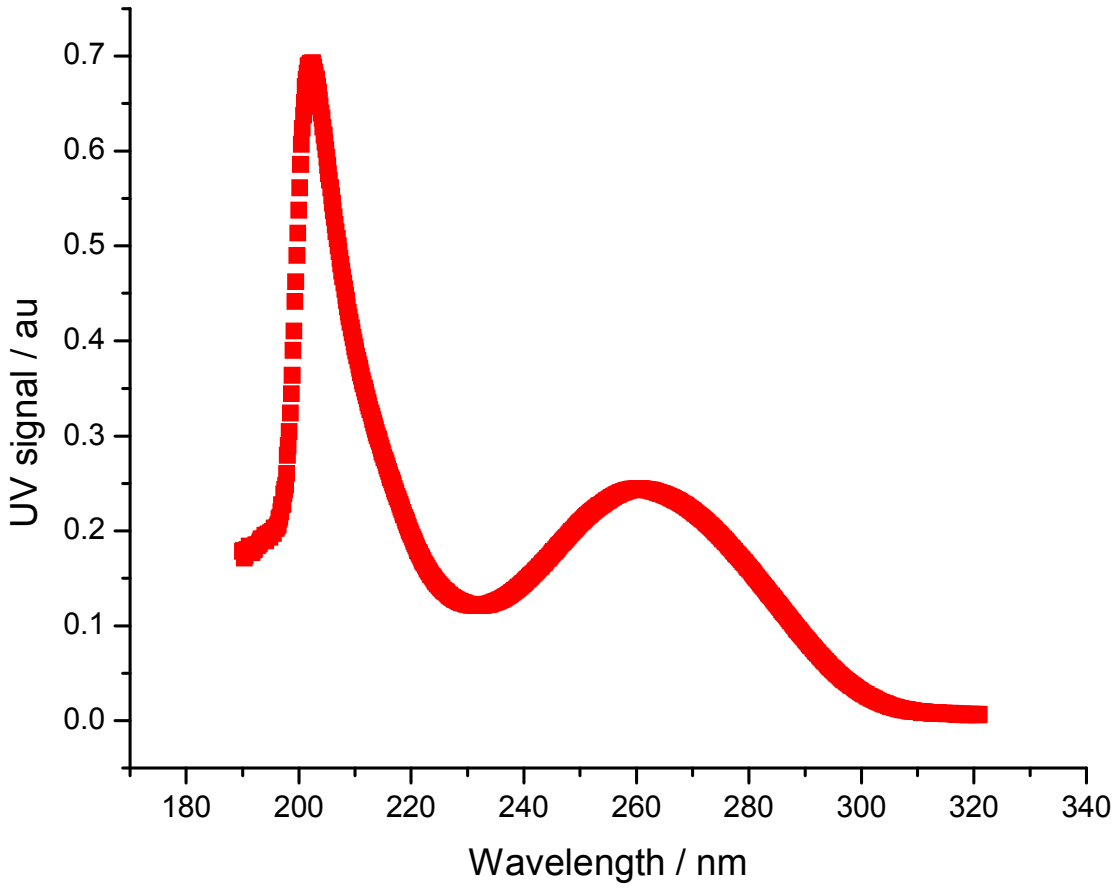

Figure A17. UV-vis measurements of DNA complexes with tetradecyltrimethylammonium bromide in methanol c=0.165 g/l

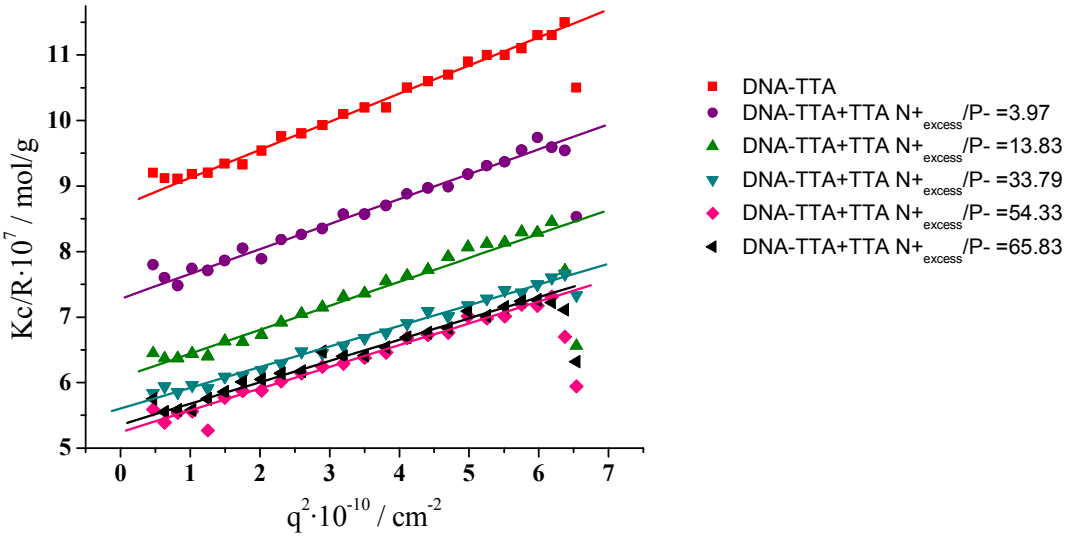

Figure A18. Static light scattering intensity (Kc/R) vs. the scattering vector (q^2) of DNA-tetradecyltrimethylammonium bromide titrated solution of 20 mM tetradecyltrimethylammonium bromide in methanol. at T=20°C. The solutions contained 1 mM LiBr.

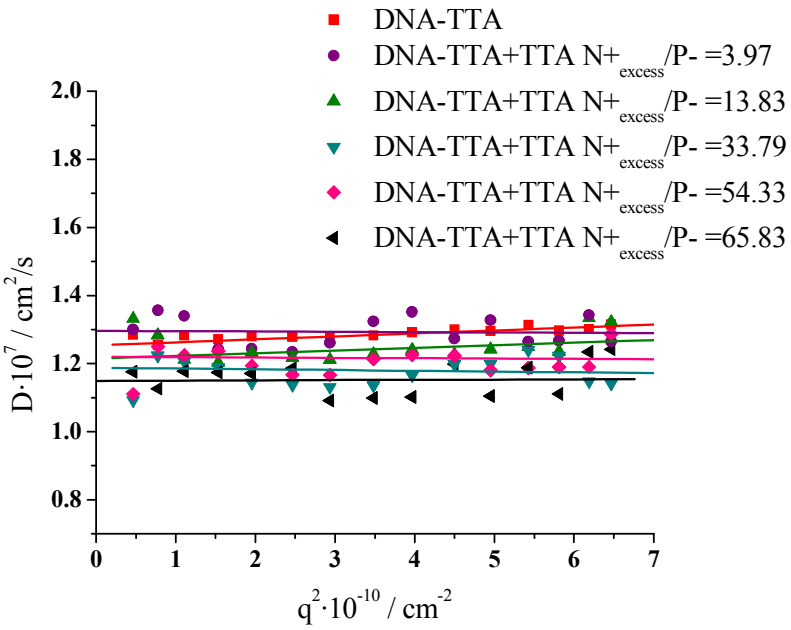

Figure A19. Diffusion coefficient (D) vs. the scattering vector (q^2) of DNA-tetradecyltrimethylammonium bromide titrated solution of 20 mM tetradecyltrimethylammonium bromide in methanol. at T=20°C. The solutions contained 1 mM LiBr.

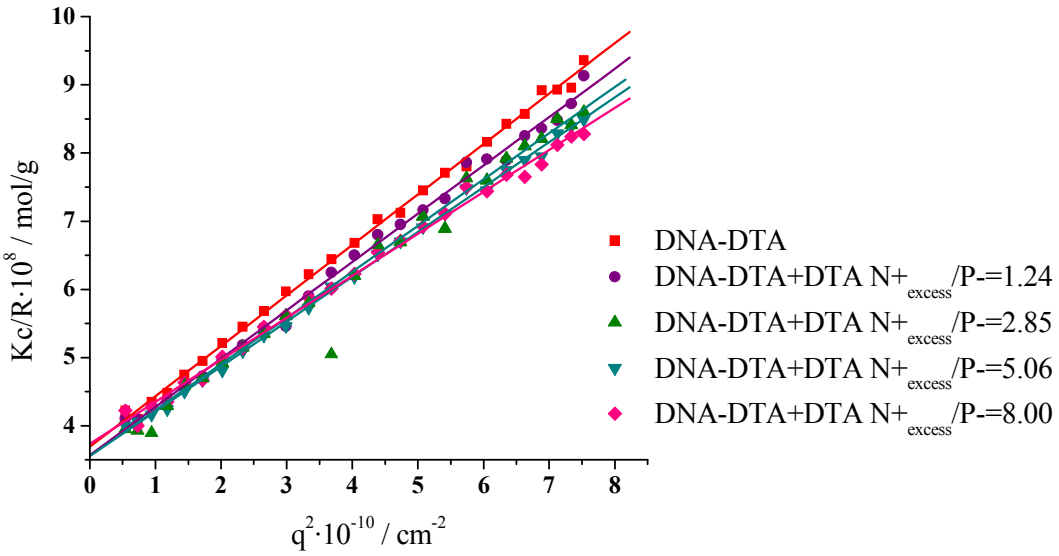

Figure A20. Static light scattering intensity (Kc/R) vs. the scattering vector (q^2) of DNA-dodecyltrimethylammonium bromide titrated solution of 20 mM dodecyltrimethylammonium bromide in DMF. at T=20°C. The solutions contained 1 mM LiBr.

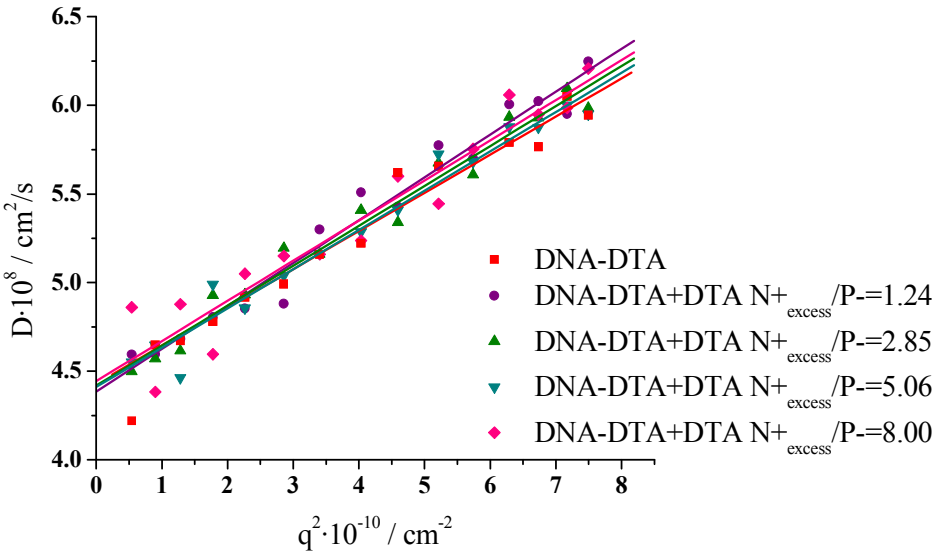

Figure A21. Diffusion coefficient (D) vs. the scattering vector (q^2) of DNA-dodecyltrimethylammonium bromide titrated solution of 20 mM dodecyltrimethylammonium bromide in DMF. at T=20°C. The solutions contained 1 mM LiBr.

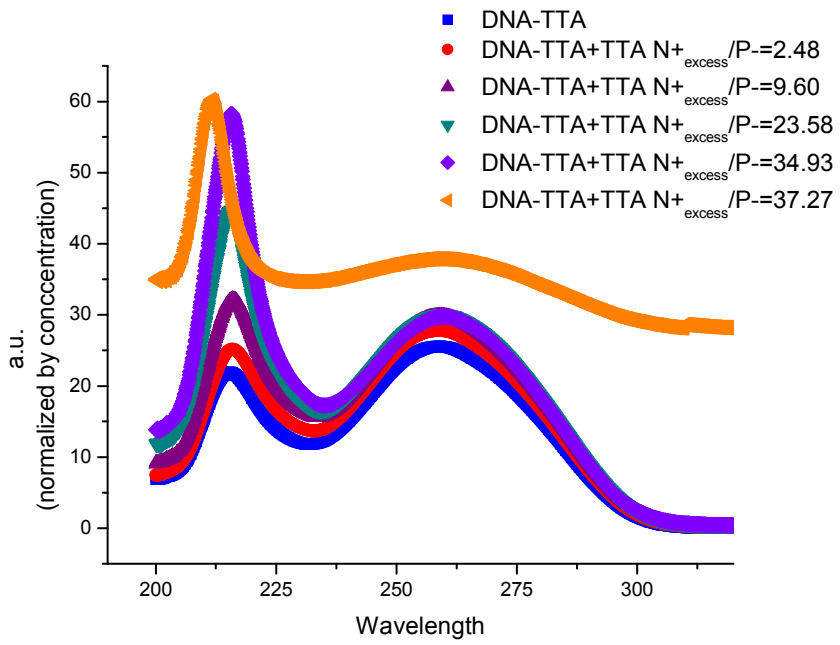

Figure A22. UV-vis measurements of DNA-tetradecyltrimethylammonium complexes (DNA-TTA) in methanol upon addition of free surfactant at T=20°C.

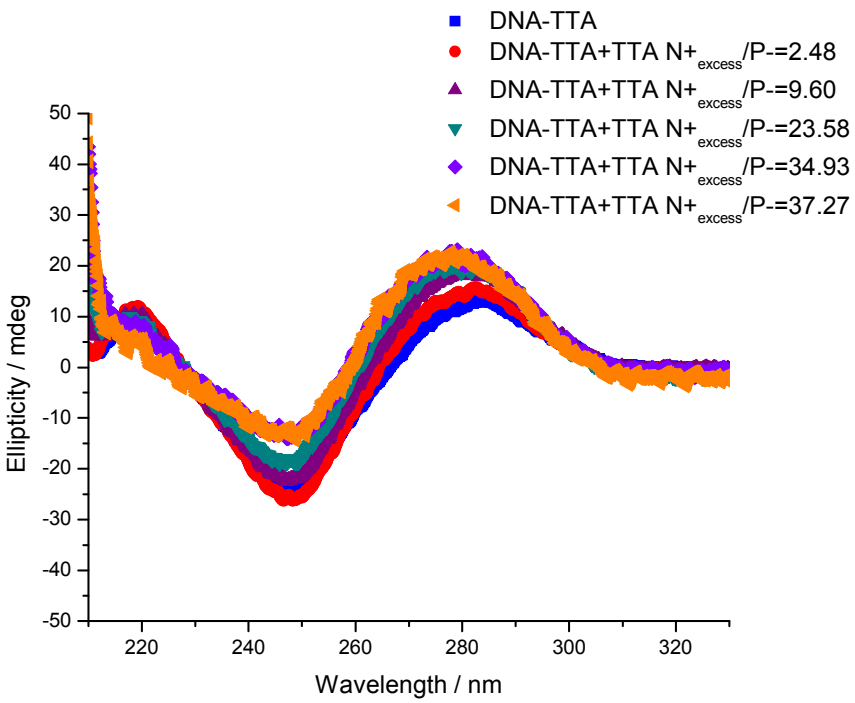

Figure A23. Circular dichroism (CD) spectroscopy measurements of DNA-tetradecyltrimethylammonium complexes (DNA-TTA) in methanol upon addition of free surfactant at T=20°C.

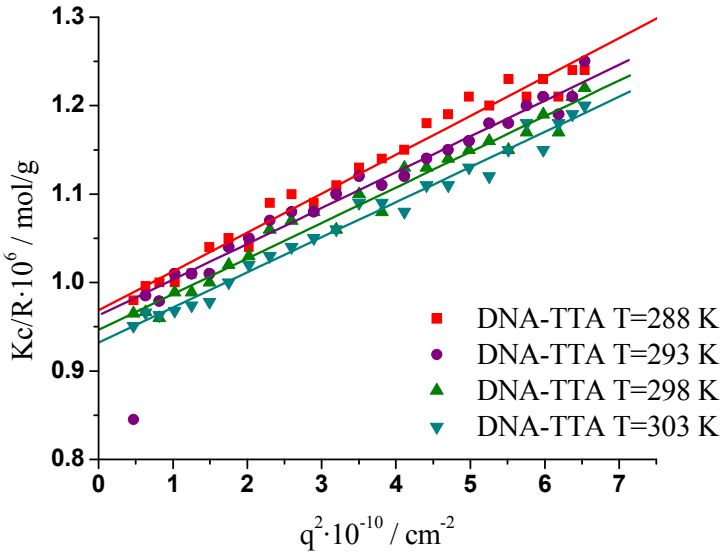

Figure A24. Static light scattering intensity (Kc/R) vs. the scattering vector (q^2) of DNA-tetradecyltrimethylammonium bromide in methanol at different temperatures. The solutions contained 1 mM LiBr.

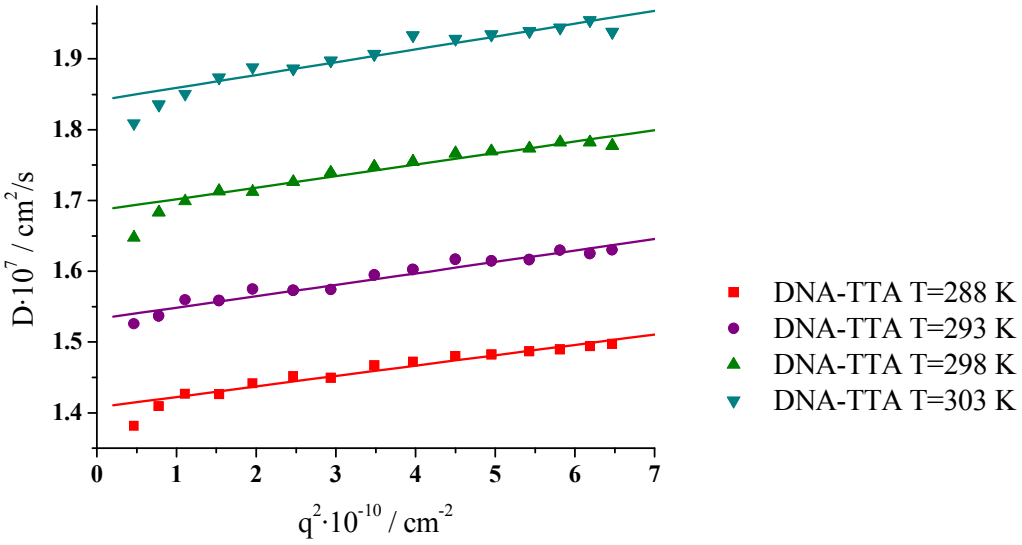

Figure A25. Diffusion coefficient (D) vs. the scattering vector (q^2) of DNA-tetradecyltrimethylammonium bromide in methanol at different temperatures. The solutions contained 1 mM LiBr.

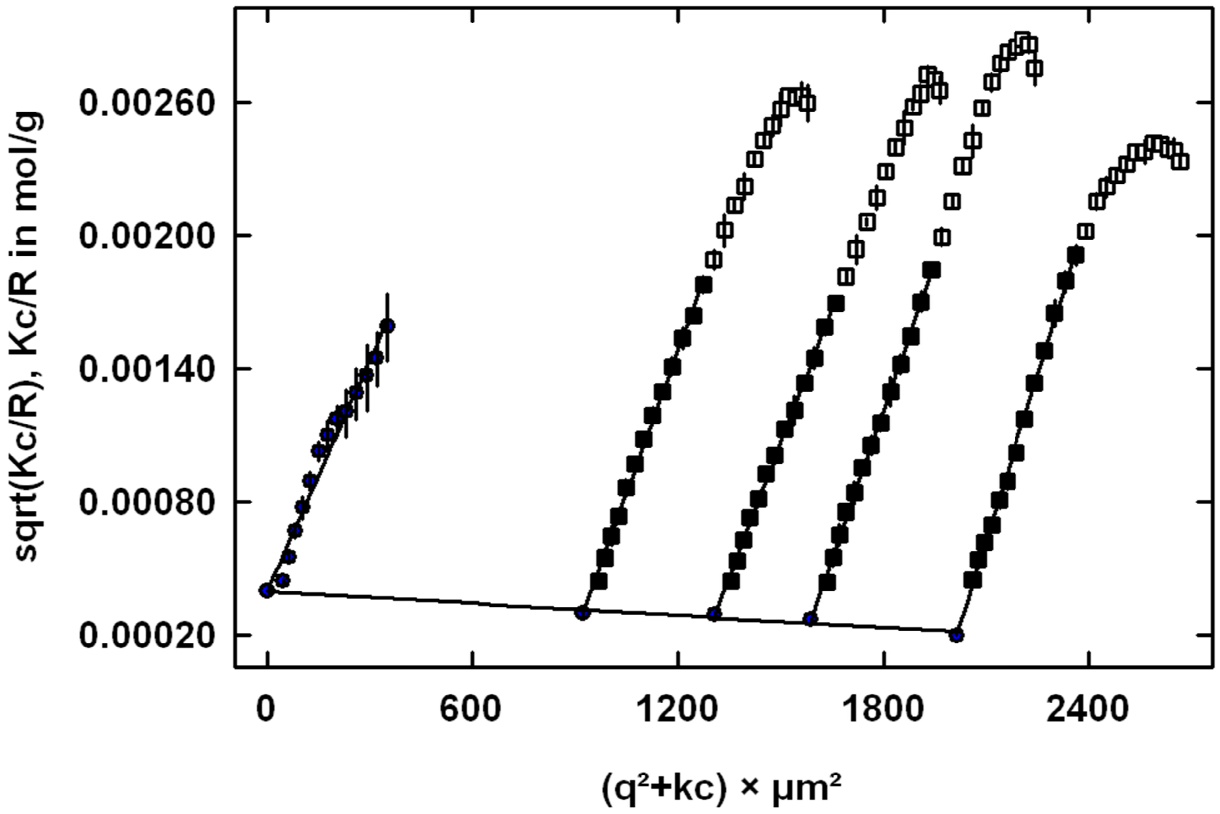

Figure A26. Berry plot of 1-2 dioleoyl-3-trimethylammonium-propane (DOTAP) in aqueous solution with no salt. SLS measurements were done from 30° to 150° with steps of 5°. T = 20°C. Concentrations: 0.2214 g/l, 0.1440 g/l, 0.1017 g/l, and 0.06675 g/l.

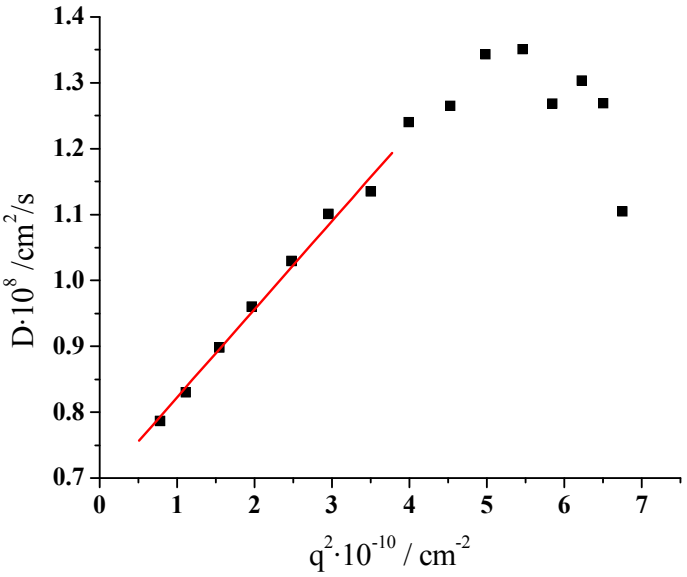

Figure A27. Diffusion coefficient (D) vs. scattering vector (q^2) of 1-2 dioleoyl-3-trimethylammonium-propane (DOTAP) in aqueous solution with no salt at 20°C and a concentration of 0.0668 g/l.

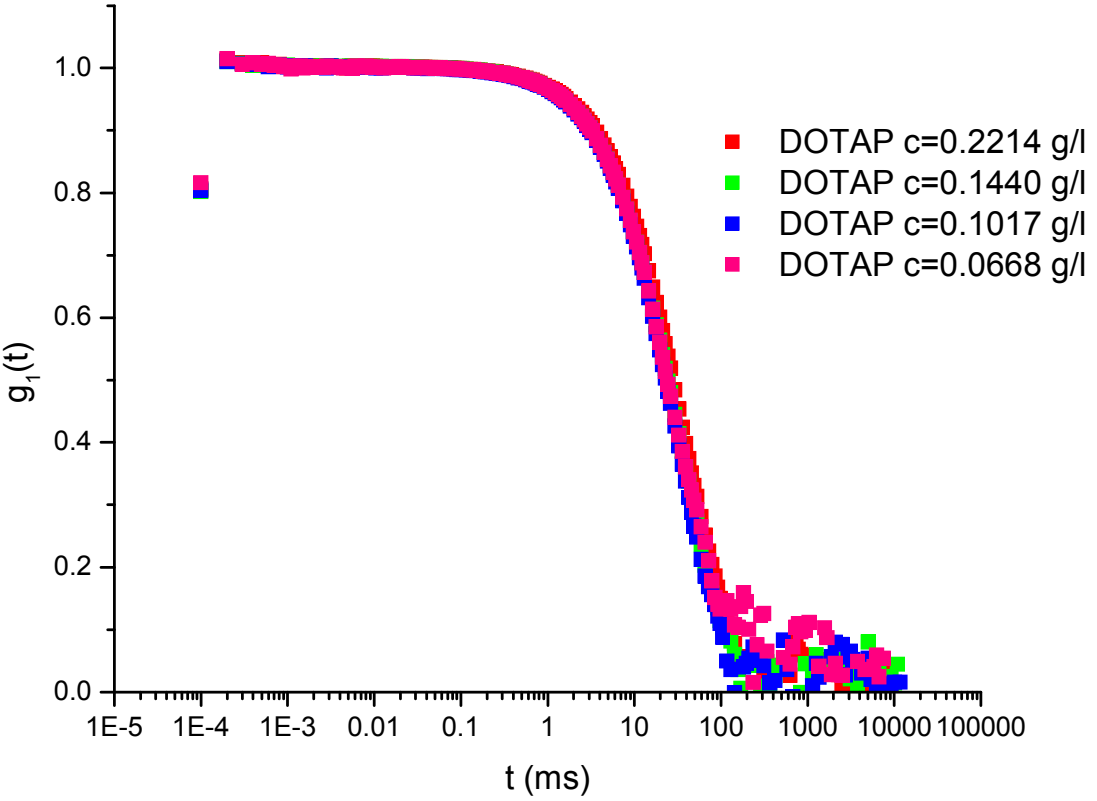

Figure A28. Intensity autocorrelation function $G_1(t)$ of 1-2 dioleoyl-3-trimethylammonium-propane (DOTAP) in aqueous solution with no salt at an angle of 30°. T = 20°C. Concentrations: 0.2214 g/l, 0.1440 g/l, 0.1017 g/l, and 0.0668 g/l.

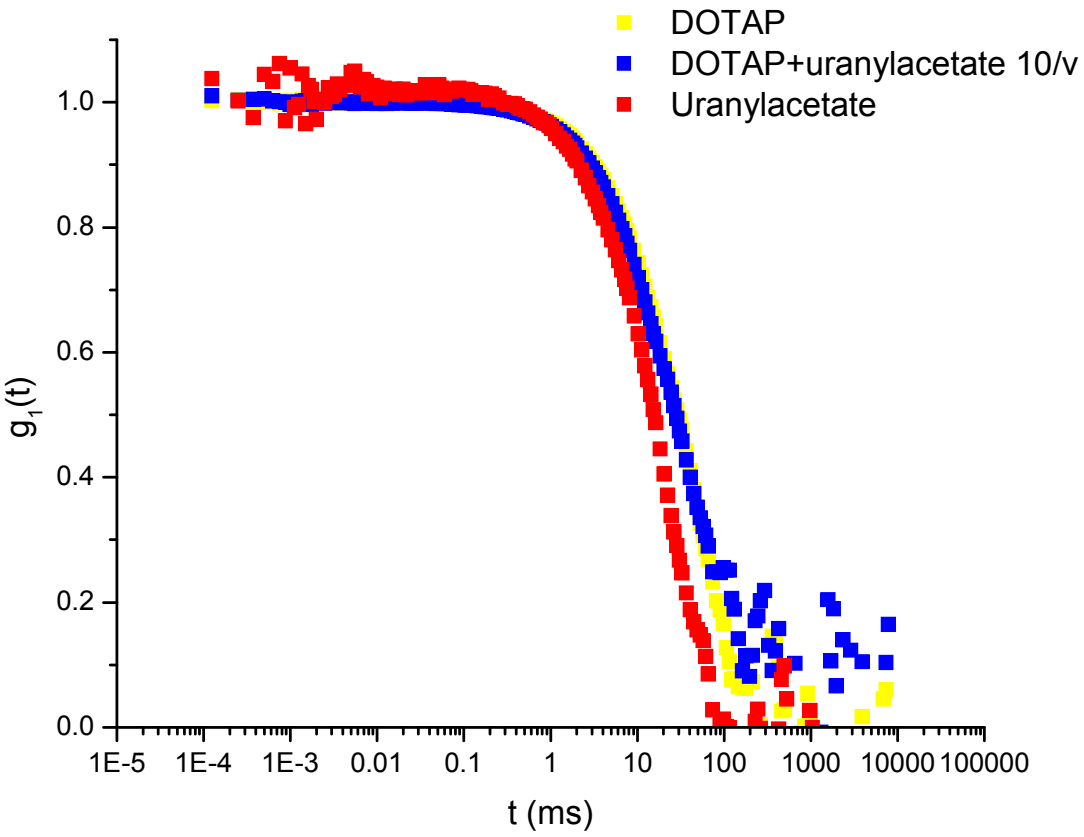

Figure A29. Intensity autocorrelation function $G_1(t)$ of 1-2 dioleoyl-3-trimethylammonium-propane (DOTAP) in aqueous solution after the addition of the staining dye uranyl acetate at an angle of 30°. T = 20°C.

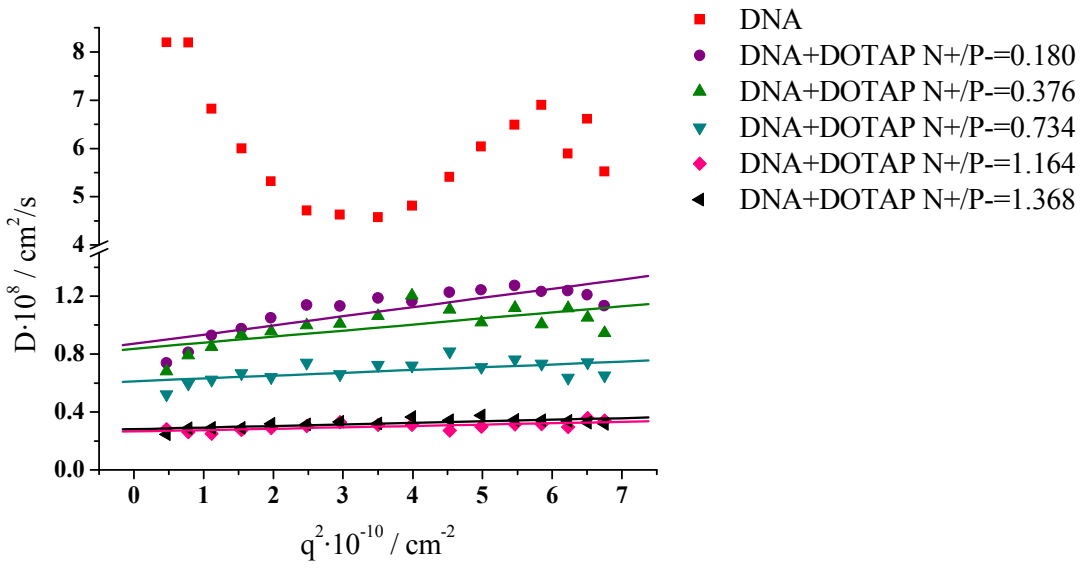

(a)

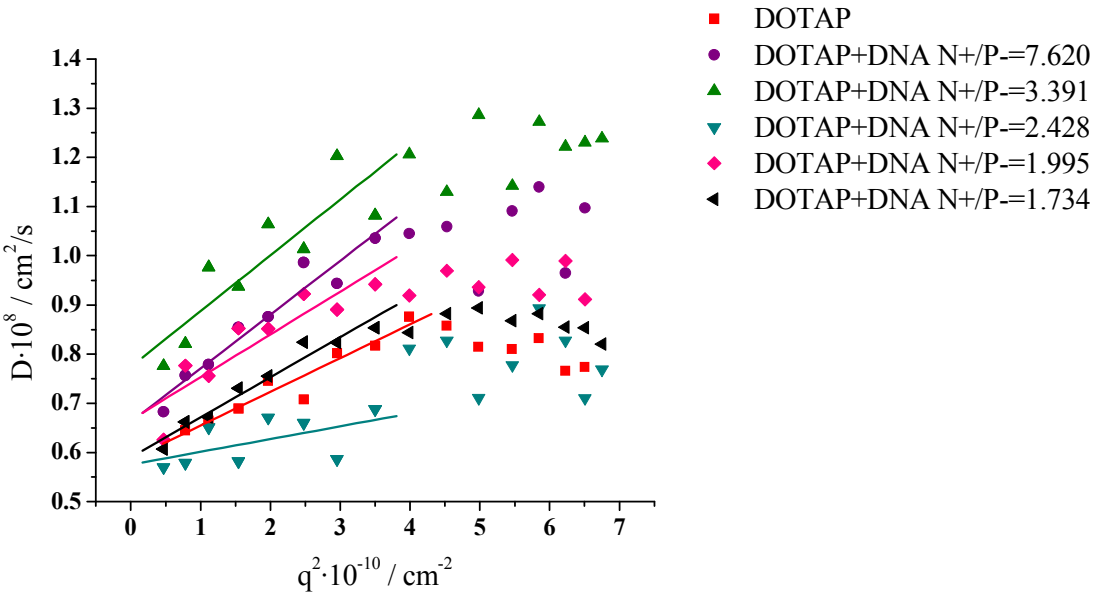

(b)

Figure A30. Diffusion coefficient (D) vs. the scattering vector (q^2) of DNA titrated with 1-2 dioleoyl-3-trimethylammonium-propane (DOTAP) (a) and DOTAP titrated with DNA (b) in an aqueous solution containing no salt. T=20°C.

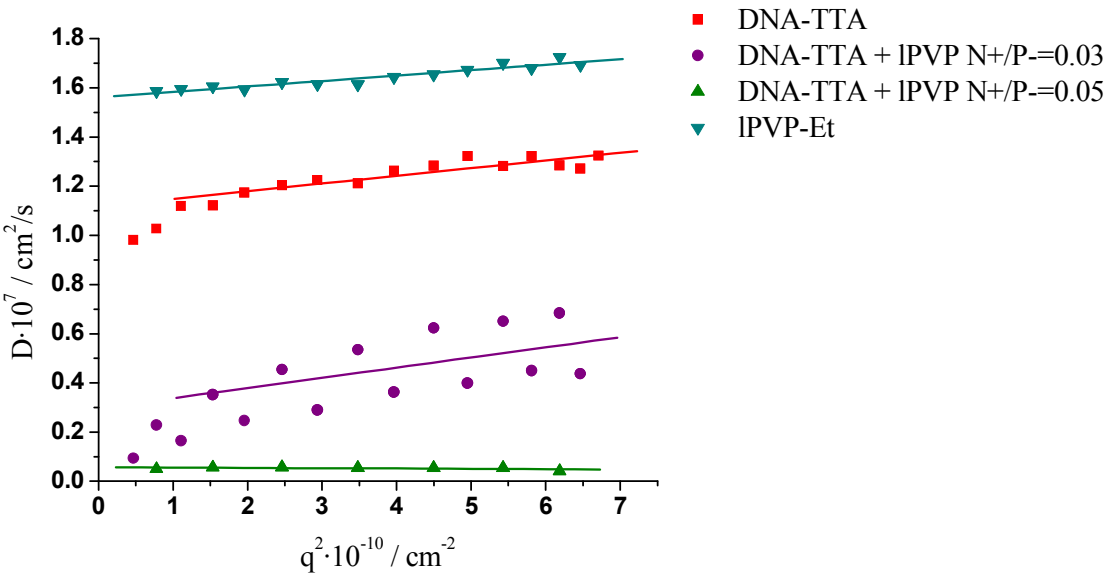

Figure A31. Diffusion coefficient (D) vs. the scattering vector (q^2) of DNA-tetradecyltrimethylammonium bromide upon the stepwise addition of a linear polyvinylpyridine (l-PVP) with 10% of quaternization in methanol at 20°C ([LiBr = 0.001 M)].

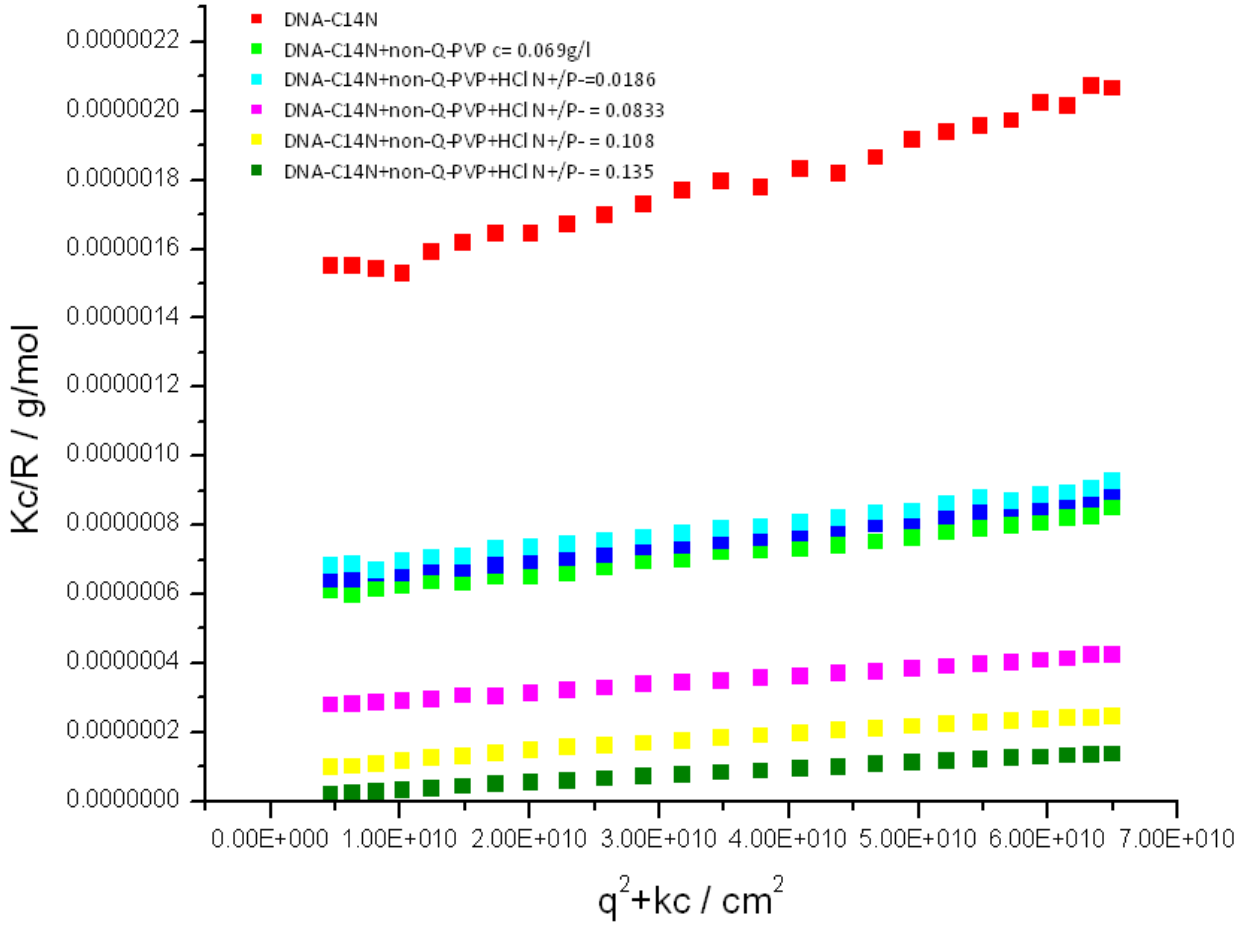

Figure A.32. Static Light Scattering measurements during the titration of the mixture of DNA-tetradecyltrimethylammonium bromide complexes and non-quaternized polyvinylpyridine with methanolic HCl. Measurements were done from 30° to 150° with steps of 5°. T = 20°C.

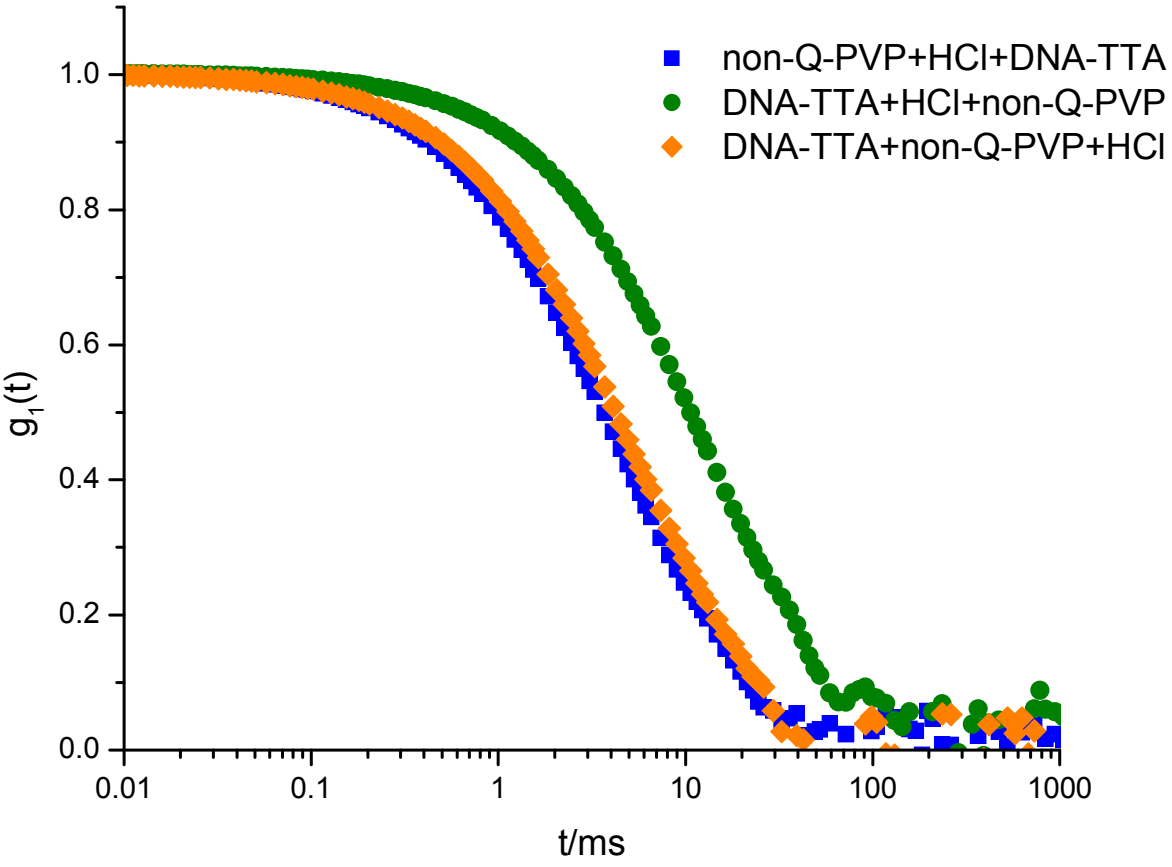

Figure A.33. Intensity autocorrelation function $G_1(t)$ at 30° of the mixture of the three components: DNA-tetradecyltrimethylammonium bromide complexes, non-quaternized polyvinylpyridine, and methanolic HCl with different order of addition at a final charge ratio of N+/P- = 0.108. T = 20°C.

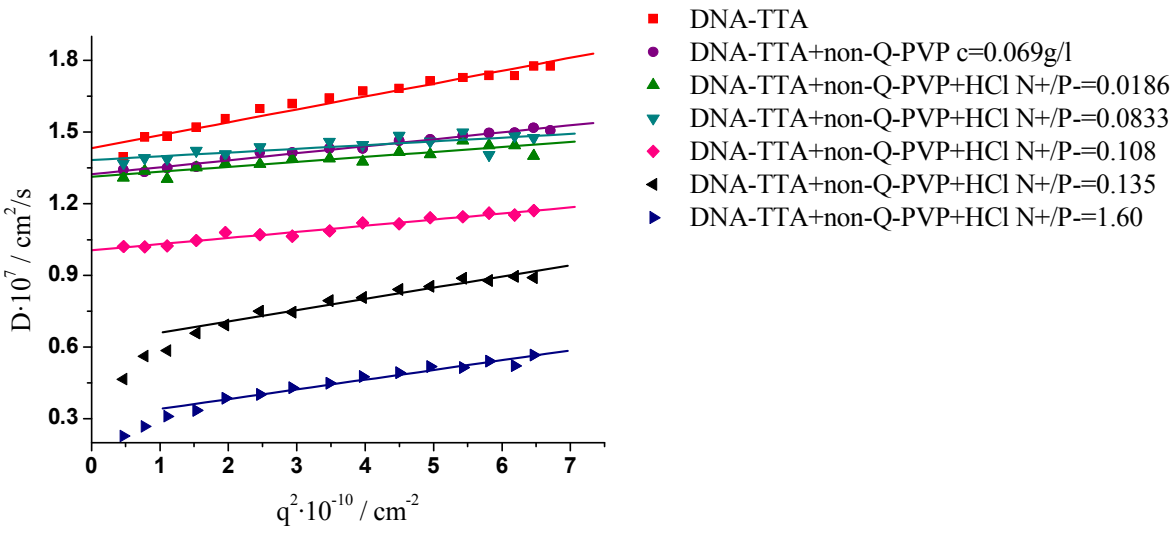

Figure A.34. Diffusion coefficient (D) vs. the scattering vector (q^2) of DNA-tetradecyltrimethylammonium bromide upon the stepwise addition of a non-quaternized polyvinylpyridine brush (non-Q-PVP) and the subsequent addition of methanol HCl in methanol at 20°C ([LiBr = 0.001 M)].

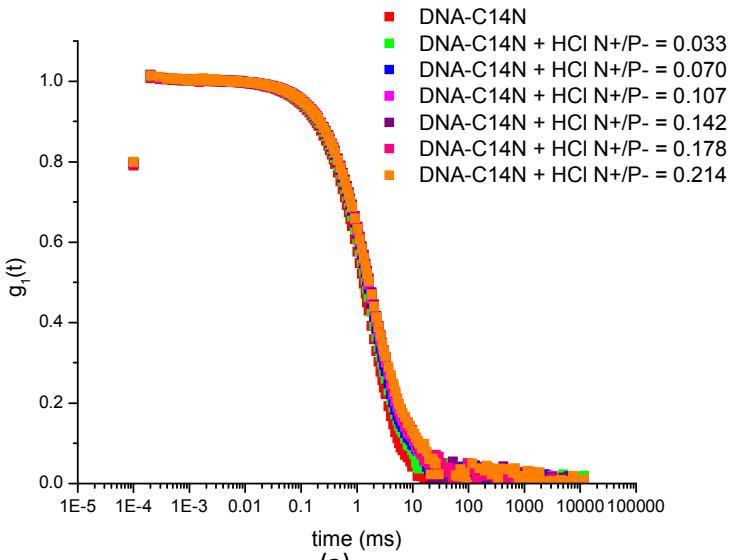

(a)

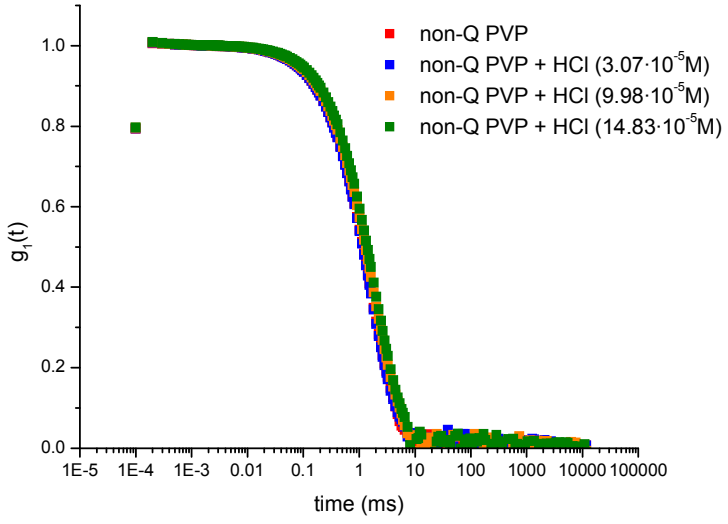

(b)

Figure A.35. Intensity autocorrelation function $G_1(t)$ at 30° of the mixtures (a) DNA-tetradecyltrimethylammonium bromide complexes with methanolic HCl and b) non-quaternized polyvinylpyridine and methanolic HCl. T = 20°C.

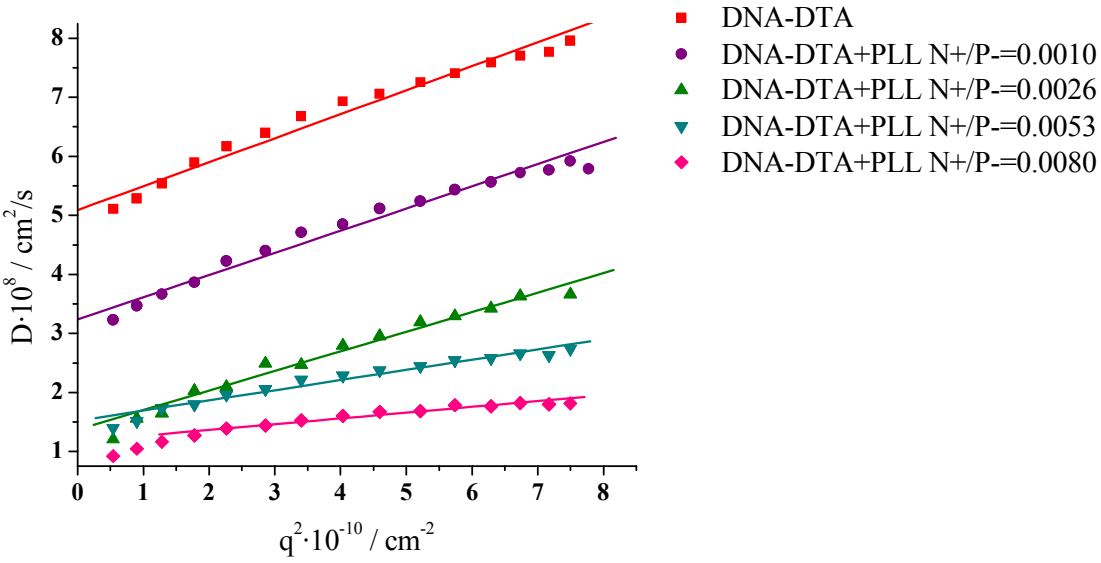

Figure A.36. Diffusion coefficient (D) vs. the scattering vector (q^2) of DNA-dodecyltrimethylammonium bromide upon the stepwise addition of a protected polylysine brush (PLL) in DMF at 20°C ([LiBr = 0.001 M)].

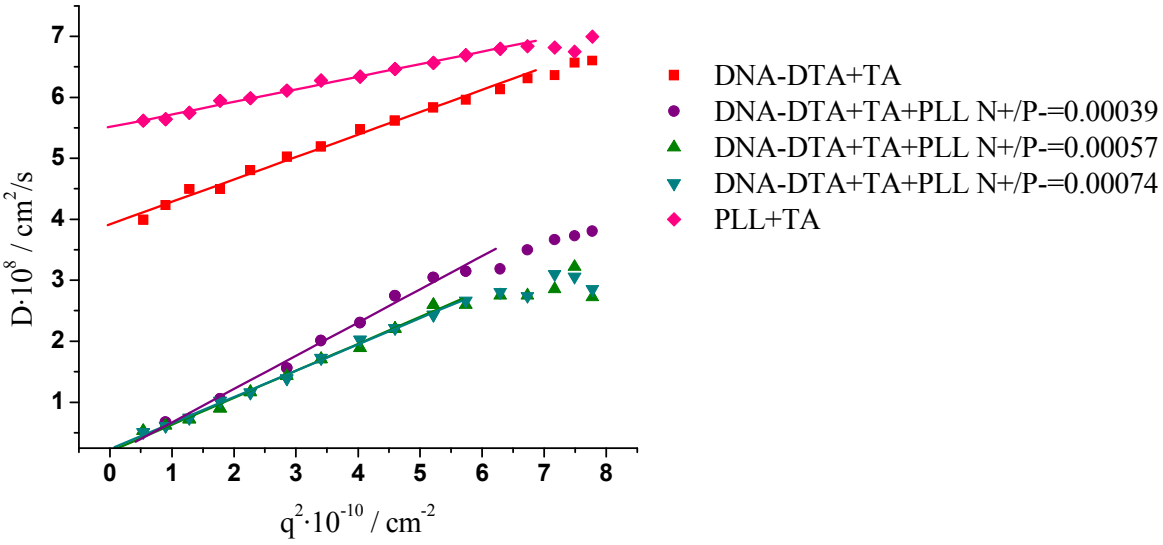

Figure A.37. Diffusion coefficient (D) vs. the scattering vector (q^2) of DNA-dodecyltrimethylammonium bromide upon the stepwise addition of a protected polylysine brush (PLL) in DMF in the presence of triethylamine (TA) 20%v/v at 20°C ([LiBr = 0.001 M)].

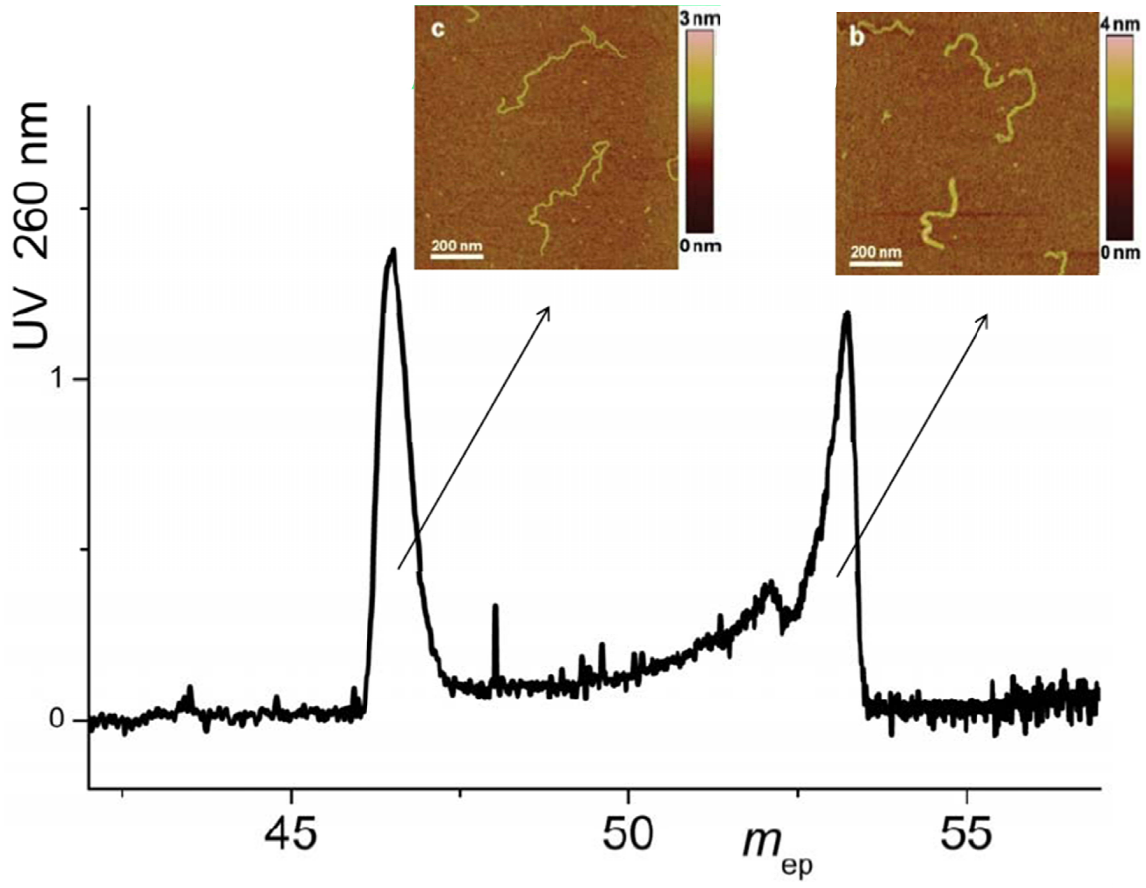

Figure A38. Electropherogram of DNApUC19 after digestion with the enzyme SpI. The digestion of DNA was not complete.The right peak correspond to supercoiled DNA and the left peak to the linear DNA.

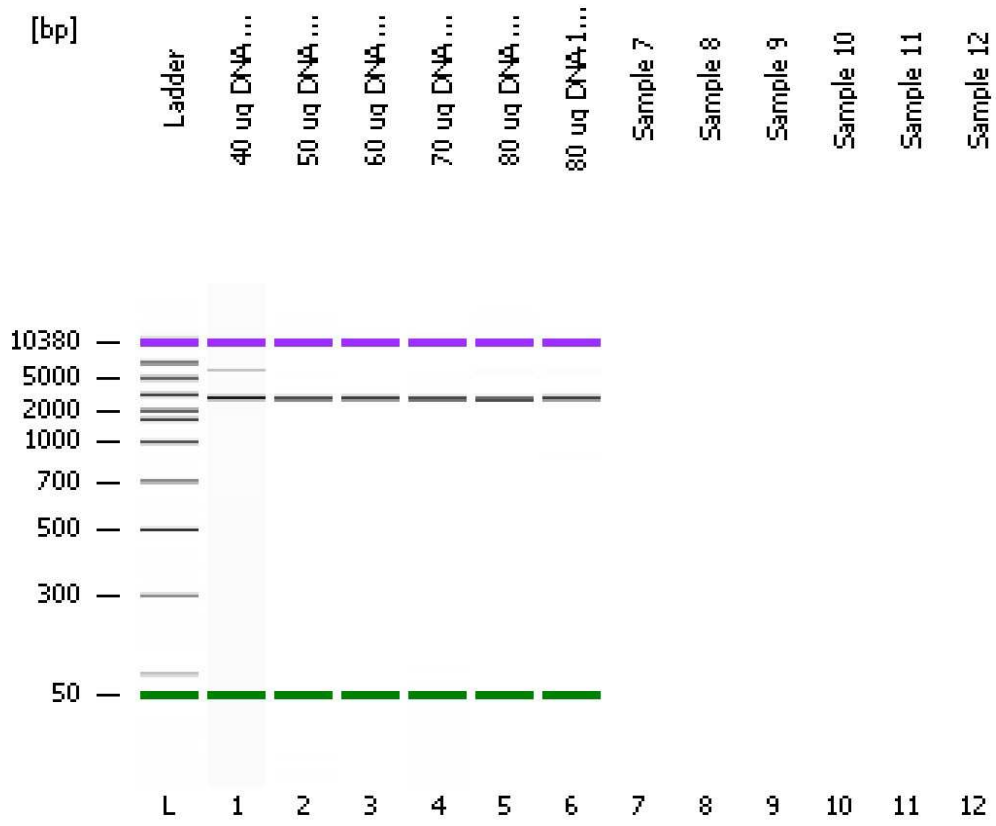

Figure A39. Electropherogram obtained after running cut DNA with SamI at different quantities in a bionanalyzer (optimized miniature gel electrophoresis). DNA was digested with 1 ul of the enzyme for 24 h. The concentration of DNA was c = 1g/l. Different volumes of this solution were used to optimize the digestion. In ladder 1) 40 ul, 2) 50 ul, 3) 60ul, 4) 70 ul, 5) 80 ul, 6) 90 ul. Subsequent DNA digestion were done by adding 60 ul of a solution 1 g/l.

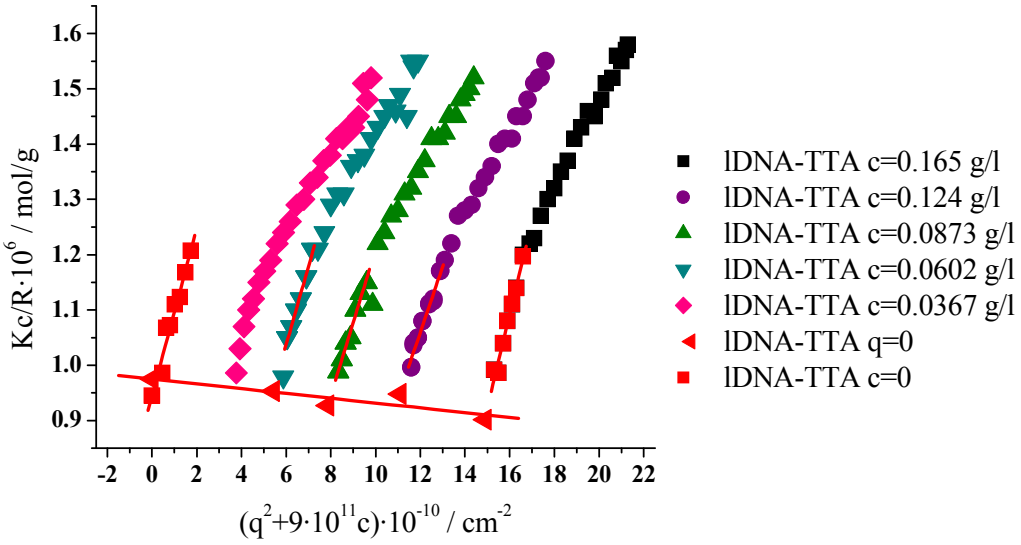

Figure A40. Zimm plot of linear DNA-tetradecyltrimethylammonium (lDNA-TTA) in methanol [LiBr]=1mM. SLS measurements were done from 30° to 150° with steps of 5°. T = 20°C. Some points were eliminated due to the presence of aggregates.

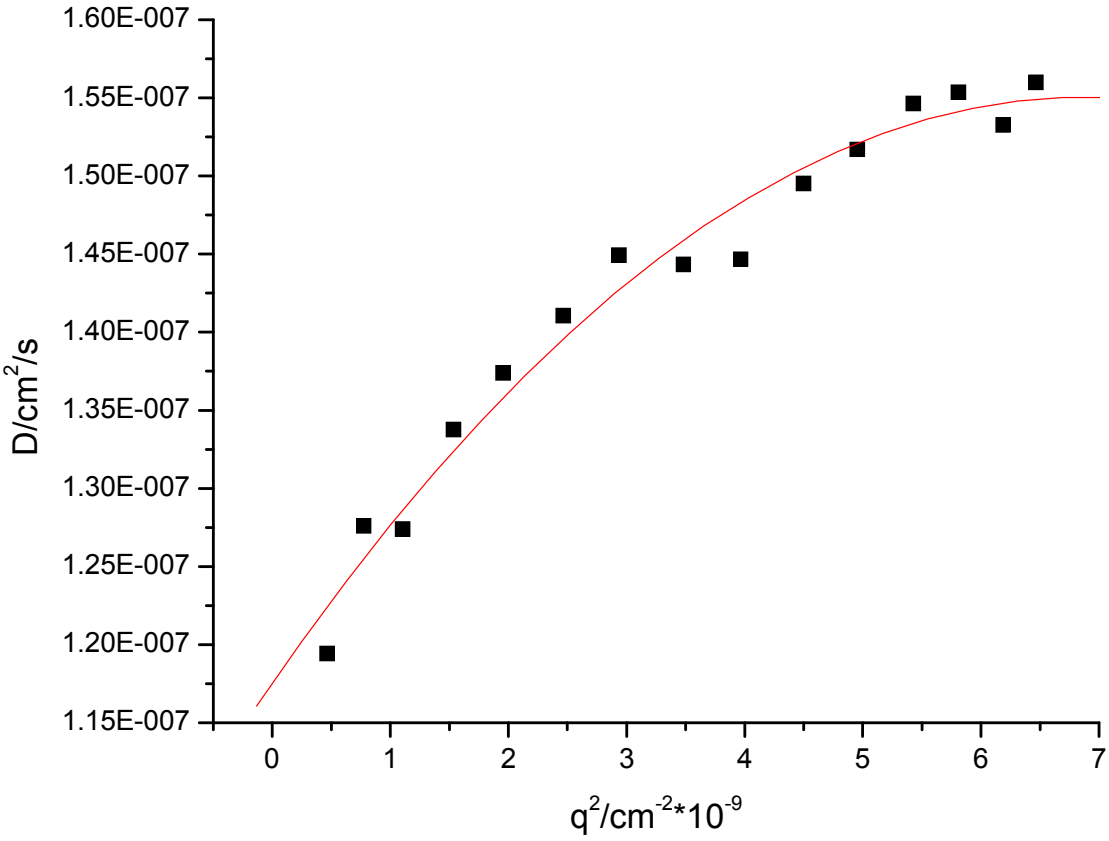

Figure A42. Diffusion coefficient vs. scattering vector q^2 of linear DNA-tetradecyltrimethylammonium bromide complex in methanol c=0.165 g/l at T=20°C. The salt LiBr at a concentration of 1mM was used to screen electrostatic interactions.

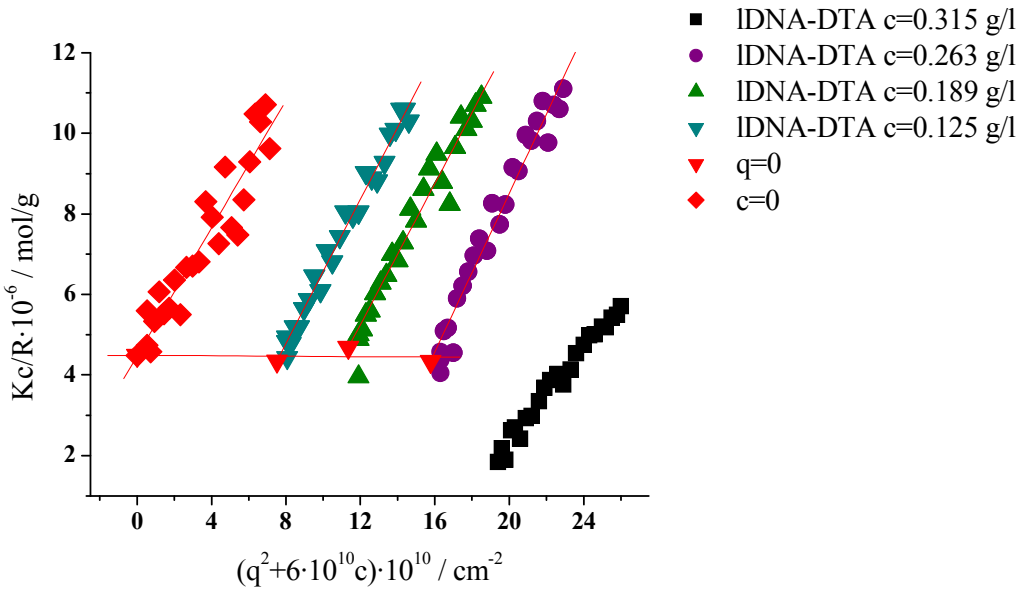

Figure A43. Zimm plot of linear DNA-dodecyltrimethylammonium (lDNA-DTA) in DMF [LiBr]=1mM. SLS measurements were done from 30° to 150° with steps of 5°. T = 20°C. Some points were eliminated due to the presence of aggregates.

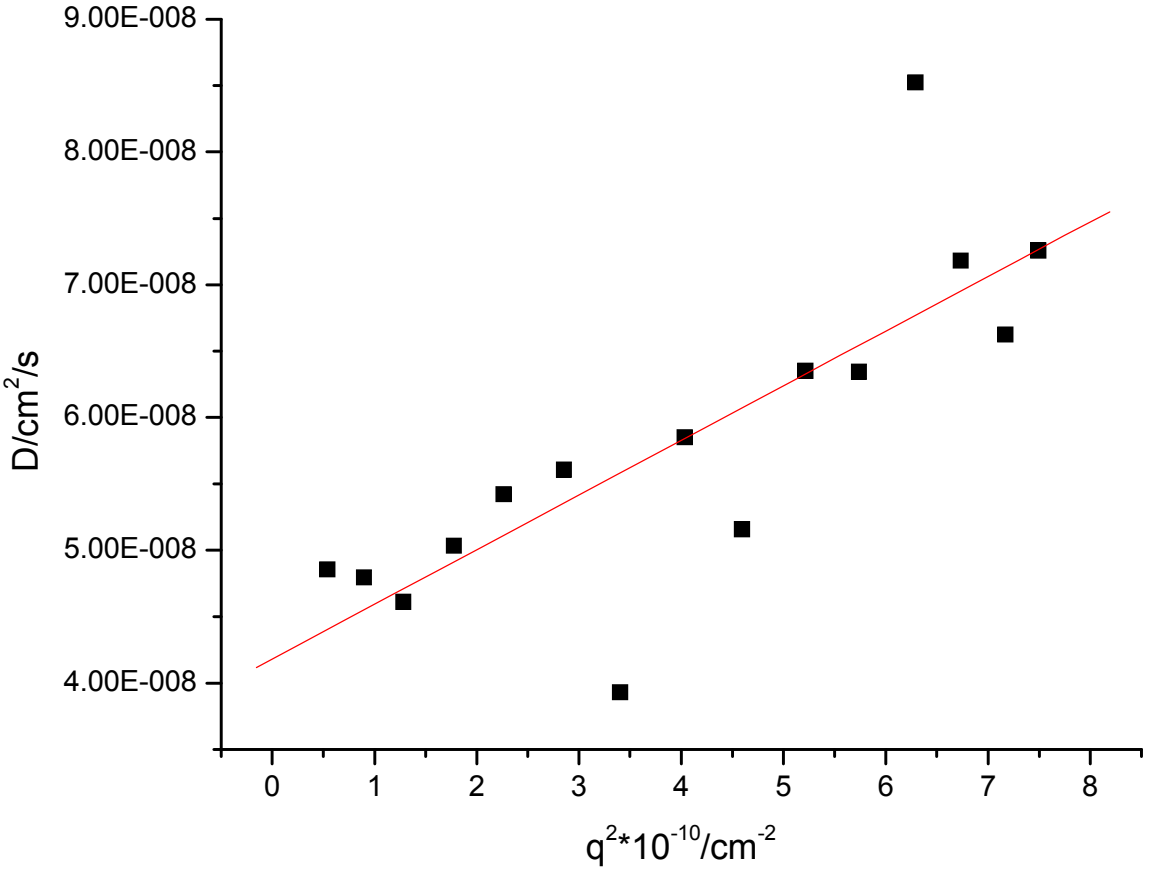

Figure A45. Diffusion coefficient vs. scattering vector q^2 of linear DNA-dodecyltrimethylammonium bromide complex in DMF c=0.1254 g/l at T=20°C. The salt LiBr at a concentration of 1mM was used to screen electrostatic interactions.

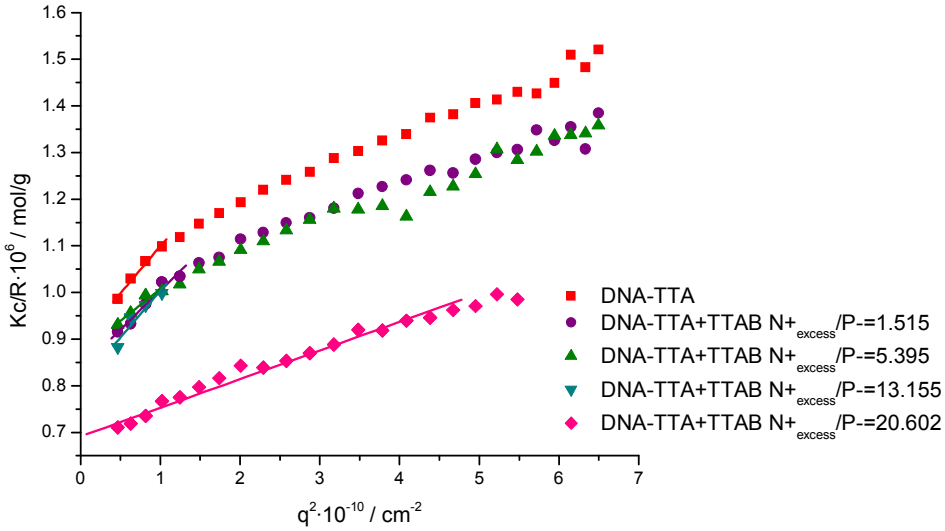

Figure A46. Static light scattering intensity (Kc/R) vs. the scattering vector (q^2) of linear DNA-tetradecyltrimethylammonium bromide titrated solution of 20 mM tetradecyltrimethylammonium bromide in methanol. at T=20°C. The solutions contained 1 mM LiBr.

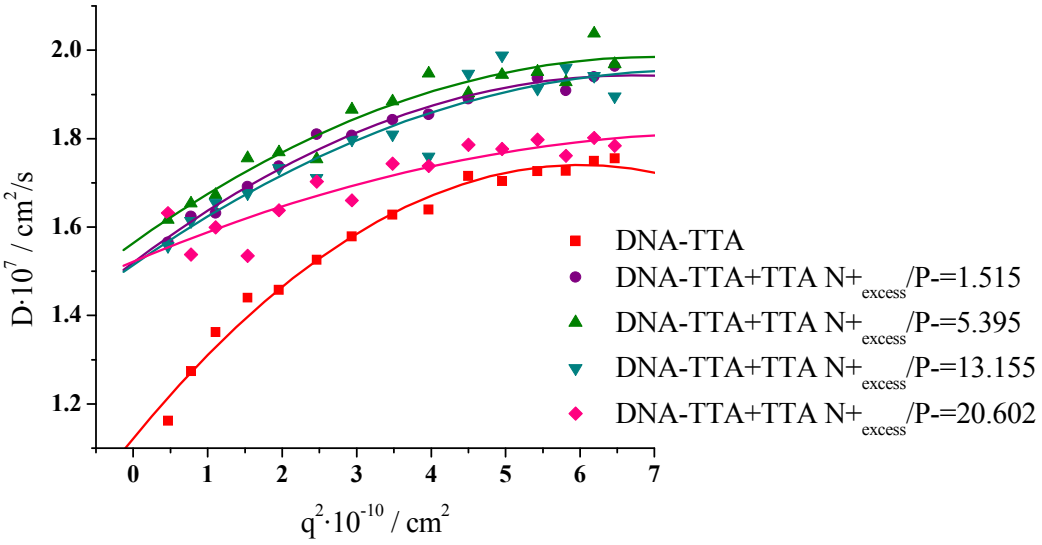

Figure A47. Diffusion coefficient (D) vs. the scattering vector (q^2) of linear DNA-tetradecyltrimethylammonium bromide titrated with a solution of 20 mM tetradecyltrimethylammonium bromide in methanol. at T=20°C. The solutions contained 1 mM LiBr.

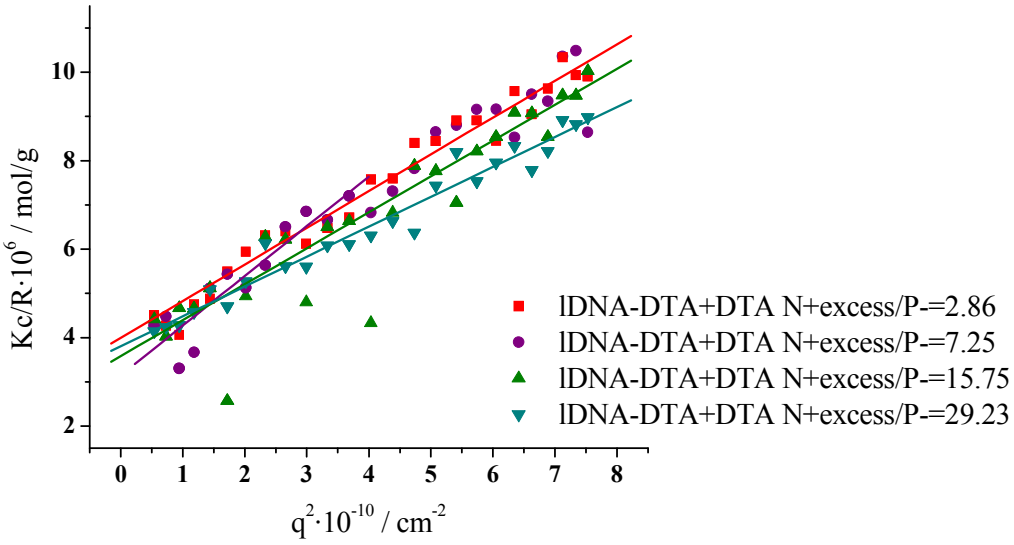

Figure A48. Static light scattering intensity (Kc/R) vs. the scattering vector (q^2) of linear DNA-dodecyltrimethylammonium bromide titrated solution of 20 mM dodecyltrimethylammonium bromide in methanol. at T=20°C. The solutions contained 1 mM LiBr.

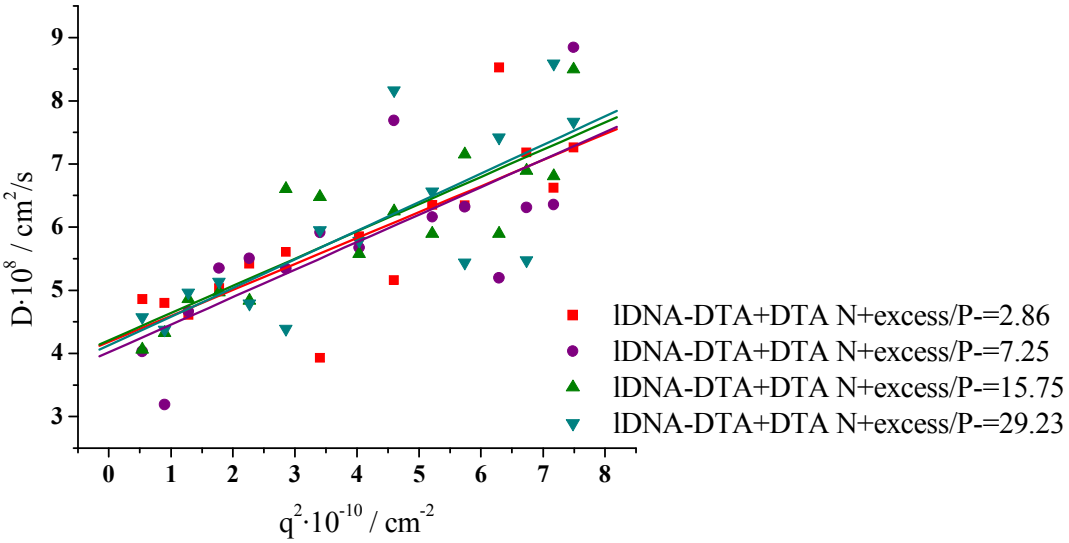

Figure A49. Diffusion coefficient (D) vs. the scattering vector (q^2) of linear DNA-dodecyltrimethylammonium bromide titrated solution of 20 mM dodecyltrimethylammonium bromide in methanol. at T=20°C. The solutions contained 1 mM LiBr.

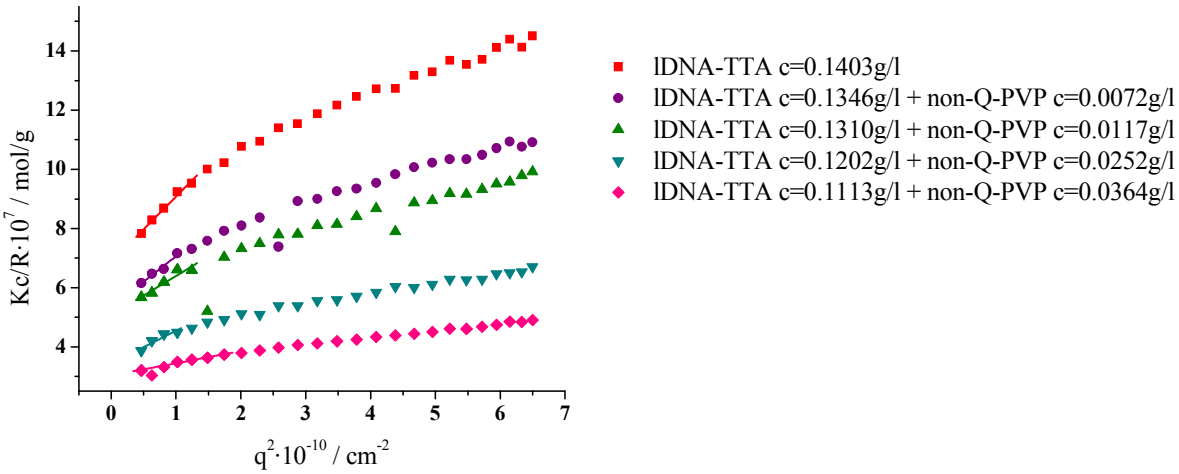

(a)

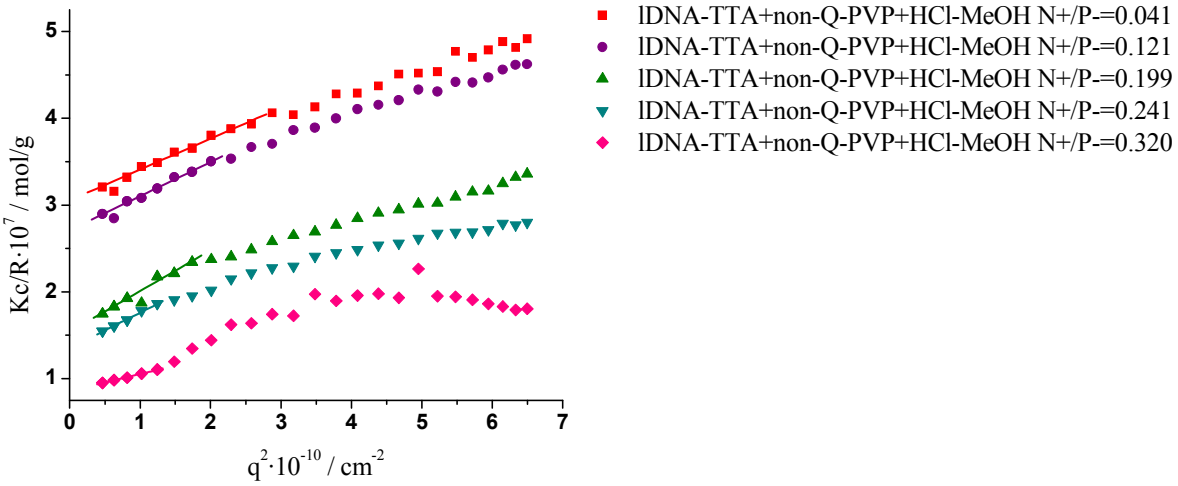

(b)

Figure A.50. Static Light Scattering measurements during the titration of the mixture of linear DNA-tetradecyltrimethylammonium bromide complexes and non-quaternized polyvinylpyridine (a) with methanolic HCl (b). Measurements were done from 30° to 150° with steps of 5°. T = 20°C.

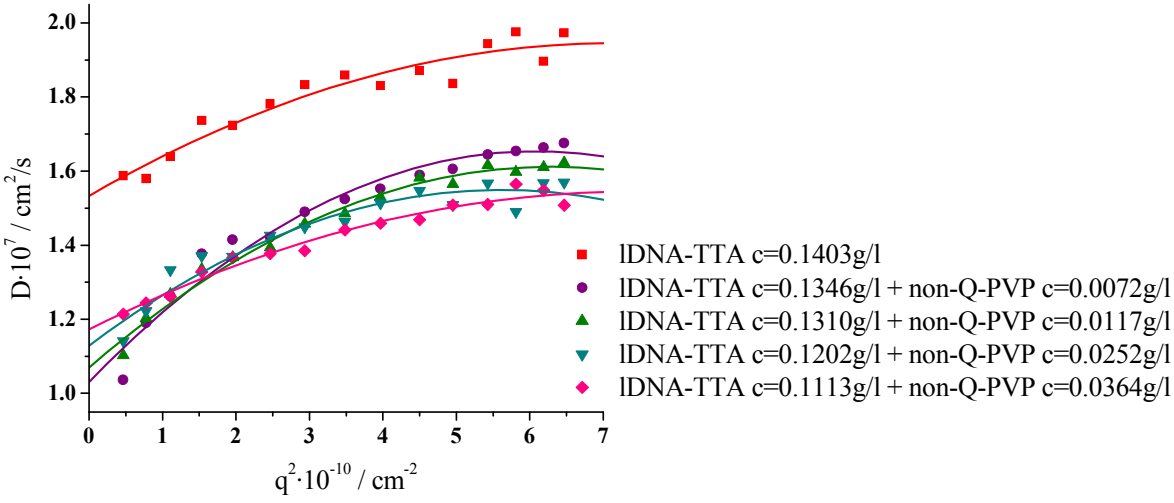

(a)

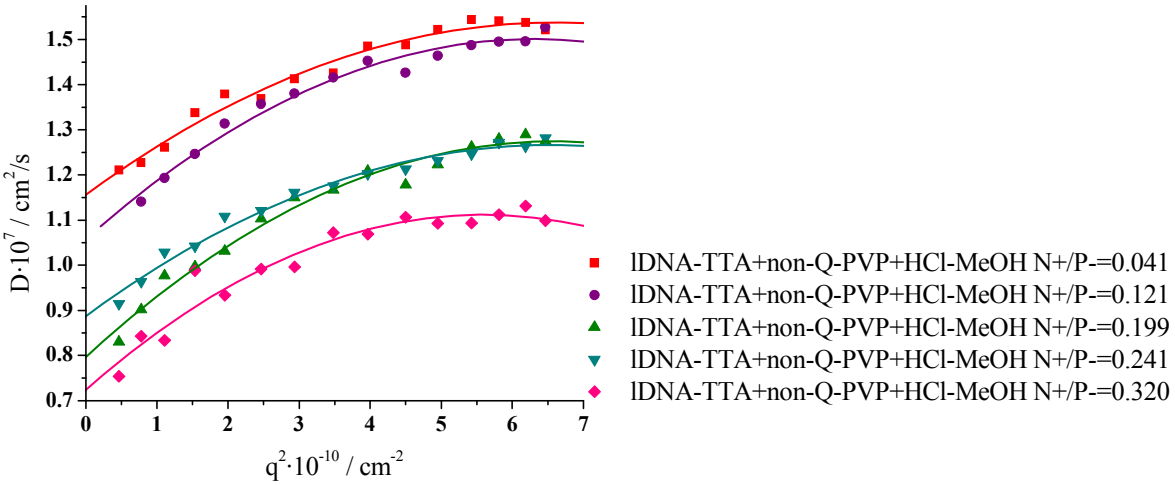

(b)

Figure A.51. Diffusion coefficient (D) vs. the scattering vector (q^2) during the titration of the mixture of linear DNA-tetradecyltrimethylammonium bromide complexes and non-quaternized polyvinylpyridine (a) with methanolic HCl (b). Measurements were done from 30° to 150° with steps of 5°. T = 20°C.

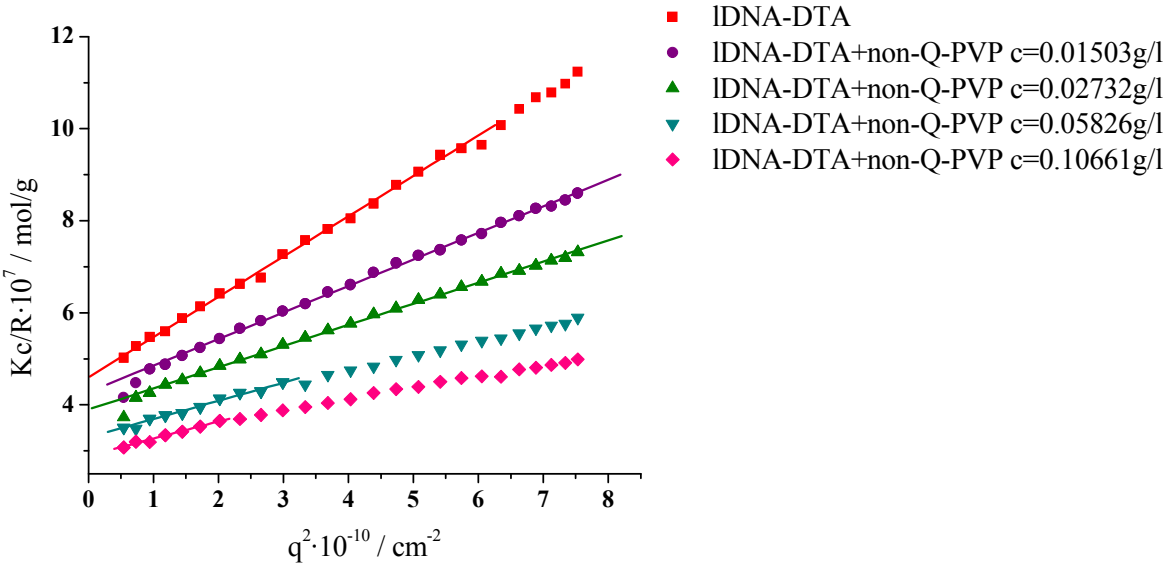

Figure A.52. Static Light Scattering measurements during the titration of linear DNA-dodecyltrimethylammonium bromide complexes with a non-quaternized polyvinylpyridine brush (non-Q-PVP) in DMF [LiBr] = 1mM. Measurements were done from 30° to 150° with steps of 5°. T = 20°C.

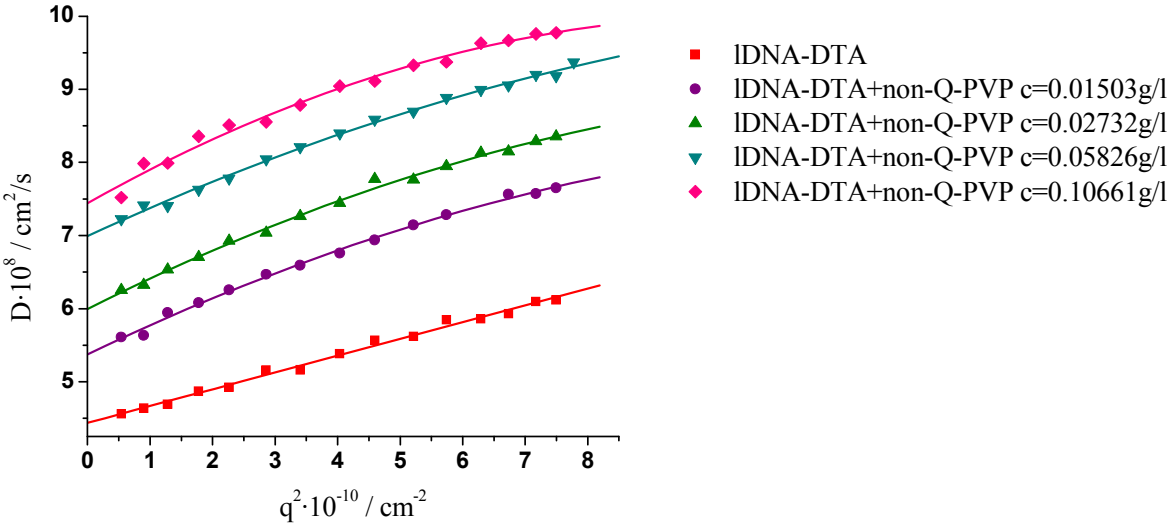

Figure A.53. Diffusion coefficient (D) vs. the scattering vector (q^2) during the titration of linear DNA-dodecyltrimethylammonium bromide complexes with a non-quaternized polyvinylpyridine brush (non-Q-PVP) in DMF [LiBr] = 1mM. Measurements were done from 30° to 150° with steps of 5°. T = 20°C.

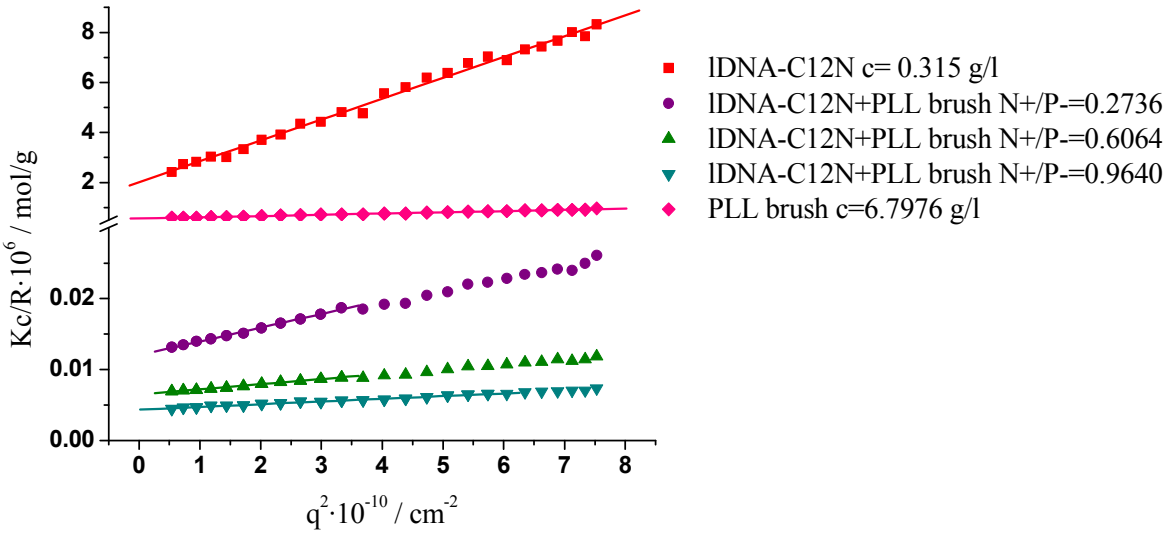

Figure A.54. Static Light Scattering measurements during the titration of linear DNA-dodecyltrimethylammonium complexes with a protected polylysine brush c=10.75 g/l. Measurements were done from 30° to 150° with steps of 5°. T = 20°C.

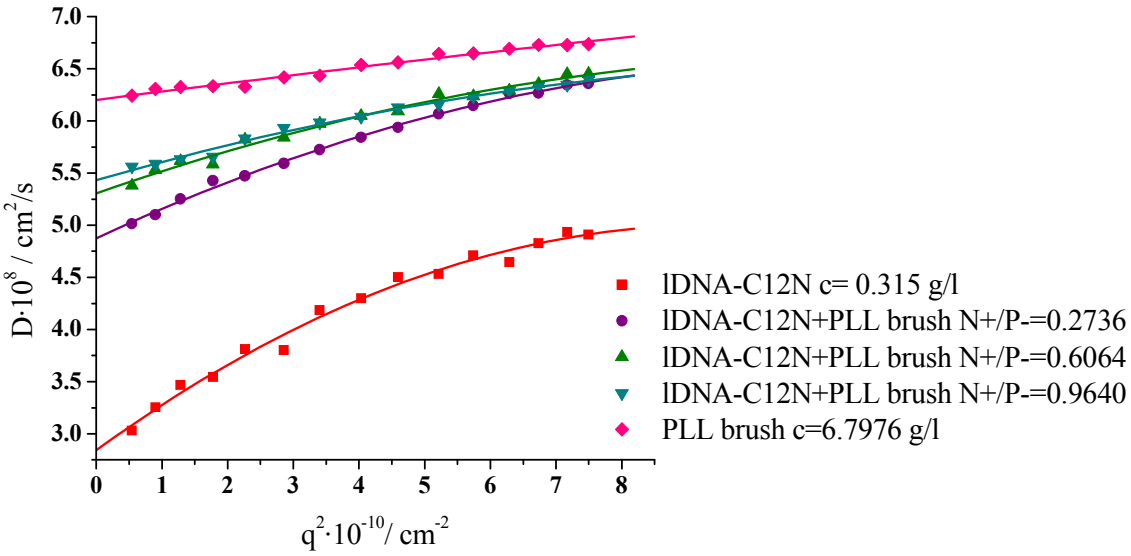

Figure A55. Diffusion coefficient (D) vs. the scattering vector (q^2) during the titration of linear DNA-dodecyltrimethylammonium complexes with a protected polylysine brush c=10.75 g/l.. Measurements were done from 30° to 150° with steps of 5°. T = 20°C.

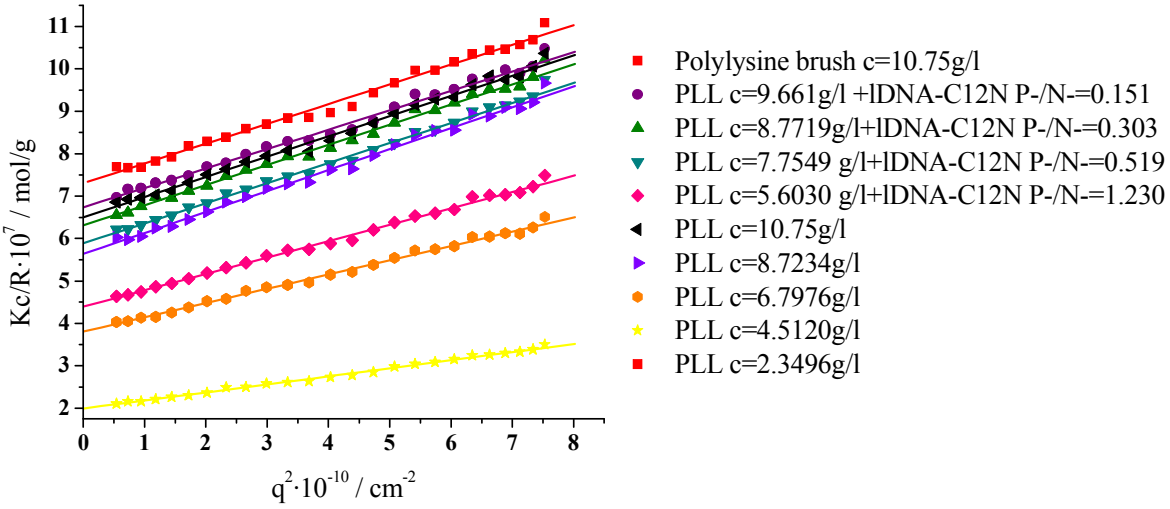

Figure A56. Static Light Scattering measurements during the titration of a protected polylysine brush c=10.75 g/l with linear DNA-dodecyltrimethylammonium complexes with a stock solution concentration of 0.315 g/l. Measurements were done from 30° to 150° with steps of 5°. T = 20°C.

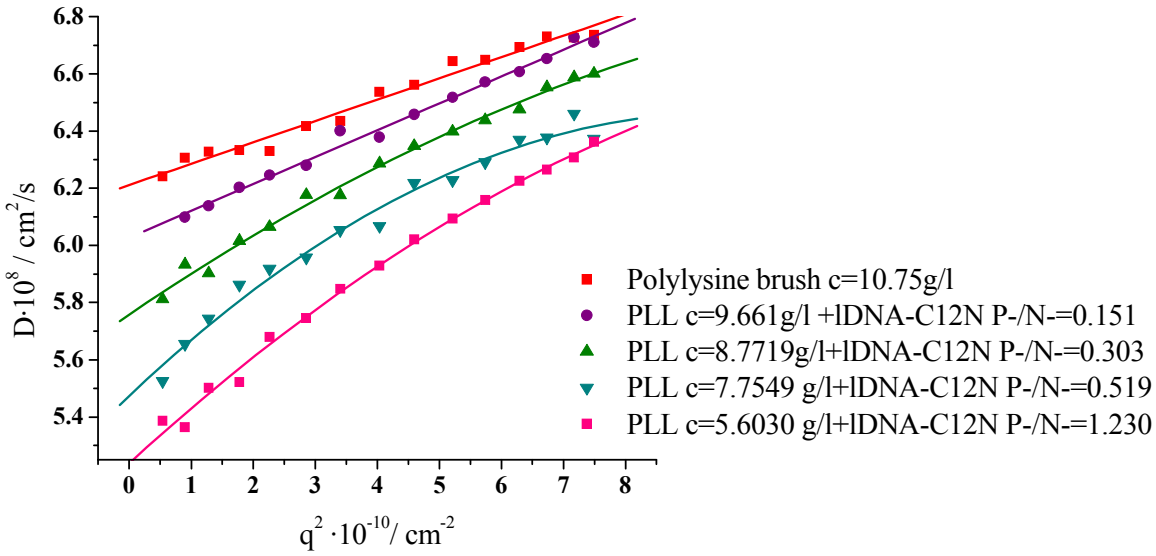

Figure A57. Diffusion coefficient (D) vs. the scattering vector (q^2) during the titration of a protected polylysine brush c=10.75 g/l with linear DNA-dodecyltrimethylammonium complexes with a stock solution concentration of 0.315 g/l. Measurements were done from 30° to 150° with steps of 5°. T = 20°C.